ENU Mutagenesis and the Quest for a Malaria Host-directed Therapy

Elinor Hortle, BSc (Hons)

Submitted in fulfilment of the requirement for the degree of Doctor of Philosophy

Australian School of Advanced Medicine
Department of Human Sciences
Macquarie University

March 2015

Table of Contents

Summary V
Copyright Statement VI
Statement of Authority of Access VI
Statement of Ethical Conduct VI
Abstracts VII
Contributions VIII
Acknowledgements IX
List of Figures X
List of Tables XI

CHAPTER 1 – LITERATURE REVIEW 1
General Introduction to Malaria 2
Lifecycle and Pathogenesis 3
Malaria Treatment and Drug Resistance 5
Malaria Vaccine 8
A New Approach is Needed for Anti-malarial Therapy 9
Host Genetic Polymorphisms and Their Prevalence 9
Haemoglobin Mutations 9
Mutation Affecting RBC Membrane Proteins 11
Enzyme Mutations 12
Immune System Mutations 14
Summary 14
Biological Mechanism of Resistance 15
Invasion 15
Growth 17
Spleen Clearance and Cytoadherence 20
Cerebral Malaria 21
Gametocytogenesis 24
Summary 24
Host-Directed Therapy 25
Current Developments in Host-directed Therapy 25
ENU Mutagenesis and the Identification of New Host-directed Therapy Targets 27
The ENU Mutagenesis Screen for Malaria Resistance Mutations in Mice 28
Previous Work on ENU Mutagenesis 31
Major Goals of the Thesis 32

CHAPTER 2 - EXPERIMENTAL PROCEDURES 33
Mouse Husbandry and Ethics 34
ENU Mutagenesis 34
Breeding RBC10 34
Whole-exome Sequencing 34
CRISPR/Cas9 36
Haematological Analysis 37
Genotyping 37
MACS Separation of Mature RBCs 38
Western Blots 39
Real-time PCR 39
Purine Analysis 40
Erythroblast Precursor Analysis 42
Plasma EPO 42
Biotin Half-life 42
Total Bilirubin 42
Lysis in Culture 42
Histology 43
Non-haem Iron 43

Osmotic Fragility 44
Phenylhydrazine Challenge 44
Eryptosis Markers 44
Infections 45
Parasitaemia 45
Growth Acceleration 45
TUNEL Staining 46
In-vivo Invasion and Growth Assay 46
Evan's Blue 47
Clinical Score 48
Plasma Cytokines 48
Lymphocyte Analysis 48
Recipes 50

CHAPTER 3 – MRI49372 BLOOD PHENOTYPE 53
Introduction 54
Results 54
MRI49372 has a macrocytic anaemia 54
The MRI49372 blood phenotype is caused by a mutation in *Ampd3* 57
The Ampd3^{T689A} mutation causes an activation of AMPD3 60
Activation of AMPD3 decreases RBC half-life 63
Shortened Ampd3^{T689A} half-life is caused by high oxidative stress 69
Discussion 71
Conclusion 76

CHAPTER 4 – MRI49372 MALARIA 77
Introduction 78
Results 80
Ampd3^{T689A} mice are resistant to erythrocytic stage *P. chabaudi* infection 80
Ampd3$^{T689A/+}$ resistance to *P. chabaudi* is affected by splenectomy 82
Ampd3$^{T689A/T689A}$ is susceptible to *P. berghei* 84
The Ampd3^{T689A} mutation stimulates reticulocytosis during infection 85
The Ampd3^{T689A} mutation causes increased gametocytogenesis 88
Ampd3^{T689A} RBCs support increased *P. chabaudi* invasion and growth 90
Discussion 93
Conclusion 98

CHAPTER 5 – RBC10 99
Introduction 100
Results 102
Kcc1^{M935K} is resistant to *P. chabaudi* and *P. berghei*. 102
Kcc1^{M935K} resistance is not cell autonomous. 106
Kcc1^{M935K} is resistant to ECM 108
Kcc1^{M935K} has an abnormal immune response to *P. berghei* infection 110
WNK3 as a novel host-directed therapy target 115
Discussion 117
Conclusion 122

CHAPTER 6 – FINAL DISCUSSION AND CONCLUSIONS 123

References 129

Appendix 153
Appendix A: Steady–state purine analysis of Ampd3^{T689A} 154
Appendix B: Ethics Approvals 156

Summary

Malaria is a disease of global concern, which causes over 800,000 deaths every year. Due to the rapid emergence of parasite drug resistance, ongoing control of malaria requires the urgent development of new anti-malarials that will have a prolonged life span. Genetic polymorphisms that provide natural resistance to malaria have existed in human populations for thousands of years without losing their efficacy. This suggests a possible new treatment strategy; drugs can be used to mimic the protective effects of such polymorphisms, in what is known as host-directed therapy (HDT). It is hoped that HDT will be able to effectively treat malaria without driving drug resistance.

An ENU mutagenesis screen was established in mice to identify novel genes mediating host resistance to malaria, and to thereby uncover potential drug targets for an anti-malarial HDT. Two mutant mouse lines were investigated: MRI49372, in which an over-activation of the enzyme AMPD3 causes striking resistance to *P. chabaudi* parasitaemia through high RBC turnover; and RBC10, in which an over-activation of the transporter KCC1 causes resistance to the development of cerebral malaria and modulation of the inflammatory response during *P. berghei* infection.

Through the work in this thesis, novel insight has been gained into the role of AMPD3 in determining red blood cell half-life, the effect of altered purine balance on intra-erythrocytic parasite growth, and the host factors affecting the immune response to malaria infection. Moreover, potential novel drug targets have been identified both for lengthening the life span of blood stored for transfusion, and for treating cerebral malaria.

Copyright Statement

To the best of my knowledge and belief, this thesis contains no material previously published or written by another person, except where due acknowledgement is made in the text. It contains no material that has been accepted for a degree or diploma by the University or any other institution, except by way of background information duly acknowledged in the thesis. It does not contain any material that infringes copyright.

Elinor Hortle
27/3/2015

Statement of Authority of Access

This thesis may be made available for loan and limited copying in accordance with the *Copyright Act 1968.*

Elinor Hortle
27/3/2015

Statement of Ethical Conduct

The research associated with this thesis abides by the International and Australian codes on human and animal experimentation, the guidelines by the Australian Government's Office of the Gene Technology Regulator and the rulings of the Safety, Ethics and Institutional Biosafety Committees of the University.

Elinor Hortle
27/3/2015

Abstracts

The following abstracts for presentation at conferences have resulted from work in this thesis.

E. Hortle, B. Nijagal, D. Bauer, S. Lampkin, M. McConville, B. McMorran, G. Burgio, S. Foote *A Role For AMP Deaminase in Malaria Resistance,* Beating Malaria, London, UK. Oral Presentation (2014)

E. Hortle, S. Lampkin, F. Rodda, B.McMorran, G. Burgio, S. Foote *Investigating New Host Factors Involved in Malaria Resistance,* MQ BioFocus Conference, Sydney, Australia. Poster Presentation (2012)

E. Hortle, S. Lampkin, F. Rodda, B.McMorran, G. Burgio, S. Foote *Investigating New Host Factors Involved in Malaria Resistance,* Australian Society of Parasitology Conference, Launceston, Australia. Oral presentation (2012)

E. Hortle, S. Lampkin, F. Rodda, B.McMorran, G. Burgio, S. Foote, *Investigating New Host Factors Involved in Malaria Resistance*, Molecular Approaches to Malaria, Lorne, Australia. Poster presentation (2012)

E. Hortle, S. Lampkin, F. Rodda, B.McMorran, G. Burgio, S. Foote, *Investigating Novel Genes Involved in Dyserythropoiesis*, Australian Flow Cytometry Users Group Conference, Hobart, Australia. Poster presentation (2011)

E. Hortle, S. Lampkin, F. Rodda, B.McMorran, G. Burgio, S. Foote, *Investigating Novel Genes Involved in Dyserythropoiesis*, SEiR Utas, Hobart, Australia. Poster presentation (2011)

Contributions

In accordance with the rules and regulations governing the degree of Doctor of Philosophy at Macquarie University, I assess my contribution the work presented in each chapter to be:

Chapter 3: 95%

- Dr Gaetan Burgio and Pr Simon Foote performed the ENU injections
- Shelley Lampkin maintained the mouse colony
- Dr Denis Bauer performed the bioinformatics analysis on the raw data resulting from exome sequencing
- Dr Brunda Nijagal conducted the LC-MS analysis of purines

Chapter 4: 95%

- Shelley Lampkin, Dr Gaetan Burgio and Emmaline Brown performed the malarial infections
- Dr Brunda Nijagal conducted the LC-MS analysis of purines

Chapter 5: 90%

- Shelley Lampkin, Dr Gaetan Burgio and Emmaline Brown performed the malarial infections
- The Australian Phenomics Facility performed the H&E staining
- Dr Gaetan Burgio and Emmaline Brown performed the CRISPR/Cas9 genome editing

Acknowledgements

I would first like to thank my three wonderful supervisors, Dr Gaetan Burgio, A/Prof Brendan McMorran, and Pr Simon Foote, for the countless hours they have devoted to my mentorship. Simon, for inspiring me to think ever bigger; Brendan for being the voice of reason and good grammar; and especially Gaetan, for fielding every Stupid Question and Nice Surprise, and for honing that most valuable of scientific tools, the ability to laugh at myself. It has been a true joy working with you all.

I also acknowledge past, present, and adopted members of the Foote group - Preethi Mayura-Guru, Diane Rowe, Karen Drysdale, Meredith Roberts-Thompson, Mariana Brizuela, Ning Huang, Bernadette Pedersen, Hong Ming Huang, Pat Lelliott, Jane Younger, Nazneen Adenwalla, Tony Jerkovic, Shelley Lampkin, and Emmaline Brown – for their invaluable advice, assistance, and fabulous company. In particular, I would like to thank Clare Smith, for making me believe I could do anything; Lucy Apps, for her punctual attendance at pub o'clock; Bernardette Schnider, for showing me that life can be lived all at once; Andy Greth, for taking me bouldering occasionally; and Ceri Flowers for holding us all together through two interstate relocations.

My thanks go to Brunda Nijagal and the team at Metabolomics Australia, as well as Noel Davies at the University of Tasmania, for contributing their LC-MS expertise to my purine adventure.

This work would not have been possible without funding from the National Health and Medical Research Council, the National Collaborative Research Infrastructure Strategy, the Education Investment Fund, the Howard Hughes Medical Institute, as well as travel funding from Macquarie University.

Lastly I would like to thank any and all of you who shouted me beers, made me dinner, or feigned interest in my sexy graphs and diagrams. It has helped me more than I can say.

List of Figures

Figure 1.1: *Plasmodium* lifecycle

Figure 1.2: Invasion of erythrocytes by *Plasmodium*

Figure 1.3: Processes involved in the development of cerebral malaria

Figure 1.4: Breeding scheme for dominant ENU RBC screen

Figure 3.1: MRI49372 macrocytic anaemia and splenomegaly

Figure 3.2: High MCV MRI49372 N2 mice have a linked region on chromosome 7

Figure 3.3: The MRI49372 phenotype is caused by a mutation in *Ampd3*

Figure 3.4: Purine metabolism in the erythrocyte

Figure 3.5: The Ampd3^{T689A} mutation causes activation of AMPD3.

Figure 3.6: Ampd3^{T689A} has elevated erythropoiesis

Figure 3.7: Ampd3^{T689A} has elevated reticulocytes

Figure 3.8: The Ampd3^{T689A} mutation shortens erythrocyte lifespan

Figure 3.9: Ampd3^{T689A} does not have iron overload in the spleen, and is not osmotically fragile

Figure 3.10: The Ampd3^{T689A} mutation causes increased oxidative stress and cell senescence

Figure 4.1: Purine metabolism in the infected erythrocyte

Figure 4.2: The Ampd3^{T689A} mutation causes resistance to *P. chabaudi*

Figure 4.3: Ampd3$^{T689A/+}$ resistance to *P. chabaudi* is spleen mediated

Figure 4.4: Ampd3$^{T689A/T689A}$ are not resistant to *P. berghei*

Figure 4.5: Ampd3^{T689A} has altered reticulocytosis in response to infection

Figure 4.6: The Ampd3^{T689A} mutation causes increased gametocytogenesis

Figure 4.7: The Ampd3^{T689A} mutation causes increased *P. chabaudi* invasion and growth

Figure 4.8: High GTP causes increased parasite growth

Figure 5.1. Schematic representation of KCC1 protein, showing the location of the M935K mutation

Figure 5.2: The Kcc1^{M935K} mutation does not increase susceptibility to infection with 1x10^5 *P. chabaudi* parasitased erythrocytes

Figure 5.3: The Kcc1^{M935K} mutation increases resistance to infection with 5x10^5 *P. chabaudi* parasitised erythrocytes

Figure 5.4: The Kcc1^{M935K} mutation causes resistance to *P. berghei*

Figure 5.5: Kcc1^{M935K} resistance is not cell autonomous

Figure 5.6: Kcc1^{M935K} resistance is independent of peripheral parasitaemia

Figure 5.7: The Kcc1^{M935K} mutation causes resistance to cerebral malaria

Figure 5.8: The Kcc1^{M935K} mutation alters the inflammatory response to *P. berghei* infection

Figure 5.9: The Kcc1^{M935K} mutation alters immune cell populations in uninfected mice

Figure 5.10: The Kcc1^{M935K} mutation causes an abnormal WBC response to infection

Figure 5.11: CRISPR/Cas9 has been used to knock-out WNK3 expression

Figure 5.12: Ion transport mediated by WNK3

List of Tables

Table 1.1: Mechanisms of resistance in common erythrocyte polymorphisms

Table 1.2: Mutant strains investigated in this thesis

Table 3.1: Haematological parameters of Wild-type, MRI49372$^{m/+}$, and MRI49372$^{m/m}$ mice.

Table 3.2: List of non-synonomous gene candidates held in common between both mutants sent for whole exome sequencing.

Table 5.1: Haematological parameters of Wild-type, Kcc1$^{M935K/+}$ and Kcc1$^{M935K/M935K}$ mice

Abbreviations

ACT	Artemesinin combination therapy
ACTB	Beta actin
ADP	Adenosine 5'-diphosphate
AGRF	Australian Genome Research Facility
AMA-1	Apical membrane antigen 1
AMP	Adenosine 5'-monophosphate
AMPD3	AMP deaminase isoform 3
Ank-1	Ankyrin-1
APC	Activated protein C
ATP	Adenosine 5'-triphosphate
BBB	Blood brain barrier
BCKDH	Branched chain keto acid dehydrogenase
bp	Base pair
BSA	Bovine serum albumin
CAM	Calmodulin
cAMP	Cyclic adenosine 5'-monophosphate
cGTP	Cyclic guanosine 5'-monophosphate
CM	Cerebral malaria
CQ	Chloroquine
CR1	Complement receptor 1
CRISPR	Clustered regularly interspaced short palindromic repeats
DARC	Duffy antigen receptor for chemokines
DNA	Deoxyribonucleic acid
DV	Digestive vacuole
E14	Embryonic day 14
EBA	Erythrocyte binding-antigen
EBL	Erythrocyte-binding-like
ECM	Experimental cerebral malaria
EDTA	Ethylenediaminetetraacetic acid
EGFR	Epidermal growth factor receptor
ENU	N-ethyl-N-nitrosourea
EPCR	Endothelial protein C receptor
EPO	Erythropoietin
EtOH	Ethanol
FACS	Fluorescence-activated cell sorting
g	G-force
G6PD	Glucose 6 phosphate dehydrogenase
GDP	Guanosine 5'-diphosphate
GMP	Guanosine 5'-monophosphate
GTP	Guanosine 5'-triphosphate
GYPA	Glycophorin A
GYPB	Glycophorin B
GYPC	Glycophorin C
HbA	Haemoglobin A
HbC	Haemoglobin C
HbS	Haemoglobin S
HDT	Host-directed therapy

HE	Hereditary elliptocytosis
hENT1	Human equilibrative nucleoside transporter
HEPES	2-[4-(2-hydroxyethyl)piperazin-1-yl]ethanesulfonic acid
hFNT1	Human facilitative nucleobase transporter
HGB	Haemoglobin
HIV	Human immunodeficiency virus
HPLC	High performance liquid chromatography
HS	Hereditary spherocytosis
Hypox	Hypoxanthine
HZ	Hemozoin
IFN	Interferon
Ig	Immunoglobulin
IL	Interleukin
IMP	Inosine 5'-monophosphate
Ino	Inosine
IP	Intraperitoneal
iRBC	Infected red blood cells
ITN	Insecticide-treated mosquito nets
IV	Intravenous
KAHRP	Knob-associated histidine-rich protein
KCC	K-Cl co-transporter
kDa	Kilodalton
kg	Kilogram
KO	Knock-out
LOD	Logarithm of odds
Macro	Macrocytic red blood cell
MACS	Magnetic-activated cell sorting
MCV	Mean corpuscular volume
MDR-TB	Multi drug resistant tuberculosis
mg	Milligram
MHC	Major histocompatibility complex
Micro	Microcytic red blood cell
ml	Millilitre
mM	Millimolar
MMPs	Matrix metalloproteinases
MS	Mass spectrometry
MSP	Merozoite binding proteins
NaCl	Sodium Chloride
NCC	Na-Cl co-transporter
NEM	N−ethylmaleimide
ng	Nanogram
NK cells	Natural killer cells
NKCC	Na-K-Cl co-transporter
NLRP3	NOD-like receptor family, pyrin domain containing 3
nm	Nano meters
NOS2	Nitric oxide synthase 2
NPP	New permeability pathway
PbA	*P. berghei* ANKA
PBS	Phosphate buffered saline

PCR	Polymerase chain reaction
PF4	Platelet factor 4
*Pf*AMPDA	*P. falciparum* AMP deaminase
*Pf*CRT	*P. falciparum* chloroquine resistance transporter
PfDHFR	*P. falciparum* dihydrofolate reductase
*Pf*EMP1	*P. falciparum* erythrocyte membrane protein 1
Pfmdr	*P. falciparum* multidrug resistance analogue
*Pf*NT1	*P. falciparum* nucleoside transporter 1
PHZ	Phenylhydrazine
PI	Inorganic phosphate
PK	Pyruvate kinase
PS	Phosphatidylserine
PV	Parasitophorous vacuole
PVM	Parasitophorous vacuole membrane
RBC	Red blood cell
RBL	Reticulocyte-binding-like
RDW	Red cell distribution width
Retic	Reticulocyte
RNA	Ribonucleic acid
RON	Rhoptry neck protein
ROS	Reactive oxygen species
rpm	Revolutions per minute
SAO	Southeast asian ovalocytosis
SCD	Sickle cell disease
SD	Standard deviation
SDS	Sodium dodecyl sulfate
SDS-PAGE	Sodium dodecyl sulfate–polyacrylamide gel electrophoresis
SEM	Standard error of the mean
SMA	Severe malarial anemia
SNP	Single nucleotide polymorphisms
SP	Sulfadoxin-pyramethamine
TB	Tuberculosis
TBIL	Total bilirubin
TCA	Tricarboxylic acid cycle
TLR9	Toll-like receptor 9
TNF	Tumour necrosis factor
TUNEL	Terminal deoxynucleotidyl transferase dUTP Nick End Labelling
USA	United States of America
UV	Ultra-violet
WBC	White blood cell
WHO	World Health Organisation
WNK	With-no-lysine kinase
WT	Wild-type
XDR-TB	Extensively drug resistant tuberculosis
XMP	Xanthosine 5'-monophosphate
µg	Microgram
µl	Microliter
µM	Micromolar

CHAPTER 1 – LITERATURE REVIEW

General Introduction to Malaria

Malaria is a lethal disease caused by the parasites of the genus *Plasmodium*. It is one of the largest public healthcare burdens worldwide, affecting some of the poorest countries and areas where access to adequate healthcare is limited. In 2013 an estimated 855, 000 deaths were caused by the disease, the majority of which were pregnant women and children under the age of 5 [1]. In recent years the combination of artemisinin based drugs, insecticide treated bed nets and indoor residual spraying of insecticides has led to substantial reductions in the burden of malaria; 43 malaria endemic countries have reported a 50% reduction in cases in the last 10 years [2]. However, the ongoing control of the disease faces a number of problems. First among these is the development of parasite resistance to anti-malarials, a problem observed for all drugs in use today [2]. Exacerbating this problem is the development of mosquito resistance to insecticides, especially pyrethroids. The development of an effective vaccine for malaria has been difficult due to the fact that the parasite is adept at avoiding immune mechanisms, and the ways it does this are not completely understood. Lasting control of malaria will require both increased access to healthcare in developing countries, and the development of new treatment strategies that are better able to avoid the development of parasite resistance. This will require deeper knowledge of the genes influencing host resistance to the disease, and the biological processes involved in the pathology of malaria.

Areas of stable malaria transmission cover almost 100 countries and 40 million square kilometres across the northern part of South America, Africa, the Middle East and South East Asia [3]. Approximately 3.4 billion people are exposed annually [2]. Transmission of malaria is dependent on the *Anopheles* mosquito, and so is limited to regions in which temperature, rainfall and humidity are suitable for *Anopheles* survival, as well as *Plasmodium* survival within the mosquito. Transmission follows seasonal changes in rainfall, as sufficient water bodies are necessary for the larval stage of *Anopheles* growth [3]. There are currently six species of *Plasmodium* known to infect humans; *Plasmodium falciparum*, *Plasmodium vivax*, *Plasmodium ovale curtisi*, *Plasmodium ovale wallikeri*, *Plasmodium malariae*, and *Plasmodium knowlesi*. Infection with *P. falciparum* causes the most lethal disease, and is most prevalent in Africa [3]. In other areas *P. vivax* accounts for roughly 50% of cases with most infection occurring in the Middle East, south Asia and the south America [4,5].

Lifecycle and Pathogenesis

The *Plasmodium* lifecycle has several stages, including sexual replication within the female *Anopheles* mosquito, and asexual replication within the human liver and bloodstream. Sporozoites, residing in the salivary glands of infected *Anopheles,* are injected into the subcutaneous tissue of the human host when the mosquito takes a blood meal. Approximately 50% of these sporozoites will then migrate to the liver, where they invade hepatocytes [6]. Here, each sporozoite undergoes a cycle of asexual schizogeny to produce several thousand merozoites, which are released into the host blood stream. This liver stage is clinically silent. Sporozoites that remain in the subcutaneous tissue are still capable of producing infective merozoites [7]. Once in the bloodstream merozoites invade red blood cells (RBCs) and begin another cycle of asexual replication. Parasites progress through a number of growth stages – from ring, to trophozoite, to schizont stage – before finally rupturing the RBC and releasing 30-40 merozoites [8]. These merozoites then invade new RBCs, where replication begins again. It is this blood stage of malaria that causes all clinical symptoms of the disease [9]; importantly, during this stage the parasite is surrounded by two membranes, and is therefore relatively isolated from the host. This makes it challenging both for the host to recognise and attack the parasite, and for anti-malarial treatments to kill the parasite. To complete its lifecycle, *Plasmodium* differentiates proportion of bloods stage parasites from asexual forms into either male or female gametocytes. Gametocyte-bearing RBCs are taken up by the feeding *Anopheles* mosquito, complete sexual replication within her, and can then be transferred to a new human host (Figure 1.1).

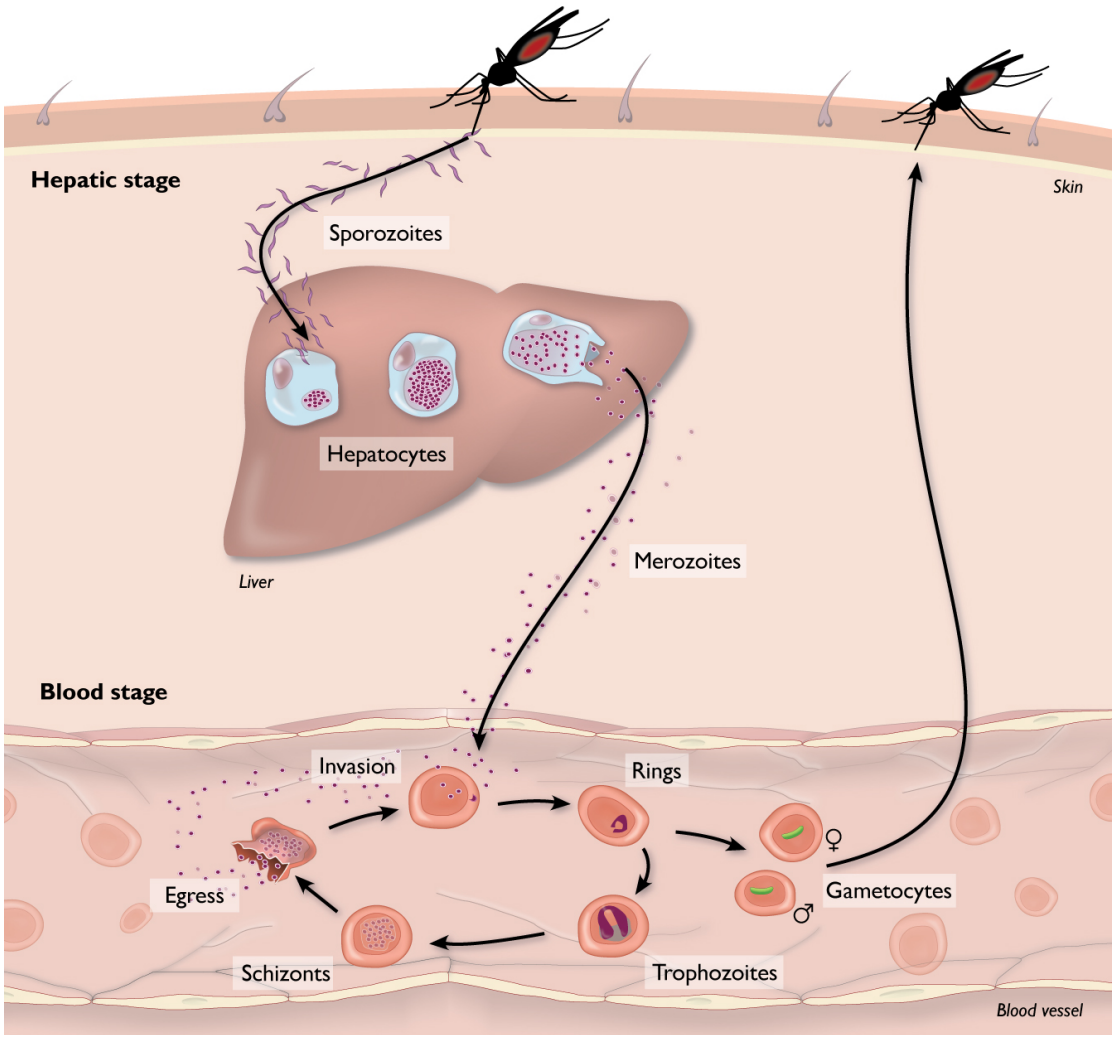

Figure 1.1 – *Plasmodium* lifecycle. The lifecycle of *Plasmodium* in humans begins when parasites residing in the salivary gland of the female anopheles mosquito are injected into the subcutaneous tissue. These sporozoites migrate to the liver, where they invade hepatocytes and undergo a cycle of clinically silent asexual replication. The parasites egress from hepatocytes as merozoites, and migrate to the bloodstream where they undergo further cycles of asexual replication within erythrocytes. This blood stage causes all the clinical symptoms of disease. A proportion of these blood stage parasites will form gametocytes, which are taken up by mosquitoes and transmitted to other human hosts. *(Illustrated by A. Greth, ASAM, 2013).*

The severity of disease symptoms depends on the species of *Plasmodium* as well as the age, genetics and acquired immunity of the infected individual. Uncomplicated malaria can cause fever, chills, nausea, vomiting, dizziness and headaches. Severe malaria is characterised by severe anemia, acute renal failure, and respiratory distress. *Plasmodium falciparum* is widely regarded as the most clinically important species of *Plasmodium*, because it has a much higher incidence of severe disease, and can cause both cerebral and placental malaria. Cerebral malaria (CM) is defined as the sudden onset of seizure and/or coma where the patient has peripheral asexual *P. falciparum* parasitaemia, and no other cause of encephalitis can be identified. Placental malaria is associated with increased risk of maternal anemia, maternal mortality, low birth weight, preterm delivery, intrauterine growth retardation, and perinatal mortality [10].

Malaria Treatment and Drug Resistance

There are many anti-malarial drugs currently available that target a range of biological processes specific to the *Plasmodium* parasite. However, it is unknown how long this arsenal will remain effective, due to the development of parasite resistance. For example chloroquine (CQ), which was the anti-malarial of choice during the 1950s, deteriorated rapidly from the first signs of resistance in Thailand in 1957, to almost complete ineffectiveness in sub-Saharan Africa by 1988 [11]. Resistance arose independently in at least six locations[12], and today CQ is ineffective against most strains of *P. falciparum* across Asia, Oceania, Africa and South America. Unfortunately the problem of resistance is common to all current anti-malarials. Resistance to artemisinin-based drugs – currently the best acting anti-malarials – has been observed in Myanmar, Thailand, Cambodia and Vietnam [13,14]. The rapid spread of anti-malarial resistance has been attributed to several factors, including the rapid lifecycle and high DNA mutation rate of the parasite [15]; the heavy use of anti-malarial mono-therapies and problems with inadequate dosing[16,17]; and the fact that anti-malarial treatment can increase rates of gametocytogenesis, which in turn leads to the preferential transmission of drug resistant parasite strains [14,18-23].

Adding to the problems outlined above is the fact that the current arsenal of anti-malarials consists of a relatively small number of chemically related compounds. These fall into four groups: aminoquinolines (chloroquine, quinine, mefloquine, amodiaquine, halofantrine, primaquine); anti-folate compounds (pyrimethamine, proguanil, chlorcycloguanil, dapsone, sulfadoxine); artemisinin and derivatives (artemisinin,

artesunate, artemether, arteether, dihydroartemisinin); and atovaquone. It has been suggested that the lack of structural diversity of these compounds has primed new drug candidates for the rapid development of drug resistance, as new compounds are simply modifications of the same basic template [17]. Indeed there is evidence that development of resistance to one anti-malarial, can affect the efficacy of others [24,25]. Therefore, the World Health Organisation now recommends the use of therapies that contain compounds of two different classes, with the preferred choice being an artemesinin derivative combined with lumefantrine, amodiaquine, mefloquine or sulfadoxine-pyrimethamine. It is thought that because these so-called artemesinin-based combination therapies (ACTs) contain two drugs, each with different modes of action, parasite resistance will develop less quickly than it has with the use of mono-therapies [26]. Examples of the mode of action and resistance of each anti-malarial type are listed below.

Aminoquinolines (Chloroquine)

The first effective Western treatment for malaria, was quinine, which occurs naturally in the bark of cinchona trees in South America. It was replaced by chloroquine as the anti-malarial of choice in the 1940s, as the latter was found to have fewer side effects [27]. During development within the RBC, *Plasmodium* parasites digest haemoglobin. This produces free haem, which can catalyse the production of free radicals. To protect itself from oxidative damage, the parasite converts free haem to inert hemozoin crystals [28-30]; chloroquine is thought to prevent the formation of hemozoin, and thereby kill the parasite through the build up of oxidative stress [31]. There is also some evidence that cholroquine may increase oxidative stress within the RBC by binding to host quinone reductase 2 [32]. Resistance to chloroquine occurs through alterations in the molecular pumps controlling the import and efflux of the drug from its site of action in the parasite's digestive vaculole (DV). These pumps are the *P. falciparum* chloroquine resistance transporter (*Pf*CRT), and multidrug resistance analogue (*pfmdr1)* [33-35]. Mutations to *Pf*CRT1 allow the protein to export CQ out of the parasite's DV. At least 30 variant residues have been identified in CQ resistant *P. falciparum* isolates across Asia, Africa, and South America. For most, resistance appears to be associated with the single amino acid substitution K76T[12]. Conversely, *Pf*MDR1 is involved in the import of CQ into the DV. Five point mutations (N86Y, Y184F, S1034C, N1042D, and D1246Y) which decrease the ability of the protein to transport CQ into the DV, as well as decreases in *Pf*MDR copy number, have been linked to CQ resistance [36].

Anti-folates (sulfadoxine-pyrimethamine)

The anti-folate drug sulfadoxine-pyrimethamine (SP) entered widespread use as the front-line treatment for malaria in areas where CQ resistance had become widespread [17,27,37]. Folate is an essential molecule that can be synthesised *de novo* by the parasite, or scavenged from its environment. It is used in the subsequent biosynthesis of purine, pyrimidine and amino acids [38]. SP combines two compounds that act within the folate synthesis pathway of *Plasmodium*. Sulfadoxine is a substrate analogue of PABA, which is metabolised by dihydropteroate synthetase (DHPS); and pyrimethamine is a specific inhibitor of *Plasmodium* dihydrofolate reductase (PfDHFR). Resistance develops due to point mutations in the genes of these enzymes. For example, a single amino acid change, from serine to asparagine, at residue 108 of PfDHFR can cause pyrimethamine resistance [39]. Several similar point mutations have been identified; 6 in PfDHFR, and 7 in PfDHPS [37]

Artemisinin

The plant *Artemesia annua* has been used in traditional Chinese medicine for treating fever and malaria for hundreds of years. The active ingredient, artemesinin, was first isolated in 1971, and began to be widely used in the 1980s[40]. It has advantages over other anti-malarials, in that it is fast acting, and is active against all stages of the parasite, including gametocytes [41,42]. Unfortunately, it has a short half-life, and therefore artemesinin is often combined with other, longer acting drugs [17]. Although it is generally understood that artemisinin kills parasites by increasing oxidative stress within the RBC [43,44], the exact mechanism of action and resistance is still unclear, and contradictory evidence is available for a number of hypotheses. For example, there is evidence that artemisinin targets the parasite ATPase *Pf*ATP6 [45,46], and mutations in *Pf*ATP6 have been associated with artemisinin resistance in some field isolates [47]. However, it has been shown *in vitro* that polymorphisms in *Pf*ATP6 do not effect *P. falciparum* sensitivity to artemisinins [48]. More recent evidence suggests that resistance may be caused by polymorphisms in the *K13* gene. K13 belongs to the kelch superfamily of proteins; resistance mutations fall within its propeller domain, which mediates a range of cellular functions including ubiquitin based protein degradation and cell adaptation to oxidative stress [49,50]. Mutations in *K13* have been associated with artemesinin resistance in Cambodia, Thailand, Myanmar, Laos, and Vietnam [14,49,51].

Atovaquone

Atovaquone-proguanil (AP) – initially licensed as Malarone – is commonly prescribed as a prophylactic drug for travellers visiting malaria endemic regions. It also has efficacy in treating uncomplicated malaria infections, but so far its high cost has prevented it from entering widespread use. As the patent for AP expired in 2013, it has been considered as a possible replacement for artemesinin in areas where parasite resistance to that drug is common. Atovaquone is a competitive inhibitor of the mitochondrial cytochrome bc1 complex. This complex plays an integral role in maintaining mitochondrial membrane potential, and is also necessary for pyrimidine synthesis. Atovaquone kills *Plasmodium* by collapsing mitochondrial membrane potential in the parasite [52]. Resistance can arise through a single point mutation in the quinol oxidation pocket of cytochrome b [53]. As such, there are concerns that the advantages gained by replacing artemesinin with AP would be short lived [54-56]

Malaria Vaccine

There has been considerable effort over the last 30 years to develop a malaria vaccine. It is thought that this is possible because individuals do develop acquired immunity to *Plasmodium*, although this appears to be due mainly to protection against the clinical symptoms of blood stage, rather than a sterilising immunity [57]. Naturally acquired immunity also depends on repeated and persistent infection and is often lost by individuals that leave endemic areas [58]. Potential vaccine targets include both liver and blood stage parasites. Of the numerous vaccine candidates under investigation, the most promising is RTS, S, which entered phase 3 trials in May 2009. This vaccine aims to induce immunity to the pre-erythrocytic form of the parasite, and thereby prevent it from invading RBCs and causing clinical symptoms. To this end, RTS, S targets the circumsporozoite protein, which is the most prominent surface antigen of the *P. falciparum* sporozoite. Results to date show that the efficacy of the vaccine varies with *Plasmodium* transmission intensity, from 60% in areas of low transmission, to 4% in areas of high transmission. Vaccine efficacy also varies with time, waning within a few years of administration [59,60]. For these reasons, RTS,S is unlikely to remain effective long term, and although many other candidate vaccines are in development, they may suffer similar problems.

A New Approach is Needed for Anti-malarial Therapy

With limited success in vaccine development, the burden of malaria treatment rests heavily on conventional anti-malarials, which suffer from the rapid development of parasite resistance. The common feature of all currently available drugs is that they are parasite-directed. They target biochemical pathways within *Plasmodium,* which means the parasite has genetic control not only over the molecule targeted by the drug, but also the metabolism, uptake and secretion of the drug. In order to overcome this problem, researchers have begun to look towards the host, to consider if it is possible to kill the *Plasmodium* by manipulating the host environment in which the parasite resides, rather than by targeting it directly. Fortunately there are many natural examples where such alterations to the host result in anti-malarial effects. These examples are host genetic polymorphisms, and are discussed below.

Host Genetic Polymorphisms and Their Prevalence

It has long been observed that in malaria endemic regions, genetic blood disorders exist in higher than predicted frequencies. In 1949 observations of the high rate of thalassemia in the Mediterranean caused Haldane to propose the malaria hypothesis: that such deleterious traits exist in high frequencies because they provide a selective advantage by rendering individuals resistant to malaria [61]. Further evidence in support of this hypothesis comes from recent observation that some traits are now disappearing from areas where malaria has been eradicated [62]. The polymorphisms providing malaria resistance affect a wide range of host cells, molecules and processes, including RBC shape and structure, RBC membrane proteins, haemoglobin and enzymes, and components of the immune system.

Haemoglobin Mutations

Haemoglobin is a tetramer made up of two α- and two β-globin chains, surrounding a haem molecule. It makes up 96% of the dry weight of the RBC, and is responsible for the oxygen and carbon dioxide carrying capacity of blood. Five major polymorphisms affecting haemoglobin have been associated with malaria resistance; three occurring from simple point mutations within the β-globin chain (haemoglobinopathies), and two affecting the production and hence total amount of the α- and β- chains (thalassaemias).

Haemoglobin S

HbS results from a glutamate to valine substitution in position 6 of the β globin molecule. In homozygous individuals HbS causes sickle cell disease (SCD) – a disorder in which RBCs distort into damaging sickle shapes under low oxygen concentration. SCD is fatal in the absence of adequate treatment, and individuals often die before the age of five. Under neutral selection, such an allele would not be expected to be present. But in populations residing in malaria endemic areas, especially Africa, the HbS allele frequency is as high as 20% [63]. It is generally believed that this is because the heterozygous allele, HbAS, provides significant resistance to *P. falciparum*. Studies have shown that HbAS individuals are protected from severe malarial anaemia, high-density parasitaemia, and cerebral malaria [64-66].

Haemoglobins E and C

HbE results from a glutamine to lysine substitution, which causes an alternate splicing site at codons 25-27 of the β-globin gene. This in turn causes reduced synthesis of β-globin and a mild thalasaemic phenotype in homozygotes. HbE is commonly found in Southeast Asia. HbC results from a glutamate to lysine substitution at position 6 of the β-globin gene. Homozygotes suffer from haemolytic anaemia. HbC is found most commonly in West Africa. Neither HbE nor HbC provide protection from uncomplicated *P. falciparum* infection, but they do provide protection from severe anaemia, high parasite densities and cerebral malaria [66-69].

Thalassaemias

α- and β- thalassaemia are disorders caused by the underproduction of α- and β-globin chains respectively. They are widely prevalent in areas where malaria is currently, or has been historically endemic [70]. Case control studies have shown 60% protection from severe malaria in α- and β- thalassaemia homozygotes, and 34% for heterozygotes [71-73]. Interestingly, there is evidence of interaction between α-thalassemia and HbS. Although both of these polymorphisms provide resistance against *P. falciparum* when carried in isolation, individuals with both mutations are almost as susceptible to clinical malaria as individuals with neither [74].

Mutation Affecting RBC Membrane Proteins

The Duffy antigen receptor for chemokines (DARC), is a glycosylated membrane protein expressed on the RBC surface, which acts as a non-specific receptor for several chemokines. Individuals with one of two point mutations in the DARC promoter have reduced or absent Duffy expression on the erythrocyte surface; this polymorphism is most prevalent in Africa, although a Duffy null allele has arisen independently in Papua New Guinea [75]. *P. vivax* binds to DARC as it invades the RBC, and therefore Duffy negative individuals are resistant to infection by that parasite. In some African regions, 100% of individuals are Duffy negative[76], and the polymorphism is thought to account for the striking lack of *P. vivax* transmission over much of the continent [77,78]. For many years it was believed that Duffy negative individuals are completely impervious to *P. vivax* infection [79], however, this paradigm has been challenged by recent reports of Duffy negative individuals infected with *P. vivax* in Madagascar, West Africa, Kenya and South America [80-84]. This may mean either that *P. vivax* is evolving to use receptors other than Duffy for invasion, or that the parasites observed are merely 'vivax-like' [82,84,85].

The erythrocyte cytoskeleton is composed of several proteins, including α- and β-spectrin, ankyrin, band 3 and protein 4.1, that interact and form complex intermolecular structures that give the RBC its form and physical properties. Hereditary spherocytosis (HS) and hereditary elliptocytsis (HE) are conditions caused by polymorphisms that disrupt the interactions between these proteins, resulting in abnormally shaped erythrocytes. These polymorphisms are highly prevalent in malaria endemic populations, but little is known about their impact on malaria susceptibility in humans [86-88]. Southeast Asian Ovalocytosis (SAO) – a type of HE caused by deletion of band 3 – has been associated with protection from cerebral malaria, but not uncomplicated *P. falciparum* infection [89-91].

The ABO antigen is a carbohydrate molecule on the RBC surface with roles in cell adhesion and hemostasis. ABO blood group has been associated with the severity of malaria outcome; A, B and AB individuals are more susceptible than those with O blood groups, and are more likely to suffer from coma due to cerebral malaria, and from severe malarial anaemia [66,92,93]. There is also some evidence that blood group O provides protection from placental malaria, although appears to be restricted to primiparae [94].

Complement receptor 1 (CR1) is a glycoprotein expressed on the RBC surface, which binds to particles and immune complexes with activated complement. Polymorphisms in CR1 can affect the size of the protein, the level of expression on the RBC surface, or Knops blood group antigens. Both of the latter have been associated with malaria. For example, Moulds et al compared the prevalence of different CR1 polymorphisms in African-Americans, European-Americans and Malians. They found the greatest association between ethnicity and the Knops blood group polymorphism Sl(a-), which was observed in <1% of Europeans, 39% of African-Americans, and 68-72% of Malians [95]. In another study, it was shown that up to 80% of healthy individuals in malaria endemic regions of Papua-New Guinea express very low levels of CR1 on their RBCs, and that this correlates with resistance to severe malaria [96]. However, in a case-control study across 12 locations in Africa, Asia and Oceania, only a weak association could be found between CR1 polymorphisms and severe malaria [66].

Other RBC surface polymorphisms common in malaria endemic regions include those in Glycophorins B and C [97,98]**.** Although their association with malaria endemicity might suggest a role in resistance, the evidence for this is unclear. For example, although null polymorphism in glycophirin C has been associated with protection from *P. falciparum in vitro,* studies in Papua New Guinea, were the mutation is commonly found, have shown no association with malaria incidence or severe anaemia [99-101]

Enzyme Mutations

Glucose 6 phosphate dehydrogenase (G6PD)

G6PD maintains cellular levels of NADPH, which in turn, maintains the levels of reduced glutathione. The latter is an essential part of the anti-oxidant defence of the RBC; insufficient amounts of reduced glutathione result in hemolyis of RBCs due to a build-up of reactive oxygen species. G6PD deficiency, also known as favism, is one of the most common erythrocyte enzyme mutations worldwide [102]. The X linked disorder can be caused by several mutations; the most common variant, G6PD A-, results in amino acid substitutions at positions 68 and 126 of the protein. Some debate exists about the protective role of G6PD deficiency in *Plasmodium* infection. Ruwende et al. reported that in two large case control studies of over 2000 African children G6PD A- was associated with a 46-58% reduction in risk of both mild and severe malaria for both female heterozygotes and male hemizygotes [103]. In contrast, Guindo et al. reported that G6PD A- provided protection for hemizygous males, but not heterozygous females. In this

study no difference in parasite density with G6PD status was observed in either sex, and protection in males was largely against cerebral malaria [104]. Other results support the protective role of the heterozygous condition, but suggest that homozygousity may make individuals more susceptible to severe malaria [66,105].

Pyruvate Kinase (PK)

PK catalyses the final step of glycolysis, converting Phosphoenolpyruvic acid to pyruvate, and generating ATP. PK deficiency - caused by any one of over 150 different mutations - is the second most common cause of haemolytic anaemia, behind G6PD deficiency, and results in lowered ATP concentration, cell shrinkage and haemolysis [106]. Various studies have estimated the occurrence of loss of function variants between 1:25 and 1:20,000 [107-109] depending on the population surveyed. Evidence of positive selection for PK deficiency in sub-Saharan Africa and Pakistan is consistent with the possibility of malarial selection [107], and individuals with PK deficiency have been associated with higher rates of uncomplicated malaria [109].

Nitric Oxide Synthase 2 (NOS2)

Phagocytes generate nitric oxide as part of the innate immune response to infection. The compound is also a potent vasodilator. Polymorphisms in the NOS2 promoter region have been found in malaria endemic regions, and have been associated with protection from severe malarial anaemia and cerebral malaria [110,111]. However, a study by Levesque et al, investigating the effects of these polymorphisms, found no difference in NOS2 promoter function between WT and mutant alleles, suggesting that the association between NOS2 polymorphisms and malaria resistance may be more complicated than previously described [112].

Plasma membrane calcium-transporting ATPase 4 (ATP2B4)

The *ATP2B4* gene encodes a calcium transporter found in the plasma membrane of erythrocytes. It was originally identified by genome wide association study (GWAS) as a malaria resistance locus [113]. A subsequent case-control study has shown that individuals carrying the derived allele at rs10900585 have a significantly higher risk of severe malaria, and those homozygous for the derived allele at rs4951074 had a decreased risk of severe malaria [66].

Immune System Mutations

There are many immune system mutations that have been identified as providing resistance to malaria. These mutations are usually non-deleterious, and affect both antigen presentation, and immune cytokines.

HLA-B and *HLA-DR* are polymorphic genes that encode MHC class I and II molecules involved in the antigen presentation necessary for parasite recognition by the immune system. Various mutations in these genes have been linked to fewer malarial attacks, lower parasitaemia and reduced fever [114,115].

Cytokine polymorphisms associated with malaria resistance include mutations to *IL4*, *IL-13* and *IFNG. IL4* encodes interleukin-4, which stimulates the differentiation of antibody producing B cells. Various alleles have been associated with higher levels of antibodies against malarial antigens, fewer malarial attacks and lower parasitaemia [114,116]. *IL-13* has been associated with increased risk of severe malarial anaemia (SMA) [117] *IFNG* encodes the pro-inflammatory cytokine interferon gamma (IFN-γ), mutations in which have been shown to protect against the development of cerebral malaria [118].

CD40 ligand (CD40L) is a glycoprotein important in the immune response to infection. It is primarily expressed by activated CD4+T cells, and is involved in B cell proliferation and Ig class switching. In a case control study of Gambian individuals, a polymorphism in the promoter region of the gene - CD40L-726C - was associated with significantly reduced risk of severe malaria, cerebral malaria and severe malarial anaemia, in hemizygous males [119]. However, in a later study, it was found that although the derived allele associated with reduced risk in The Gambia, it is associated with increased risk in Kenyan individuals [66].

Summary

The naturally occurring polymorphisms outlined above underscore the significance of host cell properties and functions in determining the course of *Plasmodium* infection. Even small changes to the host environment can provide significant protection from the worst symptoms of disease; and perhaps more strikingly, can provide protection from malaria on a scale that has not been achieved by conventional anti-malarials. For example, the Duffy negative mutation has prevented the establishment of *P. vivax* in Africa, and has continued to provide protection from infection for several thousand

years [77,120]. This thesis is based on the hypothesis that host genetics may hold the key to developing a more lasting control of malaria. That is, by using pharmaceuticals that target host products essential for parasite survival, it may be possible to minimise or even avoid parasite drug resistance from developing, as well as providing completely new classes of anti-malarials. It is therefore of considerable importance to understand the mechanisms by which host polymorphisms confer resistance.

Biological Mechanism of Resistance

During its lifecycle within the erythrocyte, *Plasmodium* interacts with a wide range of host products, as well as substantially remodelling the RBC, and influencing the host response to infection. The following section outlines the current understanding of some of these interactions, and the ways in which host polymorphisms disrupt them.

Invasion

The invasion of erythrocytes by the merozoite has been well characterised, and is summarised in Figure 1.2. It is a dynamic process that can be separated into four stages, involving a reversible attachment, reorientation, formation of a tight junction and finally internalisation.

For invasion to proceed, binding has to occur between several parasite proteins and their respective receptors on the erythrocyte surface. For *P. vivax,* Duffy binding protein (DBP) facilitates invasion, by binding DARC[121]. In *P. falciparum* the parasite proteins EBA-175 and EBL-1 bind to host glycophorin A (GYPA) and glycophorin B (GYPB) respectively [122,123]; both STEVOR and PfEBP-2 bind glycophorin C (GYPC) [124,125]; PfRh4 and PfRh5 bind complement receptor 1 and basigin [126,127]; and the merozoite surface protein MSP1 binds to band 3 [128]. Disruptions to the expression of each of these host proteins have been shown to decrease the parasite's ability to invade RBCs. The importance of each of these interactions has been shown *in vitro*. By using antibodies or peptides to block GYPB[123], STEVOR[125], PfRh4[126], basigin[127], MSP-1[128] or CR1[129], *P. falciparum* merozoite invasion can be reduced. The same is true for DARC and *P. vivax*[130]. Perhaps unsurprisingly, a number of the erythrocyte polymorphisms known to be involved in malaria resistance disrupt the expression of receptors used by *Plasmodium* for invasion. Through *ex vivo* studies conducted with blood from individuals

carrying these polymorphisms, it has been shown that Duffy negative RBCs resist *P. vivax* invasion[131]; and that reduced or absent expression of CR1[126], GYPB[132], GYPC[133,134], 4.1[134] or band 3[135] results in reduced rates of *P. falciparum* invasion. Cells which express a variant form of basigin, which has a weak affinity for PfRh5, also show reduced rates of invasion [127].

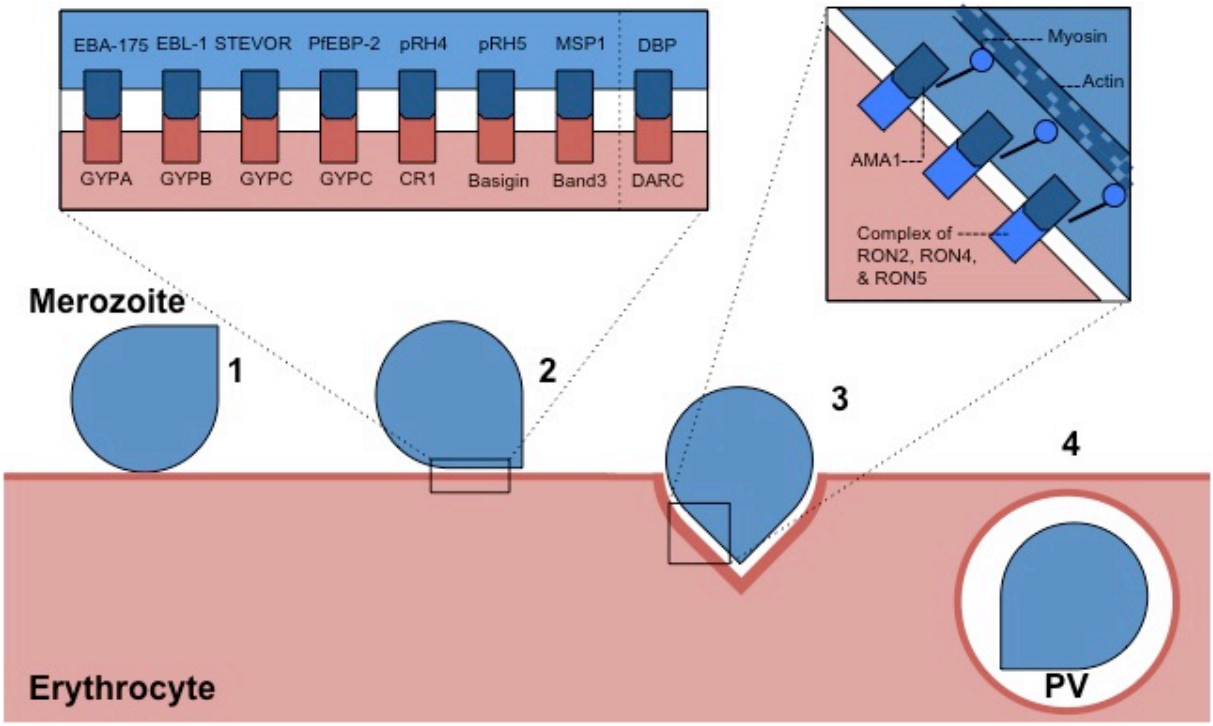

Figure 1.2. Invasion of erythrocytes by *Plasmodium*. (1) The merozoite forms a reversible attachment to the RBC. (2) It then reorients so that its apical end is facing the erythrocyte surface, and binds to various host ligands. These include Duffy antigen for *P. vivax*, and the glycophorins for *P. falciparum*. (3) Proteins are secreted by the merozoite and embedded in the erythrocyte surface. A tight junction is formed and an actin myosin motor is initiated. (4) This allows the parasite to become engulfed and enter the erythrocyte by endocytosis. Finally, the erythrocyte cytoskeleton is returned to its normal state.

One aspect of invasion that is less well understood, is how the parasite 'chooses' which cells to enter. Although *P. falciparum* invades erythrocytes of all ages, other species such as *P. vivax* (and its rodent equivalent *P. berghei*) show a clear preference for invading reticulocytes. Some of this selectivity is mediated by erythrocyte and reticulocyte binding proteins (EBL and RBL respectively)[136], however, there is increasing evidence

that the energy status of the RBC may have important implications for invasion. As early as 1969, it was noted that parasitaemia was positively correlated with the ATP concentration of RBCs [137]. More recently, it has been shown that *P. berghei* needs a functional TCA cycle to generate enough ATP to live within mature cells. In the absence of BCKDH - the *P. berghei* equivalent of pyruvate dehydrogenase - it can only survive within reticulocytes [138].

Levano-Garcia et al showed that extracellular ATP released from the RBC is an essential signal for invasion [139]. Hypothesising that ATP might have an effect on the parasite's ability to bind to RBCs, Ramalingam et al. interrogated known *Plasmodium* invasion proteins for nucleotide binding motifs. They found putative domains within all members of the RBL protein family. Further experiments determined that these domains were able to bind ATP, and that this binding produced conformational changes that exposed the erythrocyte-binding domain of the protein [140]. As it has been observed that the initial, reversible, contact between merozoite and RBC causes a wave of deformation across the erythrocyte surface [141], and it is known that membrane deformation can cause ATP release from the RBC, it has been postulated that this may form part of the parasites ability to 'sense' healthy cells to invade [136]. Although this part of the invasion process is still largely speculative, it may provide insight into the malaria resistance observed in pyruvate kinase deficient individuals. PK deficiency results in low levels of cellular ATP, and has been consistently associated with impaired merozoite invasion [142].

Growth

Once inside the red cell, the parasite occupies the unusual position of inhabiting a cell that is relatively resource scarce, separated from the nutrient rich plasma by three membranes. Therefore, *Plasmodium* must remodel the erythrocyte to facilitate the import of nutrients, and to export metabolic waste products during its rapid growth phase.

The parasite acquires most of the amino acids needed for protein synthesis, as well as clearing space for further growth, by digesting host haemoglobin (HGB). This occurs within an acidic organelle termed the digestive vacuole; other essential nutrients required by the growing parasite are imported from outside the host RBC, and to this purpose the infected erythrocyte undergoes a large increase in permeability to low molecular weight solutes. This is facilitated by a number of transport pathways,

collectively termed the NPP (new permeability pathways) [143]. The NPP allows uptake of essential nutrients, including pantothenic acid [144], and isoleucine [145], as well as the efflux of metabolic by-products such as lactate [146]. Other essential nutrients such as purine nucleosides and nucleobases are imported from the plasma, using the hosts cell's endogenous transporters, hENT1 and hFNT1 [147].

One of the problems faced by the parasite during this growth phase is the build-up of oxidative stress. The main function of RBCs is oxygen transport, and as such, they are constantly exposed to high levels of potential reactive oxygen species (ROS), to which the parasite adds by its high metabolic rate. Furthermore, haemoglobin digestion produces methaemoglobin and free haem, both of which can catalyse the production of free radicals. To protect itself from oxidative damage, the parasite converts most free heme into inert hemozoin crystals [28-30], but even a small amount of free haem can cause RBC lysis.

Although *Plasmodium* spp. have well developed redox systems (reviewed in [148,149]), they don't have catalase or glutathione peroxidase [150]. Therefore, to maintain redox equilibrium they rely heavily on reduced glutathione, thioredoxin, superoxide dismutase and peroxiredoxin [151-153]. It is therefore unsurprising that in G6PD deficiency - where levels of reduced glutathione are low - oxidative stress is postulated as the main mechanism of resistance [154]. However, this is not the only host polymorphism with a postulated link between oxidative stress and malaria resistance. Both HbS and HbC are unstable, and readily oxidise to methaemoglobin. The increased oxidative stress that this causes may impair the parasite's ability to remodel the host erythrocyte, and effectively transport virulence factors to the RBC surface, thereby providing protection to the host [155].

The oxidative stress that occurs with *Plasmodium* infection also causes changes in the RBC membrane akin to accelerated ageing and senescence, which can increase phagocytosis of infected RBCs by monocytes [156]. These changes are even more pronounced in RBCs from individuals with haemoglobin polymorphisms. Investigating this phenomenon *in vitro,* Ayi et al found that even though parasites developed normally in cells with HbS and β-thalassaemia, membrane bound hemichromes, aggregated band 3, autologous IgG binding and phagocytosis by monocytes were significantly elevated in both mutants, suggesting that they may share a common mechanism of resistance [157].

Table 1.1: Mechanisms of resistance in common erythrocyte polymorphisms

Erythrocyte polymorphisms	Invasion	Growth	Cytoadherence/ rosetting	Phagocytosis/ IgG binding	Oxidative stress	References
Sickle cell trait (HbAS)	↓	↓ or normal	↓ or normal	↑	↑	157-163
Sickle cell disease (HbSS)	Unknown	↓	↓ (low oxygen)	↑	↑	162-165
HbAC	Normal	↓	↓ or normal	↑	↑	158,162,163,166,167
HbCC	Normal	↓	↓	↑	↑	162,163,166-169
HbAE	↓	↓	Unknown	↑	↑	68,170,171
HbEE	Normal	↓	Unknown	↑	↑	68,170,171
α thalassemia	Normal	↓ or normal	↓ or normal	↑	↑	172-174
β thalassemia	↓	↓ or normal	↓	↑	↑	157,174-176
G6PD deficiency	Normal	Normal	Unknown	↑	↑	154,177
PK deficiency	↓	Normal	Unknown	↑	Unknown	142
Duffy negativity	↓ #	Unknown	Unknown	Unknown	Unknown	79,131
Blood group O	Normal	Normal	↓	Normal	Unknown	161,178,179
CR1 deficiency	↓	Unknown	↓	Unknown	Unknown	129,180
GYPA deficiency	↓	Unknown	Unknown	Unknown	Unknown	181
GYPB deficiency	↓ or normal	Unknown	Unknown	Unknown	Unknown	132
GYPC deficiency	↓	Normal	Unknown	Unknown	Unknown	133,134
Basigin deficiency	↓	Unknown	Unknown	Unknown	Unknown	127
Southeast Asian ovalocytosis (band3)	↓ or normal	Normal	↓	Unknown	Unknown	135,182,183
Hereditary elliptocytosis (α spectrin)	Normal	↓	Unknown	Unknown	Normal	182,184
Hereditary elliptocytosis (4.1)	Normal	↓	Normal	Unknown	Normal	182,185
Hereditary spherocytosis (ankyrin)	↓* or normal	↓* or normal	Unknown	Unknown	Unknown	182,186

↓ decreased, ↑ increased. All experiments are with *P. falciparum*, except where indicated as # *P. vivax,* or * *P. chabaudi.* Growth refers only to the ability of the parasite to undergo replication within the cell.

Spleen Clearance and Cytoadherence

In healthy individuals, abnormal or senescent erythrocytes are cleared from circulation by the spleen (Groom, Schmidt et al. 1991). Every 100-200 minutes, the entire RBC population passes through the splenic sinusoids [187], where the cells are forced through narrow inter-endothelial slits. Those erythrocytes that are not sufficently deformable, cannot pass through [188-191], and are retained in the red pulp, where they are expoed to macrophages for phagocytosis and recyclying. Erythrocytes with exposed phosphatidyl serine, or other stress markers will also be retained [192-194].

During malaria infection, the spleen plays a crucial role in removing parasitised erythrocytes from circulation; therefore *Plasmodium* species have developed various methods to escape splenic entrapment. *P. vivax* infected erythrocytes almost double in deformability and therefore pass easily through the spleen [195,196]. Conversely *P. falciparum* progressively increases RBC rigidity as it matures [197-200], and even the mild alterations of early ring forms can cause increased splenic retention [190,198]. Therefore, to avoid clearance, *P. falciparum* alters the adhesive properties of its host RBC, allowing it to bind to the endothelium of the microvasculature and avoid passing through the spleen during vulnerable stages of maturation [197]. The same alterations in adhesiveness also cause iRBC to bind to uninfected RBC in a process known as rosetting. Numerous host polymorphisms have been postulated to provide *P. falciparum* resistance by interrupting cytoadherence and rosetting, and therefore increasing splenic clearance. These include CR1 expression, blood group A, α-thalassaemia, HbS and HbC.

P. falciparum cytoadherence and rosetting (reviewed in [201]) are mediated largely through the parasite virulence factor *Pf*EMP1, which localises to knob-like protrusions on the RBC surface [202]. The protein is encoded by a family of roughly 60 *var* genes [203]; through its variant forms, it is able to bind at least 12 different host endothelial receptors, although most research has focused on ICAM1 and CD36 [201]. Recent research has shown that the parasite proteins STEVOR and RIFIN can also contribute to cytoadherence independent of *Pf*EMP1 [125]. These proteins are trafficked to the erythrocyte surface via Maurer's clefts; unilamellar membrane profiles located within the RBC cytosol, and anchored to the erythrocyte cytoskeleton [204]. Localisation and attachment of Maurer's clefts occurs through a network of host-derived actin filaments, which have also been associated with protein containing vesicles [155,205,206].

To form rosettes, *Pf*EMP1 binds to CR1 and Blood group A on uninfected cells. Therefore, polymorphisms resulting in reduced expression of CR1 or blood group A result in decreased rosetting [96,180,207,208]. Similarly, α thalassaemia has been shown to decrease rosetting through low expression of CR1 [96,209]. There is also evidence that HbS and HbC provide protection against malaria by disrupting the formation of actin filaments necessary for correct expression of virulence factors on the RBC surface [155,205]

Cerebral Malaria

A further complication of iRBC cytoadherence and rosetting in *P. falciparum* infections is the development of cerebral malaria (CM). CM has a mortality rate of up to 18% [66], and a great deal of research into its cause has been conducted (reviewed in [210]). Early post-mortem studies of CM patients noted an accumulation of *P. falciparum* infected RBCs within the microvasculature of the brain, therefore the cause of CM was initially postulated to be mechanical obstruction of the vessels by sequestered iRBCs [211]. Increasingly however, research suggests that CM is caused by a dynamic interaction of host and parasite factors, including iRBC sequestration, endothelial activation, breakdown of the blood brain barrier, and inflammation [212] (Figure 1.3).

Binding of iRBCs to the endothelium not only causes mechanical obstruction of the microvasculature, but is also able to contribute to pathogenic inflammation and endothelial activation. For example, some *Pf*EMP1 variants can bind to the endothelial protein C receptor (EPCR). This receptor normally binds activated protein C (APC), which in turn, exerts a cytoprotective role on the endothelium. By binding to EPCR, *Pf*EMP1 can outcompete APC, causing inflammation and the upregulation of several adhesion molecules including ICAM1 [213]. Although there are likely to be several mechanisms by which iRBC binding can cause endothelial activation, expression of the subset of *Pf*EMP1 molecules able to bind EPCR, has been associated with severe malaria in children [214]. Sequestration of iRBCs is also thought to be the major cause of placental malaria. Through specific *Pf*EMP1 variants, iRBCs adhere to Chondroitin sulfate A[215] and hyularonic acid expressed on placental syncytiotrophoblasts[216]. This results in the accumulation of parasitized red cells in the placenta, increased inflammation, and reduced blood flow to the foetus [217,218].

Alongside iRBCs, human studies have found platelets accumulated in the brains of CM patients, suggesting they also contribute to pathology [219]. *In vitro* studies have shown

that platelets help mediate iRBC clumping [220], and in mice it has been shown that inhibition of platelet binding to the brain endothelium protects against experimental cerebral malaria (ECM) [221]. Platelets also contribute to pathogenic inflammation during malaria infection [222]. However, it has been shown that platelets are able to bind to iRBCs and kill the parasites within them during the early stages of uncomplicated malaria [223], suggesting that they may have both beneficial and pathogenic roles during infection. This hypothesis is further supported by mouse studies showing that platelet depletion 24 hrs prior to infection leads to higher parasitaemia and is not survival protective, but depletion 24hrs after infection reduces ECM [224].

One of the major host processes known to contribute to the development of cerebral malaria is an over-active inflammatory response. Much of what is known about this comes from studies in mice using *P. berghei* ANKA (PbA), although there is some debate about the relevance of this model to human CM [225]. Studies with knock-out mice and *in vivo* neutralisation of host molecules have shown that cerebral malaria can be prevented by depletion of IFN-γ [226,227], TNFα [228], lymphotoxin [229], CD4+ T cells [230], and CD8+ T cells [230]. CM resistance is also observed in mice with ENU mutations in Jak3, which causes impairment in thymic development of CD8+ T cells, B cells and NK cells, and defective T cell dependent IFN-γ production [231]. Claser et al used luciferase-expressing PbA to narrow this even further; they showed that time dependent accumulation of iRBCs in the brain is mediated almost entirely by CD8+T cells and IFN-γ [232].

All of the mechanisms outlined above can result in endothelial damage, and may contribute to the eventual breakdown of the blood brain barrier (reviewed in [233]). Both adhesion of platelets[234] and iRBCs has been shown to trigger apoptosis of endothelial cells; it can also lead to endothelial activation, which reduces the expression of tight-junction proteins. Reduced blood flow caused by sequestration of leukocytes, platelets and RBCs can create an environment where glucose and oxygen are low, and toxins secreted from metabolically active parasites build-up, causing increased permeability of endothelial cells. It has also been hypothesised that IFN-γ activation of endothelial cells causes them to phagocytose parasite products, and express parasite derived epitopes on major histocompatibility complex I and II (MHC-I, and MHC-II) [235]. On recognising these epitopes, activated malaria-specific CD8+T cells attack and destroy the cells presenting them [236].

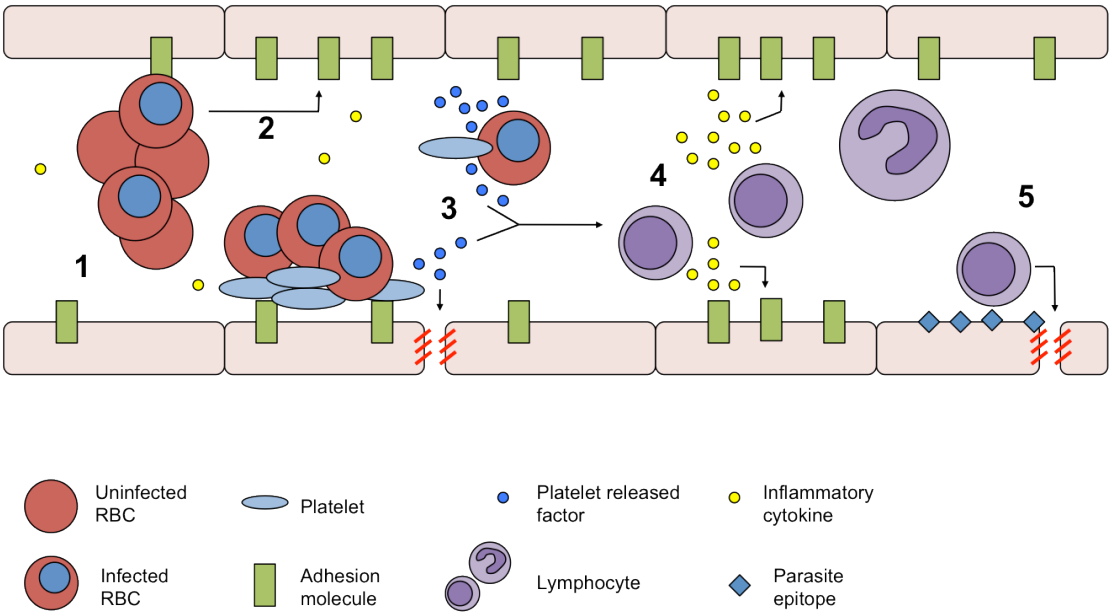

Figure 1.3: Processes involved in the development of cerebral malaria. (1) Infected RBCs form rosettes and clumps by binding to uninfected RBCs and platelets respectively. Adherence of rosettes and clumps to the vascular endothelium can cause mechanical obstruction of blood flow, resulting in tissue hypoxia. (2) Binding of iRBCs also causes endothelial activation and up-regulation of adhesion molecules, including ICAM-1. (3) Platelets are activated on binding iRBCs and release factors including PF4, which participates in parasite killing, inflammation, and T cell recruitment; and TGF-beta1, which can induce apoptosis of endothelial cells. (4) Lymphocytes are recruited to the brain microvasculature and release inflammatory cytokines, which contribute to endothelial activation and the up-regulation of adhesion molecules. Of particular importance are both CD8+ T cells, and IFN-γ. (5) Presentation of parasite-derived epitopes on MHC-I and MHC-II of activated endothelial cells marks these cells for destruction by malaria-specific CD8+ T cells. This leads to breakdown of the blood brain barrier.

It is well established that several host polymorphisms provide protection from cerebral malaria. For those affecting the production of IFN-γ, IL-4 and IL-13, resistance is easily attributed to an altered inflammatory response. For others - such as the haemoglobinopathies - the mechanism of resistance is less clear, and may be due to multiple factors. For example, the protection afforded by HbS has been variously attributed to lower levels of iRBC cytoadherence [159], impaired parasite invasion and growth [237], improved host adaptive immunity [161], improved host antioxidant response, and reduced CD8+T cell expansion [160]. Contradictions also occur when comparing *in vitro* results with those obtained from patients. For example several studies have

shown that parasites cultured in cells from HbS and HbC individuals have impaired expression of *Pf*EMP1 on the erythrocyte surface and therefore lower levels of cytoadherance [159,167]. However, a recent *ex vivo* study of Malian children found no difference in cytoadherence between parasites from HbA, HbS or HbC individuals, prompting the hypothesis that *in vivo,* parasites expressing more adhesive *Pf*EMP1 variants are selected for to compensate for lower levels of expression [158].

Gametocytogenesis

It has been estimated that any long-term control of malaria will depend, not only on treating infections, but also in blocking transmission to the mosquito. As such considerable effort has been made to understand the mechanism behind commitment to gametocytogenesis.

In vitro experiments with *P. falciparum* have shown that parasites are able to increase gametocytogenesis in response to the addition of several factors, including reticulocytes, red cell lysate, and lymphocytes [238-242]. This suggested that the parasite is able to adapt to changes in the host environment, and led to the general hypothesis that the conditions associated with late infection – high parasitaemia, dyserythropoiesis, cell lysis and anaemia – are the trigger for gametocytogenesis, and that the parasite invests in transmission as a way to escape from a hostile host environment [243]. More recent experiments have suggested that parasites default to sexual replication, and that a basal level of gametocytogenesis will occur without any specific stress signal, and even before the onset of symptoms or high parasitaemia [244-246]. The role of host genetic polymorphisms in gametocytogenesis is less well understood, but both HbS and HbC have been associated with increased gametocytogenesis and transmission in a crossectional study in Burkina Faso [247], and HbS has been associated with increased gametocyte density in asymptomatic infection [248].

Summary

During its lifecycle within humans, *Plasmodium* interacts with numerous host products and processes. Given the complexity of these interactions it is perhaps unsurprising that we still do not clearly understand how host polymorphisms provide resistance to infection. Even for those like HbS, which have been recognised for decades as host malaria resistance factors, are not fully explained. Indeed, in this case several hypotheses exist, which are not necessarily mutually exclusive. Greater understanding

of the biological processes involved in the host response to infection may provide insights into host products that could be targeted as potential new therapies for malaria.

Host-Directed Therapy

Host directed therapy (HDT) is an approach to treating disease that aims to avoid the problem of drug resistance. Rather than attacking the pathogen directly, HDT aims to render the host environment inhospitable. This is achieved by targeting a specific host protein necessary for the pathogen's survival. Because conventional therapies target processes within the pathogen, resistance can arise relatively quickly with mutations to the drug target itself, or the targeted process. HDT aims to avoid this, by acting on factors outside the pathogen's genetic control. The disadvantage of this strategy is that by acting on the host, HDTs have the potential to cause serious side effects. Nevertheless, HDT has been investigated for a variety of pathogens. Of particular interest are those that readily develop drug resistance, especially viruses [249]. Recent developments in HDT for some of these pathogens are detailed below.

Current Developments in Host-directed Therapy

Tuberculosis (TB)

There have been multiple efforts to treat tuberculosis with HDT. These include therapies against multi- and extensively drug resistant tuberculosis, known as MDR-TB and XDR-TB respectively. Targets have included the host kinase AKT1, which is necessary for the growth of *M. tuberculosis* within human macrophages [250], host proteases called MMPs, which contribute to the transmission of tuberculosis [251], and the host phosphodiesterase Pde3 [252]. Inhibitors of each of these targets have had success in preventing bacterial growth, and shortening the time taken to clear infection. More recently, Stanley et al, used a screen of small molecules to identify host products important for *M. tuberculosis* growth. Through this screen they identified host EGFR as a potential target, and were able to use the inhibitor gefitinib to prevent bacterial replication in mice [253]. Mayer-barber et al. showed that IL-1 is able to confer host resistance to TB, through the induction of eicosanoids. By using drugs to augment host prostaglandin E2 levels, they were able to increase the survival of infected mice [254].

Human immunodeficiency virus (HIV)

HIV binds to two receptors to invade host cells; CD4 and as well as either CXCR4 or CCR5. The virus that uses the CCR5 receptor is more common, and is found in 80% of patients [255]. Efforts to develop an HIV HDT have focused on the CCR5 receptor, and several antagonists have been developed. The most successful of these has been Maraviroc, which was approved for use by the US food and drug administration in 2007 [256]. Despite its success as an HDT [255], in some patients HIV has rapidly acquired resistance to Maraviroc. Although this process is not completely understood, it appears to have occurred through two mechanisms. The first is due to the fact that *in vivo*, infections will often contain both CCR5 and CXCR4 tropic viruses; resistance in these instances results from selection of the CXCR4 virus. The second mechanism relies on the virus evolving the ability to use inhibitor-bound CCR5 for invasion [256-258].

Myxoviruses

The myxoviruses are a group of enveloped, negative-strand RNA viruses that are transmitted through the respiratory route; they include influenza, mumps virus and measles virus [259]. In recent years a number of bioinformatics studies have identified several host factors essential for the replication of influenza within the host, with the aim of developing effective HDT for the virus [260,261]. Krumm et al. mined data from a large scale high-throughput chemical screen to find potential host-directed candidates for the treatment of Myxoviruses. The lead compound they identified, JMN3-003, was able to prevent the growth of measles virus in a manner consistent with a compound acting on the host, rather than the virus. They then tested the ability of the virus to develop resistance to JMN3-003. In their study, conventional therapies showed development of resistance within 20 days; JMN3-003 was still effective after 90 days [259], supporting the hypothesis that HDTs are able to avoid the development of pathogen resistance.

Malaria

Host directed therapies for malaria have also been tried by targeting two pathways within the RBC that are used by the parasite. Sicard et al found that *P. falciparum* activates the PAK-MEK kinase pathway of erythrocytes. The parasite does not have orthologues of either PAK or MEK, but rather activates the host enzymes even during ring stage development. Pharmacological inhibition of these two proteins was able to kill blood stage parasites both *in vitro* and *in vivo*, as well as liver stage parasites *in*

vitro [262]. Similarly, Smith et al. discovered that host ferrochelatase (FECH) is required for *P. falciparum* growth; significant growth inhibition was seen when parasites were cultured in the cells of FECH deficient individuals. Pharmacological inhibition of host FECH was also able to kill parasites *in vitro* [263].

ENU Mutagenesis and the Identification of New Host-directed Therapy Targets

In order to design an effective host-directed therapy for malaria, a greater understanding of the genes involved in the host response to malaria will be needed. Most of the polymorphisms outlined above were discovered because they are associated with a disease state; an ideal HDT would not target products that are going to cause such deleterious side effects. It has been estimated that our current understanding accounts for only a fraction of the total number of polymorphisms involved in malarial resistance [264]. Therefore, a number of strategies have been employed to identify more.

One such strategy has been to conduct genome wide linkage (GWL) and association studies (GWAS) in African populations. Unfortunately, these studies have had limited success due to high levels of genetic diversity between ethnic groups - even those inhabiting the same geographical location [265]. Such genetic stratification increases the risk of false positive associations, and necessitates the use of vastly more SNPs than comparable European studies [264]. Nevertheless, GWAS have found associations between malaria susceptibility and ATP2B4, an erythrocyte calcium pump; MARVELD3, a tight junction protein; and the transcription factor FOXO3A [113,266]. GWL have uncovered associations between several loci and clinical outcome. These include malarial fever episodes (10p15.3–10p14), clinical *P. falciparum* attacks (5p15-p13 and 13q13-q2), maximum parasite density (12q21-q23), and asymptomatic infection (5q31) (Timmann, Evans et al. 2007, Sakuntabhai, Ndiaye et al. 2008). However, due to the large number of genes within these loci, polymorphisms responsible for the associated phenotypes have not yet been identified.

Another method that has been used to identify genes associated with malaria resistance is to investigate the host response to infection in mice. The rodent parasites *P. chabaudi* and *P. berghei* are commonly used, and provide reasonable models for blood stage *P. falciparum* and cerebral malaria respectively. Through the creation of various congenic lines (crosses between naturally resistant and naturally susceptible mouse strains) several loci involved in resistance to both *P. chabaudi* [267-271] and *P. berghei* [272-275]

have been discovered. However, these crosses are restricted by the small number of strains available, and the low spontaneous mutation rate of mice [276]. This has lead mouse geneticists to search for mutagens that can efficiently generate novel mutations. One of these is N-ethyl-N-nitrosurea, commonly known as ENU. It was initially discovered in 1951 by William Russel at the Oak Ridge National laboratory in Tennessee, and has been widely used in genetic studies since 1970 [276].

ENU mutagenesis

ENU is an alkylating agent; it transfers its ethyl group to nucleic acids. During DNA replication, these changes cause mispairing of bases, most commonly A to T transversions and A to G transitions [277,278]. These point mutations may cause gain of function, or loss of function of a gene. The majority of ENU induced mutations that cause a detectable phenotype are missense mutations, but they may also introduce premature termination codons, splicing errors or perturb gene expression control elements [278]. The number of mutations will depend on the dose of ENU, but typically they occur randomly every 2 megabases, resulting in approximately one exonic mutation per chromosome [277].

In a standard ENU screen, male mice are treated with ENU, which targets the spermatogonial stem cells [279]. Mutagenized mice will then be crossed with untreated females, and the progeny screened for the phenotype of interest. ENU screens have been structured to identify both dominant mutations and recessive mutations. They have also been established to identify genes that predispose individuals for particular conditions [280]. To date, ENU has been used to investigate processes as varied as male infertility [281], craniofacial development [282], skeletal morphology [283], lung disease [284], and the host response to infection [285-288]. The advantage of ENU mutagenesis is that it does not rely on a priori knowledge of mechanisms and genes controlling a given phenotype. Rather, it enables an unbiased interrogation of the entire genome for genes affecting the trait of interest [276,277]. Moreover, by disrupting gene function, ENU creates a phenotype that could be recreated with a small compound or drug. Currently, the Foote lab is using ENU mutagenesis to find targets for malaria host directed therapy.

The ENU Mutagenesis Screen for Malaria Resistance Mutations in Mice

This project is derived from an ENU screen established by Pr Simon Foote, A/Pr Brendan McMorran, and Dr Gaetan Burgio, to search for novel genes involved in resistance to malaria. In this screen, male *P. chabaudi* susceptible SJL/J mice are treated

with ENU and crossed with untreated SJL/J. The resulting G1 are then screened for RBC abnormalities and increased survival to *P. chabaudi* infection. Screening for RBC abnormalities is relatively simple and utilised a haematological analyser to determine red cell measures such as cell number, cell size and haemoglobin content. Since the blood stage replication of *Plasmodium* occurs within the erythrocyte, it was reasonable to assume that mutations affecting the RBC may also impact on the susceptibility. Screening for survival to *P. chabaudi* infection, while more time consuming, can identify mutations that are completely unrelated to the RBC, which may implicate pathways previously unknown to affect the host response to infection. G1 mice displaying either a blood or survival phenotype of interest are crossed again to SJL/J, and the resulting progeny (G2) are tested to determine the presence of a true heritable mutation (Figure 1.4). To date, the screen has identified over 90 lines – both RBC mutants and survival mutants – that show positive progeny testing of G2.

ENU mutagenesis screens using RBC parameters, and screens using malaria survival as their phenotype of interest, have previously had success in identifying novel genes involved in malaria resistance. Some examples are detailed below.

RBC screen

Investigating the host response to *Plasmodium chabaudi*, the Foote lab set up a dominant ENU screen in order to identify mutations that affect the RBC. The mutant MRI23420 was identified due to an MCV over two standard deviations below average. The cause of this microcytosis was found to be an A-T transversion causing a premature stop codon within exon 11 of *Ank-1*. When infected with *P. chabaudi*, mice heterozygous for the MRI23420 mutation were found to be significantly resistant to infection, with survival rates increased from 10% in WT females to 94% in mutant females. This mutation was found to affect not only the ability of the parasite to invade RBCs, but also to grow within them [186].

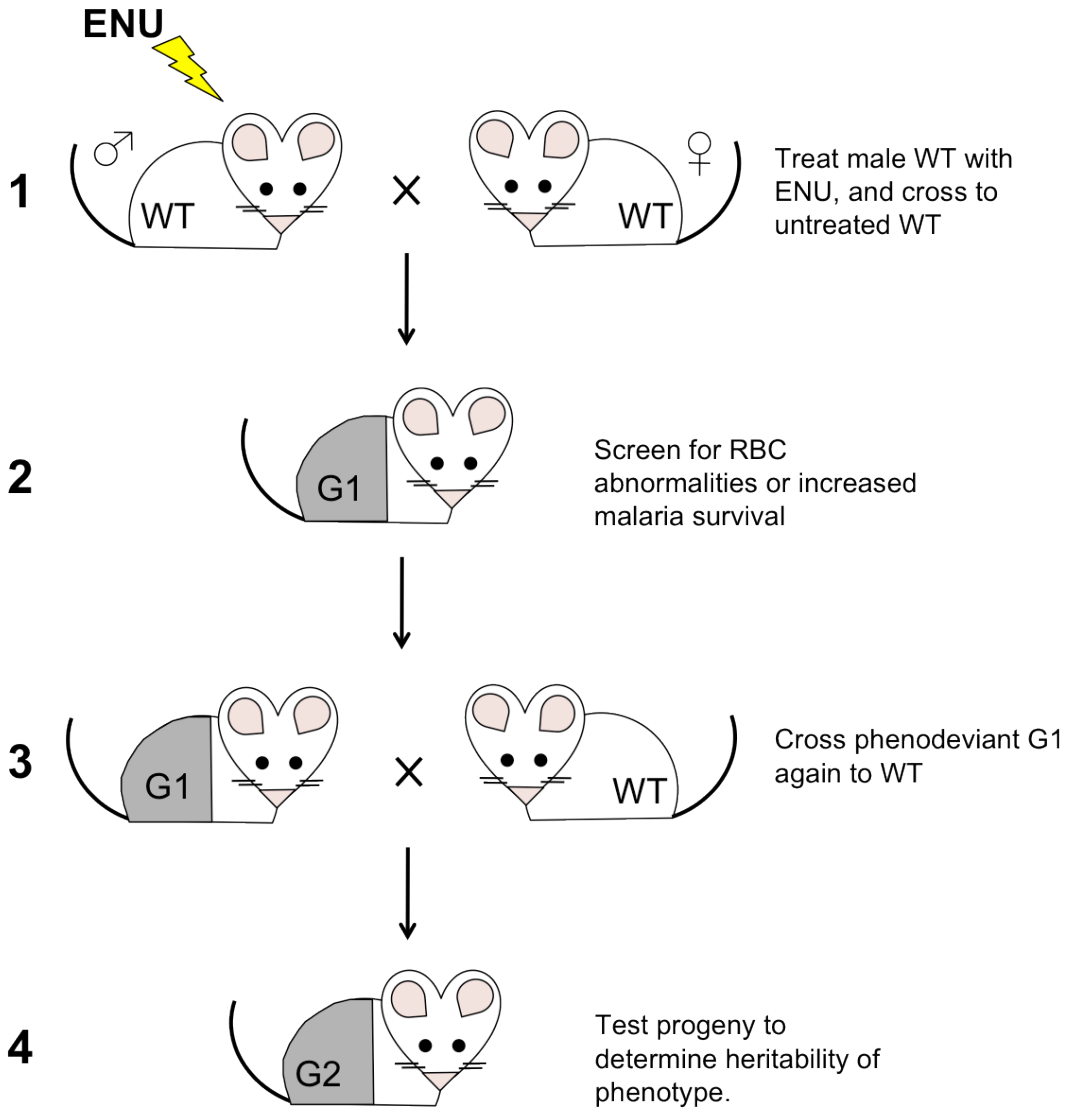

Figure 1.4: Breeding scheme for dominant ENU RBC screen (1) Male SJL/J mice are treated with ENU and crossed to untreated female SJL/J. (2) Resulting G1s are screened for abnormal blood parameters. (3) G1s displaying a blood parameter of interest are crossed again to SJl/J. (4) Resulting G2s are screened for abnormal blood parameters; if the parental G1 phenotype is caused by a heritable mutation, ~50% of these mice should display the same blood phenotype. A colony is then maintained by crossing G2xG2 or G2xSJL/J.

Malaria survival screen

Investigating the host response to cerebral malaria (CM), the Phillippe Gros lab at McGill University set up an ENU screen in order to identify recessive mutations affecting the response to *P. berghei*. By infecting the progeny of mutagenized C57BL/6J and C56BL/10J mice with a lethal dose of the parasite, and selecting those mutants that failed to develop cerebral symptoms, they have identified genes involved in the pathogenesis of CM. For example, they showed that a mutation in *Jak3* prevented 35% of mice from developing cerebral symptoms. The W81R amino acid substitution at the N-terminus of the protein disrupts the interaction of Jak3 with various cytokine receptors on immune cells, and therefore impairs the CD8+ T cell response to *P. berghei* infection [231]. Mutation in a second gene, *Ccdc88b*, was also found to increase survival. A cryptic splice site, resulting in a frame-shift and therefore premature stop-codon, increased survival to 40% in heterozygotes and 80% homozygotes. Resistance was caused by defective T cell maturation and activation, and impaired production of IFN-γ and TNF-α [289].

Previous Work on ENU Mutagenesis

This project was conducted as part of the ongoing ENU mutagenesis screen described above. The mutant MRI49372 was investigated; it was initially identified because it displayed the abnormal blood phenotype of MCV over two standard deviations above WT SJL/J. This project also investigated a mutant line RBC10, which was identified through a dominant ENU mutagenesis screen conducted by Pr Benjamin Kile, Pr Stephen Jane and A/Pr David Curtis. In this screen, male C57BL/6 mice are treated with ENU and crossed with untreated C57BL/6. The resulting G1 are examined for abnormal blood phenotype, and phenodeviants crossed again to C57BL/6 to determine the presence of a true heritable mutation. The mutant RBC10 was initially identified because it displayed MCV over three standard deviations below WT C57BL/6. The two mutants investigated in this thesis are summarised in Table 2.

Table 1.2: Mutant strains investigated in this thesis

Mutant strain	Selected for	MCV			Chapter
		G1	Affected G2	Normal G2	
MRI49372	Abnormal blood phenotype	58.4	59.7±0.5	54.4±0.5	3 & 4
RBC10	Abnormal blood phenotype	39.0	39.2±0.7	44.5±0.8	5

MCV=mean corpuscular volume.

Major Goals of the Thesis

The aim of this work was to investigate the host response to malaria infection, with the view to finding potential new targets for host directed therapy. The major goals were as follows:

1: Identify novel genes associated with malaria resistance

Mice with abnormal blood parameters that had been identified in the ENU screens described above, were challenged with *Plasmodium chabaudi* to identify lines that were resistant to malaria. A combination of linkage analysis and next generation sequencing, was used to discover the ENU induced mutation responsible for that resistance, and therefore the gene mediating an altered response to malaria.

2. Determine the biological mechanism of malaria resistance

Once a gene was identified, the way that gene (and the ENU mutation) mediated the observed blood phenotype and resistance to malaria was identified. In uninfected animals, protein expression, erythroblast production, and other indices relevant to the particular ENU mutation were investigated, to determine the cause of the blood phenotype. In infected animals the kinetics of infection were investigated to elucidate the mechanism of resistance.

CHAPTER 2 - EXPERIMENTAL PROCEDURES

Mouse Husbandry and Ethics

Mouse husbandry was conducted under a continuously controlled specific pathogen-free (SPF) hygiene standard according the NHMRC guidelines. Mice were housed under controlled temerature (21°C) with a 12:12hr light-dark cycle. All animal experiments were conducted with the authorisation of, and in accordance with the policies of, the University of Tasmania Animal ethics committee (A0010470), and the Macquarie University animal ethics committee (ARA2012/019).

ENU Mutagenesis

Seven-week-old SJL/J male mice were injected IP with 150 mg/kg of ENU at 1 week intervals. Mutagenized G0 mice were then crossed with the background SJL/J. G1s were bled at seven weeks, for haematological analysis. The G1 49372 was identified due to MCV three standard deviations higher than average. 49372 was then crossed with SJL/J and the resulting G2s used for further experiments. N2 mice were generated by first crossing 49372 with C57BL/6 to create F1. Haematological analysis was then conducted on the F1 mice, and those with high MCV (>56fL) were selected for further breeding. High MCV F1 were crossed again to C57BL/6 to produce N2s. Haematological analysis was also conducted on the N2 mice, and those with high MCV were selected for use in genotyping experiments.

Breeding RBC10

RBC10 mice were on a mixed BALB/c C57BL/6 background. For experiments, WT x WT and Kcc1$^{M935K/M935K}$ x Kcc1$^{M935K/M935K}$ breeding pairs were maintained. To exclude the possibility that the resistance phenotype was due to the mixed background, and carried by chance in mutant breeding pairs, Kcc1^{M935K} was periodically crossed back to WT, and new WT x WT and Kcc1$^{M935K/M935K}$ x Kcc1$^{M935K/M935K}$ pairs established from the progeny.

Whole-exome Sequencing

DNA was extracted from the ear tissue of 2 phenodeviant MRI49372. DNA was extracted using a Qiagen DNeasy extraction kit following the manufacturer's protocol. 10µg of DNA was prepared for paired-end genomic libraries using a paired-end preparation kit from Illumina, following the manufacturer's instructions. Exome enrichment was

performed using an Agilent Sure select mouse exome kit according to the manufacturer's protocol. Enriched libraries were tested for enrichment using quantitative PCR. The samples were then sequenced on an Illumina Hiseq 2000 platform, which generated paired-end reads of 100 nucleotides. The libraries were multiplexed and barcoded. The exome coverage was 50x on target.

Sequencing alignment and variant detection pipeline

Sequencing alignment and variant detection was performed by Dr Denis Bauer (CSIRO). Genomes of offspring were grouped by founder, and the identified mutations compared to those from other founder-groups previously sequenced. Only investigating mutations that occur in all offspring from one founder (complete) and not in those from other founders (exclusive) will robustly separate segregating ENU-triggered mutations from strain-specific variants or sequencing errors. The subsequent section describes the mapping, variant-calling, and filtering process. Where not stated otherwise, the default settings were used.

Calling mutations from raw sequencing data (fastq) combines the result from four separate mapping and variant calling pipelines (P1-P4), which make use of different combinations of mappers and variant callers to avoid the loss of variants due to algorithm bias and were triggered with NGSANE [290]. P1 and P2 uses Burrow-Wheeler Aligner (BWA V0.6.1) [291] and BOWTIE2 V2.1.0 [292] to the mouse genome reference sequence (GRCm38 or mm10) in conjunction with SAMTOOLS V0.1.19 [293] to call variants (mpileup -q1 -D) in each of the offspring groups individually after removal of duplicates (rmdup) and subsequent filtering. P3 and P4 also map with BWA, but in addition use GATK 2.5 [294] to realign reads and recalibrate the quality score to improve the read location and base-pair call-accuracy. While P3 again uses SAMTOOLS, P4 uses GATK's UnifiedGenotyper with subsequent hard filtering of variants to call variants over all mouse genomes in the study simultaneously. In all cases, reads were mapped against Genome Reference Consortium Mouse Build 38 (equivalent to UCSC mm10). The known mouse variants used during realignment, recalibration and GATK variant calling were downloaded from UCSC (dbSNPv128, mm9) and lifted over to mm10. Only variants in the targeted regions as provided by Agilent (lifted over from mm9) were considered.

After variants are available from P1-P4 the information from all founder-groups is combined using GATK and annotated using GATK with dbSNPv128 and variants from

Sanger's The Mouse Genomes Project (lifted over from mm9). Then, only complete and exclusive variants that have not been annotated previously are retained (dbSNP, Sanger) using in-house python scripts. These scripts also filter out variants that are only supported by one method (P1-P4) well as specific genotypes (homo- or heterozygous mutation), that can be ruled out based on prior genetic information.

The resulting high-confidence variants are then functionally annotated using ANNOVAR [295] (Ensembl, MGI, dbSNP137, phastConsElements60way).

CRISPR/Cas9

CRISPR (Clustered Regularly Interspaced Short Palindromic Repeats) is a microbial nuclease system involved in defence against invading phages and plasmids. CRISPRs together with Cas (CRISPR-associated) proteins recognise and cut exogenous DNA in a manner analogous to RNAi in eukaryotic organisms. This nuclease system has recently been harnessed to facilitate genome editing [296]; delivery of the bacterial Cas9 nuclease along with appropriate guide RNAs, allows that cell's genome to be cut at any desired location.

For CRISPR/Cas9 genome editing to knock-out WNK3, guide RNA was designed to target the start codon of this gene.

GACTGAAGAGTGAAACAAGAACAAATTTAGTGCCAACCTTAGTTACAATGGCCACTGATTCT
GGGGAGCCAGCTAGCACAGAAGATTCTGAGAAGCCTGATGGAGTTTCCTTTGAAAACAGGGC
TGCCCGGGCTGTTGCCCCTCTGACTGTAGAAG

gRNA: GTTACAATGGCCACTGATTCTG

Green highlighting shows the position of the gRNA. Underlined letters show the position of the start codon. The guide RNA was cloned into a Px461 plasmid encoding for a Cas9-D10 according to the published protocol [297].

Embryo donor mice were first primed with Pregnant Mare Serum Gonadotrophin (PMSG) and Human chorionic Gonadotrophin (hCG) to induce superovulation. Female C57BL/6 mice were injected IP with 5 IU PMSG. 46-48 hours later they were injected IP

with 5 IU hCG, and placed immediately with a fertile stud male. Embryos were collected at day 0.5 post conception.

5 ng/µl of modified Px461 plasmid was injected into the pronucleus of the zygotes in two different injection sessions and transferred into psuedopregnant females. Resulting pups were genotyped and positives pups for WNK were bred for germline transmission. The following primers were used for genotyping:

WNK_X1_F: GACTGAAGAGTGAAACAAGAACAAA
WNK_X1_R: GATGTTTTCCCCGGAAGC

Haematological Analysis

Peripheral blood was collected by mandibular bleed into an EDTA lined tube. Complete blood counts were obtained using an ADVIA® 2120 haematology system (Bayer HealthCare, NY, USA) using the CBC/DIFF/RETIC settings, species Mouse C57BL/6. Samples were diluted 1:1 with MT-PBS.

Genotyping

DNA was extracted from 0.4 cm sections of tail using a DNEasy kit (Qiagen) to the maker's instructions.

Primers pairs:

Amplicon	Forward	Reverse
Cpeb1	gccttgggaggagtactgtg	caggaaggggtcagatggta
Pde3b	catggtgtggacagcacatt	gtgagaactgccagggtagc
Ampd3	cattgtaggccctcagtgct	catggtgacctcacaaggttt
Trim34a	aagaggcagctgtgacttcaa	gaggtaagaaagggtggtataagaa
Mgam	ggagtggggtgggtaagagt	tttgctatgaaaatgagatgtttt
Ptpn4	cagtgctacatgtgtgtgcat	cccagcaagtgttgttcttaac
Dhrs7	gtggcacctgtgaagactcc	tgctgacaacctttgatttga
Gpr98	tgagccttatctggttgaaaa	ccacgacgtcatccagaag
Atp13a4	atcccatttagagctgagca	aaaggattgaagggaattaacac
Kcc1	ccaccaatcatgcatcctg	ccaccaagcctagtcctgaa
rs32156288	gcctttcaaggcagctagtc	tgatactttaacatccttctcatgc

rs36514000	tccttagccacacgagttcc	gatggagcaagggacagatg
rs32613342	actgaagttaggtgccaagc	gggtccccagaaactgaga
rs225043648	gctcaacccaatttggaaac	agtgttctccaagggctgaa

GoTaq® DNA polymerase was used for all PCR reactions (Promega Corporation, Wisconsin, USA), which were conducted under the following conditions:

Stage	Temp (°C)	Time (m:ss)
Hold	50	5:00
	95	0:30
Cycle x 35	58	0:30
	72	0:30
Hold	72	5:00

PCR product was purified using either a Wizard SV PCR Clean-Up Kit (Promega) according to the manufacturer's instructions

OR

by ExoSap enzymatic digestion. Briefly, 0.025ul Exonuclease 1 and 0.25µl Shrimp alkaline phosphatase (New England Biolabs) were added to 9µl H_2O and 25µl PCR product. Samples were then incubated at 37°C for 30 minutes, then heated to 95°C for 5 minutes.

Purified PCR product was sequenced at the Australian Genome Research Facility (AGRF) in Melbourne, and analysed using Codoncode Aligner (Codoncode Corporation, Massachusetts, USA).

MACS Separation of Mature RBCs

Whole blood from MRI49372 mice was collected by mandibular bleed and pooled (~450µl), centrifuged at 1500xg for 5 minutes and the plasma and buffy coat were removed. Blood was then washed in MACS buffer. Cells were stained with 5µl CD71-FITC in 1ml MACS buffer, for 45 minutes at 4°C, with constant mixing. Cells were washed three times, and resuspended in 400µl MACS buffer with 80µl anti-FITC magnetic beads (Miltenyi Biotech, Germany), and incubated at 4°C for a further 15 minutes with constant mixing. Cells were then washed once, and loaded onto a primed LS MACS separation column (Miltenyi Biotech, Germany). The negative fraction was collected and

analysed by flow cytometry to check the purity. Samples with <1% FITC+ events were used for further experiments.

Western Blots

For Western blotting, whole blood, MACS sorted CD71- RBCs, or erythroblasts from E14 livers were lysed using MT-PBS containing 1% TritonX, and complete Protease Inhibitor Cocktail (Roche, Basel, Switzerland). Protein concentration was determined by BCA assay (Thermo Fisher Scientific), and 10µg of each sample was separated by non-denaturing SDS-PAGE [298] using 8% gradient gels. Lysates were not heated to 95°C prior to SDS-PAGE. For immunoblotting, samples were transferred to nitrocellulose membranes using an iBlot® Dry Blotting System (Life Technologies) using the default P3 setting. The membrane was then incubated with either mouse monoclonal ACTB (Abcam, NSW), or rabbit polyclonal AMPD3 (Abcam, NSW). Membranes were then washed extensively prior to incubation with peroxidase-conjugated secondary antibodies. After further washes, the blots were visualized using enhanced chemiluminescence reagents (Amersham Biosciences, Piscataway, NJ).

Real-time PCR

RNA was extracted from WT and MRI49372 E14 livers using RNeasy columns (Qiagen, Limburg, Netherlands) to the maker's instructions. CDNA was synthesised using a Transcriptor High Fidelity cDNA Synthesis kit (Roche, Basel, Switzerland) to the maker's instructions. PCR was conducted using an *Ampd3* TaqMan® Gene Expression assay, according to the manufacturer's instructions. Briefly, 1ul TaqMan® Gene Expression assay probe was added to 10ul TaqMan® Gene Expression Master Mix, and 100ng CDNA. RNAse free water was added to make the reaction volume up to 20ul. PCR reaction was conducted on an Applied Biosystems ViiA™ 7 Real-Time PCR System, using standard conditions:

Stage	Temp (°C)	Time (mm:ss)
Hold	50	2:00
Hold	95	10:00
Cycle x 40	95	0:15
	60	1:00

Purine Analysis

Steady State

Blood was collected either by mandibular bleed or cardiac puncture and placed immediately in EDTA lined tubes on ice. Blood from WT, Heterozygous and Homozygous mice was pooled, centrifuged at 1000xg for 5 minutes, and the plasma and buffy coat were removed. Cells were stained with CD71-FITC, and depleted of CD71+ cells using MACS separation columns. Cells were then washed again in ice cold PBS. 20µl aliquots of packed cells were snap frozen, then sent to Metabolomics Australia analysis.

Labelled AMP

MACS-separated mature RBCs were incubated at 37°C, 50% hematocrit in HBSS, containing either 0.002M AMP or 0.002M13C15N-AMP. Samples were taken at T=0, T=1, and T=2hrs, and washed in MT-PBS. 20µl aliquots of packed cells were snap frozen, then sent to Metabolomics Australia analysis.

Labelled GTP

Human erythrocytes were incubated at 37°C, 10% hematocrit in CCM, containing 5mg/ml 13C-GTP. Samples were taken at T=0, T=2 and T=4hrs, and washed in CCM wash. 20µl aliquots of packed cells were snap frozen, then sent to Metabolomics Australia analysis.

Metabolomics Analysis

On receipt of the RBC aliquots at Metabolomics Australia ten times the volume of ice cold extraction solution (Acetonitrile/Water (80:20) containing 10µM 13C-sorbitol, 13C,15N-Valine, 13C,15N-AMP and 13C,15N-UMP (internal standards)) was added to the RBCs to quench and lyse the cells. RBC extracts were scraped (10-times) and sonicated (2mins) to ensure homogenous mixing and lysis. Extracts were then centrifuged at maximum speed for 10mins at 4°C to remove any cell debris. Cell lysate (supernatant) was transferred to glass HPLC vials containing small volume glass inserts and capped to prevent any volume change. Pooled biological quality control (pbQC) samples were prepared by pooling 20µl of all lysate samples into a fresh glass insert. The samples were stored in the autosampler, which was maintained at a temperature of 4°C, in preparation for LCMS analysis.

An untargeted metabolome-wide analysis was performed on LC-MS. LC analysis was performed on an Agilent HPLC system (Agilent 1260) using a ZIC®-pHILIC column (column ID = 4.6mm (Merck SeQuant®)) with a 40 minute gradient containing a 5min washout and 5 min equilibration. Buffer A: 20mM ammonium carbonate pH 9, Buffer B: acetonitrile. The elution gradient consisted of a starting composition of 80% B and this decreased to 20% B in 30 mins followed by a column wash out at 5% B for 5mins and finally re-equlibrating the column at 80% B for 5mins (to prevent sample carry over). Sample volumes of 20 µL were injected onto the column, which was maintained at 25 °C, at a flow rate of 300 µL/min.

The LC system was directly connected to a ESI source (on an Agilent 6520 Accurate Mass QTOF MS) and ionization performed with a capillary voltage of 3.5kV, drying gas flow of 9.0 L/min (N_2) and temperature of 325°C, nebulizer pressure of 35 psi, fragmentor and skimmer cap voltage of -175V and -65V, respectively. Ions were analyzed in negative mode with a full scan range of 25 to 1200 *m/z* at a rate of 0.9 spectra/sec.

Mass calibration was performed for the negative polarity before analysis using the standard Agilent mass calibration solution. To ensure accurate mass and correct for instrumental mass drift over the span of the run an Agilent reference ion solution for internal mass calibration was continuously sprayed into the ESI at a flow rate of 0.2ml/min. The reference ion solution contained purine (119.036320) and hexakis(1H,1H,3H-tetrafluoropropoxy)phosphazine (981.99509).

Samples were run in a randomised order, with a pbQC every 5-10 samples to monitor instrument reproducibility. To aid identification and quantification of the nucleotides being investigated, calibration standard solutions ranging in concentration (100, 40, 10, 2, 0.4 and 0.1 µM) were prepared and analysed with each batch. Standard Mix 1 contained ADP, Cytidine, CDP, GTP, Uridine and UDP. Standard Mix 2 contained Adenosine, ATP, CTP, Guanosine, GDP and UTP. Standard Mix 3 contained AMP, CMP, GMP and UMP. The retention time, mass and peak shape were used for identification and the peak area was utilised to determine relative amounts of the metabolites in the samples.

Erythroblast Precursor Analysis

Bone marrow was collected from the femur of mutant and WT mice, and passed through a 70µm BD Falcon Cell Strainer with 0.5ml of MT-FACS buffer. $1x10^6$ cells from each sample were resuspended in 100µl MT-FACS buffer, and stained with 0.5µl FC block for 15 minutes at 4°C. Cells were then further stained with 1µl of TER119-FITC and 1µl CD44-APC for 1hr at RT. Cells were then washed twice and resuspended in 500µl MT-FACS buffer. Stained cells were analysed on a BD FACSARIA™™-II flow cytometer, recording 10,000 events per sample. Populations were gated as described in [299].

Plasma EPO

Blood was collected from adult uninfected WT and mutant mice, centrifuged at 11,000x g for 5 minutes, and plasma collected. A Quantikine Mouse/Rat Immunoassay (R & D Systems, Minneapolis) was used to measure the concentration of erythopoietin (EPO) according to the manufacturer's instructions.

Biotin Half-life

RBC half-life was determined by *in vivo* biotinylation. Mice were injected IV with 1mg of NHS-biotin-ester (Pierce Scientific) dissolved in saline. At selected time-points post injection a drop of blood (2µl) was collected by tail snip, stained with Ter119-APC and Streptavidin-PE analysed via flow cytometry.

Total Bilirubin

Plasma bilirubin was measured using TBIL strips on the VetTest® Chemistry Analyzer (IDEXX Laboratories). Blood from mutant and WT mice was collected either by cardiac puncture or mandibular bleed, and centrifuged at 11,000xg for 5 minutes. Plasma was collected and either analysed immediately, or stored at -20°C until analysis.

Lysis in Culture

10µl of blood from WT and mutant mice was added to 1ml mouse culture media, and incubated at 37°C for 24 hrs. Samples were centrifuged at 500 x g for 5 minutes, and 200µl supernatant were collected for analysis by absorbance at 595nm. %lysis was calculated by comparison to samples that were completely lysed by freeze/thawing.

Histology

Wright Giemsa

Thin smears were fixed for 1 minute in 100% methanol, air dried and stained for 30 seconds in Wright-Giemsa Modified stain (Sigma). Stained smears were then placed in deionized water for 10 minutes without agitation, before being washed briefly and allowed to air dry.

Giemsa

Thin smears were fixed for 1 minute in 100% methanol, air-dried and stained for 10 minutes in 10% giemsa solution. Stained smears were then washed and allowed to air dry.

Perl's Prussian Blue

Spleens from uninfected WT and Ampd3$^{T689A/T689A}$ mice were collected and fixed in 10% formalin for 24hrs, dehydrated on a Leica ASP200 S Tissue Processor (Leica Microsystems), and embedded in paraffin wax. 5μM sections were fixed to glass slides and stained with Perl's Prussian Blue.

Hematoxylin and Eosin

Spleens from both uninfected and infected WT and Kcc1$^{M935K/M935K}$ were collected and fixed in 100% ethanol. Samples were then sent to the Australian Phenomics Network for hematoxylin and eosin staining and analysis.

Non-haem Iron

Liver and spleen tissue were dissected from uninfected animals. Between 50 and 100mg of each tissue was dried at 45°C for 48 hours and then placed in a 10% hydrochloric acid / 10% trichloroacetic acid solution to digest for 48 hours at 65°C. Samples were then centrifuged at 13000rpm for five minutes. 200μl of supernatant was then added to 1ml of 1,10-Phenanthroline monohydrate solution (Sigma-Aldrich) and incubated for 15 minutes at room temperature. After incubation, 300μl of sample was transferred to a flat bottom plate (Corning®) and absorbance measured at 508nm. All samples were analysed in duplicate.

Osmotic Fragility

Blood was collected from mutant and WT mice by mandibular bleed, and incubated 1:100 in NaCl solutions ranging from 0 to 160mmol in concentration. After 30 minutes at 37°C, Samples were centrifuged at 500xg for 5 minutes. 100µl of supernatant was collected and its absorbance measured at 545nm. Percentage lysis was calculated by assuming 100% lysis at 0mmol NaCl.

Phenylhydrazine Challenge

Acute hemolysis was achieved by IP injection of 60mg/kg Phenylhydrazine on two consecutive days. On days 1 to 7 post the second injection, 2µl blood was collected by tail snip, washed and centrifuged at 500xg for 5 minutes. Cells were then stained with 0.5µlFC block in 100ul MT-FACS for 15 minutes at 4°C. 1µl TER119-FITC and 1µl CD71-APC, were then added, and cells were incubated for 40 minutes at room temperature. Cells were then centrifuged at 500xg for 5 minutes, and resuspended in 300µl MT-FACS containing counting beads at a concentration of 108 beads/µl. Samples were analysed by flow cytometry on a BD FACSAria™ II. 100000 events were recorded per sample, and the number of TER119+ and CD71+ cells calculated per bead.

Eryptosis Markers

PS exposure/Annexin binding

2µl of RBC pellet were added to 100µl Annexin Binding Buffer (150mM NaCl, 10mM HEPES and 2.5mM $CaCl_2$) containing 5µl Annexin V-FITC (Invitrogen, NY, USA), and incubated at room temperature for 20 minutes in the dark. Volume was then increased to 500µl with Annexin Binding Buffer, cells were put on ice, and analysed by flow cytometry. 10,000 events were captured on a BD FACSAria™ II, and the percentage of FITC positive cells calculated.

Reactive oxygen species (ROS)

2µl of RBC pellet were added to 500µl RPMI containing 2µg/ml H2DCFDA (Invitrogen, NY, USA) and incubated at 37°C for 20 minutes. Cells were then centrifuged at 500xg for 5 minutes, resuspended in 500µl MT-FACS, put on ice, and analysed by flow cytometry. 10,000 events were captured on a BD FACSAria™ II. ROS content was calculated by mean FITC flourescnece.

Intracellular Calcium

2µl of RBC pellet were added to 100µl RPMI containing 1µg/ml FLUO 3/AM (Merk Millipore, Germany), and incubated at 37°C for 20 minutes. Cells were then centrifuged at 500xg for 5 minutes, resuspended in 500µl MT-FACS and incubated for a further 30 minutes at 37°C. Cells were then put on ice, and analysed by flow cytometry. 10,000 events were captured on a BD FACSAria™ II. Calcium content was calculated by mean FITC fluorescence.

Infections

Experiments used either the rodent parasite *P. chabaudi chabaudi AS* or *P. berghei ANKA*. Parasite stocks were prepared from passage through resistant C57BL/6 and SJL/J mice respectively. 250 µl stock was injected into the intraperitoneal cavity of C57BL/6 male mice. When these mice reached 5-10% parasitaemia, blood was collected via mandibular bleed and diluted into 25ml Krebs buffer. Using the assumption that mice contained $9x10^9$ RBC/ml, dilutions were calculated to give a final concentration of either $1x10^3$ or $1x10^4$ parasitised RBC. Experimental mice were infected IP. Mice used to measure survival were infected at a dose of $1x10^4$ parasitised RBC; mice used for all other experiments were infected at a dose of $1x10^3$ parasitised RBC.

Parasitaemia

Blood stage parasitaemia was determined by counting Giemsa stained thin smears from tail blood. Slides counts differed depending on ENU line and parasite species. For MRI49372 at least 600 cells were counted per slide, including infected and uninfected reticulocytes, and infected and uninfected mature cells. For *P. chabaudi* RBC10 at least 300 cells were counted per slide, including infected and uninfected mature cells only. For *P. berghei* RBC10 at least 300 cells were counted per slide, including infected and uninfected cells. For gametocytogenesis measurements 1000 infected cells were counted per slide.

Growth Acceleration

P. falciparum 3D7 were maintained between 0.5 and 10% parasitaemia in purified AB+ human erythrocytes, in a 1% 0_2/5% $C0_2$ atmosphere, according to the method of Trager and Jensen [300]. The cell culture medium (CCM) comprised RPMI supplemented with 1x

Glutamax, 0.2% albumax (all from Gibco, NY, USA), 4% pooled AB+ human serum (Invitrogen, NY, USA), 10mM D-Glucose, 25 µg/ml gentamycin, 6mM HEPES and 0.2 mM hypoxanthine (all from Sigma, MO, USA).

Uninfected RBCs were pre-incubated with GTP for 3hrs at 37°C, then washed with CCM Wash to remove excess GTP. Trophozoite stage *P. falciparum* 3D7 parasites were synchronised by percoll density gradient [301] then added to pre-treated cells at 0.5-0.7% parasitaemia and cultured for a further 48hrs. Thin blood smears were made at 0 and 48hrs, fixed in 100% methanol, and stained in 10% Giemsa solution. Parsitaemia was determined by counting 1000 cells per slide under a light microscope. Growth was calculated by dividing the parasitaemia at T=48 by the parasitaemia at T =0. Growth acceleration was calculated as the percentage increase in growth observed in treated cells when compared to untreated cells.

TUNEL Staining

Thin tail smears from *P. chabaudi* infected mice were fixed in 100% MeOH. For all TUNEL staining, an APO-BrdU TUNEL assay kit was used (Invitrogen, Carlsbad, CA). Slides were initially washed three times with 1ml of wash buffer solution before being incubated with 50µl of DNA labelling solution mix (according to manufacturer's instructions) overnight at room temperature. The next day slides were rinsed three times with 1ml rinse solution with two minutes incubation time each. Stained sections were then incubated with 100µl of BrdU-antibody for one hour in the dark at room temperature with subsequent washes in 1%BSA/ 1x MT-PBS (three times with a two minute soak each). Slides were then further labelled with 100µl of nuclear yellow (Invitrogen, Carlsbad, CA) (1:5000 in 1% BSA/ 1 x MT-PBS) for one minute in the dark. After further washes with 1ml MT-PBS (three times with a two minute soak each) sections were affixed with Fluorescent Mounting Medium (DakoCytomation). Once the medium dried, slides were examined on an upright epifluorescence microscope (ZIESS) 600x magnification. 10 fields of view were counted for each slide.

***In-vivo* Invasion and Growth Assay**

Blood from Mutant and WT uninfected mice was collected by cardiac puncture. 1800µl of blood was collected and pooled for each genotype, then halved and stained with either

NHS-Atto 633 (1µl/100µl) or sulfobiotin-LC-NHS-Biotin (1µl/100µl of 25mg/ml in DMF) to achieve the following combinations:

WT-Biotin
WT-Atto
Mutant-Biotin
Mutant-Atto

Cells were then incubated at RT for 30 minutes, and washed twice in MTPBS. Stained cells were combined in equal proportions to achieve the following combinations:

1) WT-Biotin + Mutant-Atto
2) WT-Atto + Mutant Biotin

Combined cells were then resuspended in 2ml MTPBS, and injected intravenously into WT *P. chabaudi* infected mice. 4 mice at 1-5% parasitaemia, plus 1 uninfected control, were injected with 200µl dye combination 1; the same numbers of mice were injected with 200µl dye combination 2. Injections were carried out when parasites were undergoing schizogeny, at ~1am.

At 30 minutes, 3hrs, 12hrs, and 20hrs post injection, 1µl tail blood was collected and stained for 30 minutes at 4°C in 50µl MTPBS containing 0.25µl CD45-APC-Cy7, 0.25µl CD71-PE-Cy5, 0.5µl Step-PE-Cy7. Next, 400µl MTPBS containing 0.5µl Hoechst 33342 and 1µl 800µg/ml Thiazole orange was added, and cells were incubated for a further 5 minutes at 4°C. Stained cells were then centrifuged at 750xg for 3 minutes, re-suspended in 700µl MTPBS, and analyzed on a BD Fortessa Flow Cytometer. $2x10^6$ cells were collected for each sample, and data was analysed using FlowJo (FlowJo, LLC, Oregon, USA).

Evan's Blue

P. berghi infected mice, and uninfected controls, were injected IV with 200µl 1% Evans Blue/PBS solution. 1hr post injection, mice were sacrificed and their brains collected and weighed. Brains were placed in 2ml 10% neutral buffered formalin at room temperature for 48hrs to extract dye. 200µl of formalin from each brain was then collected and absorbance measured at 620nm. Amount of Evans blue extracted per gram

brain tissue was calculated using a standard curve ranging from 40µg/ml to 0µg/ml. Injections were carried out on the day of infection that the first mouse died.

Clinical Score

Mice were monitored three times daily, and given a score from 0 to 5 based on the type and severity of their symptoms. '0' indicated no symptoms; '1' reduced or languid movement; '2' rapid breathing and/or hunched posture; '3' ruffled fur, dehydration and/or external bleeding; '4' fitting and/or coma; '5' death. Mice were considered comatose if they were unable to right themselves after being placed on their side. The highest score recorded for each mouse on each day was used to generate daily averages.

Plasma Cytokines

Peripheral blood was taken either by cardiac puncture or mandibular bleed (as described in **Haematological Analysis),** and centrifuged for 4 minutes at 11,000xg. Plasma was then taken into a separate tube and stored at -20°C until needed.

Cytokine analysis was conducted using a CBA Mouse Th1/Th2/Th17 Cytokine Kit (BD biosciences). Samples were prepared to the maker's instructions. Briefly, cytokines were reconstituted in assay diluent, and a serial dilution was performed to make a standard curve. 50µl of each standard and plasma sample were then added to 50µl of mixed capture beads and 50µl of Th1/Th2/Th17 PE detection reagent, and then incubated at 2 hours at room temperature protected from light. Samples were then washed by centrifuging at 200xg for 5 minutes, removing the supernatant and adding 150µl of wash buffer to each. This wash step was then repeated.

Samples were acquired using a BD Fortessa flow cytometer. A total of 2100 events were captured (300 per cytokine) per sample. The results were exported and analysed using FCAP Array™ software (BD biosciences). Of the calculated parameters, final concentration was used in analysis. Statistical significance was determined using the Student's T test.

Lymphocyte Analysis

150 µl blood was diluted in 2 ml of MT-PBS and mixed well. Using a Pasteur pipette, 2 ml of this blood/MT-PBS mix was then layered carefully on top of 2 ml room temperature Ficoll-Paque™ , so that as little mixing as possible occurred at the interface. This was centrifuged for

20 minutes at 1500xg at room temperature. After centrifugation a white, lymphocyte layer was clearly visible at the interface. This layer was removed using a Pasteur pipette and transferred into a new tube. 10 ml of MT-PBS was added to the lymphocytes, mixed and centrifuged at 800xg for 10 minutes. The supernatant was removed and the pellet re-suspended in 5 ml MT-PBS. The centrifugation was repeated, and the supernatant discarded. Cell suspension was then incubated with 1µg Fc-block/10^6 cells/100µl MT-FACS for 10 minutes at 4°C.

Both spleen and thymus were prepared for flow cytometry using the same method. ½ of each organ was passed through a 70µm BD Falcon Cell Strainer with 0.5 ml of MT-FACS buffer, and then centrifuged at 300xg for 5 minutes at 4°C. The supernatant was removed and the pellet resuspended in 5 ml cold MT-FACS buffer. A 200 µl aliquot of this suspension was then incubated with 0.8 µl Fc-block.

Each sample was incubated in 0.5µl CD4-PacificBlue, 0.5µl CD11-PE, 1µl CD8-FITC, 1µl CD25-PECy7, 1µl CD19-PERCPCy5.5 and 1µl CD3-APCCy7 for 20 minutes at 4°C. Cells were then washed in 1ml MT-FACS buffer and centrifuged at 250xg for 5 minutes at 4°C. The supernatant was discarded, 300 µl of MT-PBS containing 1% formalin and 1% BSA was added, and the suspension incubated for at least 10 minutes at 4°C. Cells were washed again in 1 ml MT-FACS buffer and centrifuged at 250xg for 5 minutes at 4°C. The supernatant was discarded, and 250µl of MT-PBS containing 0.1% saponin and 1%BSA was added. This was incubated at 4°C for 20 minutes. The cells were washed in 1ml MT-FACS buffer, centrifuged at 250xg for 5 minutes at 4°C, and the supernatant was discarded. 1µl of FoxP3-APC was then added to each sample, and incubated on ice for 20 minutes. Cells were then re-suspended in 300µl of MT-FACS buffer.

Samples were acquired using a BD FACSAria™ II flow cytometer, and analysed using BD FACSDiva™ software (BD Biosciences). Statistical significance was calculated using the Student's T Test.

Recipes

CCM

RPMI

1.6% Glutamax,

0.2% albumax

4% pooled AB+ human serum

10mM D-Glucose

25µg/ml gentamycin

6mM HEPES

0.2 mM hypoxanthine

CCM wash

1x Glutamax,

10mM D-Glucose

25µg/ml gentamycin

6mM HEPES

MACS buffer

2.5g BSA

10ml 100mM EDTA

make up to 500ml with MT-PBS

MT-FACS buffer

MT-PBS

1% BSA

Krebs Ringer solution

79.72g Sodium Chloride

2.05g Potassium chloride

1.90g Sodium phosphate monobasic

24.03g Sodium bicarbonate

5.5L cold deionised water

Krebs buffer

750ml Krebs Ringer solution

750ml deionised water

3ml 2mM Calcium Chloride

3ml 1mM Magnesium Sulfate

4g Glucose.

Mouse culture media

250ml RPMI

62.5ml FCS

5ml glutamine

0.125ml gentamycin

1.5g HEPES

0.5g $NaHCO_3$

CHAPTER 3 – MRI49372 BLOOD PHENOTYPE

Introduction

The ENU mutant mouse line MRI49372 was identified by screening 1st generation ENU injected mice for an abnormal blood phenotype. It was characterised by increased mean corpuscular volume (MCV). This chapter aimed to identify the causative ENU mutation that underlies this macrocytic phenotype, and characterise how the mutation affects the blood phenotype and physiology of MRI49372.

Results

MRI49372 has a macrocytic anaemia

The ENU G1 mouse MRI49372 was first identified due to MCV over two standard deviations higher than wild-type (WT) SJL/J. The mouse MRI49372 was crossed to SJL/J, and G2 generation mice were tested for the heritability of the high MCV phenotype. Phenodeviant G2s were crossed together, and the resulting G3 mice were categorised as WT, m/+ or m/m based on the severity of their MCV phenotype (WT ≤ 55fL, m/+ 56-61fL, m/m ≥62fL). These mice were then subjected to analysis of their complete blood count. Mutants were found to differ significantly from WT for several parameters. They exhibited leucocytosis, reticulocytosis, and anisocytosis (Table 3.1). Conversely, the number of RBCs and the total amount of haemoglobin were both significantly decreased (Table 3.1). Wright-Giemsa stained blood smears confirmed a macrocytic anaemia, and also showed increased target cells, blister cells, and acanthocytes (RBCs with the appearance of a 'bullseye', RBCs with haemoglobin concentrated on one side, and RBCs with spiked membranes respectively) (Figure 3.1). This suggested that MRI49372 might have a haemolytic anaemia. Mutants exhibited splenomegaly, with m/m showing an almost 5 fold increase in spleen index (Figure 3.1).

Table 3.1: Haematological parameters of Wild-type, MRI49372$^{m/+}$, and MRI49372$^{m/m}$ mice.

Automated full blood analysis on WT (n=15), MRI49372$^{m/+}$ (n=21), and MRI49372$^{m/m}$(n=14) mice. WBC = number of white blood cells x 10^3 cells/µl; RBC = number of red blood cells x 10^6 cells/µl; HGB = total haemoglobin g/L; MCV = mean corpuscular volume fL; RDW = percentage red cell distribution width; %Macro = macrocytic cells; %micro = microcytic cells. Values are average ± SEM. *P<0.05, **P<0.01, ***P<0.001.

	Wild-type	MRI49372$^{m/+}$	MRI49372$^{m/m}$
WBC	9.6 ± 0.7	10.6 ± 0.5	20.2 ± 2.3**
RBC	10.3 ± 0.2	8.8 ± 0.4	5.9 ± 0.4***
HGB	106.1 ± 8.2	93.0 ± 7.7	71.2 ± 7.9**
MCV	53.1 ± 0.5	56.2 ± 0.4*	71.6 ± 2.1*
RDW	14.6 ± 0.2	14.1 ± 0.2	21.9 ± 1.0***
%Retic	2.3 ± 0.3	6.0 ± 1.1*	52.6 ± 6.5**
%Macro	0.3 ± 0.1	1.3 ± 0.3**	40.2 ± 5.5***
%Micro	0.4 ± 0.04	0.2 ± 0.01***	0.7 ± 0.1***

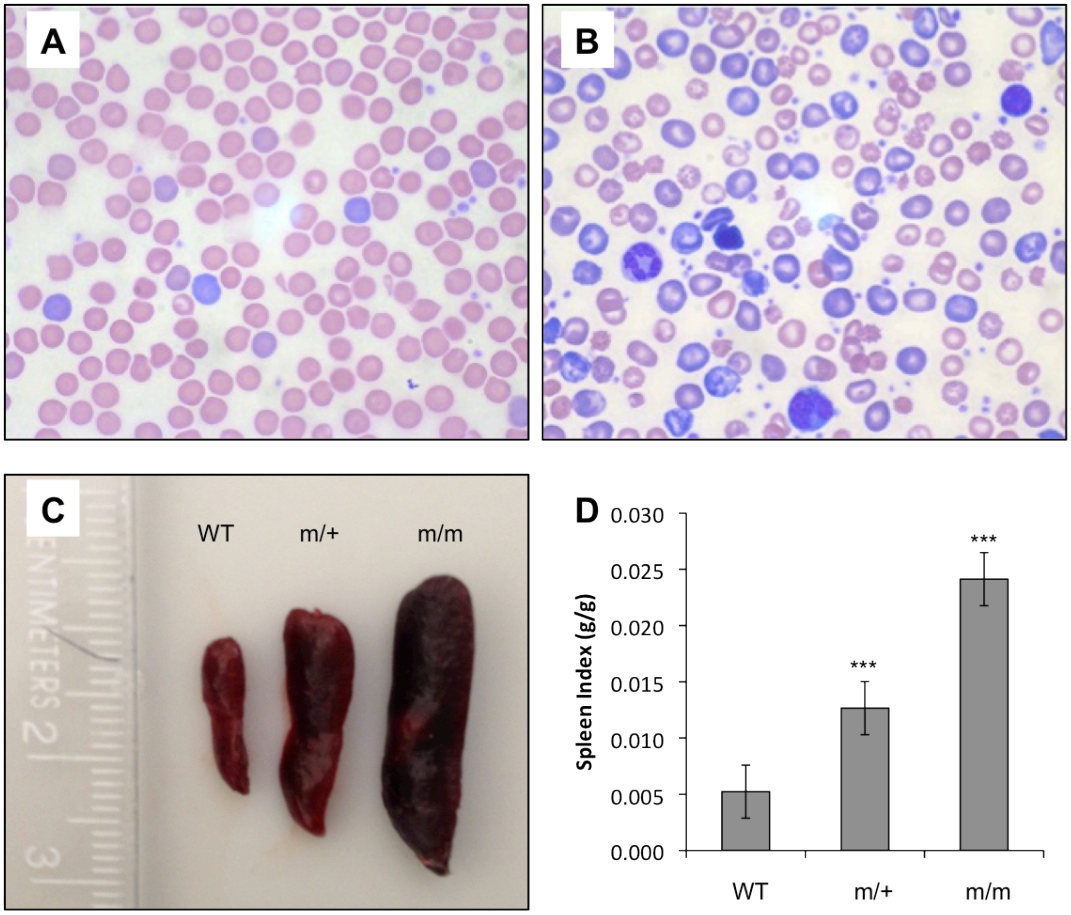

Figure 3.1: MRI49372 macrocytic anaemia and splenomegaly. (A) Representative light microscopy image of Wright-Giemsa stained WT thin smear. **(B)** Representative light microscopy image of Wright-Giemsa stained MRI49372$^{m/m}$ thin smear. **(C)** Representative spleens from WT, MRI49372$^{m/+}$, MRI49372$^{m/m}$ mice. **(D)** Average spleen index ± SEM, calculated as spleen weight (g)/mouse weight (g) for WT (n=7), MRI49372$^{m/+}$ (n=8), MRI49372$^{m/m}$ (n=7). ***P<0.001.

The MRI49372 blood phenotype is caused by a mutation in *Ampd3*

To discover the causative mutation of the MRI49372 phenotype, whole-exome sequencing was performed on two phenodeviant (m/m) G3s on a Hiseq 2000 platform using an Agilent exome enrichment kit. After filtering out previously reported common SNPs, and selecting for novel, non-synonymous, exonic mutations held in common by both animals, 9 mutations remained for further investigation. By conducting Sanger sequencing on these candidate variants in a larger cohort of mice from 3 generations, a mutation in *Ampd3*, at location 7:117953361, remained the only variant to associate 100% with the blood phenotype, with a LOD score of 6.55 (Table 3.2).

In order to further confirm this location as the site of the causative mutation, N2 mice were generated by crossing phenodeviant MRI49372 mice to Balb/c. Known SNPs on chromosome 7 were genotyped, between 90 and 120 megabases. 12/13 affected mice were heterozygous across 3 SNPs (Chr7:99912442-120255269), giving a LOD score of 2.38, and suggesting linkage between the MCV phenotype and the region of the genome containing *Ampd3* (Figure 3.2).

The mutation in *Ampd3* is an A to G transition, causing an amino acid substitution of alanine for threonine at position 689 in the AMPD3 protein (Figure 3.2). This residue falls within the AMP deaminase domain, which is highly conserved between species (Figure 3.3).

For the rest of this chapter, mutant MRI49372 will be referred to as $Ampd3^{T689A}$.

Table 3.2: List of non-synonomous gene candidates held in common between both mutants sent for whole exome sequencing.

Between 4 and 32 mice were sequenced for each candidate mutation. Mutants were categorised as WT, m/+ or m/m based on the severity of their MCV phenotype (WT ≤ 55fL, m/+ 56-61fL, m/m ≥62fL)

Chrom	Location	Base		Gene name	LOD score	n
		Ref	Var			
7	81356970	A	T	*Cpeb1*	0.69	32
7	114536169	A	T	*Pde3b*	2.58	21
7	110809847	A	G	*Ampd3*	6.55	22
7	104260195	G	A	*Trim34a*	0.51	11
6	40680762	C	T	*Mgam*	0	6
1	119678820	T	G	*Ptpn4*	1.19	4
12	72652426	T	A	*Dhrs7*	0.23	4
13	81521252	C	G	*Gpr98*	1.19	4
16	29409849	T	A	*Atp13a4*	0.23	4

SNP	Postion	Affected			Unaffected			
rs32156288	Chr7:90180905							
rs36514000	Chr7:99912442							
rs31984795	Chr7:105389927							
rs32613342	Chr7:120255269							
Number of mice		11	1	1	1	1	5	3

Figure 3.2: High MCV MRI49372 N2 mice have a linked region on chromosome 7. Genotype for SNPs from 90 to 120 megabases on chromosome 7, for affected (MCV>53) and unaffected (MCV<53) N2s. Grey boxes represent heterozygousity.

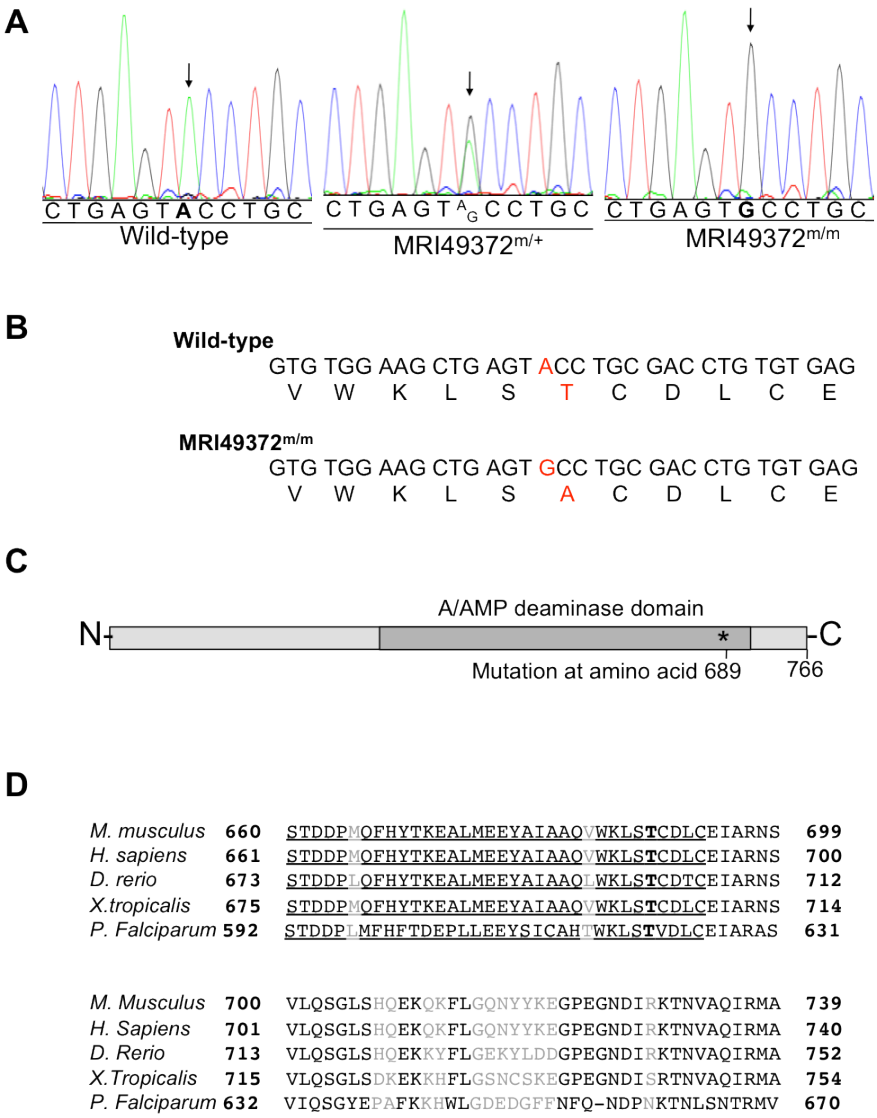

Figure 3.3: The MRI49372 phenotype is caused by a mutation in *Ampd3*. (A) DNA sequence electropherograms showing the A to G transition in exon 14 of *Ampd3*. **(B)** Nucleotide and amino acid sequences, showing the threonine to alanine missense mutation in red. **(C)** Representation of the position of the mutation within the protein. **(D)** Sequence alignment showing conserved residues in AMPD3. Black letters represent residues conserved in 4/5 listed species. Underlined letters represent plecstrin homology domain. Bold 'T' is the position of the MRI49372 mutation.

The Ampd3^{T689A} mutation causes an activation of AMPD3

AMPD3 is the erythrocyte specific isoform of AMP deaminase; it catalyses the conversion of AMP to IMP, an important reaction involved in purine metabolism within the RBC (Figure 3.4).

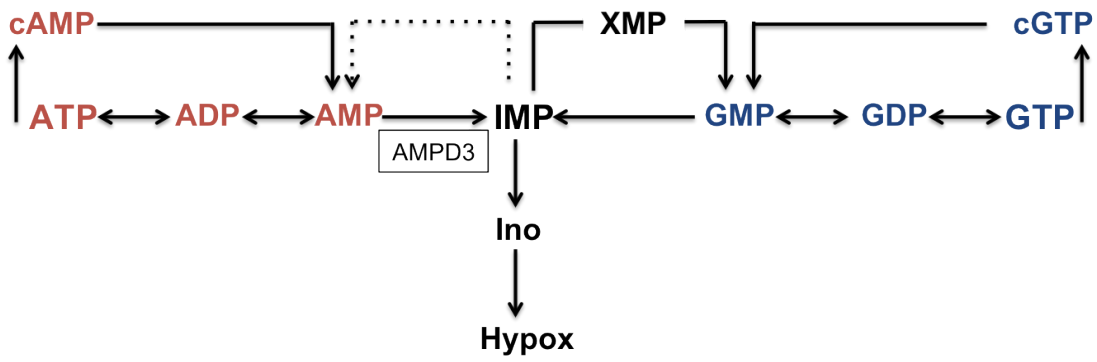

Figure 3.4: Purine metabolism in the erythrocyte, showing reaction catabolised by AMPD3. Dotted line indicates reaction that does not proceed in human RBCs. It is not known if this reaction proceeds in mouse RBCs **ATP**, adenosine 5'-triphosphate; **ADP**, adenosine 5'-diphosphate; **AMP**, adenosine 5'-monophosphate; **IMP**, inosine 5'-monophosphate; **XMP**, xanthosine 5'-monophosphate; **GMP**, guanosine 5'-monophosphate; **GDP**, guanosine 5'-diphosphate; **GTP**, guanosine 5'-triphosphate; **Ino**, inosine; **Hypox**, hypoxanthine; **cAMP**, cyclic AMP; **cGTP**, cyclic GTP.

To determine if the Ampd3^{T689A} mutation affects expression of the enzyme, real time PCR was conducted on E14 livers, which are composed primarily of erythroblasts. No significant difference was observed between Ampd3$^{T689A/+}$ and WT, and a 1.4 fold increase in expression was observed between Ampd3$^{T689A/T689A}$ and WT (Figure 3.5). To determine if this change in expression translated into a difference in protein abundance, the amount of AMPD3 present in peripheral RBCs was assayed by Western Blot. There was a dramatic increase in the amount of AMPD3 in mutant whole blood. However, it is known that the expression of many erythrocytic proteins varies as the erythrocyte

matures [302], which raises the possibility that results obtained from whole blood will be confounded by the high proportion of reticulocytes in Ampd3^{T689A}. A recent transciptome analysis of human and murine erythroblasts found no significant changes in the expression of *Ampd3* during maturation [302]; however blots were repeated with isolated mature (CD71-) RBCs, and erythroblasts (E14 livers) to eliminate the possibility that the observed difference in AMPD3 abundance was caused by the level of reticulocytosis. In these experiments, no difference in protein level was observed, suggesting that the Ampd3^{T689A} mutation does not affect the amount of enzyme present in the RBC (Figure 3.5).

To determine if the Ampd3^{T689A} mutation affects the activity of the enzyme, the relative abundance of several purines within the mature (CD71-) RBC was assayed by HPLC/MS (Appendix A). Mutant cells had significantly more IMP, GMP, GDP and GTP when compared to WT; they also had significantly less ATP, ADP and AMP. Together, these results suggest an over activation of AMPD3. To confirm this, mature (CD71-) RBCs were incubated with 13C15N labelled AMP, and the accumulation of labelled IMP was measured over a period of 4 hours. The conversion of AMP to IMP occurred six times faster in *Ampd3*$^{T689A/T689A}$ than Ampd3$^{T689A/+}$. No labelled IMP was observed in WT mice at all, suggesting that under normal circumstances, AMPD3 is completely inhibited in mature erythrocytes (Figure 3.5).

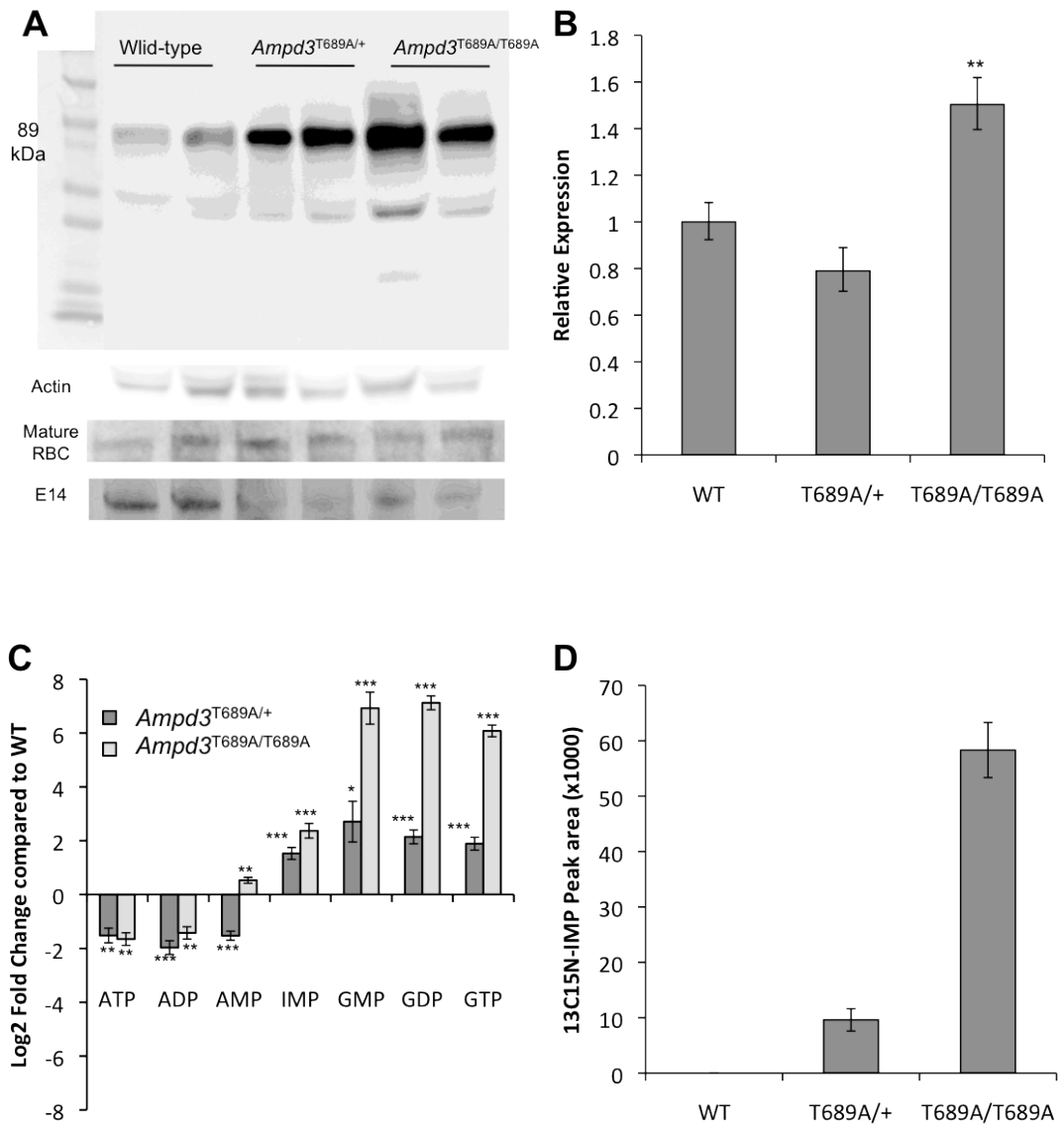

Figure 3.5: The Ampd3^{T689A} mutation causes activation of AMPD3. (A) Western blot of whole blood, showing AMPD3 band at 89kDa for WT, Ampd3$^{T689A/+}$ and Ampd3$^{T689A/T689A}$, as well as actin loading control for the same blot. AMPD3 blots for MACS sorted mature RBCs (CD71-), and E14 livers are also shown. **(B)** RT PCR analysis showing average ± SEM fold change in expression of *Ampd3* in E14 livers for Ampd3$^{T689A/+}$ (n=2) and Ampd3$^{T689A/T689A}$ (n=2) compared to WT (n=4). *Ampd3* expression was calculated relative to *ACTB* expression **(C)** Average ± SEM fold change in purine concentration in mature RBCs (CD71-) for Ampd3$^{T689A/+}$ and Ampd3$^{T689A/T689A}$ compared to WT. Data shows average of technical replicates (n=4), from pooled biological replicates (n=6) **(D)** Accumulation of labelled IMP in mature WT, Ampd3$^{T689A/+}$ and Ampd3$^{T689A/T689A}$ RBCs (CD71-) incubated at 37°C for 2 hours with labelled AMP. Data shows average of technical replicates (n=3) from pooled biological replicates (n=3). *P<0.05, **P<0.01, ***P<0.001. P values calculated using the student's T test.

Activation of AMPD3 decreases RBC half-life

To understand the cause of macrocytosis and reticulocytosis in Ampd3^{T689A}, erythropoiesis was investigated by flow cytometry of CD44+TER119+ erythroblasts. Plasma levels of the hormone that stimulates erythropoiesis, erythropoietin (EPO), were also assayed by ELISA. Significantly higher proportions of erythroblasts were observed in the spleen and bone marrow, and significantly higher concentrations of EPO were found in the plasma of both Ampd3$^{T689A/+}$ and Ampd3$^{T689A/T689A}$ mice (Figure 3.6). These results are consistent with an elevated erythropoiesis in the mutants. To determine if erythropoiesis was occurring at a constant rate, the percentage of peripheral reticulocytes was monitored by giemsa stained thin smears over the course of 11 days. Consistent with the results from the automated complete blood count (Table 3.1), a significantly higher proportion of reticulocytes were observed in both Ampd3$^{T689A/+}$ and Ampd3$^{T689A/T689A}$. However, while both WT and Ampd*3*$^{T689A/+}$ showed little variation over the course of the experiment, reticulocytosis in Ampd3$^{T689A/T689A}$ oscillated between 30% and 60% in a 5-day cycle (Figure 3.7A). When the data from each individual Ampd3$^{T689A/T689A}$ mouse were adjusted so that the peaks of reticulocytosis were aligned, this cycle was even more evident (Figure 3.7B). The fact that Ampd3^{T689A} have increased RBC production, but lower numbers of mature erythrocytes, suggests that the phenotype results from increased RBC destruction. In support of this hypothesis, a 1.5 fold increase in plasma bilirubin – a product of heme catabolism - was observed in Ampd3$^{T689A/+}$, and a 2.7 fold increase was observed in Ampd3$^{T689A/T689A}$ (Figure 3.8).

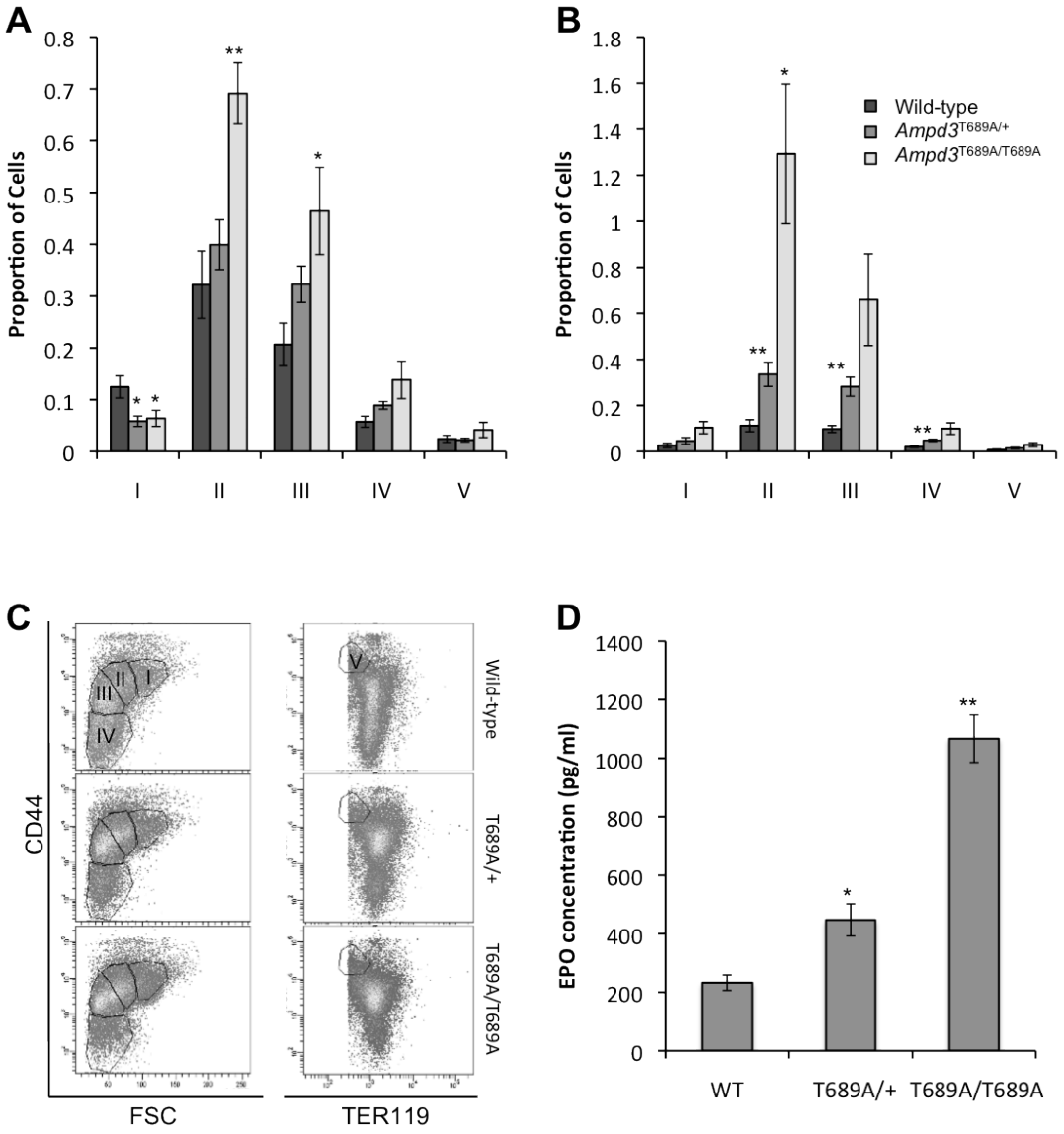

Figure 3.6: Ampd3^{T689A} has elevated erythropoiesis. Proportion of TER119+ erythroblast populations in the **(A)** bone marrow and **(B)** spleen, calculated relative to the number of TER119- cells, for WT, Ampd3$^{T689A/+}$ and Ampd3$^{T689A/T689A}$. I = RBCs, II = reticulocytes, III = polychromatic erythroblasts, IV = basophilic erythroblasts and V = proerythroblasts **(C)** Representative plots showing flow cytometry gating strategy, using CD44 and TER119 staining. **(D)** EPO concentration in the plasma of WT, Ampd3$^{T689A/+}$ and Ampd3$^{T689A/T689A}$. Values are average ± SEM. *P<0.05, **P<0.01, ***P<0.001. P values calculated using the student's T test.

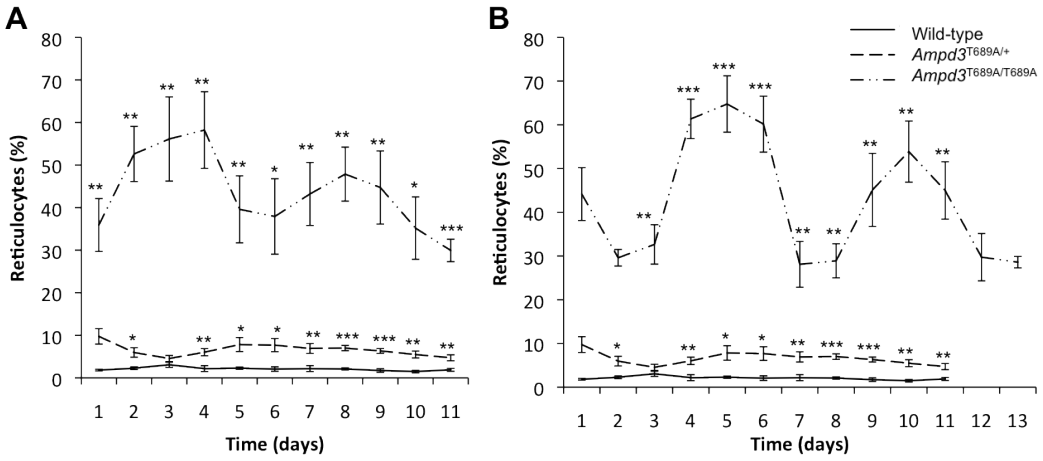

Figure 3.7: Ampd3^{T689A} has elevated reticulocytes. Average ± SEM percentage peripheral reticulocytes in WT (n=4), Ampd3$^{T689A/+}$ (n=8), and Ampd3$^{T689A/T689A}$ (n=5) mice **(A)** over the course of 11 days. **(B)** Values from Ampd3$^{T689A/T689A}$ have been adjusted so that the peaks of reticulocytosis align. *P<0.05, **P<0.01, ***P<0.001. P values calculated using the student's T test.

To determine if RBC destruction is increased in Ampd3^{T689A}, mice were injected intravenously with biotin, and the loss of labelled cells from circulation was monitored over a period of 4 weeks by flow cytometry. Both Ampd3$^{T689A/+}$ and Ampd3$^{T689A/T689A}$ showed a decrease in RBC half-life, from 15.5 days in WT, to 8.5 days in heterozygotes, and 2.5 days in homozygotes (figure 3.8a). Given that splenomegaly is observed in mutant mice, we hypothesised that this was caused by an increased rate of splenic clearance.

To determine if shortened RBC half-life was mediated by aberrant splenic clearance, biotinylation of RBCs was performed in splenectomised mice. Although half-life was lengthened by splenectomy in homozygotes, this amounted to an increase of only 1.45 days, indicating that half-life in Ampd3^{T689A} is not spleen dependent (figure 3.8b). In further support of this, no evidence of iron overload in the spleen was observed, either by Perl's blue staining, or by total non-haem iron (Figure 3.9), indicating that a normal amount of RBC destruction is occurring in the spleen. Similarly, there was no difference in osmotic fragility – a trait that often results in increased splenic clearance - between Ampd3^{T689A} and WT (Figure 3.9). Therefore, to determine if Ampd3^{T689A} RBCs lyse spontaneously, mutant and wild-type RBCs were incubated for 24 hrs *in vitro*. The level of lysis was almost three times higher in cells from Ampd3$^{T689A/T689A}$ than in those from WT mice (Figure 3.8). Together, these results indicate that the shortened life-span of Ampd3^{T689A} RBCs is determined by factors autonomous to the erythrocyte, and that RBC turnover is occurring independently of the spleen.

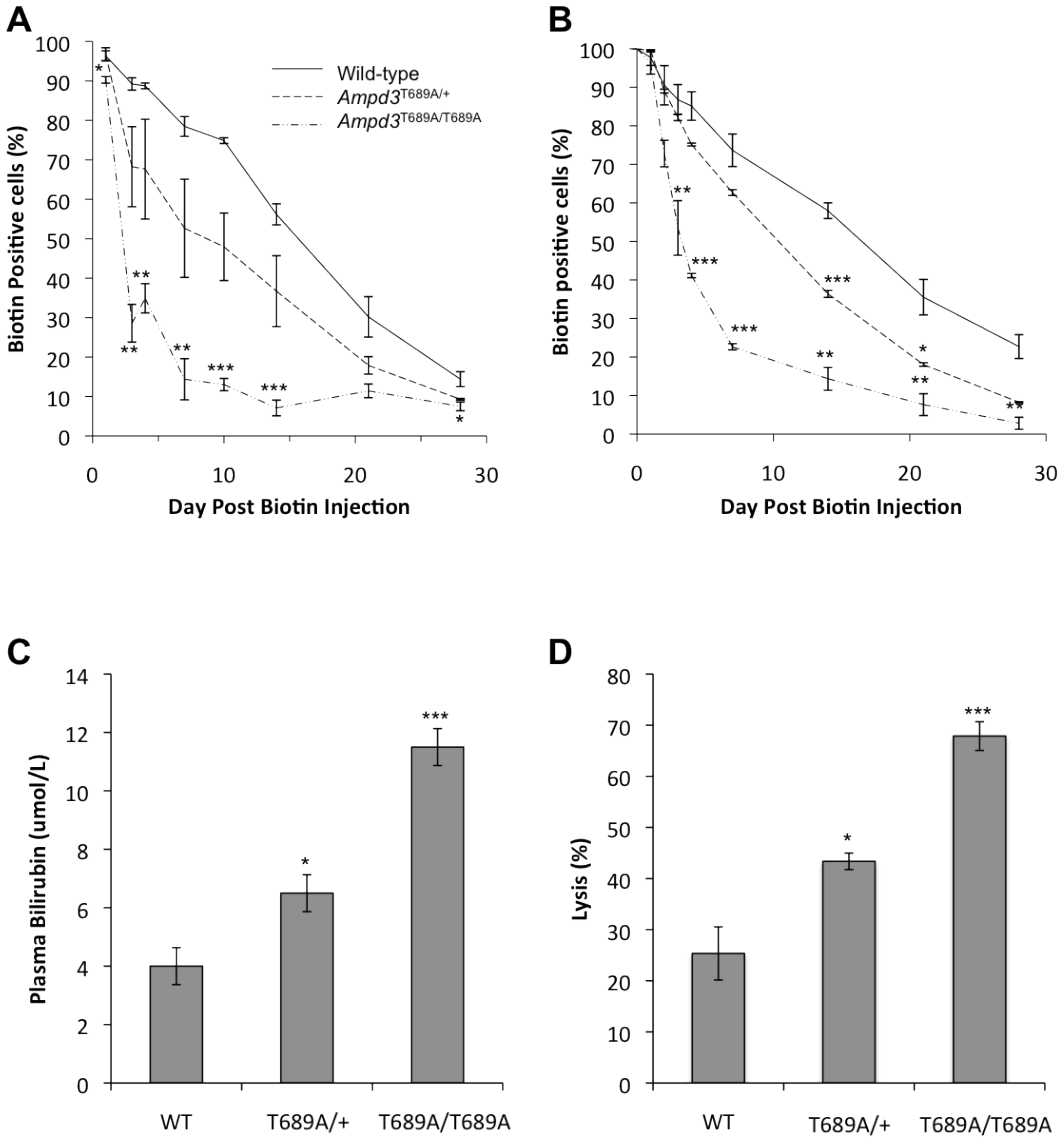

Figure 3.8: The Ampd3^{T689A} mutation shortens erythrocyte lifespan. (A) RBC half-life in WT, Ampd3$^{T689A/+}$ and Ampd3$^{T689A/T689A}$ mice, as measured by loss of biotinylated cells from circulation. **(B)** RBC half-life in splenectomised WT, Ampd3$^{T689A/+}$ and Ampd3$^{T689A/T689A}$ as measured by loss of biotinylated cells from circulation. **(C)** Amount of bilirubin in the plasma of WT, Ampd3$^{T689A/+}$ and Ampd3$^{T689A/T689A}$ mice. **(D)** Amount of lysis for WT, Ampd3$^{T689A/+}$ and Ampd3$^{T689A/T689A}$ cells incubated *in vitro* at 37°C for 24hrs. Measured by absorbance at 545nm, and compared to 100% lysis. Values are average ± SEM. *P<0.05, ***P<0.001. P values calculated using the student's T test.

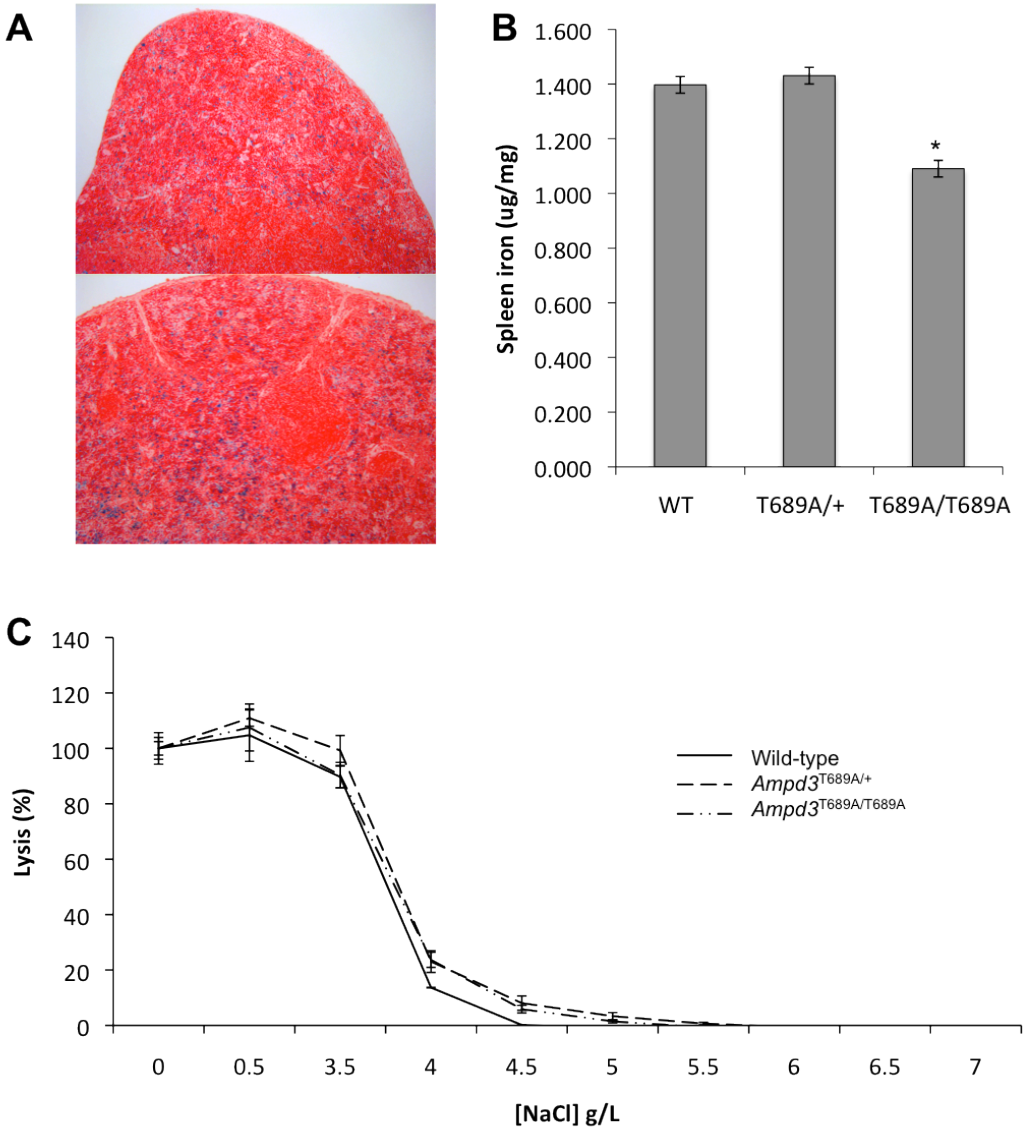

Figure 3.9: Ampd3^{T689A} does not have iron overload in the spleen, and is not osmotically fragile. **(A)** Perls blue stained spleen sections of WT (top) and Ampd3$^{T689A/T689A}$ (bottom). **(B)** Amount of non-haem iron in the spleen of WT (n=2), Ampd3$^{T689A/+}$ (n=2), Ampd3$^{T689A/T689A}$ (n=4). **(C)** osmotic fragility of WT, Ampd3$^{T689A/+}$, and Ampd3$^{T689A/T689A}$ (all genotypes n=3). Values are average ± SEM. *P<0.05. P value calculated using the student's T test.

Shortened Ampd3^{T689A} half-life is caused by high oxidative stress

To determine the cause of short RBC half-life, the susceptibility of Ampd3^{T689A} RBCs to oxidative stress was investigated by intraperitoneal injection of phenylhydrazine (PHZ). This chemical causes RBC lysis by increasing reactive oxygen species (ROS) within the cell. Significantly more lysis was observed in Ampd3$^{T689A/+}$ and Ampd3$^{T689A/T689A}$ one day after injection. Only 12.5% of RBCs remained in heterozygotes, and 5.3% in homozygotes, compared to 22.9% in WT, indicating that mutant cells are more susceptible to oxidative stress (Figure 3.10A). To determine if this increased sensitivity to PHZ was due to higher baseline oxidative stress, the amount of ROS was measured within mutant and WT RBC, using the ROS activated fluorescent dye H_2DCFDA and flow cytometry. The amount of ROS, as measured by change in mean fluorescence intensity, was significantly higher in mutant mice. Ampd3$^{T689A/+}$ displayed ROS 1.7 fold higher than WT, and Ampd3$^{T689A/T689A}$ reached 5 fold higher, indicating that mutant cells experience a higher level of oxidative stress than wild type, and may be undergoing eryptosis (Figure 3.10C). This was further supported by the observation that Ampd3^{T689A} RBCs had significantly higher levels of phosphatidyl serine exposure (measured by annexin binding and flow cytometry) and intracellular calcium (measured by Fluo3am dye and flow cytometry); both are markers of RBC senescence (Figure 3.10B and D).

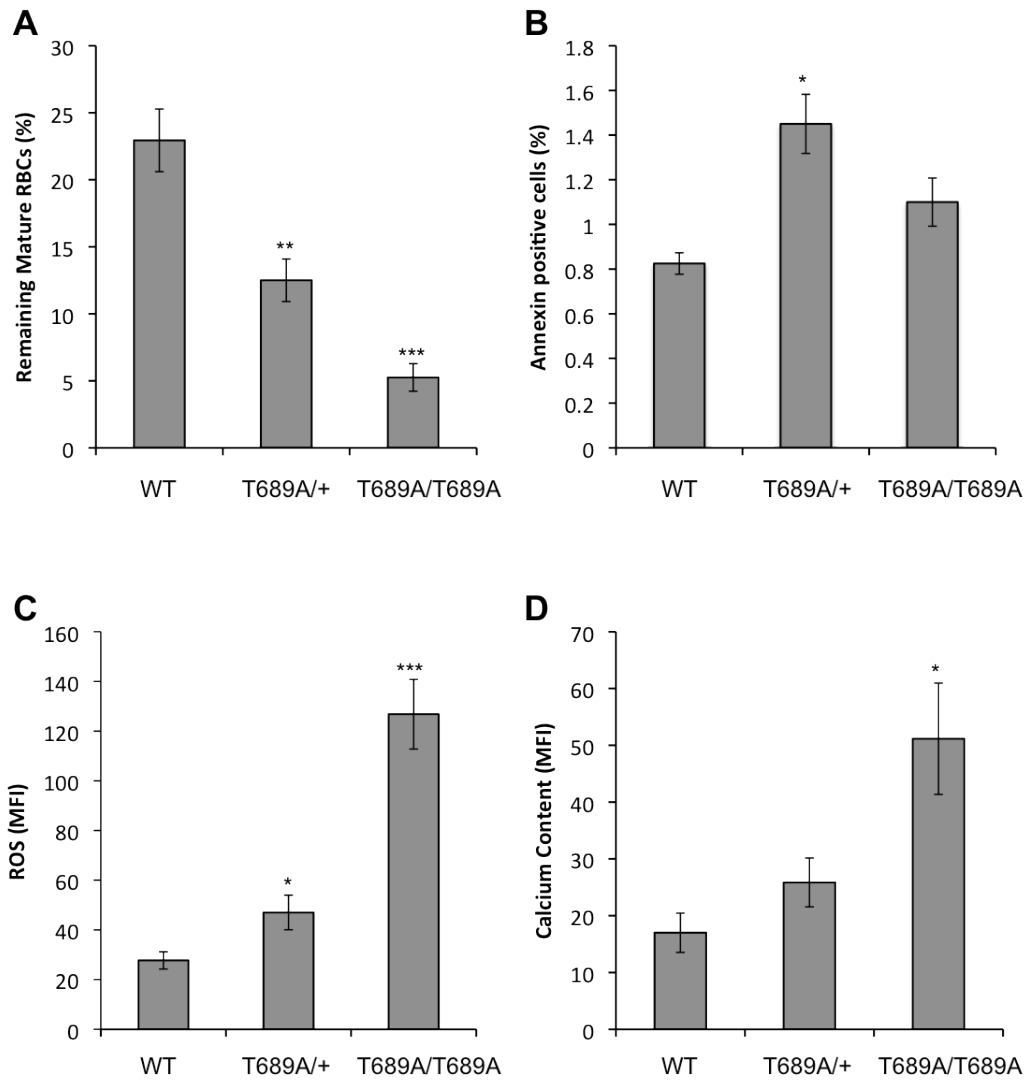

Figure 3.10: The Ampd3^{T689A} mutation causes increased oxidative stress and cell senescence.
(A) Proportion of RBCs remaining in circulation one day post phenylhydrazine injection for WT (n=5), Ampd3$^{T689A/+}$ (n=4), and Ampd3$^{T689A/T689A}$ (n=5). **(B)** Proportion of mature RBCs (CD71-) that were Annexin V positive (n=4). **(C)** Amount of reactive oxygen species in mature RBCs (CD71-) as measured by mean fluorescence intensity of H_2DCFDA, for WT (n=7), Ampd3$^{T689A/+}$ (n=7), and Ampd3$^{T689A/T689A}$ (n=6). Combined results of two independent experiments. **(D)** Amount of calcium in mature RBCs (CD71-) as measured by mean fluorescence intensity of FLUO3-am, for WT (n=7), Ampd3$^{T689A/+}$ (n=7), and Ampd3$^{T689A/T689A}$ (n=6). Combined results of two independent experiments. Values are average ± SEM. *P<0.05, ***P<0.001. P values calculated using the student's T test.

Discussion

This chapter investigated the ENU mutant line MRI49372, with the aim to identify both the causative mutation and biological mechanism behind its blood phenotype. It shows that phenodeviant MRI49372 carry a missense mutation in the *Ampd3* gene, which is associated with erythrocytic ATP depletion, as well as a build up of GTP and oxidative stress. Mutant mice also display shortened erythrocyte lifespan, and macrocytic anaemia, with rapid RBC turnover, splenomegaly and leukocytosis.

The MRI49372 blood phenotype is caused by a gain of function mutation in Ampd3

Through both whole-exome and Sanger sequencing, it was discovered that 100% of mice with the MRI49372 blood phenotype also carried a mutation in *Ampd3*. This mutation was not associated with changes in AMPD3 protein abundance in the mature RBC, but was associated with a significant increase in the rate of conversion of AMP to IMP in the same cell type. Therefore, it was concluded that the MRI49372 blood phenotype is caused by a gain of function mutation in *Ampd3* that causes over-activation of the AMPD3 enzyme.

AMPD3 catalyses the conversion of AMP to IMP, one of the many interconnected reactions involved in purine metabolism. Balanced purine metabolism is important for maintaining the necessary levels of cellular ATP and other energy molecules. Within most cell types IMP can be converted back to AMP, in a two-step process catalysed by adenylosuccinate synthase (ADSS) and adenylosuccinate lyase. Within the human erythrocyte however, IMP cannot be converted back to AMP due to the fact that ADSS is inactive (figure 4) [303,304]. This means that conversion of AMP to IMP results in the irreversible loss of ATP in mature red cells. Furthermore, the loss of ATP through this pathway has been associated with haemolysis and anaemia [305]. This suggests that tight regulation of AMPD3 may be essential to maintain the homeostasis of the RBC. It is not known whether IMP can be converted back to AMP in mouse erythrocytes. However, the experiments with labelled AMP described here, showed that AMP was not converted to IMP in WT mice, suggesting that AMPD3 is not functional in mouse erythrocytes under normal circumstances. It should also be noted that neither cAMP nor cGTP could be measured in this analysis (Appendix A). These cyclic nucleotides act as secondary messengers in a large range of metabolic processes, and it is unknown if activation of

AMPD might alter their relative abundance, and consequently their ability to regulate essential cellular processes.

The activity of AMPD is regulated through multiple mechanisms, including phosphorylation, protein interactions, monovalent cations, ROS, and PI [306-310]. Both ATP and GTP can inhibit the enzyme at low concentrations, and activate it at high concentrations [306,311]. Moreover, AMPD3 is able to bind to the erythrocyte cell membrane, and in this form it is less active. Ca^{2+}, through its interaction with calmodulin, can inhibit membrane binding, and releases AMPD3 into the cytosol where it is more active [312]. Changes in pH are also able to affect the localisation, and hence activity of AMPD3 [313]. It is possible that the Ampd3^{T689A} mutation may impair one or more of these negative regulatory mechanisms and thus lead to a more active enzyme.

Membrane binding is mediated largely through the N terminal end of the protein [313], so the Ampd3^{T689A} mutation, which sits at the C terminal end, is unlikely to affect this process directly. However, the mutation may affect the ability of AMPD3 to respond to endogenous signals that determine the location of the protein. For example, Sims *et al.* found that phosphoinositides are able to bind AMPD3, and alter the ratio of soluble and membrane-associated protein. The study predicted that the phosphoinositide binding site may be one of two pleckstrin homology domains located within the C terminal end of the protein (shown in Figure 3.3D); although it is still only speculation, the Ampd3^{T689A} mutation falls within the second of these domains, and may therefore affect phosphoinisitide mediated alteration of AMPD3 activity [314]. Another possible mechanism by which the Ampd3^{T689A} mutation might cause activation of the enzyme is by removing an amino acid residue that is normally phosphorylated. A query of the Human Protein Reference Database suggests that the WKLSTCD motif that includes the mutation is a likely site for phosphorylation. By changing the threonine in this motif to an alanine, the Ampd3^{T689A} mutation may disrupt this. So far, no studies have investigated whether phosphorylation has a role in the activation of AMPD3. However, studies of AMPD1 have shown that the enzyme is phosphorylated by protein kinase C in the presence of Ca^{2+} and PS, and that this increases its activity [308,315]. Further studies into the mechanism of AMPD3 activation in these mutants should investigate whether AMPD3 is membrane bound in mutant erythrocytes, as well as any changes in phosphorylation of the protein.

Ampd3^{T689A} has a shortened RBC half-life and increased oxidative stress

Mice carrying the Ampd3^{T689A} mutation were found to have significantly decreased RBC half-life. This was shown for homozygous mutants both before and after splenectomy, and for heterozygous mutants after splenectomy. Mutant mice also exhibited significant increases in plasma EPO, the number of erythroblasts in the spleen and bone marrow, and the number of peripheral reticulocytes. When erythrocytes were isolated in culture, mutant cells lysed spontaneously at a significantly faster rate than WT.

Shortened RBC half-life can be caused either by defective red cell maturation (dyserythropoiesis), increased RBC destruction (either intra- or extra-vascular haemolysis), or a combination of both. The presence of elevated reticulocytes with low numbers of mature RBCs in the Ampd3^{T689A} strain is suggestive of increased destruction. This is further supported by the fact that both plasma EPO, and the number of erythroblasts are elevated, suggesting mutants are able to upregulate erythropoiesis in response to anaemia. Increased RBC destruction could be mediated either by excessive splenic clearance, or by spontaneous lysis due to intrinsic red cell factors. In hereditary spherocytosis - a disorder where changes to membrane deformability cause excessive destruction of RBCs in the spleen - the resulting chronic haemolysis and shortened RBC half-life can be improved by even partial splenectomy [316]. However splenectomy only marginally increased the RBC half-life in Ampd3$^{T689A/T689A}$ mice. Therefore, it can be assumed that aberrant splenic clearance is not the cause of haemolysis. Given that mutant cells life-span is also decreased *in vitro,* cell intrinsic factors may be more important in determining the cell half-life phenotype.

The life-span of RBCs is tightly regulated, lasting some 150 days in humans, and 51 days in mice [317]. Senescent RBCs are destroyed by eryptosis; a controlled programme of cell death. Similar to the apoptotic process in non-erythroid cells, eryptosis involves cell shrinkage, breakdown of cell membrane asymmetry, and eventual phagocytosis[318]. Eryptosis differs from apoptosis in that it does not involve mitochondrial depolarisation and condensation of nuclei, due to the lack of these organelles in the mature RBC, and it does not require the involvement of caspases [319,320]. Eryptosis can be triggered by a number of stimuli, including oxidative stress [321,322], energy depletion [323], small molecules [318], anti-A IgG [324] and conjugated bilirubin [325]. Enhanced eryptosis is also observed in a number of diseases, including haemolytic anaemia, malaria, sickle cell disease,

thalassaemia, G6PD deficiency, and hereditary spherocytosis (reviewed in [318]). Eryptosis begins with an increase in cytosolic Ca^{2+}, which stimulates several events. These include cell membrane scrambling, resulting in the externalisation of phosphatidylserine (PS); activation of ion channels, resulting in the dehydration and shrinkage of the cell; and activation of a Ca-activated protease called calpain, which degrades cytoskeletal proteins and results in membrane blebbing. Eryptotic cells are then phagocytosed by both splenic and circulating macrophages; they are recognised by exposed PS, and novel antigens resulting from cleavage of Band 3, which can bind IgG [326].

To date, no studies have investigated directly whether AMPD3 has a role in programmed RBC death. However a number of observations from this study suggest that Ampd3^{T689A} erythrocytes are undergoing accelerated senescence and eryptosis; they have increased intracellular calcium, increased PS exposure, and an increased proportion of microcytic cells. Ampd3^{T689A} RBCs also exhibit a decreased concentration of adenosyl nucleotides and significantly increased amounts of ROS, both of which are known to trigger eryptosis[326]. Taken together, these observations suggest the following mechanism of reduced RBC half-life: activation of AMPD3 causes depletion of ATP, and therefore loss of ATP-dependant oxidative metabolism, which in turn increases oxidative stress. Increased oxidative stress then triggers Ca^{2+} influx, cell shrinkage, PS exposure and cell death. Interestingly, other studies have found that increases in both ROS and Ca^{2+} can also cause activation of AMPD3 [310,312]. It is therefore possible that eryptosis involves some positive feedback loops, which the Ampd3^{T689A} mutation may act on to accelerate the process.

If the mutation-induced activation of AMPD3 is indeed causing accelerated ageing and senescence of RBCs, it raises the question of whether inhibition of AMPD3 would have the opposite effect and delay RBC ageing. Several polymorphisms in *Ampd3* have been reported in humans, all of which cause either partial or complete loss of enzyme activity. Individuals with AMPD3 deficiency are clinically asymptomatic, with the only notable change being elevated ATP levels in the red cell [327]. Knockout mice have been generated for *Ampd3* and are reported to be similarly asymptomatic, aside from a build-up of adenosine nucleotides, and loss of GTP [328]. To date, no studies have investigated whether RBC half-life in either humans or mice with AMPD3 deficiency is lengthened, but it is intriguing to note that the changes in purine balance observed in these models appear to be the opposite to those changes observed in Ampd3^{T689A}. It is therefore

possible that the opposite effects on red cell half-life may also occur in Ampd3-deficient cell, i.e. extended cell half-life. If AMPD3 deficiency does lengthen the lifespan of erythrocytes, it opens the possibility that pharmacological inhibition of AMPD3 may also be able to delay senescence. This would be of particular benefit to blood banks, as donated RBCs suffer from storage lesion – a process similar to RBC senescence - which limits the time blood can be kept for transfusion [329].

Another interesting and novel finding of this study is that Ampd3$^{T689A/T689A}$ mice display cyclic reticulocytosis, in which the percentage of immature RBCs oscillates between 30% and 60% over a 5-day cycle. Spontaneous cyclic reticulocytosis has not previously been described in mice, however similar phenotypes have been observed in a number of clinical conditions, including cyclic neutropenia (CN), periodic chronic myelogenous leukemia, cyclic thrombocytopenia and periodic autoimmune haemolytic anaemia (AIHA) [330-332]. For some of these conditions, the causes of pathology have been identified [331,333-335], but these do not always explain why oscillations occur. For example, it is known that AIHA occurs when antibodies directed against an individual's own RBCs cause them to lyse, but this does not explain why some patients exhibit periodicity in their erythropoiesis and some do not [336].

Mackey *et al.* used mathematical modelling to determine if the oscillations observed in periodic AIHA could be explained purely by changes in RBC half-life. They found that a simple model of erythropoiesis - in which the rate of RBC destruction was varied and all other parameters were kept constant - accounted for the observed oscillations in hematocrit in experimentally induced AIHA in rabbits [336,337]. In this model, erythropoiesis occurred at a constant rate at low levels of RBC destruction, but when the rate of RBC destruction was increased above a certain threshold, erythropoiesis became unstable and began to oscillate. The Ampd3^{T689A} phenotype is similar to AIHA in that it appears to be caused by increased rates of RBC destruction. Although the experiments detailed in this chapter do not exclude the possibility that a more complex mechanism is causing cyclic reticulocytosis in homozygous mutants, this mathematical model provides a simple explanation for the fact that reticulocytosis does not oscillate in Ampd3$^{T689A/+}$, but does in Ampd3$^{T689A/T689A}$.

Conclusion

This chapter describes an ENU mutant mouse line with dramatically shortened RBC half-life. The causative mutation was found to be a novel gain-of-function amino acid substitution in *Ampd3* that leads to an apparent over-activation of the Ampd3 enzyme; this in turn causes a build-up of oxidative stress and accelerated senescence in the erythrocyte. This is the first time a mutation in AMPD3 has been shown to affect RBC half-life. The data suggests it may be an important mediator of RBC life span, and provides a novel avenue for future research into the causes of RBC ageing and senescence. Future studies should focus on the possibility that AMPD3 inhibition may lengthen the life span of the RBC, and the potential of this hypothesis, for example, to increase the shelf life of blood stored for transfusion.

CHAPTER 4 – MRI49372 MALARIA

Introduction

The previous chapter of this thesis described the mouse line MRI49372, which carries an ENU induced gain-of-function mutation in *Ampd3.* The Ampd3^{T689A} amino acid substitution and consequent over-activation of the AMPD3 enzyme causes an imbalance in RBC purine concentrations, characterised by low [ATP] and extremely high [GTP], [GDP] and [GMP]. Mutant mice also exhibit significantly shortened RBC half-life, increased reticulocytosis and splenomegaly. These aspects of the Ampd3^{T689A} phenotype potentially have large impacts both on *Plasmodium* growth within the erythrocyte, and the host response to malaria infection.

Plasmodium parasites need a large supply of purines and pyrimidines for DNA synthesis. They are able to synthesise the latter *de novo*, but because their genome contains only one of the 10 enzymes involved in the biosynthesis of purines (PRPP to IMP), these nucleotides must be scavenged from the host [338]. In fact, the parasite's demand for purines is so high that it exceeds the endogenous supply of the RBC, and therefore *Plasmodium* increases the uptake of exogenous purines through host erythrocyte nucleobase transporters [147,339]. Transport of purines into the parasite across the parasite plasma membrane occurs via *Pf*NT1, a high affinity, saturable nucleoside transporter that has a broad substrate specificity for purine nucleosides and their L-stereoisomers [340]. To date, *Plasmodium* is only known to import 7 purines (6 via *Pf*NT1, and one via a putative transporter that has yet to be identified) but has the full complement of enzymes necessary to recycle these into all other purines needed for growth [338,339,341,342] (Figure 4.1). As such, there has been wide interest in developing anti-malarials that block *Pf*NT1 (reviewed in [339]).

Two recent metabolomics surveys have attempted to quantify the final purine balance within the parasite. The first looked at RBCs infected with asynchronous *P. falciparum*; compared to uninfected RBCs, it found significant increases in ADP, AMP, and adenine, along with decreases in IMP and inosine [343]. The second compared isolated *P. falciparum* schizonts to uninfected RBCs, and found significant increases in ADP, AMP, IMP, GMP, GDP and several other purines, but notably, significant decreases in ATP and GTP [344]. Ampd3^{T689A} provides an interesting model to study the effect of host RBC purine balance on *Plasmodium* growth.

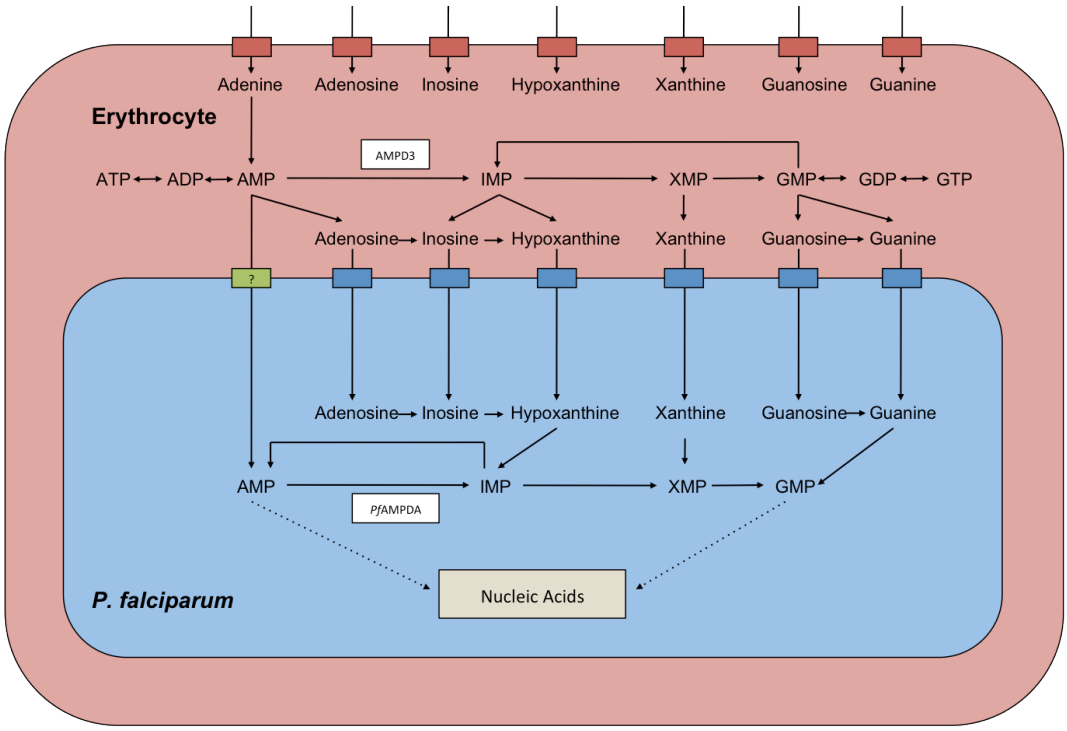

Figure 4.1: Purine metabolism in the infected erythrocyte. *P. falciparum* imports purines from the host cell, as well as increasing erythrocytic uptake of exogenous purines. White boxes show the reaction catalysed by human AMPD3, and the corresponding reaction within the parasite, catalysed by *Pf*AMPDA. Red boxes represent human erythrocyte nucleobase transporters; Blue boxes represent *P. falciparum* NT1 transporter; green box represents a putative AMP transporter. **ATP**, adenosine 5'-triphosphate; **ADP**, adenosine 5'-diphosphate; **AMP**, adenosine 5'-monophosphate; **IMP**, inosine 5'-monophosphate; **XMP**, xanthosine 5'-monophosphate; **GMP**, guanosine 5'-monophosphate; **GDP**, guanosine 5'-diphosphate; **GTP**, guanosine 5'-triphosphate.

The spleen has an essential role in malaria resistance, both in clearing infected erythrocytes, and the extramedullary erythropoiesis essential for staving off severe anaemia [345,346]. In both naïve and immune individuals, parasitaemia is higher and death more frequent after splenectomy [187]. Moreover, less severe disease has frequently been associated with the presence of splenomegaly [347]. Therefore, the Ampd3^{T689A} phenotype of splenomegaly may protect the host from severe disease.

Although timely erythropoiesis is essential to recover from the anaemia induced by infection [348], studies have also shown that the production of new RBCs too early in infection can aid the parasite by giving it a greater number of cells to invade, and therefore can result in increased mortality [348]. Therefore, the Ampd3^{T689A} phenotype of increased erythropoiesis and RBC turnover, could either mitigate or exacerbate anaemia.

The aim of this chapter was to determine if parasite growth or the host response to malarial infection is affected by the Ampd3^{T689A} mutation, and to investigate the mechanisms of any observed differences.

Results

Ampd3^{T689A} mice are resistant to erythrocytic stage *P. chabaudi* infection

To determine if mice carrying the Ampd3^{T689A} mutation are resistant to rodent malaria, mice were infected with *P. chabaudi* by intraperitoneal injection of parasitised erythrocytes. Survival and peripheral parasitaemia were monitored daily from the 7th day post infection.

Survival was significantly increased in both homozygous and heterozygous mice for both sexes. In female mice, 100% of Ampd3$^{T689A/T689A}$ and 60% of Ampd3$^{T689A/+}$ survived infection, compared to 0% of WT. In male mice, 60% of Ampd3$^{T689A/T689A}$ survived infection, compared to 0% in both Ampd3$^{T689A/+}$ and WT (Figure 4.2A and B).

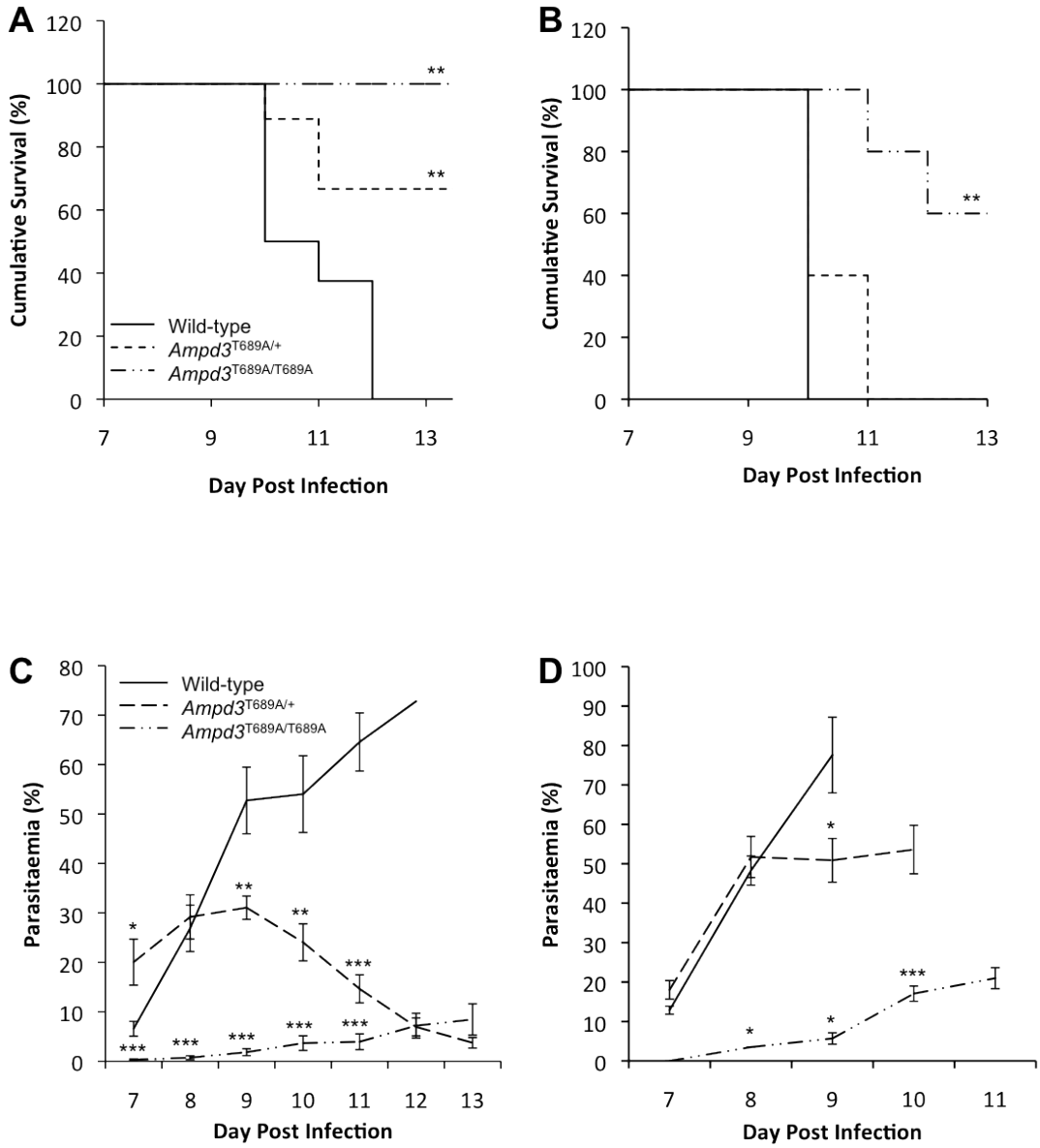

Figure 4.2: The Ampd3^{T689A} mutation causes resistance to *P. chabaudi*. Cumulative survival for **(A)** female WT (n=17), Ampd3$^{T689A/+}$ (n=11), and Ampd3$^{T689A/T689A}$ (n=6), and **(B)** male WT (n=4), Ampd3$^{T689A/+}$ (n=5), and Ampd3$^{T689A/T689A}$ (n=5) infected with *P. chabaudi*. **(C)** and **(D)** Average ± SEM parasitaemia for WT, and Ampd3$^{T689A/+}$, and Ampd3$^{T689A/T689A}$ female and male mice respectively (same n values as A and B). *P<0.05, **P<0.01, ***P<0.001. P values calculated using Log rank test **(A)** and **(B) or** student's T-test **(C)** and **(D)**.

The marked increases in survival correlated with significant reductions in overall peripheral parasitaemia. In females mean peak parasitaemia reached just 10% in Ampd3$^{T689A/T689A}$, and 31% in Ampd3$^{T689A/+}$, compared to 72% in WT. Male mice, while generally more susceptible to *P. chabaudi,* showed the same trend in lowered peak parasitaemia (Figure 4.2C and D). The growth curve was also altered in Ampd3$^{T689A/+}$. In female mice, Ampd3$^{T689A/+}$ showed significantly higher parasitaemia than WT on day 7,

but reached peak by day 9, before reducing parasite burden to 3% by day 13. In contrast, both WT and Ampd3$^{T689A/T689A}$ showed steady increases in parasitaemia, until days 12 and 13 respectively. A similar trend was observed in males, with parasitaemia peaking for Ampd3$^{T689A/+}$ on day 8, WT steadily increasing until day 9 and Ampd3$^{T689A/T689A}$ steadily increasing until day 11.

Together, these results suggest that Ampd3^{T689A} is significantly resistant to *P. chabaudi* infection, although the level of resistance appears to vary, depending on whether mice carry one or two copies of the mutation. Ampd3$^{T689A/+}$ exhibits rapid parasite replication in the early part of infection, followed by enhanced clearance and survival; Ampd3$^{T689A/T689A}$ exhibits a very slow rate of replication throughout the infection.

Ampd3$^{T689A/+}$ resistance to *P. chabaudi* is affected by splenectomy

In chapter 3 of this thesis, it was shown that mice carrying the Ampd3^{T689A} mutation exhibit splenomegaly, which is positively correlated with malaria resistance, both through increased clearance of parasitised cells and increased erythropoiesis. Therefore, it was hypothesised that the spleen might play a role in the resistance observed in Ampd3^{T689A}. To investigate this, female mice were splenectomised and then infected with *P. chabaudi.* Cumulative survival and peripheral parasitaemia were monitored daily.

All the splenectomised mice eventually succumbed to infection. However, compared to WT mice, a significant extension in the time to death was observed in Ampd3$^{T689A/T689A}$. No difference in survival was observed between WT and Ampd3$^{T689A/+}$ (Figure 4.3A). Significant differences were also observed in peripheral parasitaemia, and interestingly, trends were similar to non-splenectomised animals. Ampd3$^{T689A/+}$ had significantly higher parasitaemia than WT on days 7 and 8 post infection, but had a lower peak parasitaemia; 50% compared to 80% in WT. Ampd3$^{T689A/T689A}$ had significantly lower parasitaemia than WT on days 7-10 post infection, and peaked at 33% (Figure 4.3B). This suggested that while overall survival of the mutant mice was dependent on the spleen, differences in parasite growth – particularly in homozygotes - was dependent on other factors.

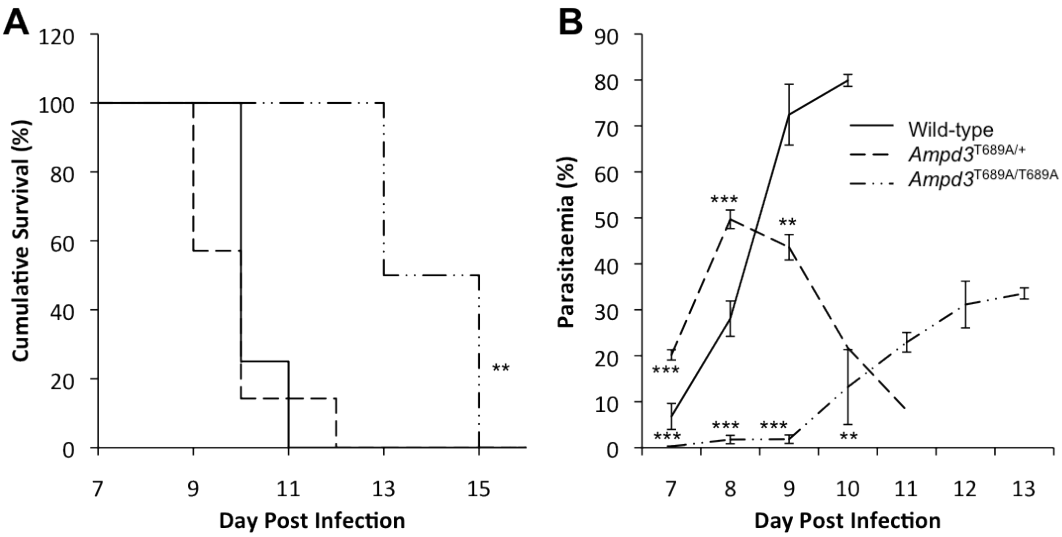

Figure 4.3: Ampd3$^{T689A/+}$ resistance to *P. chabaudi* is spleen mediated. **(A)** Cumulative survival and **(B)** Average ± SEM parasitaemia for splenectomised female WT (n=8), Ampd3$^{T689A/+}$ (n=8), and Ampd3$^{T689A/T689A}$ (n=4) infected with *P. chabaudi*. **P<0.01, ***P<0.001. P values calculated using the Log rank test **(A)** or student's T-test **(B).**

Ampd3$^{T689A/T689A}$ is susceptible to *P. berghei*

In chapter 3 of this thesis, it was shown that Ampd3$^{T689A/T689A}$ have severely accelerated erythrocyte ageing and shortened half-life; these mice lose approximately a quarter of their RBCs every day. This phenotype was only marginally improved by splenectomy, and may be exacerbated during infection, as it has been shown *in vitro* that *P. falciparum* is able to induce biochemical changes in the membranes of uninfected and infected erythrocytes alike, that cause accelerated ageing of RBCs [349]. It is therefore possible that the slow increase in parasitaemia observed in Ampd3$^{T689A/T689A}$ is caused by the fact that many merozoites are invading cells that will be eliminated during their replication cycle. To determine if the short half-life of RBCs was contributing to the low parasitaemia observed in *P. chabaudi* infection, mice were infected with *P. berghei,* which has a tropism for reticulocytes. By favouring immature cells, *P. berghei* is far more likely than *P. chabaudi* to invade RBCs that are going to remain in circulation for the full 24 hours needed to complete replication. Therefore the shortened half-life phenotype will have much less affect on *P. berghei* than *P. chabaudi.*

During *P. berghei* infection, no significant difference in survival was observed between the *Ampd3*$^{T689A/T689A}$ and WT. Significantly more Ampd3$^{T689A/+}$ survived to day 14 (P=0.0325), but by day 22 all mice had succumbed to infection (Figure 4.4A). Ampd3$^{T689A/T689A}$ had significantly higher parasitaemia than WT on days 7-10 post infection, peaking at 46%, compared to 11% in WT. Ampd3$^{T689A/+}$ had significantly higher parasitaemia than WT on days 9 and 10 post infection, peaking at 27%. (Figure 4.4B). Together these results suggest that Ampd3$^{T689A/T689A}$ is not resistant to *P. berghei*, and that short RBC half-life may be a major contributor to the resistance observed in *Ampd3*$^{T689A/T689A}$ during *P. chabaudi* infection

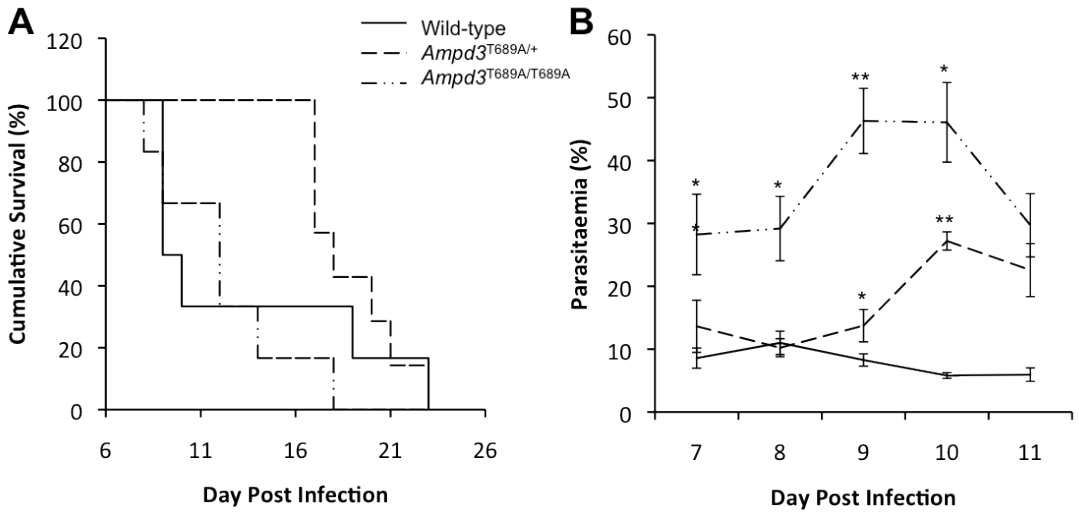

Figure 4.4: Ampd3$^{T689A/T689A}$ are not resistant to *P. berghei*. (A) Cumulative survival, **(B)** Average ± SEM parasitaemia and for WT (n=6), Ampd3$^{T689A/+}$ (n=7), and Ampd3$^{T689A/T689A}$ (n=6) infected with *P. berghei*. **P<0.01, ***P<0.001. P values calculated using the Log rank test **(A)** or student's T-test **(B and C).**

The Ampd3^{T689A} mutation stimulates reticulocytosis during infection

Severe anaemia is one of the major causes of morbidity and mortality during *Plasmodium* infection. Given that Ampd3^{T689A} mice have increased rates of erythropoiesis when uninfected, it was hypothesised that they may be able to increase RBC production in response to infection more efficiently than WT, and that this may play a role in their increased survival.

To determine if Ampd3^{T689A} increase erythropoiesis in response to infection, circulating reticulocyte numbers were monitored daily over the course of *P. chabaudi* infection in both splenectomised and non-splenectomised female mice. Concordant with the results from uninfected mice (discussed in chapter 3), Ampd3^{T689A} had a significantly higher proportion of reticulocytes than WT. On day 7 of infection in non-splenectomised mice, the average proportion of reticulocytes was 2% in WT, 10% in Ampd3$^{T689A/+}$, and 46% in Ampd3$^{T689A/T689A}$. The same trend was observed in splenectomised mice on day 7; the average proportion of reticulocytes was 2% in WT, 12% in Ampd3$^{T689A/+}$, and 43% in Ampd3$^{T689A/T689A}$.

Differences between mutant and WT mice were also apparent in the rate of reticulocytosis observed over the course of infection. In non-splenectomised mice, Ampd3$^{T689A/T689A}$ and WT mice maintained steady reticulocytosis between 46-61% and 2-5% respectively. Conversely, Ampd3$^{T689A/+}$ steadily increased reticulocytosis from 10% to 58% over the course of infection (Figure 4.5A). In splenectomised mice this trend was unchanged for WT, but was altered for both mutants; reticulocytosis remained between 8-16% in Ampd3$^{T689A/+}$, and fell from 43% to 19% in Ampd3$^{T689A/T689A}$ (Figure 5B). In both splenectomised and non-splenectomised mice the level of reticulocytosis did not appear to be related to the level of *P. chabaudi* parasitaemia.

Reticulocytosis was also monitored over the course of infection with *P. berghei.*
At the beginning of infection, on day 7, reticulocytosis was significantly higher in the mutants; 3.8% in Ampd3$^{T689A/+}$ and 23% in Ampd3$^{T689A/T689A}$, compared to 0.5% in WT. In Ampd3$^{T689A/T689A}$ the proportion of reticulocytes increased to 49% over the course of infection. In Ampd3$^{T689A/+}$ the proportion of reticulocytes increased from 3.8% to 28% over the same period. In WT mice the percentage of reticulocytes remained below 1.5% until day 9, then rose to 7.4% by day 11 (Figure 4.5C). In *P. berghei* infection, parasitaemia was closely related to the level of reticulocytosis in both homozygous and heterozygous mutants, but appeared to be unrelated in WT mice.

Although the percentage of reticulocytes observed in homozygous mutants during both *P. chabaudi* and *P. berghei* infection was remarkably high when compared to WT, it was not higher than the average peak (64%) observed in uninfected mice (discussed in chapter 3, Figure 3.7). Ampd3$^{T689A/+}$ however, increased far above its highest average when uninfected (9.7%). Therefore, these results show that non-splenectomised Ampd3$^{T689A/+}$ are able to increase erythropoiesis in response to *Plasmodium* infection, even at low parasitaemia. This may help to alleviate anaemia, and therefore increase survival.

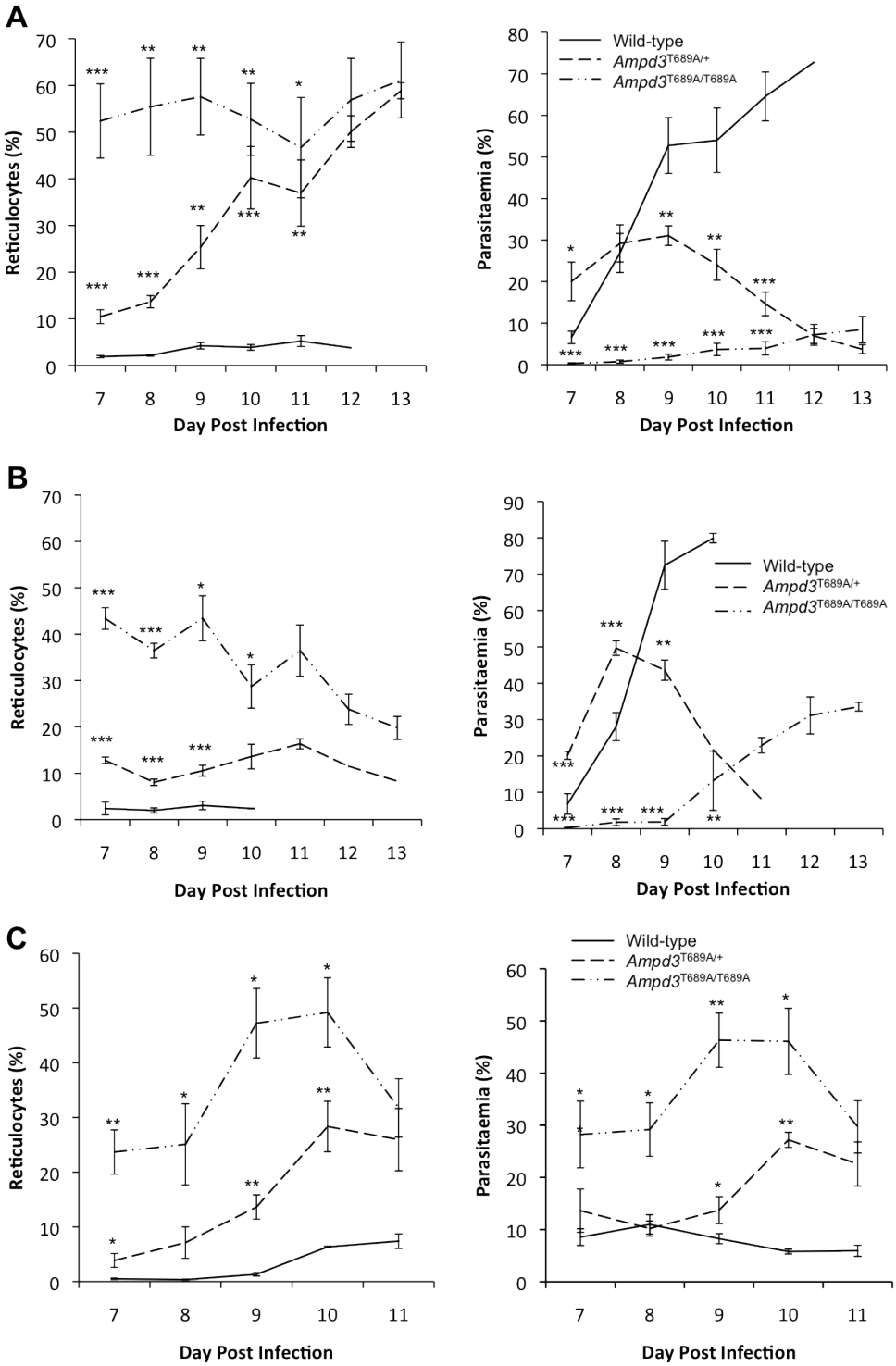

Figure 4.5: Ampd3^{T689A} has altered reticulocytosis in response to infection. Average ± SEM proportion of reticulocytes and parasitaemia in **(A)** *P. chabaudi* infected female WT (n=17), Ampd3$^{T689A/+}$ (n=11), and Ampd3$^{T689A/T689A}$ (n=6). **(B)** Splenectomised *P. chabaudi* infected female WT (n=8), *Ampd3*$^{T689A/+}$ (n=8), and Ampd3$^{T689A/T689A}$ (n=4). **(C)** *P. berghei* infected WT (n=6), Ampd3$^{T689A/+}$ (n=7), and Ampd3$^{T689A/T689A}$ (n=6). *P<0.05, **P<0.01, ***P<0.001. P values calculated using the student's T test.

The Ampd3^{T689A} mutation causes increased gametocytogenesis

During the blood stage of infection, some merozoites will divert from asexual replication to form either male or female gametocytes. The precise cause of commitment to gametocytogenesis remains unclear, but several potential triggers have been identified, including increased numbers of reticulocytes [239], and parasite density [241]. Observations made during the *P. chabaudi* and *P. berghei* infections detailed above suggested that Ampd3^{T689A} might be producing increased amounts of gametocytes. Therefore, an examination of gametocytogenesis was conducted.

During *P. chabaudi* infection, the rate of gametocytogenesis was very low in WT mice; the average proportion of gametocytes compared to asexual parasites was 0.1%. This was significantly increased to 2.7% in Ampd3$^{T689A/+}$, and 1.6% in Ampd3$^{T689A/T689A}$. In splenectomised mice, gametocytogenesis in WT remained at 0.1%, but in mutants was reduced to 0.7% in Ampd3$^{T689A/+}$ and 0.3% in Ampd3$^{T689A/T689A}$ (Figure 4.6A). Significantly higher gametocytogenesis was also observed in *P. berghei* infection, although the increase was far smaller than in *P. chabaudi*; gametocytes were observed at an average of 0.4% in WT, 0.7% in Ampd3$^{T689A/+}$ and 1% in Ampd3$^{T689A/T689A}$ (Figure 4.6C).

Interestingly, for *P. chabaudi*, gametocytogenesis was not associated with the number of reticulocytes present; homozygotes had consistently lower gametocytogenesis than heterozygotes, despite having up to five times the proportion of immature cells. A similar trend was observed in relation to parasite density; the highest levels of gametocytogenesis were observed in non-splenectomised Ampd3$^{T689A/+}$ despite these mice having lower peak parasitaemia than both WT mice and splenectomised Ampd3$^{T689A/+}$. Some of the *P. chabaudi* gametocytes were also observed to contain large vacuoles.

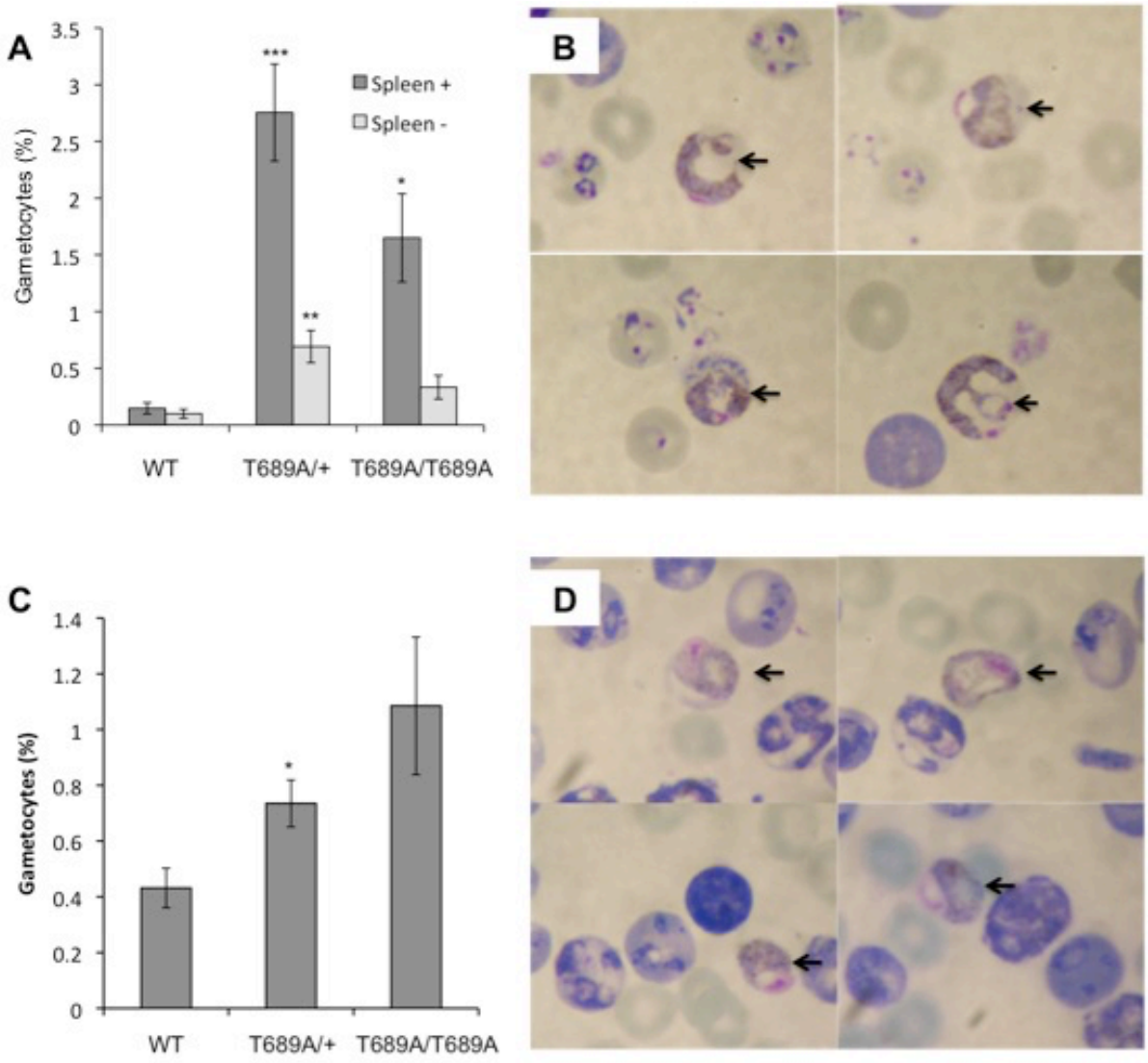

Figure 4.6: The Ampd3^{T689A} mutation causes increased gametocytogenesis. **(A)** Average ± SEM proportion of parasites that are gametocytes, counted on the day of peak parasitaemia, for splenectomised (-) and non-splenectomised (+) female WT (n=6), Ampd3$^{T689A/+}$ (n=7), and Ampd3$^{T689A/T689A}$ (n=6) infected with *P. chabaudi.* **(B)** Light microscopy images of Giemsa stained thin smears from *P. chabaudi* infected Ampd3$^{T689A/+}$. Arrows indicate gametocytes. **(C)** Average ± SEM proportion of parasites that are gametocytes, counted on the day of peak parasitaemia, for WT (n=6), Ampd3$^{T689A/+}$ (n=6), and Ampd3$^{T689A/T689A}$ (n=4) infected with *P. berghei.* **(D)** Light microscopy images of Giemsa stained thin smears from *P. berghei* infected Ampd3$^{T689A/+}$. Arrows indicate gametocytes. *P<0.05, ** P<0.01, ***P<0.001. P values calculated using the student's T-test.

Ampd3^{T689A} RBCs support increased *P. chabaudi* invasion and growth

Despite an increase in survival to *P. chabaudi* infection, the *Ampd3*$^{T689A/+}$ female mice displayed a higher parasitaemia than WT mice during the early stages of infection. A possible explanation for this observation is that the parasites are able to invade and/or grow in the *Ampd3*$^{T689A/+}$ cells at a greater rate that WT cells.

To investigate this hypothesis an *in vivo* invasion and growth assay was conducted as previously described [350]. Blood was collected from both Ampd3$^{T689A/+}$ and WT mice, and labelled with different fluorescent markers (Atto-633 and Biotin). The labelled blood was mixed in equal proportions and injected into *P. chabaudi* infected WT mice between 12:00 and 2:00 am, while the parasites were undergoing schizogony. Blood samples were collected at different times following injection and analysed by flow cytometry. The parasitaemia of each labelled population was monitored over a period of 21 hours to determine if there were any differences in the rate of parasite invasion and growth.

At all time points analysed, a higher proportion of parasites was observed in Ampd3$^{T689A/+}$ than WT cells. (Figure 4.7A) Although this difference was modest (1.1 fold on average) it was significant at both 3 and 12 hours post injection.

In this experiment, parasites were detected by thiazole-orange, which stains RNA, and Hoechst, which stains DNA. At the 12-hour timepoint, two populations were visible that were positive for both dyes: one with high, and one with low levels of staining. It was assumed that the 'low' population represented ring stage parasites with small amounts of RNA and DNA, and that the 'high' population represented trophozoite and/or schizont stage parasites that are undergoing translation and replication, and therefore have a higher amount of RNA and DNA. In these samples, the proportion of 'high' parasites in mutant cells was almost double that of WT – 39% compared to 20% - suggesting that parasites are able to mature faster within Ampd3$^{T689A/+}$ RBCs (Figure 4.7B).

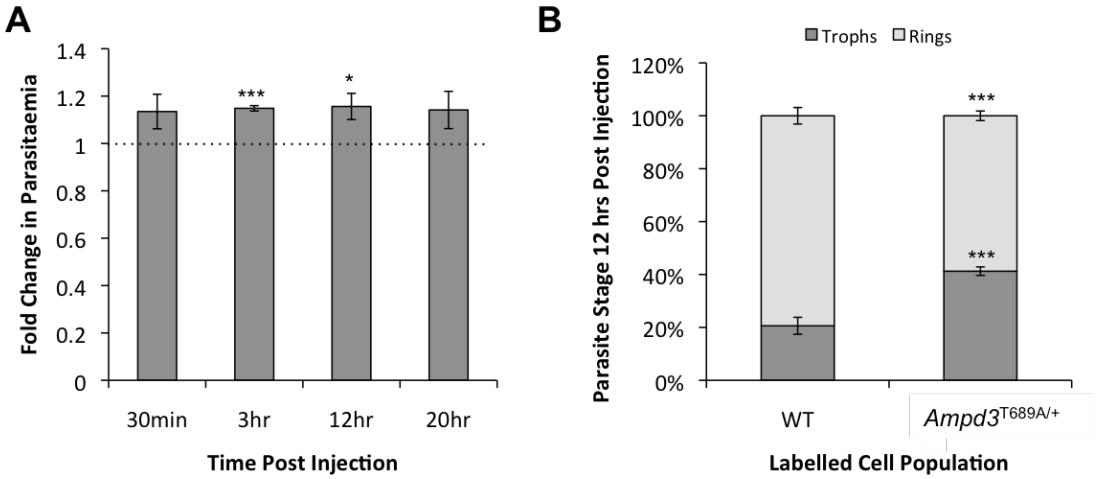

Figure 4.7: The Ampd3^{T689A} mutation causes increased *P. chabaudi* invasion and growth.

(A) Average ± SEM fold change in parasitaemia compared to WT, for Ampd3$^{T689A/+}$ labelled RBCs. Dotted line indicates equal ratio of WT to mutant. **(B)** Average ± SEM proportion of ring (thizol-orange^{low}, hoechst^{low}), and trophozoite (thizol-orange^{high}, hoechst^{high}) stage parasites within labelled WT and Ampd3$^{T689A/+}$ cells. N=7, *P<0.05, ***P<0.001. P values calculated using the student's T-test.

Given the dramatically altered purine balance within Ampd3^{T689A} cells, it was hypothesised that high GTP levels, either directly or indirectly, may be responsible for the increased parasite growth observed in mutant cells. Therefore, the effect of GTP on *P. falciparum* growth was measured *in vitro*. First, in order to determine if the purine can cross the RBC membrane, human erythrocytes obtained from the Red Cross Blood Service as expired transfusion material were incubated with 13C-labelled GTP. After incubation in 5mg/ml 13C-GTP, labelled GTP was observed within the RBC at 80 times the abundance of unlabelled GTP. This is approximately equal to the increase in GTP concentration observed in the RBCs of Ampd3$^{T689A/T689A}$. Conversion of 13C-GTP to both 13C-GDP and 13C-GMP was also observed. The proportion of these species compared to their unlabelled counterparts was 9 and 2.6 fold respectively (Figure 4.8A). This indicated that not only can GTP be taken up by human red cells maintained under *in vitro* culture conditions, but that purine metabolism is active in these cells, and that GTP levels equivalent to those in the Ampd3$^{T689A/T689A}$ mouse can be achieved.

To determine the effect of GTP on *P. falciparum* growth, RBCs were incubated in increasing concentrations of GTP to alter their GTP content. The cells were then washed to remove exogenous GTP, and used to culture *P. falciparum* for 48 hours. GTP increased parasite growth in a dose dependant manner, with up to 40% more parasites at the highest concentration of 5mg/ml, than in untreated cells (Figure 4.8B). This concentration should be equivalent to the levels of GTP observed in Ampd3$^{T689A/T689A}$ RBCs.

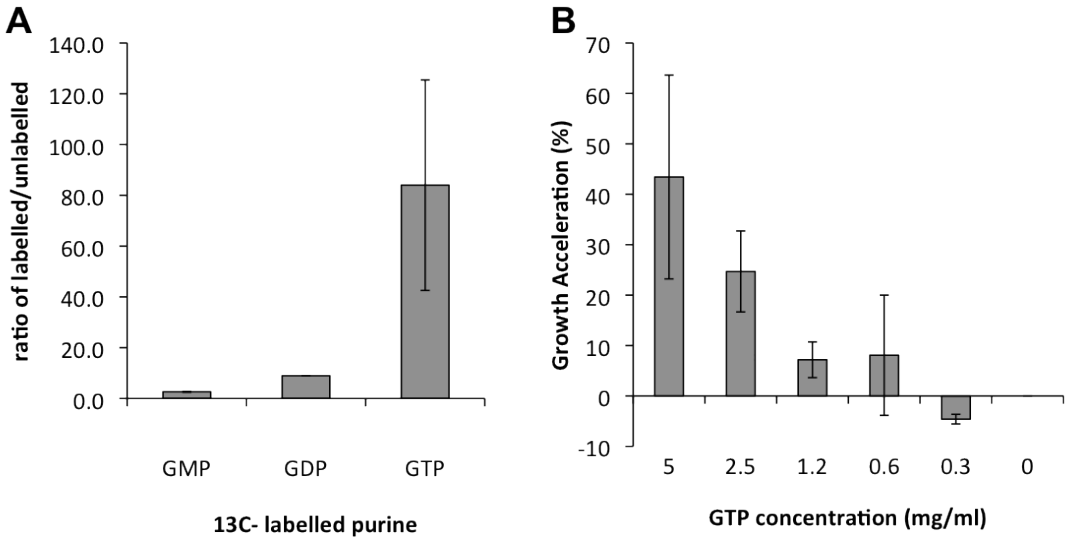

Figure 4.8: High GTP causes increased parasite growth. **(A)** Average ± SEM ratio of 13C-labelled purines within RBCs incubated for ~ 20 seconds (T=0hrs) with 13C-GTP. **(B)** Average ± SEM percentage increase in parasite growth, for parasites cultured in RBCs treated with GTP compared to untreated cells. Combined results of two independent experiments.

Discussion

This study provides the first evidence that AMPD3 has a role in the host response to malaria infection. It shows that activation of the enzyme leads to resistance to *P. chabaudi*, but not *P. berghei.* It also shows that changes to the purine balance within the RBC can affect both invasion and growth of the parasite. Erythrocyte polymorphisms can have both RBC-autonomous and systemic effects that change the course of malaria infection. That is, they may alter the RBC's ability to support parasite growth, or they might cause changes to the immune or erythropoietic systems that make the animal more resistant to the pathology of disease. In the case of Ampd3^{T689A} it appears that both processes are involved; the mutation makes each individual RBC more habitable to *Plasmodium*, but also causes increases in erythropoiesis and RBC turnover that enable mice to better survive infection.

Ampd3^{T689A} resistance to P. chabaudi *is meditated by the spleen, and by high RBC turnover.*

Both Ampd3$^{T689A/+}$ and Ampd3$^{T689A/T689A}$ were observed to be significantly resistant to *P. chabaudi* infection. However, differences were observed in the parasitaemia curves of homozygous and heterozygous mutants, suggesting the mechanism of resistance might be different in each case. Splenectomy abrogated the increased survival in heterozygotes, but not homozygotes. In *P. berghei* – which was used to remove the effect of RBC half-life - heterozygotes still had increased survival, but homozygotes were no longer significantly different to WT. Together, these results suggest that the spleen mediates Ampd3$^{T689A/+}$ resistance, and short RBC half-life mediates Ampd3$^{T689A/T689A}$ resistance.

The spleen has three important roles in the host response to malaria infection: it removes infected RBCs from circulation; it forms part of the immune response by producing dendritic cells, T cells and B cells; and it produces new erythrocytes to help alleviate anaemia (reviewed in [351]). The experiments detailed here did not investigate the immune response to infection; therefore the possibility that it has some role in Ampd3^{T689A} resistance cannot be excluded. In *P. chabaudi* infection, Ampd3$^{T689A/+}$ parasitaemia peaks on day 8 or 9, and then decreases to below 10%. This could be explained by a more active adaptive immune response causing increased removal of parasitised erythrocytes from circulation. However, it should be noted that the heterozygous mutants are able to limit parasitaemia both in the presence and absence of their spleens. This suggests that if the immune system is causing the decrease in

parasitaemia observed in these animals, systemic and peripheral protective factors are more likely to be involved.

The Ampd3^{T689A} mutation causes increased reticulocytosis during malaria infection.

Investigation of erythropoiesis during infection showed that Ampd3$^{T689A/+}$ was able to increase reticulocytosis in response to both *P. chabaudi* and *P. berghei* infection. This did not occur in splenectomised mice, suggesting the spleen mediated the observed increase in erythropoiesis. Given that splenectomy also reduced cumulative survival in Ampd3$^{T689A/+,}$ it is likely that increased RBC production is an important factor in the survival of these animals. Although no increase in reticulocytosis was observed over the course of *P. chabaudi* infection in Ampd3$^{T689A/T689A}$, it is worth noting that the oscillations in reticulocytosis normally observed in these animals (discussed in chapter 3) appear to be absent. This may simply be a factor of sample size, or perhaps small changes due to infection that make the oscillations harder to observe. Alternately, 60% may represent the maximal rate of reticulocytosis, and so 'increased' erythropoiesis in these mutants means just that the 'troughs' of the cycle are removed. As in Ampd3$^{T689A/+}$, splenectomy resulted in a lower level of reticulocytosis in homozygous mutants over the course of infection, suggesting that the spleen mediated the maintenance of reticulocytosis above 40% in these animals.

Death from *P. chabaudi* is caused by severe anaemia, therefore splenomegaly and extramedullary erythropoiesis are key components of survival in resistant mouse lines [345,346]. During malaria infection erythropoiesis is not always able to compensate for the loss of RBCs, and anaemia can be exacerbated by an abnormal decrease in circulating reticulocytes [352]. This proved true for WT mice, in which the proportion of reticulocytes remained static over the course of infection in both the presence and absence of spleens. Dyserythropoisis during malaria infection can be caused by several mechanisms, including low EPO production [353,354], parasite suppression of erythropoiesis via hemozoin [355-357], and host suppression of erythropoiesis via inflammatory cytokines [358,359]. It is possible that differences in one of these mechanisms enable Ampd3^{T689A} to maintain and up-regulate erythrocyte production during infection, and because of this, they are protected from severe anaemia and survive. Future research into the hormone and cytokine profiles of infected mutants may shed more light on the causes of severe malarial anaemia, and uncover ways to stimulate erythropoiesis in infected individuals.

The Ampd3^{T689A} mutation causes increased gametocytogenesis

Associated with the high rates of erythropoiesis in Ampd3^{T689A} was significantly elevated gametocytogenesis. It is known that the parasite is able to adapt its rate of gametocytogenesis to changes in the host environment [238]. *In vitro*, gametocytogenesis has been shown to increase in response to the addition of reticulocytes [239], erythroid progenitors [360], red cell lysate [238], human serum and lymphocytes [240], parasite density [241], as well the hormones insulin, progesterone, 17-beta-estradiol and testosterone [242]. In chickens, reticulocytosis has been shown to change the male/female ratio of *P. gallinaceum* gametocytes, but not the number [361]. In Ampd3^{T689A}, during *P. chabaudi* infection, gametocytogenesis was most highly elevated in non-splenectomised mice; that is, mice that were actively increasing their rate of erythropoiesis. In splenectomised mice, where erythropoiesis remained static, the level of gametocytogenesis was dramatically reduced. The work presented here did not investigate if the two phenomena were linked, and it is possible that they are occurring coincidentally. However, this suggests that the trigger for increased gametocytogenesis may be the same trigger that allows *Ampd3*$^{T689A/+}$ to increase erythropoiesis in response to infection. Similarly, the level of gametocytogenesis was highest in Ampd3$^{T689A/+}$, despite these mice having five times fewer reticulocytes than Ampd3$^{T689A/T689A}$. This suggests that gametocytogenesis is not caused by the presence of reticulocytes as such, but rather by increases in EPO or some other signal associated with the host response to anaemia. It is of note that the *P. chabaudi* gametocytes appear to have large vacuoles, which are not normally observed in this species. Further research into whether these gametocytes are able to infect mosquitoes may provide novel insight into the conditions necessary for gametocytogenesis, and ways in which sexual development can be altered.

High [GTP] causes increased parasite growth

The fact that higher parasitaemia was observed in both Ampd3$^{T689A/+}$ early in *P. chabaudi* infection, and in Ampd3$^{T689A/T689A}$ in *P. berghei* infection, suggested that the Ampd3^{T689A} mutation causes RBC autonomous effects that favour parasite growth. This was further supported by the *in vivo* invasion assay, which suggested that *P. chabaudi* might able to invade Ampd3$^{T689A/+}$ cells more easily and grow faster within them. Further, *in vitro* assays with *P. falciparum* and human red cells showed that GTP is able to increase parasite growth in a dose dependent manner.

It is worth being cautious when interpreting the *P. berghei* results, beyond the observation that the parasite can grow well within mutant cells. Besides its tropism for immature RBCs, *P. berghei* differs from *P. chabaudi* in a number of metabolic enzymes, which might be affected by purine balance [138,362]. Furthermore, *P. berghei* is known to cause cerebral malaria in some mouse lines, although it is not usually observed in the SJL/J mice used in these experiments [363]. Neither of these traits was investigated in this chapter, therefore the possibility that they cause the varied susceptibility of Ampd3^{T689A} to *P. chabaudi* and *P. berghei* cannot be excluded.

The fact that Ampd3$^{T689A/+}$ cells have equal or slightly increased rates of invasion when compared to WT is surprising, given the purine balance within them. Past research has consistently shown that higher ATP concentration is associated with greater rates of invasion [137,139], and that loss of ATP is associated with lower rates of invasion [364]; yet this is not observed in Ampd3$^{T689A/+}$, despite a twofold decrease in ATP concentration (Chapter 3, Figure 5C). Research investigating the effect of purines on *Plasmodium* invasion tends to focus heavily on ATP, and therefore it is unknown if the receptors and ligands involved in this process respond equally well to other purines - such as GTP – which are present at high concentrations in *Ampd3*$^{T689A/+}$ RBCs.

The increased growth of *P. chabaudi* in mutant cells is also surprising. There are several notable changes in the purine balance of Ampd3$^{T689A/+}$ cells, the most obvious of which is a 4 fold increase in [GMP] and [GDP], and a 2 fold increase in [GTP] (Figure 3.5C). However, it is difficult to speculate on how these changes could influence parasite growth. Purine metabolism involves a multitude of interconnected and tightly regulated reactions, which are further complicated in the parasitised erythrocyte by transport across the PVM. The only purines known to be imported into the parasite are adenosine, inosine, hypoxanthine, xanthine, guanine, guanosine and AMP (reviewed in [339]) (Figure 4.1). Of these, adenosine, inosine, and guanosine could not be measured in mutant cells; hypoxanthine, xanthine and guanine were not significantly different between WT and Ampd3$^{T689A/+}$; and AMP was significantly less abundant in Ampd3$^{T689A/+}$ (Appendix A). Given the fact that the parasite is able to import exogenous purines and recycle them to suit its requirements, it is possible that the changes in host purine balance are not affecting the parasite directly, but through their impact on other host factors used by the parasite.

The ability of GTP to increase parasite growth in a dose dependent manner *in vitro*, suggests that the high concentration of GTP found within Ampd3^{T689A} cells may provide an environment that is more favourable to *Plasmodium* growth than WT. Besides its importance in DNA synthesis, GTP provides an essential source of chemical energy, and acts as a co-factor for a wide range of metabolic reactions necessary for cell growth and protein synthesis [365-370]. However, this study faced a number of limitations that make it difficult to determine exactly how GTP might increase parasite growth. First, although the experiments with labelled GTP indicate that the purine is able to cross the RBC membrane, the time course used in this experiment was not optimal for gaining an accurate picture of how this is occurring. Even at the T=0hrs time-point, large amounts of 13-C GTP were observed within the RBC. This could indicate that either GTP is moving across the RBC membrane within a matter of seconds, or that 13-C GTP is simply sticking to the RBC membrane, and is therefore not removed from the extracellular environment during washing steps. Therefore, it is unclear from these experiments if GTP is acting on the parasite directly, or through secondary changes to the RBC membrane or to the concentration of other purines. It should also be noted that in the *in vitro* studies high [GTP] is occurring with normal [ATP], but in the mutants high [GTP] occurs with low [ATP]. ATP is also an essential source of chemical energy, and therefore, the *in vitro* studies may not capture changes to growth that are caused when high [GTP] is coupled with a lack of adenosyl nucleotides.

Nevertheless, the results described here are concordant with a recent study, which showed that GTP was able to increase bacterial growth in a dose dependent manner [371]. Interestingly, this study also showed that when GTP concentration increased past a threshold, it became toxic and began to slow cell growth again. It is possible that the same is true for *P. chabaudi,* and that such a mechanism may explain the slow parasite growth observed within Ampd3$^{T689A/T689A}$, which have a 74 fold increase in [GTP] compared to WT. However, incubation with 5mg/ml was able to elevate erythrocyte GTP concentration 80 fold, and this concentration was also able to increase *P. falciparum* growth by 40%. Although *P. falciparum* and *P. chabaudi* are different species, and so may have different susceptibilities to [GTP], this result suggests that GTP is beneficial, rather than detrimental to parasite growth in Ampd3$^{T689A/T689A}$. Further research is needed to determine if GTP is being imported into the parasite from the host erythrocyte, and if so, how it is effecting increased parasite growth.

Conclusion

In this chapter it has been shown that the Ampd3^{T689A} mutation causes two different alterations to *Plasmodium* growth within the host. The high erythrocyte turnover and increased erythropoiesis caused by AMPD3 activation, provides dramatic resistance to *P. chabaudi* infection. At the same time, reticulocytosis was associated with greatly increased gametocytosis. Finally, high GTP within the RBC may promote parasite growth. This highlights the complexities of altering erythrocyte enzymes in the quest for a host-directed therapy. Further investigation of this mutant may uncover a way to activate erythropoiesis during infection, and protect an individual from developing severe malarial anaemia. However, if the same therapy also increases intrinsic parasite growth and gametocytosis (and therefore malaria transmission), this would make it a less desirable as a potential treatment approach.

.

CHAPTER 5 – RBC10

Introduction

A mouse line expressing an activated form of KCC1 was produced using ENU mutagenesis, by our collaborators at Monash University. The induced dominant mutation is an M to K substitution at amino acid 935 of the protein, which is predicted to lie in a cytoplasmic domain of the membrane-bound protein (Figure 5.1). Functionally, the mutation is known to impair phosphorylation of the neighbouring regulatory threonines, leading to over-activation of the transporter. The resulting increase in K+ efflux from the RBC causes $Kcc1^{M935K}$ mice to display a microcytic anaemia, with homozygous mutants showing a 21% decrease in MCV, 8% decrease in total haemoglobin, and 21% increase in number of red cells (Table 5.1).

The potassium content of the RBC has a large effect on intra-erythrocytic *Plasmodium*. 12-18 hrs after invasion, K+ efflux and Na+ influx through the new permeability pathway adjusts the high potassium environment within the erythrocyte to more closely resemble the low potassium environment of the plasma [372]. This outwardly directed K+ gradient is needed for normal parasite growth, and helps maintain the parasite plasma membrane potential [373,374].

KCC channels - transporters of potassium and chloride ions - mediate potassium efflux in the uninfected RBC. Three KCC isoforms - KCC1, KCC3, and KCC4 - are expressed in the erythrocyte. KCC3 is expressed consistently throughout the lifespan of the RBC, and is thought to be the major mediator of erythrocyte K-Cl transport; the expression of both KCC1 and KCC4 declines with erythrocyte age [375]; KCC1 is normally most active within reticulocytes as they undergo the volume changes associated with maturation [375-377]. Overactivity of KCC1 is one of the features of Sickle Cell Disease, and is thought to contribute to pathogenic cell sickling by dehydrating the RBC. Interestingly, K+ efflux through KCC1 has been postulated as a mechanism for the malaria resistance observed in HbAS individuals, as it has been associated with parasite death, independent of cell sickling [378].

The aim of this chapter was to determine if $Kcc1^{M935K}$ mice have an altered susceptibility to malaria, and if so, how this response is mediated.

Table 5.1: **Haematological parameters of Wild-type, Kcc1$^{M935K/+}$ and Kcc1$^{M935K/M935K}$ mice.** Full blood analysis was carried out by Fiona Brown at Monash University, on 7 week old male WT (n=12), Kcc1$^{M935K/+}$ (n=19), and Kcc1$^{M935K/M935K}$ (n=11) mice. MCV = mean corpuscular volume; MCH = mean corpuscular haemoglobin; MCHC = mean corpuscular haemoglobin concentration; RDW = red cell distribution width. Values are mean ± SD. *p <0.05 compared with wild type animals (WT); #p<0.05 compared with Kcc1$^{M935K/+}$ animals. P values calculated using a two-tailed student's T test.

	Wild-type	Kcc1$^{M935K/+}$	Kcc1$^{M935K/M935K}$
Hemoglobin (g/dL)	16.66 ± 0.51	15.87 ± 0.39*	15.33 ± 0.55*
Red cells (x 10^{12}/L)	11.17 ± 0.32	12.31 ± 0.47*	13.61 ± 0.40*#
Hematocrit (%)	49.71 ± 0.95	48.23 ± 1.59*	47.51 ± 1.96*#
MCV (fl)	44.52 ± 0.84	39.20 ± 0.67*	34.91 ± 0.92*#
MCH (pg)	14.90 ± 0.56	12.91 ± 0.37*	11.26 ± 0.33*#
MCHC (g/dL)	33.45 ± 0.81	32.95 ± 0.80	32.31 ± 1.01
RDW (%)	15.97 ± 1.81	18.05 ± 1.20*	19.45 ± 0.89*#
Reticulocytes (%)	2.68 ± 0.53	2.74 ± 0.60	3.0 ± 0.50
Platelets (x10^9/L)	1007 ± 98	1020 ± 116	1113 ± 119
White cells (x10^9/L)	8.48 ± 1.38	8.23 ± 2.27	10.36 ± 3.02

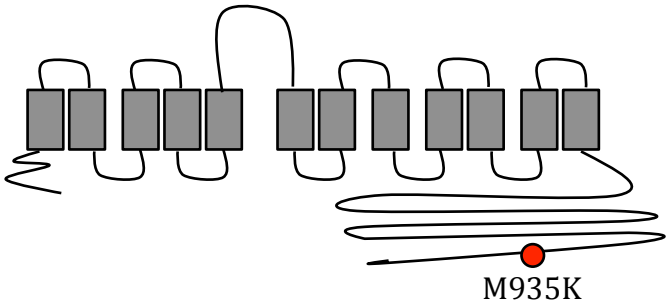

Figure 5.1. Schematic representation of KCC1 protein, showing the location of the M935K mutation.

Results

Kcc1^{M935K} is resistant to *P. chabaudi* and *P. berghei*.

To determine if the Kcc1^{M935K} mutation causes resistance to malaria, mice were challenged with *P. chabaudi* and with *P. berghei.* Cumulative survival and peripheral parasitaemia were monitored daily over the course of infection. The Kcc1^{M935K} mutation is carried on a mixed BALB/c and C57BL/6 background; homozygotes are viable and exhibit the strongest RBC phenotype. Therefore, only wild-type Kcc1$^{+/+}$ (referred to as WT) and homozygous Kcc1$^{M935K/M935K}$ mice were used in these experiments. Mice were derived from WT x WT and Kcc1$^{M935K/M935K}$ x Kcc1$^{M935K/M935K}$ breeding pairs, which were established from WT and Kcc1$^{M935K/M935K}$ littermates.

When infected with *P. chabaudi* by intraperitoneal injection of 1x10^{5} parasitised erythrocytes, no differences in survival or parasitaemia were observed (Figure 5.2). This suggested that Kcc1$^{M935K/M935K}$ were not more susceptible to *P. chabaudi* than WT. However, given ≥90% of mice survived infection, this experiment could not indicate whether Kcc1$^{M935K/M935K}$ mice were more resistant to infection. Therefore mice were infected with a higher dose of *P. chabaudi*, to lower the rate of survival.

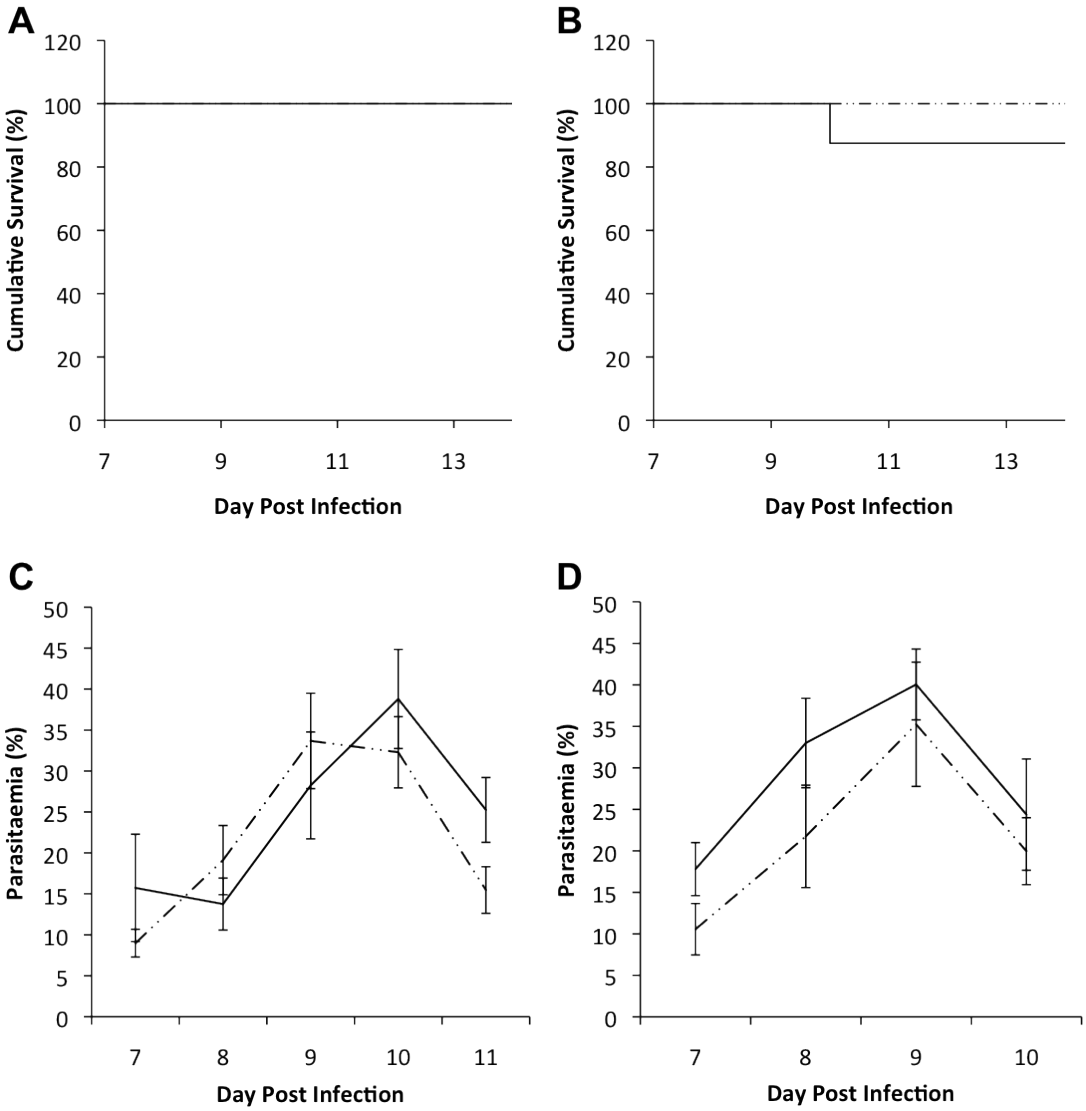

Figure 5.2: The Kcc1^{M935K} mutation does not increase susceptibility to infection with 1x10^{5} *P. chabaudi* parasitased erythrocytes. (A) and **(B)** Cumulative survival for WT (solid lines) and Kcc1$^{M935K/M935K}$ (dashed lines) male and female mice respectively. **(C)** and **(D)** average ± SEM parasitaemia for WT (solid lines) and Kcc1$^{M935K/M935K}$ (dashed lines) male and female mice respectively. WT male n=10, WT female n=8, Kcc1$^{M935K/M935K}$ male n=10, Kcc1$^{M935K/M935K}$ female n=8.

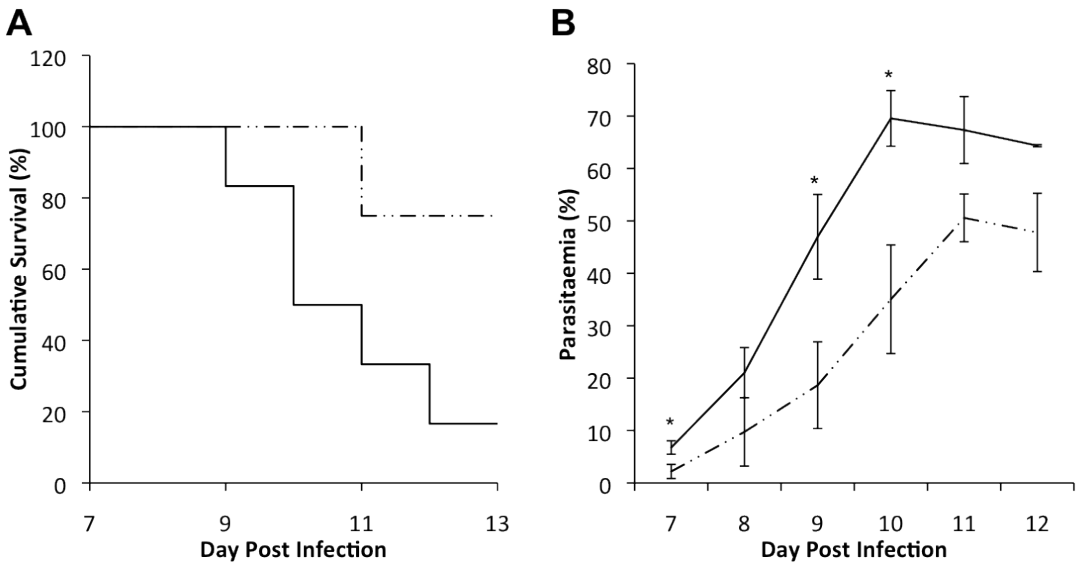

Figure 5.3: The Kcc1^{M935K} mutation increases resistance to infection with 5x10^5 *P. chabaudi* parasitised erythrocytes. (A) Cumulative survival and **(B)** average ± SEM parasitaemia for WT (solid lines) and Kcc1$^{M935K/M935K}$ (dashed lines) female mice. WT n=6, Kcc1$^{M935K/M935K}$ n=4. *P<0.05. . P values calculated using Log rank test **(A)** , or the student's T-test **(B)**.

When infected with 5x10^5 *P. chabaudi* parasitised erythrocytes, 75% of Kcc1$^{M935K/M935K}$ survived infection, compared to 16% in WT. Although this difference was not significant (P=0.07), this may have been due to small sample size. Parasitaemia in WT rose from an average of 6.7% on day 7, to 69.5% on day 10, before returning to 64.3% on day 12 post infection. Parasitaemia was significantly lower in Kcc1$^{M935K/M935K}$ on days 7, 9 and 10 post infection, rising from an average of 2.2% on day 7, to a peak of 50.5% on day 11, before returning to 47.8% on day 12 post infection (Figure 5.3).

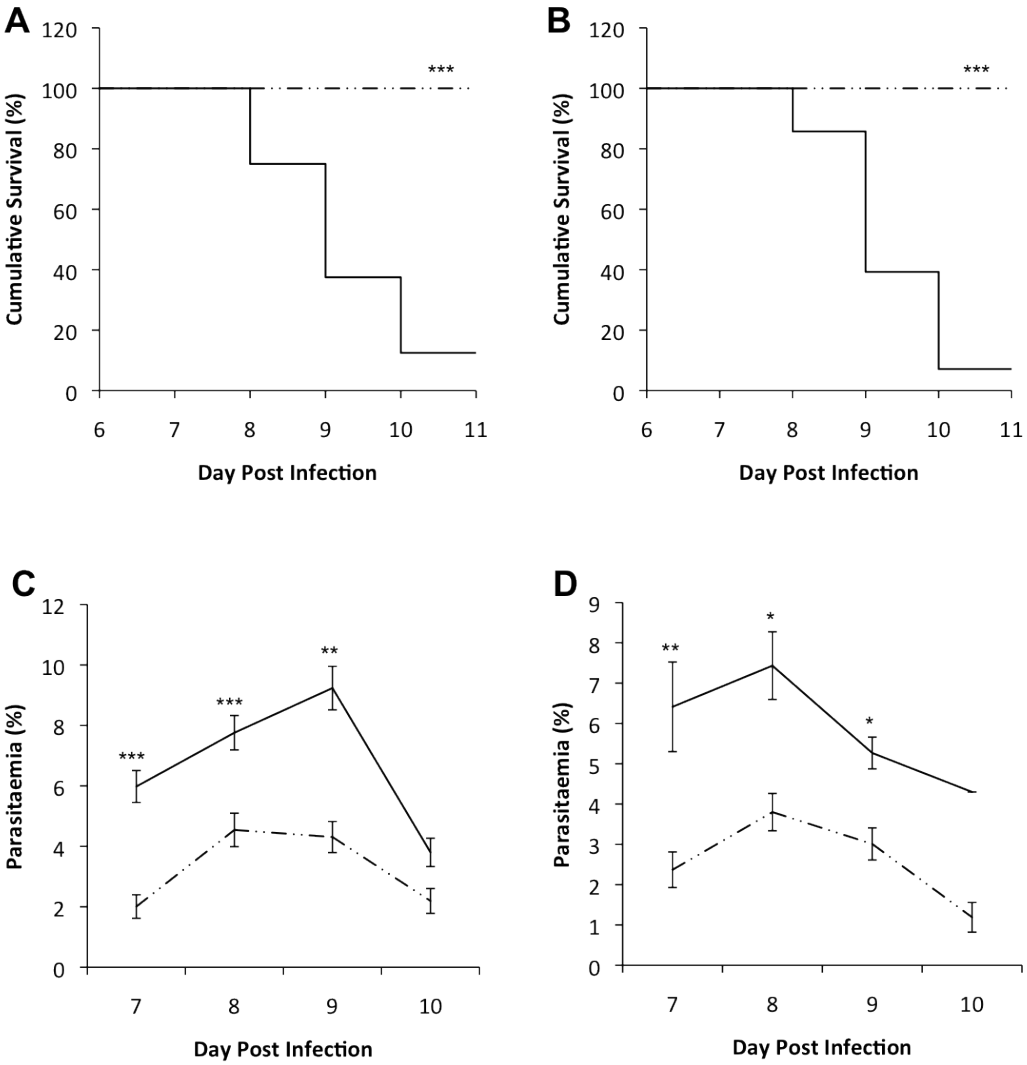

Figure 5.4: The Kcc1^{M935K} mutation causes resistance to *P. berghei*. (A) and **(B)** Cumulative survival for WT (solid lines) and Kcc1$^{M935K/M935K}$ (dashed lines) male and female mice respectively. **(C)** and **(D)** average ± SEM parasitaemia for WT (solid lines) and Kcc1$^{M935K/M935K}$ (dashed lines) male and female mice respectively. WT male n=28, WT female n=8, Kcc1$^{M935K/M935K}$ male n=14, Kcc1$^{M935K/M935K}$ female n=10. Combined results of two independent experiments. *P<0.05, **P<0.01, ***P<0.001. P values calculated using Log rank test **(A)** and **(B)**, or the student's T-test **(C)** and **(D)**.

When mice were infected with 1x10^4 *P. berghei* parasitised red cells, survival was significantly increased in the mutants, with 100% of homozygotes surviving infection, compared to 7% of WT females, and 11% of WT males. Significantly lower parasitaemia was also observed in the Kcc1^{M935K} on days 7, 8, and 9 post inoculation. (Figure 5.4). Together, these results suggest that Kcc1^{M935K} is resistant to both *P. chabaudi* and *P. berghei* when compared to WT.

The Kcc1^{M935K} mutation has an RBC autonomous effect.

Although KCC1 plays an integral role in volume regulation of the RBC, it is also expressed in many other cell types; notably it is expressed in macrophages and T cells, which are known to play important roles in the host response to *Plasmodium* (although the functional role for KCC1 in these cells has not been determined). It was therefore important to determine if the resistance observed in Kcc1$^{M935K/M935K}$ was autonomous to the mutant RBC. To investigate this, an *in vivo* invasion and growth assay was conducted with *P. berghei* as previously described [350] and in chapter 4.

At all time-points the mutant cell population had a higher parasitaemia than the WT population, and this increased to significance by 13 and 21hrs post injection (Figure 5.5A). The total number of labelled cells remained stable across all time points, indicating there was no disproportionate loss of WT cells from circulation (Figure 5.5B). Together, these results suggest that Kcc1$^{M935K/M935K}$ cells support increased invasion and/or growth, and that the Kcc1^{M935K} mutation has an RBC autonomous effect.

This result was counterintuitive, given that in normal *P. berghei* challenge, mutant mice have significantly lower parasitaemia on days 7-10 post infection. One possible explanation was that the parasites might be dying within the mutant RBCs post invasion. To investigate this possibility, thin smears were taken from mice on day 9 of infection and stained with TUNEL. This method labels fragmented DNA, which is present during late stage apoptosis. Therefore, TUNEL is used as a marker for dying parasites. No difference in the percentage of TUNEL positive parasites was observed. Therefore the proportion of viable parasites present in the circulation is not different, and the disparity between the apparent increase in parasite invasion/growth and lower peripheral parasitaemia may be due to other factors (Figure 5.5C).

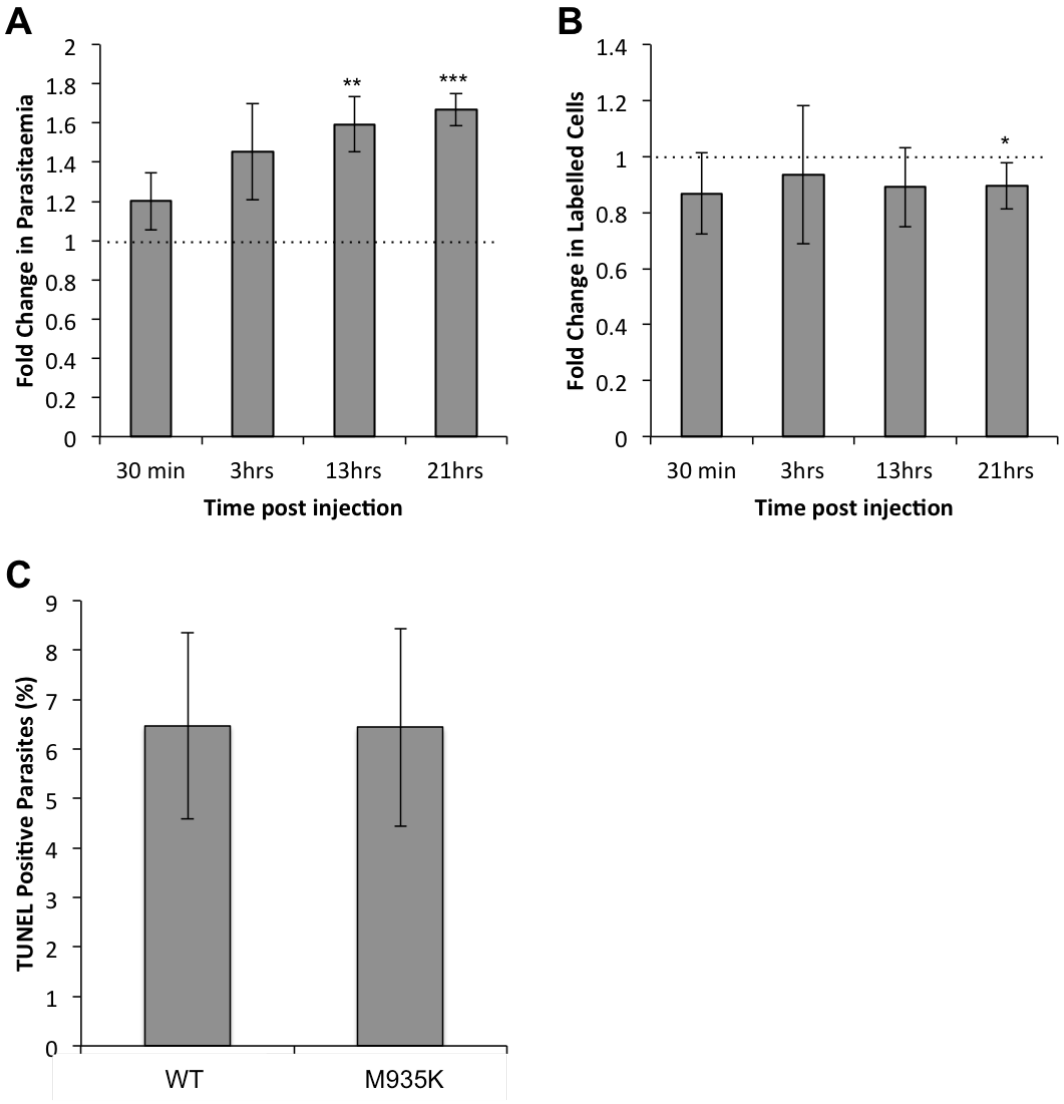

Figure 5.5: Kcc1^{M935K} resistance is not cell autonomous. **(A)** Fold change in parasitaemia of Kcc1$^{M935K/M935K}$ labelled cells compared to WT labelled cells injected into the same *P. berghei* infected host (n=8) **(B)** Fold change in proportion of Kcc1$^{M935K/M935K}$ labelled cells compared to WT labelled cells injected into the same *P. berghei* infected host (n=8). Dotted line represents equal proportion compared to WT **(C)** Percentage of parasites that are TUNEL positive in WT (n=8) and Kcc1$^{M935K/M935K}$ (n=7) mice. Values are average ± SEM. *P<0.05, **P<0.01, ***P<0.001. P values calculated using the Student's T-test.

Kcc1^{M935K} is resistant to ECM

When infected with *P. berghei* in the experiments described above, most WT mice died between days 8 and 10 post infection. Death at this point in *P. berghei* infection is usually caused by experimental cerebral malaria (ECM), and unrelated to the level of peripheral parasitaemia. To confirm that the survival phenotype of Kcc1$^{M935K/M935K}$ was not caused by its significantly lower pararitaemia, mice were infected with a high dose of *P. berghei* at 1x10^{7} parasitised red cells. Under these conditions, Kcc1$^{M935K/M935K}$ showed a similar resistance to infection as in low dose experiments. 90% of Kcc1$^{M935K/M935K}$ survived infection, compared to 0% of WT; parasitaemia was also significantly lower in the mutants on days 7-9 of infection, peaking at an average of 8.6% compared to 14.8% in WT. Importantly, Kcc1$^{M935K/M935K}$ remained resistant to death, despite showing higher peripheral parasitaemias than those at which WT mice began to die in low dose experiments (Figure 5.6). Together these results suggest that increased survival in Kcc1$^{M935K/M935K}$ is not caused by their low parasitaemia.

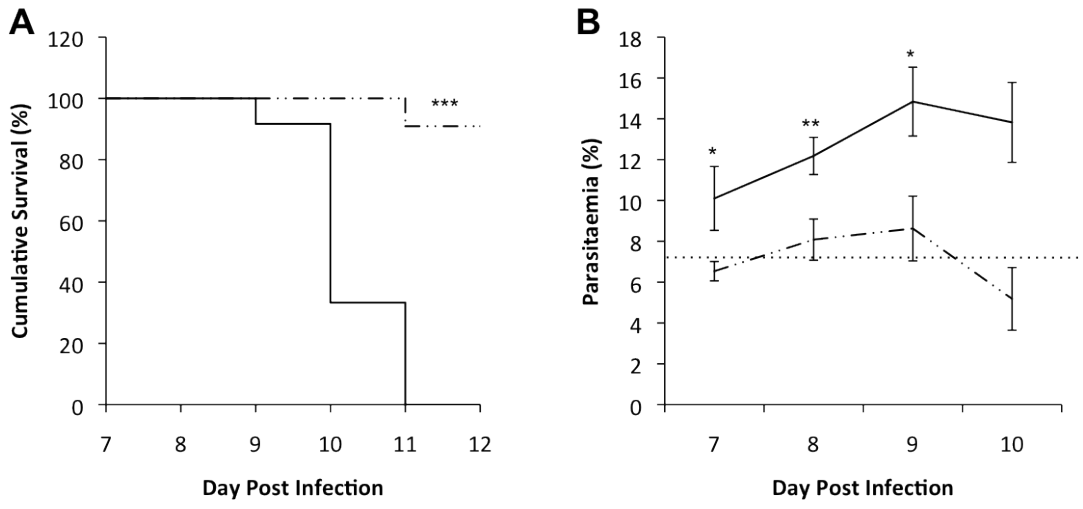

Figure 5.6: Kcc1^{M935K} resistance is independent of peripheral parasitaemia. **(A)** Cumulative survival and **(B)** average ± SEM parasitaemia for WT (solid lines) and Kcc1$^{M935K/M935K}$ (dashed lines) female mice, over the course of infection with high-dose *P. berghei.* Dashed horizontal line in (B) represents the parasitaemia at which WT mice began dying in low-dose *P. berghei* infection. WT n=12, Kcc1$^{M935K/M935K}$ n=11. *P<0.05, **P<0.01. P values calculated using the or Log rank test **(A)** student's T-test **(B).**

To determine if the WT mice dying from *P. berghei* infection were succumbing to ECM, mice were injected with *P. berghei* and symptoms of ECM were scored according to severity, from 0 (no symptoms) to 5 (death).

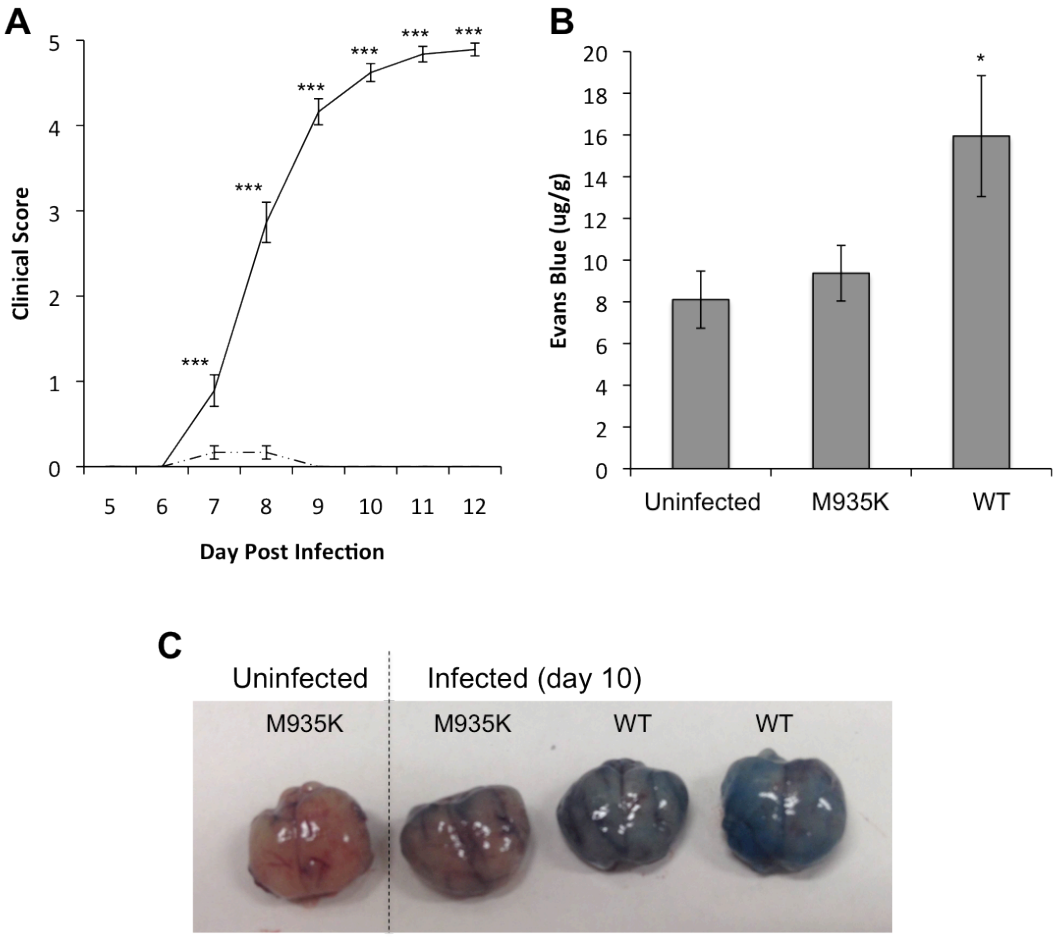

Figure 5.7: The Kcc1^{M935K} mutation causes resistance to cerebral malaria. **(A)** Clinical score for WT (solid lines n=37) and Kcc1$^{M935K/M935K}$ (dashed lines n=24) mice infected with *P. berghei* 0= no symptoms, 1= reduced movement, 2= rapid breathing/hunched posture, 3= ruffled fur/external bleeding, 4= fitting/coma, 5= death. **(B)** Amount of Evan's Blue dye extracted from *P. berghei* infected Kcc1$^{M935K/M935K}$ (n=8), WT (n=7) and uninfected (n=4) brains. **(C)** Representative brains dissected from mice injected with Evan's Blue dye. Values are average ± SEM. *P<0.05, **P<0.01, ***P<0.001. P values calculated using the Student's T-test.

Severe clinical symptoms were observed in WT mice, with most dying from seizures, whereas Kcc1$^{M935K/M935K}$ remained asymptomatic for the length of the experiment (Figure 5.7A). One of the key hallmarks of cerebral malaria is breakdown of the blood brain barrier. Therefore, mice were injected intravenously with Evan's Blue to assess blood brain barrier integrity. Significantly more dye was observed in the brains of WT mice compared to uninfected controls; this was not observed in the brains of Kcc1$^{M935K/M935K}$ mice (Figure 5.7B). Together, these results suggest that WT mice are dying from ECM, and that Kcc1$^{M935K/M935K}$ are resistant to the development of this condition.

Kcc1^{M935K} has an abnormal immune response to *P. berghei* infection

One of the major host processes known to contribute to the development of cerebral malaria in *P. berghei* infection is an over-active inflammatory response. Both *in vivo* neutralisation of host molecules, and studies with knock-out mice have shown that cerebral malaria can be prevented by depletion of the pro-inflammatory cytokines IFN-γ [226,227] and TNFα [228], and can be induced by depletion of the anti-inflammatory cytokine IL-10 [379]. CM resistance is also observed in mice with impaired thymic development of CD8+ T cells, and defective T cell dependent IFN-γ production [231]. KCC1 is expressed in both CD4+ and CD8+ T cells, and is highly expressed in macrophages. Therefore, it was hypothesised that the Kcc1^{M935K} mutation might cause alterations to the immune response that mediate the observed resistance to ECM. To investigate this, plasma cytokine levels were measured in both uninfected mice and mice infected with *P. berghei.* Samples were taken on both days 9 and 10 of infection, when mice normally begin succumbing to ECM.

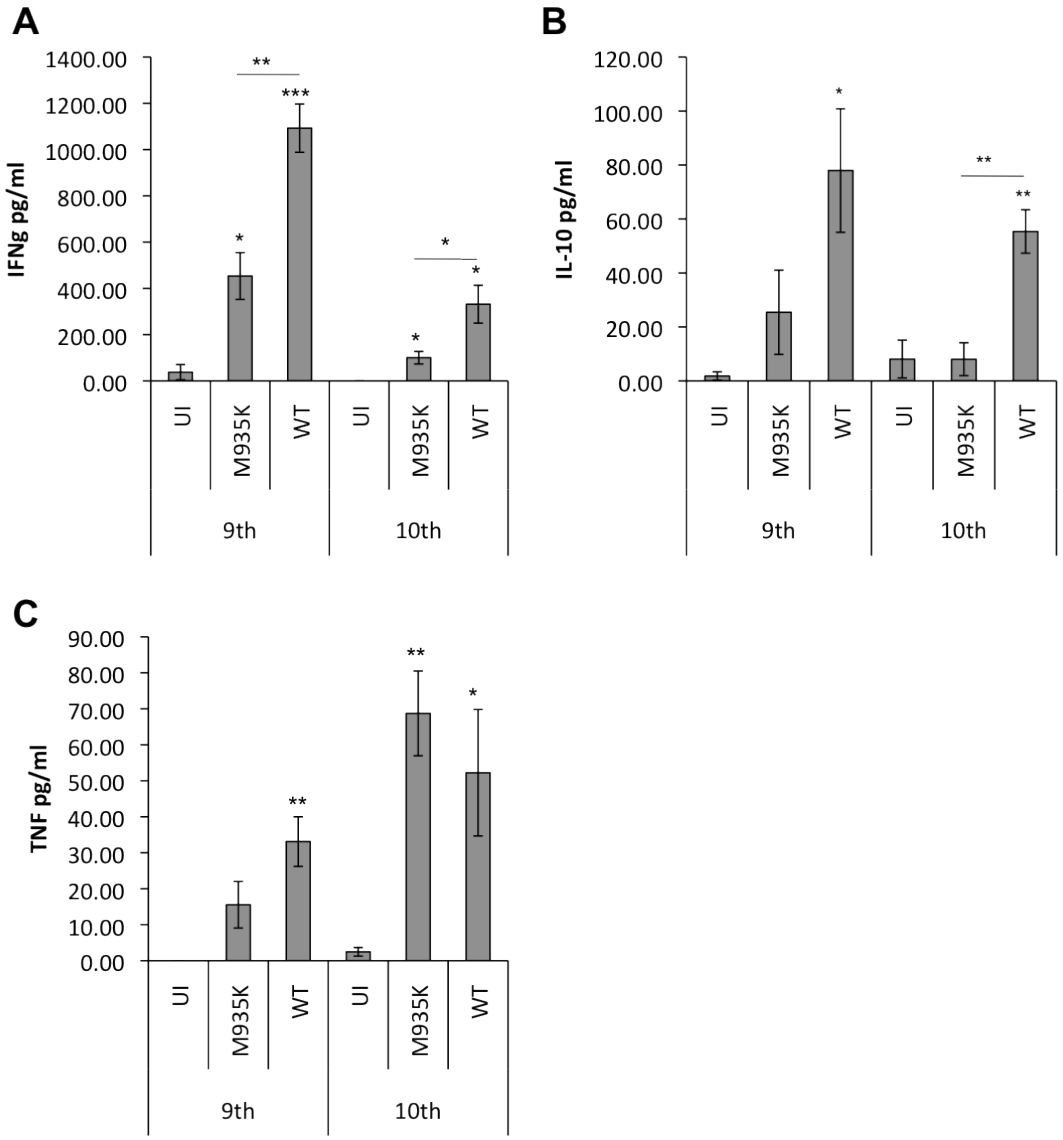

Figure 5.8: The Kcc1^{M935K} mutation alters the inflammatory response to *P. berghei* infection. Average ± SEM concentration of cytokines in the plasma of uninfected (UI n=4), WT (n=5) and Kcc1$^{M935K/M935K}$ (n=5) mice on the 9th and 10th days post infection with *P. berghei*. Uninfected include both WT and Kcc1$^{M935K/M935K}$ mice combined. **(A)** Interferon-γ. **(B)** Interleukin 10. **(C)** Tumour necrosis factor α. *P<0.05, **P<0.01, ***P<0.001. P values calculated using the Student's T-test.

Kcc1$^{M935K/M935K}$ showed no difference in plasma cytokine levels when uninfected, suggesting that the mutation has no obvious effect on immune homeostasis. During infection however, lower levels of IFNγ and IL-10 were observed in the mutant on both days 9 and 10 post infection. TNFα levels were slightly lower in the mutants on day 9, but this difference disappeared by day 10 (Figure 5.8).

It has been shown that depletion of CD4+ and CD8+ T cells can also prevent the development of ECM [230,232]. Therefore, to determine if the Kcc1^{M935K} mutation causes differences in immune cell populations, the relative proportion of CD4+, CD8+, CD11c+, T regulatory cells and B cells were measured by flow cytometry in the blood, spleen and thymus, both before and during *P. berghei* infection. H&E stained sections of spleen were also taken, in order to observe any changes in spleen architecture both before and during infection.

In both infected and uninfected animals, no significant differences were observed between Kcc1$^{M935K/M935K}$ and WT in the proportion of CD4+ or CD8+ T cells in either the blood, spleen or thymus (Figure 5.9A and B). In uninfected animals the proportion of dendritic (CD11c+) cells was significantly higher in the mutant thymus; conversely the amount of T regulatory (CD4+CD25+FoxP3+) cells was significantly lower in the mutant spleen and thymus (Figure 5.9C and D). While these significant differences disappeared during infection, the trends remained. Spleen histology showed no difference in architecture between uninfected WT and Kcc1$^{M935K/M935K}$, however a marked hyperproliferation of WBCs was observed in the spleens of infected mutants, which was not evident in the spleens of infected WT mice (Figure 5.10).

Together these results suggest that the Kcc1^{M935K} mutation alters the inflammatory response to infection, and may also alter the expansion of some lymphocyte populations in response to infection.

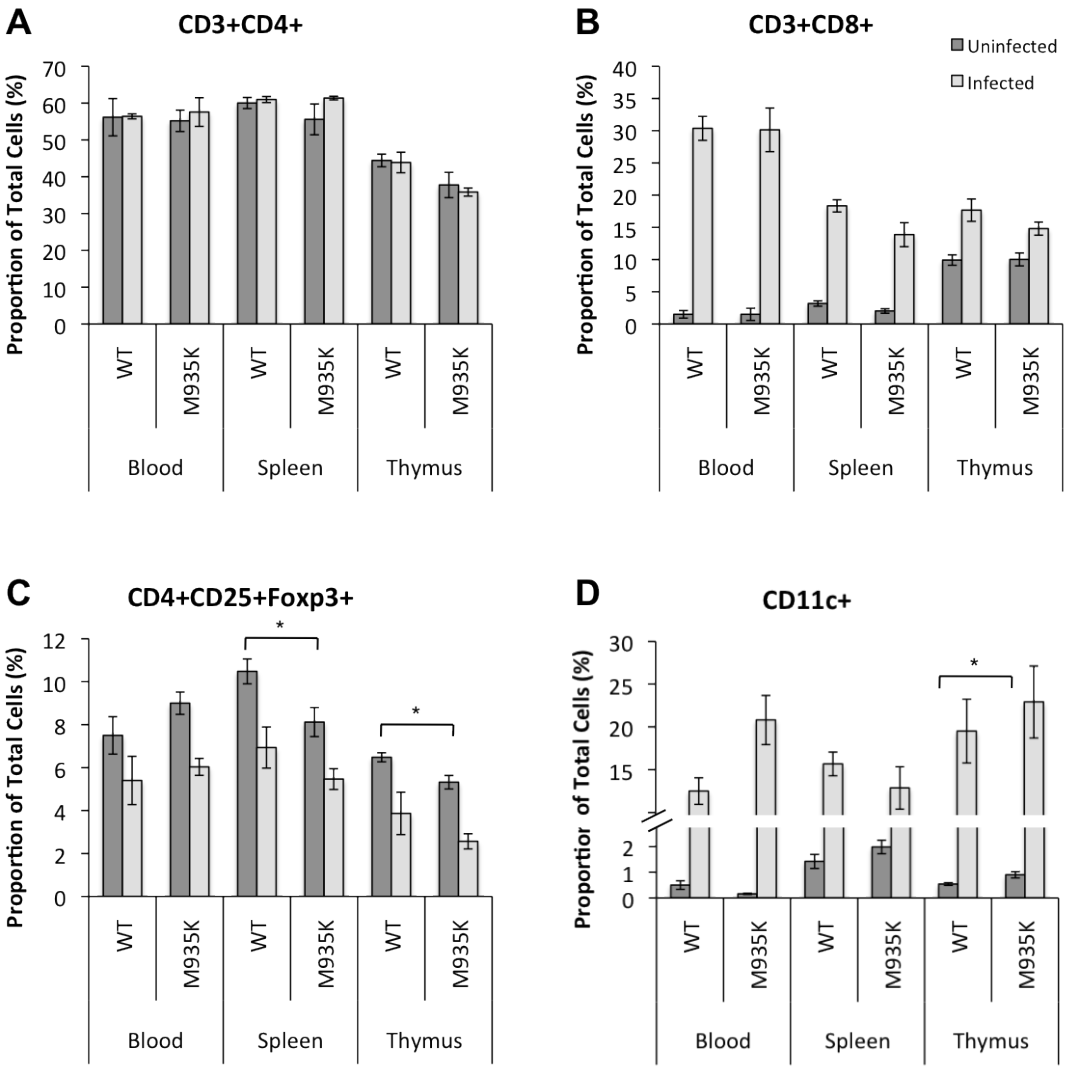

Figure 5.9: The Kcc1^{M935K} mutation alters immune cell populations in uninfected mice Average ± SEM proportion of lymphocytes that are **(A)** CD3+CD4+, **(B)** CD3+CD8+, **(C)** CD4+CD25+Foxp3+, and **(D)** CD11c+ in the blood, spleen, and thymus, of WT and Kcc1$^{M935K/M935K}$ mice. In uninfected mice n=5 for each genotype; infected n=3 for each genotype. *P<0.05. P values calculated using the Student's T-test.

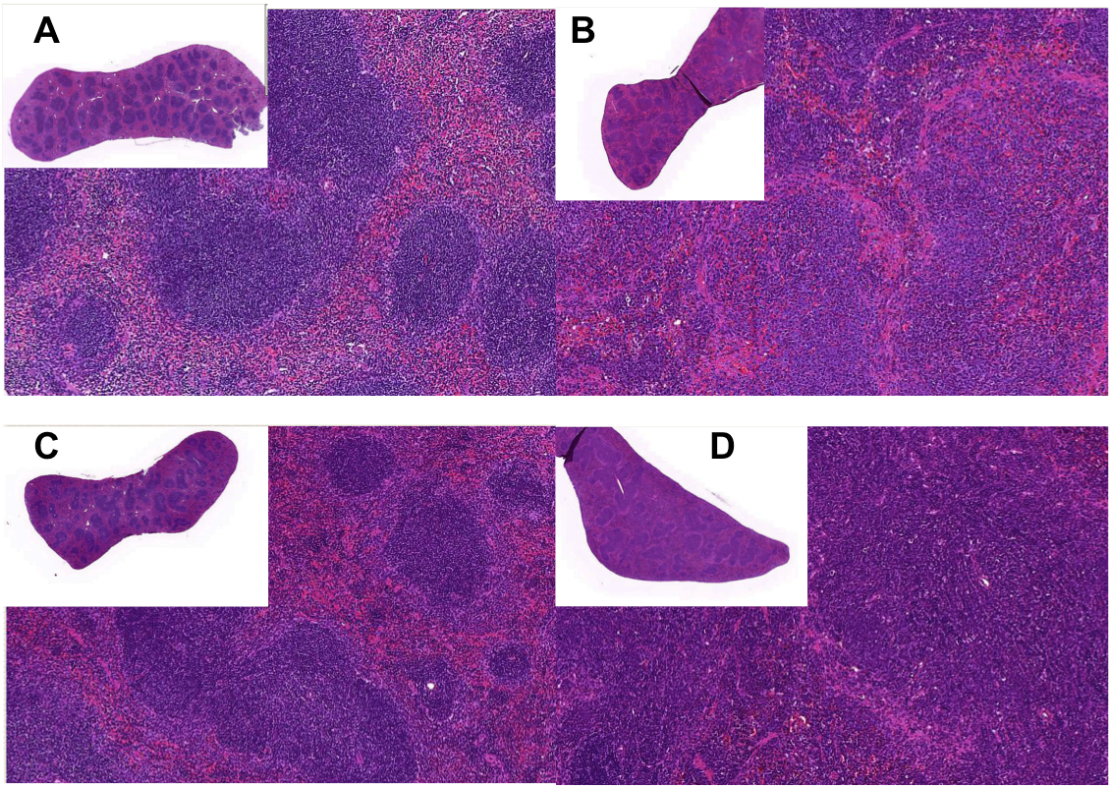

Figure 5.10: The Kcc1^{M935K} mutation causes an abnormal WBC response to infection. H&E stained spleen sections from **(A)** uninfected WT, **(B)** infected WT, **(C)** uninfected Kcc1$^{M935K/M935K}$, and **(D)** infected Kcc1$^{M935K/M935K}$ mice, showing hyperproliferation of WBCs (stained purple). Sections are at 5x magnification; insets at 0.625x magnification.

WNK3 as a novel host-directed therapy target

The Kcc1^{M935K} mutation provides striking resistance to the development of ECM, and does not produce severe pathology in homozygous mutants. Therefore, activation of KCC1 presents an attractive target for a host-directed therapy that may treat or prevent cerebral malaria.

KCC1 activity is regulated by WNK3 (with-no-lysine kinase 3); this kinase activates SPAK/OSR1, which in turn phosphorylates KCC1 and inhibits its activity [380,381]. Because WNK kinases have a known role in hypertension, several screens have identified inhibitors of WNK signalling [382,383], suggesting that WNK3 may be an easily drugable target. Therefore, CRISPR/Cas9 genome editing technology was used to create a WNK3 knockout mouse, in order to genetically test the hypothesis that inhibition of WNK3 will recreate the same phenotype as the Kcc1^{M935K} mutation, and provide protection from ECM.

Guide RNA was designed to disrupt the start codon of WNK3, aiming to induce a frameshift mutation leading to a premature stop codon and therefore complete knockout of the gene (Figure 5.11). Using CRISPR/Cas9 genome editing technology, five novel mutations were generated and are listed below. The first is a compound heterozygous mouse resulting in two alleles, each with a 7 base pair deletion, which will induce a frame shift 1 and 8 bp from the start codon respectively. The second is also a compound heterozygous mouse; each of its two alleles has a 6 base pair deletion, removing amino acids 4-5 and 2-3 from the protein respectively. The third mutant is heterozygous, with one wild-type allele and one allele containing an extra thiamine, which induces a frame shift 9 bp from the start codon. The fourth mutant is homozygous for a 6 base pair deletion removing amino acids 4-5 from the protein. The fifth mutant has three alleles; one WT, one with a 3 base pair deletion removing the amino acid 5 from the protein, and one with a single bp deletion, causing a frame shift 7 bp from the start codon. Of these mutants, those with frame shifts are being tested for their effect on the protein and their germline transmission. The mice are currently breeding and the progeny will tested with *P. berghei* for their susceptibility to ECM.

A

GGGCAGCCCTGTTTTCAAAGGAAACTCCATCAGGCTTCTCAGAA
TCTTCTGTGCTAGCTGGCTCC**CCAGAATCAGTGGCCATtgtaac**
taaggttggcactaaatttgttcttgtttcactcttcagtctac

B

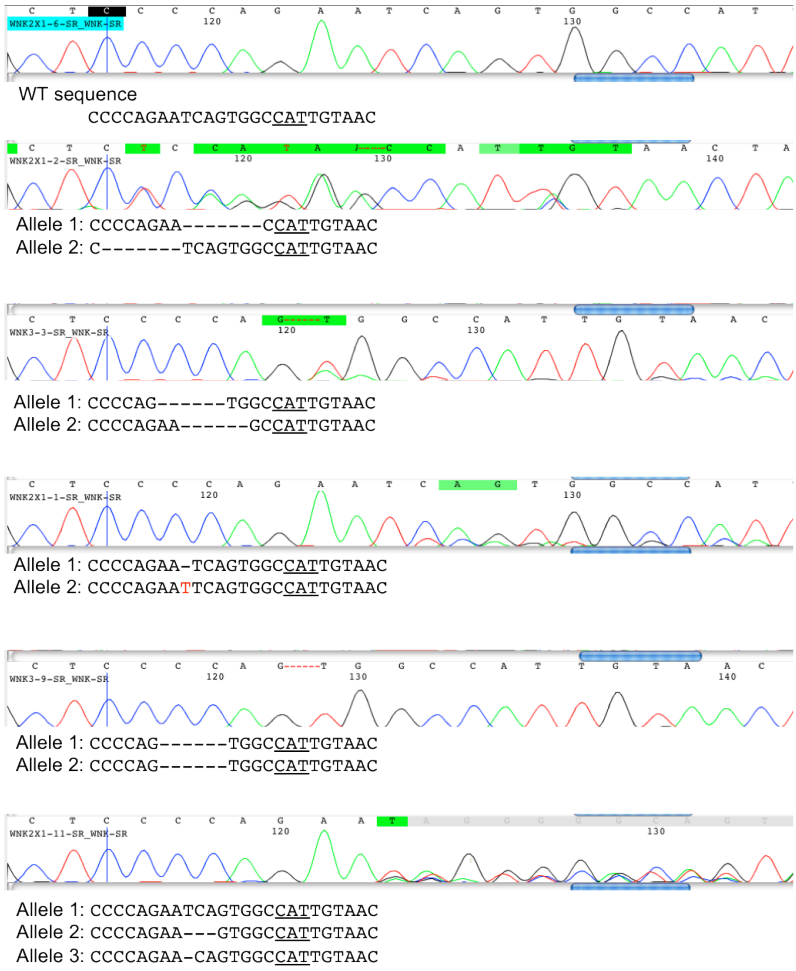

Figure 5.11: CRISPR/Cas9 has been used to knock-out WNK3 expression. (A) WNK3 sequence (reverse complement) showing the site targeted by CRISPR/Cas9. Lower case letters represent 5'UTR, upper case letters represent exon 1. Bold letters show the position of the RNA guide. Underlined letters show the position of the start codon. **(B)** Electropherograms (reverse complement) from 5 mice with mutant alleles.

Discussion

This study provides the first evidence that host KCC1 plays a role in the host response to malarial infection. Mice expressing only a mutant form the protein, which results in unregulated activation of K+ transport in the red cell, display a marked resistance to infection and concomitant suppression of peripheral parasitaemia when challenged with both *P. chabaudi* and P*. berghei.* In the later infection, the basis for the resistance may be due to effects of the mutation of the immune response. However reasons for the resistance to the former parasite are difficult to deduce.

Kcc1^{M935K} is resistant to P. chabaudi *and* P. berghei.

In both *P. chabaudi*, and *P. berghei* infection, Kcc1$^{M935K/M935K}$ had significantly lower parasitaemia that WT. Survival was also significantly increased in *P. berghei* infection. Although the observed difference in survival was not significant during *P. chabaudi* infection, this is likely due to the small sample size used in this experiment. Therefore it was concluded that Kcc1^{M935K} is resistant to both *Plasmodium* species.

The Kcc1^{M935K} mutation has an RBC specific effect on P. berghei

To determine if the resistance observed in Kcc1$^{M935K/M935K}$ was caused by intrinsic factors within the RBC, an *in vivo* invasion/growth assay was conducted, and it was observed that 21 hours after injection, a significantly higher proportion of parasites were found in mutant cells compared to WT cells. One explanation for this result is that Kcc1$^{M935K/M935K}$ cells support a higher rate of parasite invasion and/or growth than WT. However, it is difficult to see how increased invasion/growth could lead to the significantly lower paraisteamia observed over the course of infection in Kcc1$^{M935K/M935K}$ animals. Moreover, the hypothesis that over-active KCC1 leads to increased invasion is not supported by previous studies, which consistently associate increased K+ efflux with lower rates of invasion [384-386].

A second explanation for these results is suggested by the fact that *P. berghei* infected RBCs have the ability to cytoadhere to the endothelium of blood vessels. Mutant cells may be sequestering at lower rates than WT cells, making more of them visible when counting peripheral parasitaemia. It is not possible to determine from this *in vivo* invasion/growth assay, whether there is any difference in sequestration between WT

and Kcc1$^{M935K/M935K}$ cells. At each time point, the number of labelled cells counted for each genotype is roughly $5x10^5$, of which around $2x10^3$ are parasitised, depending on the parasitaemia of the animal. Therefore, even a large change to the number of parasites being removed from circulation through sequestration will have a small impact on the total number of labelled cells. The proportion of WT to mutant labelled cells did not change over the course of the infection, but this only suggests that there was no preferential splenic clearance of uninfected cells during the assay. However, the hypothesis of reduced cytoadherance fits well with the observation that Kcc1$^{M935K/M935K}$ has lower parasitaemia over the course of infection; lower levels of sequestration leaves more late stage parasites vulnerable to splenic clearance, and therefore results in reduced parasite burden [387].

Kcc1^{M935K} is resistant to ECM and has an abnormal immune response to infection

Results from both clinical observations and from assessment of blood brain barrier integrity with Evan's Blue suggest that as well as being resistant to *P. berghei* infection, Kcc1$^{M935K/M935K}$ is resistant to the development of cerebral malaria. This is the first description of a mutation in a transporter that has an effect on ECM; other previously discovered genes have involved host cytokines, antigen presentation [115,118], or erythrocyte membrane proteins [92,93,135].

Given ECM is a pathology largely mediated by T cells and inflammatory cytokines, it was hypothesised that the Kcc1^{M935K} mutation may have effects on the immune system. In uninfected animals it was observed that the proportion of dendritic cells was significantly higher in the mutant thymus and that the amount of T regulatory cells was significantly lower in the mutant spleen and thymus. During *P. berghei* infection, Kcc1$^{M935K/M935K}$ was found to have significantly altered plasma concentrations of inflammatory cytokines, and to exhibit hyperproliferation of WBCs in the spleen.

The results from measuring cytokines during *P. berghei* infection suggest the mutation causes an attenuated inflammatory response. This fits well with previous reports that lowering IFNγ and/or TNFα levels results in protection from ECM [226-228]. However, IL-10 has been shown to have a protective role, with *in-vivo* neutralisation of the cytokine leading to the development of ECM in normally resistant mice [379]. It is therefore surprising that the ECM resistant Kcc1$^{M935K/M935K}$ mice have a significantly lower IL-10

response than WT in these experiments. The plasma samples used in this experiment were obtained on days 9 and 10 of infection; it is therefore unknown if Kcc1$^{M935K/M935K}$ had a higher inflammatory response than WT earlier in infection. It is well established that effective control of *Plasmodium* infection relies on an appropriate balance between inflammatory and regulatory cytokine responses. Inflammatory cytokines are necessary in the early part of infection to control parasitaemia, but later need to be regulated in order to prevent pathology from developing (reviewed in [388]). Future experiments could investigate the cytokine response of Kcc1$^{M935K/M935K}$ over the course of infection, to determine if Kcc1$^{M935K/M935K}$ has an elevated inflammatory response during the early part of infection.

It is unclear from these experiments if the altered immune response observed in Kcc1$^{M935K/M935K}$ is the cause or the effect of low parasitaemia in these animals. The RBC autonomous effects of the mutation may lead to lower parasitameia, and therefore a proportionally lower cytokine response; alternately the Kcc1^{M935K} mutation may have direct effects on both the erythrocyte and the immune system independently. The previously mentioned hypothesis - that the mutation reduces the ability of infected Kcc1$^{M935K/M935K}$ red cells to cytoadhere - can be used to explain most of the observed results. Reduced sequestration would expose more infected cells to the spleen, resulting in higher clearance rates and lower parasitaemia; greater exposure of parasitised cells to the spleen may also result in a faster expansion of WBCs within that organ. Lower rates of cytoadherence in the brain may result in reduced inflammation and protection from ECM [389,390]. However, as it was observed that the populations of both T regulatory and dendritic cells were significantly altered in uninfected mutant animals, the possibility that the Kcc1^{M935K} mutation has an intrinsic effect on the immune system cannot be excluded.

During *Plasmodium* infection, parasite products like *Pf*EMP1 and hemozoin can actively suppress dendritic cell function, and dampen the early inflammatory response to infection [391-393]. It is possible that activation of KCC1 interferes with this inhibition, allowing the host to respond to infection more quickly and keep parasitaemia low. This may occur through increased immune recognition of infected cells leading to higher rates of phagocytosis; through reduced cytoadherence of infected cells, and therefore greater splenic clearance; or through a reduced inflammatory response and therefore less damage to the host. Therefore, further investigation of the immune response to

infection will be needed if the exact mechanism behind Kcc1^{M935K} resistance to infection is to be discovered.

WNK3 as a novel HDT target

The WNK3 knock-out mice generated using CRISPR/Cas9 will allow investigation of the hypothesis that the ECM resistant phenotype of Kcc1$^{M935K/M935K}$ can be recreated by inhibiting WNK3. The Kcc1^{M935K} mutation causes activation of KCC1 by impairing the phosphorylation of key regulatory threonines. Under normal conditions, KCC1 is phosphorylated and inactivated by WNK3[380,381]. Therefore, it was hypothesised that inhibition of WNK3 may prevent the inhibition of KCC1, leading to over-activation of the transporter and recreating the Kcc1^{M935K} phenotype.

WNK3 plays a key role in the maintenance of cellular Cl^- balance, by modulating the activity of several transporters (Figure 15.11). The K-Cl transporters - including KCC1, KCC2, KCC3 and KCC4 - mediate Cl- efflux, and are inhibited when phosphorylated by WNK3. The Na-(K)-Cl cotransporters - including NCC and NKCC1/2 - mediate Cl- influx, and are activated when phosphorylated by WNK3 [380,381] (Figure 5.12). Three isoforms of KCC are expressed in the erythrocyte; KCC1, KCC3 and KCC4. Of these, KCC3 is thought to be the major mediator of K^+ efflux [375]. Complete knock-out of WNK3 should effect all three isoforms, as well as other transporters mediating K^+ influx in the RBC. Therefore WNK3 KO may produce a more pronounced RBC phenotype than Kcc1^{M935K}. The effect of WNK signalling on cells of the immune system have been less well studied, although it is known that both T cells and macrophages express isoforms of both WNK and KCC. Given it is not yet known which cell type or types are mediating the resistance to malaria observed in Kcc1^{M935K}, it is difficult to speculate on how WNK3 KO might recreate a similar phenotype.

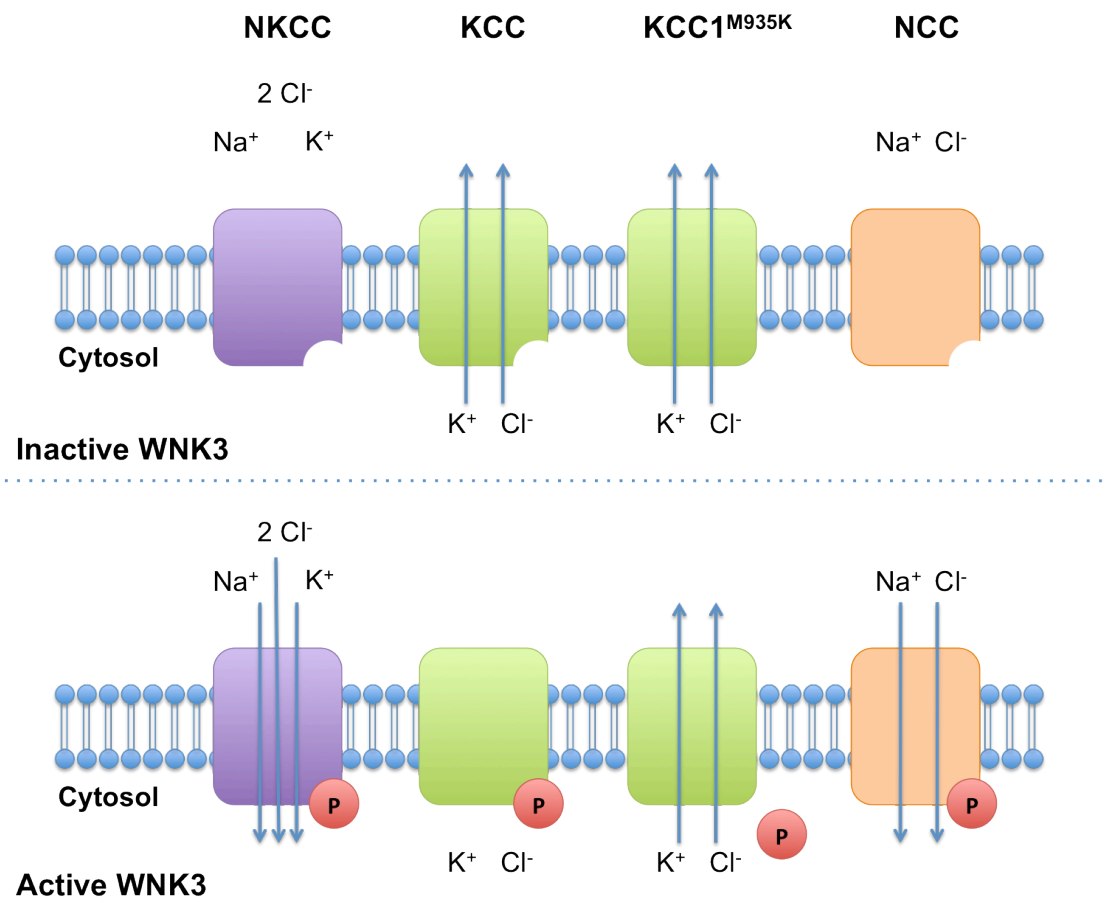

Figure 5.12: Ion transport mediated by WNK3. Active WNK3 phosphorylates NKCC, KCC and NCC transporters. This causes activation of NKCC and NCC, and inhibition of KCC, resulting in net K^+ influx. The Kcc1^{M935K} mutation prevents phosphorylation of KCC1 by WNK3. This causes the transporter to remain constitutively activated, and increases cellular K^+ efflux.

Further experiments with WNK3 mutant lines will involve infecting KO mice with *P. berghei* to determine if they have improved symptoms and survival compared to WT C57BL/6. If the WNK3 KO mice prove to be resistant to ECM, this will open the possibility of investigating WNK3 inhibitors as host-directed therapies for the treatment of cerebral malaria. CM is the most severe complication of *P. falciparum* infection in humans. The occurrence of CM varies from region to region, with a case fatality rate ranging from 8.5% in Africa, to 15% in Southeast Asia [210]. In a recent multicenter study, 52% of severe malaria cases developed cerebral malaria, and the fatality rate after treatment was 18% [66]. Therefore, an HDT that could improve outcomes for individuals at risk of developing CM would be of great benefit in reducing both morbidity and mortality associated with *P. falciparum* infection.

Conclusion

In this chapter it has been shown that activation of KCC1 causes reduced parasitaemia in both to *P. chabaudi* and *P. berhgei* infection. This may be mediated through intrinsic effects to the RBC that result in reduced sequestration of infected cells. Activation of KCC1 also induces resistance to *P. berghei* by preventing the development of experimental cerebral malaria. This is the first description of a mutation in a transporter that has an effect on ECM. Future research into WNK3 inhibition might lead to the development an HDT for cerebral malaria.

CHAPTER 6 – FINAL DISCUSSION AND CONCLUSIONS

The malaria parasite has a complex interaction with its host. Residing within the RBC, it can be affected by the intracellular environment, by the host's immune system, by the rate of RBC turnover, and more. For decades it has been known that host polymorphisms can provide resistance to malaria, but despite many years of research and great advances in our understanding of parasite biology, the precise mechanisms by which many of these polymorphisms provide resistance remain elusive.

In this project, ENU mutagenesis experiments have allowed the study of two novel host mutations that confer resistance to rodent malaria parasites, gaining insight into both the host response to infection, and the conditions necessary for parasite growth within the RBC. The major aim of this thesis was to uncover novel mutations affecting malaria susceptibility that might provide targets for host-directed therapy (HDT). Investigation of the two mutant mouse lines aimed to discover both how these mutations affect the physiology of the host, and how they affect the interaction of the parasite with the host.

The first mouse line investigated was found to carry a mutation in AMPD3 – Ampd3^{T689A} - which is an enzyme involved in purine metabolism, specifically converting AMP to IMP. Studies were then directed towards determining the aetiology of the Ampd3^{T689A} blood phenotype, and the effect of the mutation on the host response to rodent malarial infection. It was found that the mutation resulted in increased activity of enzyme in the red cell; AMPD3 activity is normally absent or significantly repressed in these cells. This resulted in red cells with greater than normal concentrations of guanylyl nucleotides (GMP, GDT and GTP) and reduced adenosyl nucleotides (AMP, ADP and ATP). These cells also displayed other unusual features, including increased oxidative stress and dramatic reduction in RBC half-life. It was therefore concluded that AMPD3 has a critical role in determining the life span of erythrocytes. This highlights one of the advantages of conducting an ENU screen; because mutagenesis occurs randomly and the effects are manifest *in vivo*, there is always the possibility of uncovering aspects of biology that were not the primary focus of the study. It was necessary to determine the aetiology of the Ampd3^{T689A} blood phenotype in order to ascertain the mechanisms behind its response to malaria. However, the information gained by this study has provided novel insight into both erythropoiesis and eryptosis, and has identified AMPD3 as a possible drug target for lengthening the lifespan of RBCs stored for transfusion. It therefore has considerable value outside the field of parasitology.

An investigation of the host response to malarial infection revealed that the Ampd3^{T689A} line was dramatically resistant to *P. chabaudi.* The underlying mechanism of resistance appeared to vary according to whether the mice carried one or two copies of the mutant allele. In homozygous mutants this resistance appeared to be mediated by severely reduced erythrocyte half-life and rapid RBC turnover, thereby preventing the establishment of high parasitaemia. In heterozygous animals parasite growth was robust, and occurred at even greater rates than normal during the early stages of infection. Unlike the wild-type littermates however, heterozygous animals were much more likely to control and resolve the infection, resulting a significant higher rates of survival. Results here indicated that the survival phenotype was dependent on the spleen, possibly by the up-regulation of splenic erythropoiesis during infection. Interestingly, investigation both *in vivo* and *in vitro* of the RBC intrinsic effects of altered purine metabolism suggested that the high [GTP] in mutant cells favours greater parasite growth.

Together, these findings suggest that AMPD3 is not a strong candidate for anti-malarial host-directed therapy. Although homozygous mutants exhibit an incredible resistance to infection, it is caused by rapid RBC turnover. Recapitulating the effect of the mutation in individuals with malaria could result in a similar increase in RBC destruction, which is not desirable for a disease that can cause anaemia. However further investigation of the heterozygous mutant phenotype may lead to new ways to stimulate erythropoiesis during malaria infection, which could be of great benefit in preventing individuals from developing severe anaemia. Of course such benefits would also have to be weighed against the possibility that this therapy would also increase the rate of parasite growth, which was the other prominent effect of this mutation against rodent malaria strains tested.

Another of the interesting findings from the Ampd3^{T689A} study was that mutants exhibit significantly increased gametocytogenesis during both *P. chabaudi* and *P. berghei* infection. While the aim of this project was to identify HDT targets that could induce parasite death, it is also important to consider the effects that these targets may have on the sexual commitment of the parasite, particularly when aiming for a therapy that is going to avoid the problem of spreading parasite resistance. Evidence from a number of studies has shown that anti-malarials that increase the rate of gametocytogenesis can contribute to the rapid spread of parasite resistance. For example, it has been shown that both CQ treatment of CQ-resistant parasites [20-22] and sulfadoxin-pyramethamine

(SP) treatment of SP resistant parasites [23], significantly increases gametocytogenesis in human infections, leading to preferential transmission of drug resistant strains. Therefore, the impact that increased gametocytogenesis has on the suitability of AMPD3 as an HDT target will depend largely on whether the gametocytes observed in Ampd3^{T689A} are capable of replicating within the mosquito and therefore transmitting parasites to a new host. If they are, this increased transmission may be a reason to avoid AMPD3 as an HDT target. However, understanding the basis for the stimulation of gametocyte production in the AMPD3 mutant line, and whether parasite differentiation occurs normally, may provide important new insights into the process of gametocytogenesis and possible new targets to interfere with the process. Such novel strategies would undoubtedly be of great benefit in endemic areas where parasite transmission is very high, and may also slow the spread of drug resistant parasite strains.

This thesis also investigated the mouse mutant line, Kcc1^{M935K}. This mutation causes dysregulation and activation of the K+ and Cl- transporter KCC1, resulting in increased efflux of K+ from the RBC. Results here suggest that KCC1^{M953K} mutation also results in changes to the host response to malarial infection, particularly the experimental cerebral malarial (ECM) induced by *P. berghei* infection. Central to these effects are alterations to the immune system that correlate with in lower peripheral parasitaemia and increased survival, however the exact mechanisms of the ECM resistance in Kcc1^{M935K} were unable to be determined. Nevertheless, unlike in Ampd3^{T689A}, resistance to rodent malaria in Kcc1^{M935K} was not associated with any severe side effects, suggesting that KCC1 might provide a good target for host-directed therapy. CM is one of the most severe complications of *P. falciparum* infection, with a case fatality rate as high as 18% in some regions [66]. Of those individuals who recover from CM, many suffer from neurological sequelae such as ataxia, hemiplegia, epilepsy and blindness. Therefore, an HDT that can both lower parasitaemia, and reduce the incidence of CM would be of great benefit in reducing both morbidity and mortality associated with malaria infection.

Direct *in vivo* pharmacological activation of KCC1 is difficult to achieve. *In vitro* experiments have shown that KCC1 can be activated by two compounds: N-ethylmaleimide (NEM) and staurosporine [377]. However, neither of these compounds is attractive as an HDT for use *in vivo*, as they are not specific to KCC1. NEM is an irreversible inhibitor of all cystidine peptidases, and can block vesicular transport; staurosporine is a broad spectrum protein kinase inhibitor. Therefore, this thesis has

investigated the possibility of activating KCC1 indirectly through the kinase WNK3. WNK kinases have been widely researched due to their known role in hypertension, and several screens have identified inhibitors of WNK signalling that have had success both *in vitro* and *in vivo* [382,383]. This suggests that WNK3 may be an easily drugable target. It remains to be seen if the WNK3 knock-out mice generated in this study will be as resistant to ECM as Kcc1$^{M935K/M935K}$. If they are, WNK3 will be a highly promising HDT target.

One of the most interesting observations of this study was that both mutations investigated had multiple effects on the course of infection. It is tempting to think that mutations altering the erythrocyte will purely affect the ability of the parasite to live and grow within the cell. Indeed many *ex vivo* and *in vitro* studies with RBCs from humans carrying protective polymorphisms have focused purely on invasion and growth phenotypes. However, an obvious point from this work is that the effects of the polymorphisms on malarial infection *in vivo* must also be considered. In some cases the reasons for the resistance may be complex, and the impacts of the mutations counterintuitive. Mutations may increase parasite growth, but at the same time cause systemic changes that tip the balance in favour of the host and result in resistance. This proved true for Ampd3^{T689A} and further investigation may find that it is also true for Kcc1^{M935K}.

Many of the host polymorphisms known to provide malaria protection induce similar alterations to the RBC, and this has lead researchers to speculate on whether there might be common mechanisms of resistance amongst different red cell polymorphisms. For example, some of the polymorphisms that cause increased resistance to infection also cause RBCs to be smaller (hereditary spherocytosis, α- and β-thalassaemia). Therefore, microcytosis has been postulated as a common cause of resistance [394]. Similarly, increased oxidative stress is observed in each of the haemoglobin disorders (HbS, HbE, HbC, and α- and β-thalassaemia) and has therefore been proposed as a common mechanism behind the decreased parasite invasion/growth observed in these individuals [155,395]. However, in this study, microcytosis in Kcc1^{M935K} was associated with equal rates of parasite survival, and in Ampd3^{T689A} increased levels of oxidative stress were associated with increased invasion and growth. This demonstrates the danger of making generalisations about the causes of resistance to infection, and highlights the importance of considering the systemic changes that may be occurring alongside alterations to the RBC.

In summary, the interactions between *Plasmodium* and the human host are complex. The investigation undertaken here has given novel insight into some of the host molecules that impact on the progression of the disease. Hopefully, through future research, they will provide us a greater understanding of host-parasite interactions, and new therapeutic avenues and even targets for host-directed therapy.

References

1 Murray, C. J. *et al.* Global, regional, and national incidence and mortality for HIV, tuberculosis, and malaria during 1990-2013: a systematic analysis for the Global Burden of Disease Study 2013. *Lancet*, doi:10.1016/S0140-6736(14)60844-8 (2014).
2 World Malaria Report 2014. (World Health Organisation, Geneva, 2014).
3 Guerra, C. A. *et al.* The limits and intensity of *Plasmodium falciparum* transmission: implications for malaria control and elimination worldwide. *PLoS Med* **5**, e38, doi:07-PLME-RA-1649 [pii] 10.1371/journal.pmed.0050038 [doi] (2008).
4 Mendis, K., Sina, B. J., Marchesini, P. & Carter, R. The neglected burden of Plasmodium vivax malaria. *Am J Trop Med Hyg* **64**, 97-106 (2001).
5 Carlton, J. M. *et al.* Comparative genomics of the neglected human malaria parasite Plasmodium vivax. *Nature* **455**, 757-763, doi:10.1038/nature07327 (2008).
6 Amino, R. *et al.* Imaging malaria sporozoites in the dermis of the mammalian host. *Nature protocols* **2**, 1705-1712, doi:10.1038/nprot.2007.120 (2007).
7 Gueirard, P. *et al.* Development of the malaria parasite in the skin of the mammalian host. *Proc Natl Acad Sci U S A* **107**, 18640-18645, doi:10.1073/pnas.1009346107 (2010).
8 Miller, L. H., Good, M. F. & Milon, G. Malaria pathogenesis. *Science* **264**, 1878-1883 (1994).
9 Kwiatkowski, D. & Nowak, M. Periodic and chaotic host-parasite interactions in human malaria. *Proc Natl Acad Sci U S A* **88**, 5111-5113 (1991).
10 Uneke, C. J. Impact of placental *Plasmodium falciparum* malaria on pregnancy and perinatal outcome in sub-Saharan Africa: II: effects of placental malaria on perinatal outcome; malaria and HIV. *The Yale journal of biology and medicine* **80**, 95-103 (2007).
11 Hyde, J. E. Drug-resistant malaria - an insight. *Febs J* **274**, 4688-4698, doi:10.1111/j.1742-4658.2007.05999.x (2007).
12 Ecker, A., Lehane, A. M., Clain, J. & Fidock, D. A. PfCRT and its role in antimalarial drug resistance. *Trends Parasitol* **28**, 504-514, doi:10.1016/j.pt.2012.08.002 (2012).
13 Tripathi, R. P., Mishra, R. C., Dwivedi, N., Tewari, N. & Verma, S. S. Current status of malaria control. *Curr Med Chem* **12**, 2643-2659 (2005).
14 Ashley, E. A. *et al.* Spread of artemisinin resistance in *Plasmodium falciparum* malaria. *N Engl J Med* **371**, 411-423, doi:10.1056/NEJMoa1314981 (2014).
15 Castellini, M. A. *et al.* Malaria drug resistance is associated with defective DNA mismatch repair. *Mol Biochem Parasit* **177**, 143-147, doi:Doi 10.1016/J.Molbiopara.2011.02.004 (2011).
16 Ursing, J. *et al.* Chloroquine is grossly under dosed in young children with malaria: implications for drug resistance. *PLoS One* **9**, e86801, doi:10.1371/journal.pone.0086801 (2014).
17 Na-Bangchang, K. & Karbwang, J. Current status of malaria chemotherapy and the role of pharmacology in antimalarial drug research and development. *Fundam Clin Pharmacol* **23**, 387-409, doi:FCP709 [pii] 10.1111/j.1472-8206.2009.00709.x [doi] (2009).
18 Barkakaty, B. N., Sharma, G. K. & Chakravorty, N. K. Studies on efficacy of treatment with sulfamethoxazole + trimethoprim and sulfalene + pyrimethamine combinations in *Plasmodium falciparum* malaria of known and unknown resistant status. *The Journal of communicable diseases* **20**, 165-174 (1988).
19 Buckling, A. G., Taylor, L. H., Carlton, J. M. & Read, A. F. Adaptive changes in Plasmodium transmission strategies following chloroquine chemotherapy.

Proceedings. Biological sciences / The Royal Society **264**, 553-559, doi:10.1098/rspb.1997.0079 (1997).

20 Handunnetti, S. M. *et al.* Features of recrudescent chloroquine-resistant *Plasmodium falciparum* infections confer a survival advantage on parasites and have implications for disease control. *Trans R Soc Trop Med Hyg* **90**, 563-567 (1996).

21 Robert, V., Molez, J. F. & Trape, J. F. Short report: gametocytes, chloroquine pressure, and the relative parasite survival advantage of resistant strains of falciparum malaria in west Africa. *Am J Trop Med Hyg* **55**, 350-351 (1996).

22 Sokhna, C. S., Trape, J. F. & Robert, V. Gametocytaemia in Senegalese children with uncomplicated falciparum malaria treated with chloroquine, amodiaquine or sulfadoxine + pyrimethamine. *Parasite* **8**, 243-250 (2001).

23 Tjitra, E., Suprianto, S. & Anstey, N. M. Higher gametocyte prevalence following failure of treatment of *Plasmodium falciparum* malaria with sulfadoxine-pyrimethamine and the combination of chloroquine plus sulfadoxine-pyrimethamine: implications for progression of anti-folate resistance. *Trans R Soc Trop Med Hyg* **96**, 434-437 (2002).

24 Ochong, E. O., van den Broek, I. V., Keus, K. & Nzila, A. Short report: association between chloroquine and amodiaquine resistance and allelic variation in the *Plasmodium falciparum* multiple drug resistance 1 gene and the chloroquine resistance transporter gene in isolates from the upper Nile in southern Sudan. *Am J Trop Med Hyg* **69**, 184-187 (2003).

25 Venkatesan, M. *et al.* Polymorphisms in *Plasmodium falciparum* chloroquine resistance transporter and multidrug resistance 1 genes: parasite risk factors that affect treatment outcomes for *P. falciparum* malaria after artemether-lumefantrine and artesunate-amodiaquine. *Am J Trop Med Hyg* **91**, 833-843, doi:10.4269/ajtmh.14-0031 (2014).

26 Organization, W. H. Guidelines for the tratment of malaira. (2010).

27 Wongsrichanalai, C., Pickard, A. L., Wernsdorfer, W. H. & Meshnick, S. R. Epidemiology of drug-resistant malaria. *Lancet Infect Dis* **2**, 209-218 (2002).

28 Loria, P., Miller, S., Foley, M. & Tilley, L. Inhibition of the peroxidative degradation of haem as the basis of action of chloroquine and other quinoline antimalarials. *Biochem J* **339 (Pt 2)**, 363-370 (1999).

29 Rosenthal, P. J. & Meshnick, S. R. Hemoglobin catabolism and iron utilization by malaria parasites. *Mol Biochem Parasitol* **83**, 131-139 (1996).

30 Francis, S. E., Sullivan, D. J., Jr. & Goldberg, D. E. Hemoglobin metabolism in the malaria parasite *Plasmodium falciparum*. *Annual review of microbiology* **51**, 97-123, doi:10.1146/annurev.micro.51.1.97 (1997).

31 Sullivan, D. J., Jr., Gluzman, I. Y., Russell, D. G. & Goldberg, D. E. On the molecular mechanism of chloroquine's antimalarial action. *Proceedings of the National Academy of Sciences of the United States of America* **93**, 11865-11870 (1996).

32 Graves, P. R. *et al.* Discovery of novel targets of quinoline drugs in the human purine binding proteome. *Molecular pharmacology* **62**, 1364-1372 (2002).

33 Foote, S. J. *et al.* Several alleles of the multidrug-resistance gene are closely linked to chloroquine resistance in *Plasmodium falciparum*. *Nature* **345**, 255-258, doi:10.1038/345255a0 (1990).

34 Fidock, D. A. *et al.* Mutations in the *P. falciparum* digestive vacuole transmembrane protein PfCRT and evidence for their role in chloroquine resistance. *Mol Cell* **6**, 861-871 (2000).

35 Babiker, H. A. *et al.* High-level chloroquine resistance in Sudanese isolates of *Plasmodium falciparum* is associated with mutations in the chloroquine resistance transporter gene pfcrt and the multidrug resistance Gene pfmdr1. *J Infect Dis* **183**, 1535-1538, doi:10.1086/320195 (2001).

36 Koenderink, J. B., Kavishe, R. A., Rijpma, S. R. & Russel, F. G. The ABCs of multidrug resistance in malaria. *Trends Parasitol* **26**, 440-446, doi:10.1016/j.pt.2010.05.002 (2010).
37 Sibley, C. H. *et al.* Pyrimethamine-sulfadoxine resistance in *Plasmodium falciparum*: what next? *Trends Parasitol* **17**, 582-588 (2001).
38 Vangapandu, S. *et al.* Recent advances in antimalarial drug development. *Med Res Rev* **27**, 65-107, doi:10.1002/med.20062 (2007).
39 Cowman, A. F., Morry, M. J., Biggs, B. A., Cross, G. A. & Foote, S. J. Amino acid changes linked to pyrimethamine resistance in the dihydrofolate reductase-thymidylate synthase gene of *Plasmodium falciparum*. *Proc Natl Acad Sci U S A* **85**, 9109-9113 (1988).
40 Klayman, D. L. Qinghaosu (artemisinin): an antimalarial drug from China. *Science* **228**, 1049-1055 (1985).
41 Bousema, T. & Drakeley, C. Epidemiology and infectivity of *Plasmodium falciparum* and *Plasmodium vivax* gametocytes in relation to malaria control and elimination. *Clin Microbiol Rev* **24**, 377-410, doi:10.1128/CMR.00051-10 (2011).
42 Price, R. N. *et al.* Effects of artemisinin derivatives on malaria transmissibility. *Lancet* **347**, 1654-1658 (1996).
43 Antoine, T. *et al.* Rapid kill of malaria parasites by artemisinin and semi-synthetic endoperoxides involves ROS-dependent depolarization of the membrane potential. *The Journal of antimicrobial chemotherapy* **69**, 1005-1016, doi:10.1093/jac/dkt486 (2014).
44 Gopalakrishnan, A. M. & Kumar, N. Anti-malarial action of Artesunate involves DNA damage mediated by Reactive Oxygen Species. *Antimicrob Agents Chemother*, doi:10.1128/AAC.03663-14 (2014).
45 Cui, L. & Su, X. Z. Discovery, mechanisms of action and combination therapy of artemisinin. *Expert Rev Anti Infect Ther* **7**, 999-1013, doi:10.1586/eri.09.68 (2009).
46 Shandilya, A., Chacko, S., Jayaram, B. & Ghosh, I. A plausible mechanism for the antimalarial activity of artemisinin: A computational approach. *Scientific reports* **3**, 2513, doi:10.1038/srep02513 (2013).
47 Krishna, S., Pulcini, S., Fatih, F. & Staines, H. Artemisinins and the biological basis for the PfATP6/SERCA hypothesis. *Trends in parasitology* **26**, 517-523, doi:10.1016/j.pt.2010.06.014 (2010).
48 Cui, L. *et al.* Lack of Association of the S769N Mutation in *Plasmodium falciparum* SERCA (PfATP6) with Resistance to Artemisinins. *Antimicrob Agents Chemother*, doi:10.1128/AAC.05943-11 (2012).
49 Ariey, F. *et al.* A molecular marker of artemisinin-resistant *Plasmodium falciparum* malaria. *Nature* **505**, 50-55, doi:10.1038/nature12876 (2014).
50 Straimer, J. *et al.* Drug resistance. K13-propeller mutations confer artemisinin resistance in *Plasmodium falciparum* clinical isolates. *Science* **347**, 428-431, doi:10.1126/science.1260867 (2015).
51 Takala-Harrison, S. *et al.* Independent Emergence of Artemisinin Resistance Mutations Among *Plasmodium falciparum* in Southeast Asia. *J Infect Dis*, doi:10.1093/infdis/jiu491 (2014).
52 Srivastava, I. K., Rottenberg, H. & Vaidya, A. B. Atovaquone, a broad spectrum antiparasitic drug, collapses mitochondrial membrane potential in a malarial parasite. *J Biol Chem* **272**, 3961-3966 (1997).
53 Fisher, N. *et al.* Cytochrome b mutation Y268S conferring the atovaquone resistance phenotype in the malaria parasite results in reduced parasite bc1 catalytic turnover and protein expression. *J Biol Chem*, doi:10.1074/jbc.M111.324319 (2012).

54 Cottrell, G. *et al.* Emergence of resistance to atovaquone-proguanil in malaria parasites: insights from computational modeling and clinical case reports. *Antimicrob Agents Chemother* **58**, 4504-4514, doi:10.1128/AAC.02550-13 (2014).
55 Guler, J. L., White, J., 3rd, Phillips, M. A. & Rathod, P. K. Atovaquone tolerance in *Plasmodium falciparum* parasites selected for high-level resistance to a dihydroorotate dehydrogenase inhibitor. *Antimicrob Agents Chemother* **59**, 686-689, doi:10.1128/AAC.02347-14 (2015).
56 Maude, R. J., Nguon, C., Dondorp, A. M., White, L. J. & White, N. J. The diminishing returns of atovaquone-proguanil for elimination of *Plasmodium falciparum* malaria: modelling mass drug administration and treatment. *Malar J* **13**, 380, doi:10.1186/1475-2875-13-380 (2014).
57 Marsh, K. & Kinyanjui, S. Immune effector mechanisms in malaria. *Parasite Immunol* **28**, 51-60, doi:10.1111/j.1365-3024.2006.00808.x (2006).
58 Taylor-Robinson, A. W. Regulation of immunity to *Plasmodium*: Implications from mouse models for blood stage malaria vaccine design. *Exp Parasitol*, doi:S0014-4894(10)00042-1 [pii] 10.1016/j.exppara.2010.01.028 (2010).
59 Bejon, P. *et al.* Efficacy of RTS,S malaria vaccines: individual-participant pooled analysis of phase 2 data. *Lancet Infect Dis* **13**, 319-327, doi:10.1016/S1473-3099(13)70005-7 (2013).
60 Rts, S. C. T. P. Efficacy and Safety of the RTS,S/AS01 Malaria Vaccine during 18 Months after Vaccination: A Phase 3 Randomized, Controlled Trial in Children and Young Infants at 11 African Sites. *PLoS Med* **11**, e1001685, doi:10.1371/journal.pmed.1001685 (2014).
61 Dronamraju, K. R., Arese, P. & Haldane, J. B. S. The Rate of Mutations of Human Genes. 169-174, doi:10.1007/0-387-28295-5_8.
62 Firdous, N., Gibbons, S. & Modell, B. Falling prevalence of beta-thalassaemia and eradication of malaria in the Maldives. *J Community Genet* **2**, 173-189, doi:10.1007/s12687-011-0054-0 (2011).
63 Salih, N. A. *et al.* Loss of balancing selection in the betaS globin locus. *BMC Med Genet* **11**, 21, doi:10.1186/1471-2350-11-21 (2010).
64 Aidoo, M. *et al.* Protective effects of the sickle cell gene against malaria morbidity and mortality. *Lancet* **359**, 1311-1312, doi:10.1016/S0140-6736(02)08273-9 (2002).
65 Williams, T. N. *et al.* Sickle cell trait and the risk of *Plasmodium falciparum* malaria and other childhood diseases. *J Infect Dis* **192**, 178-186, doi:10.1086/430744 (2005).
66 Rockett, K. A. *et al.* Reappraisal of known malaria resistance loci in a large multicenter study. *Nat Genet* **46**, 1197-1204, doi:Doi 10.1038/Ng.3107 (2014).
67 Agarwal, A. *et al.* Hemoglobin C associated with protection from severe malaria in the Dogon of Mali, a West African population with a low prevalence of hemoglobin S. *Blood* **96**, 2358-2363 (2000).
68 Chotivanich, K. *et al.* Hemoglobin E: a balanced polymorphism protective against high parasitemias and thus severe *P. falciparum* malaria. *Blood* **100**, 1172-1176 (2002).
69 Modiano, D. *et al.* Haemoglobin C protects against clinical *Plasmodium falciparum* malaria. *Nature* **414**, 305-308, doi:10.1038/35104556 (2001).
70 Weatherall, D. J. The definition and epidemiology of non-transfusion-dependent thalassemia. *Blood reviews* **26 Suppl 1**, S3-6, doi:10.1016/S0268-960X(12)70003-6 (2012).
71 Allen, S. J. *et al.* alpha+-Thalassemia protects children against disease caused by other infections as well as malaria. *Proc Natl Acad Sci U S A* **94**, 14736-14741 (1997).

72 Oppenheimer, S. J. *et al.* The interaction of alpha thalassaemia with malaria. *Trans R Soc Trop Med Hyg* **81**, 322-326 (1987).
73 Williams, T. N. *et al.* High incidence of malaria in alpha-thalassaemic children. *Nature* **383**, 522-525, doi:10.1038/383522a0 (1996).
74 Williams, T. N. *et al.* Negative epistasis between the malaria-protective effects of alpha+-thalassemia and the sickle cell trait. *Nature genetics* **37**, 1253-1257, doi:10.1038/ng1660 (2005).
75 Zimmerman, P. A. *et al.* Emergence of FY*A(null) in a *Plasmodium vivax*-endemic region of Papua New Guinea. *Proc Natl Acad Sci U S A* **96**, 13973-13977 (1999).
76 Hamblin, M. T. & Di Rienzo, A. Detection of the signature of natural selection in humans: evidence from the Duffy blood group locus. *Am J Hum Genet* **66**, 1669-1679, doi:10.1086/302879 (2000).
77 Culleton, R. L. *et al.* Failure to detect *Plasmodium vivax* in West and Central Africa by PCR species typing. *Malar J* **7**, 174, doi:10.1186/1475-2875-7-174 (2008).
78 Hodgson, J. A. *et al.* Natural selection for the Duffy-null allele in the recently admixed people of Madagascar. *Proceedings. Biological sciences / The Royal Society* **281**, 20140930, doi:10.1098/rspb.2014.0930 (2014).
79 Miller, L. H., Mason, S. J., Clyde, D. F. & McGinniss, M. H. The resistance factor to *Plasmodium vivax* in blacks. The Duffy-blood-group genotype, FyFy. *N Engl J Med* **295**, 302-304, doi:10.1056/NEJM197608052950602 (1976).
80 Menard, D. *et al. Plasmodium vivax* clinical malaria is commonly observed in Duffy-negative Malagasy people. *Proc Natl Acad Sci U S A*, doi:0912496107 [pii] 10.1073/pnas.0912496107 [doi] (2010).
81 Cavasini, C. E. *et al. Plasmodium vivax* infection among Duffy antigen-negative individuals from the Brazilian Amazon region: an exception? *Transactions of the Royal Society of Tropical Medicine and Hygiene* **101**, 1042-1044, doi:10.1016/j.trstmh.2007.04.011 (2007).
82 Mendes, C. *et al.* Duffy negative antigen is no longer a barrier to *Plasmodium vivax*--molecular evidences from the African West Coast (Angola and Equatorial Guinea). *PLoS Negl Trop Dis* **5**, e1192, doi:10.1371/journal.pntd.0001192 (2011).
83 Ryan, J. R. *et al.* Evidence for transmission of *Plasmodium vivax* among a duffy antigen negative population in Western Kenya. *Am J Trop Med Hyg* **75**, 575-581 (2006).
84 Ngassa Mbenda, H. G. & Das, A. Molecular evidence of *Plasmodium vivax* mono and mixed malaria parasite infections in Duffy-negative native Cameroonians. *PLoS One* **9**, e103262, doi:10.1371/journal.pone.0103262 (2014).
85 Qari, S. H. *et al.* Identification of *Plasmodium vivax*-like human malaria parasite. *Lancet* **341**, 780-783 (1993).
86 Eng, L. I. Hereditary ovalocytosis and haemoglobin E-ovalocytosis in Malayan aborigines. *Nature* **208**, 1329 (1965).
87 Lecomte, M. C. *et al.* [Hereditary elliptocytosis in West Africa: frequency and repartition of spectrin variants]. *Comptes rendus de l'Academie des sciences. Serie III, Sciences de la vie* **306**, 43-46 (1988).
88 Glele-Kakai, C. *et al.* Epidemiological studies of spectrin mutations related to hereditary elliptocytosis and spectrin polymorphisms in Benin. *Br J Haematol* **95**, 57-66 (1996).
89 Lin, E. *et al.* Minimal association of common red blood cell polymorphisms with Plasmodium falciparum infection and uncomplicated malaria in Papua New Guinean school children. *Am J Trop Med Hyg* **83**, 828-833, doi:10.4269/ajtmh.2010.09-0713 (2010).
90 Doumbo, O. K. *et al.* High Levels of *Plasmodium falciparum* Rosetting in All Clinical Forms of Severe Malaria in African Children. *Am J Trop Med Hyg* **81**, 987-993, doi:10.4269/ajtmh.2009.09-0406 (2009).

91 Allen, S. J. *et al.* Prevention of cerebral malaria in children in Papua New Guinea by southeast Asian ovalocytosis band 3. *Am J Trop Med Hyg* **60**, 1056-1060 (1999).
92 Fischer, P. R. & Boone, P. Short report: severe malaria associated with blood group. *Am J Trop Med Hyg* **58**, 122-123 (1998).
93 Fry, A. E. *et al.* Common variation in the ABO glycosyltransferase is associated with susceptibility to severe *Plasmodium falciparum* malaria. *Hum Mol Genet* **17**, 567-576, doi:10.1093/hmg/ddm331 (2008).
94 Bedu-Addo, G. *et al.* Reduced prevalence of placental malaria in primiparae with blood group O. *Malar J* **13**, 289, doi:10.1186/1475-2875-13-289 (2014).
95 Moulds, J. M. *et al.* Identification of complement receptor one (CR1) polymorphisms in west Africa. *Genes Immun* **1**, 325-329, doi:10.1038/sj.gene.6363676 (2000).
96 Cockburn, I. A. *et al.* A human complement receptor 1 polymorphism that reduces *Plasmodium falciparum* rosetting confers protection against severe malaria. *Proc Natl Acad Sci U S A* **101**, 272-277, doi:10.1073/pnas.0305306101 (2004).
97 Lowe, R. F. & Moores, P. P. S-s-U-red cell factor in Africans of Rhodesia, Malawi, Mozambique and Natal. *Human heredity* **22**, 344-350 (1972).
98 Patel, S. S., King, C. L., Mgone, C. S., Kazura, J. W. & Zimmerman, P. A. Glycophorin C (Gerbich antigen blood group) and band 3 polymorphisms in two malaria holoendemic regions of Papua New Guinea. *Am J Hematol* **75**, 1-5, doi:10.1002/ajh.10448 (2004).
99 Maier, A. G. *et al. Plasmodium falciparum* erythrocyte invasion through glycophorin C and selection for Gerbich negativity in human populations. *Nature Medicine* **9**, 87-92, doi:10.1038/nm807 (2003).
100 Patel, S. S. *et al.* The association of the glycophorin C exon 3 deletion with ovalocytosis and malaria susceptibility in the Wosera, Papua New Guinea. *Blood* **98**, 3489-3491 (2001).
101 Tavul, L. *et al.* Glycophorin C delta(exon3) is not associated with protection against severe anaemia in Papua New Guinea. *Papua and New Guinea medical journal* **51**, 149-154 (2008).
102 Weatherall, D. J. *et al.* Malaria and the red cell. *Hematology Am Soc Hematol Educ Program*, 35-57 (2002).
103 Ruwende, C. *et al.* Natural selection of hemi- and heterozygotes for G6PD deficiency in Africa by resistance to severe malaria. *Nature* **376**, 246-249, doi:10.1038/376246a0 (1995).
104 Guindo, A., Fairhurst, R. M., Doumbo, O. K., Wellems, T. E. & Diallo, D. A. X-linked G6PD deficiency protects hemizygous males but not heterozygous females against severe malaria. *PLoS Med* **4**, e66, doi:10.1371/journal.pmed.0040066 (2007).
105 Sirugo, G. *et al.* G6PD A- deficiency and severe malaria in The Gambia: heterozygote advantage and possible homozygote disadvantage. *Am J Trop Med Hyg* **90**, 856-859, doi:10.4269/ajtmh.13-0622 (2014).
106 Zanella, A., Fermo, E., Bianchi, P. & Valentini, G. Red cell pyruvate kinase deficiency: molecular and clinical aspects. *Br J Haematol* **130**, 11-25, doi:10.1111/j.1365-2141.2005.05527.x (2005).
107 Berghout, J. *et al.* Genetic diversity in human erythrocyte pyruvate kinase. *Genes Immun* **13**, 98-102, doi:10.1038/gene.2011.54 (2012).
108 Beutler, E. & Gelbart, T. Estimating the prevalence of pyruvate kinase deficiency from the gene frequency in the general white population. *Blood* **95**, 3585-3588 (2000).

109 Machado, P. *et al.* Pyruvate kinase deficiency in sub-Saharan Africa: identification of a highly frequent missense mutation (G829A;Glu277Lys) and association with malaria. *PLoS One* **7**, e47071, doi:10.1371/journal.pone.0047071 (2012).
110 Hobbs, M. R. *et al.* A new NOS2 promoter polymorphism associated with increased nitric oxide production and protection from severe malaria in Tanzanian and Kenyan children. *Lancet* **360**, 1468-1475, doi:10.1016/S0140-6736(02)11474-7 (2002).
111 Kun, J. F. *et al.* Nitric oxide synthase 2(Lambarene) (G-954C), increased nitric oxide production, and protection against malaria. *J Infect Dis* **184**, 330-336, doi:10.1086/322037 (2001).
112 Levesque, M. C. *et al.* Malaria severity and human nitric oxide synthase type 2 (NOS2) promoter haplotypes. *Hum Genet* **127**, 163-182, doi:10.1007/s00439-009-0753-3 (2010).
113 Timmann, C. *et al.* Genome-wide association study indicates two novel resistance loci for severe malaria. *Nature* **489**, 443-446, doi:10.1038/nature11334 (2012).
114 Kwiatkowski, D. P. How malaria has affected the human genome and what human genetics can teach us about malaria. *Am J Hum Genet* **77**, 171-192, doi:S0002-9297(07)62909-7 [pii]
10.1086/432519 [doi] (2005).
115 Hill, A. V. *et al.* Common west African HLA antigens are associated with protection from severe malaria. *Nature* **352**, 595-600, doi:10.1038/352595a0 (1991).
116 Tangteerawatana, P. *et al.* Relative levels of IL4 and IFN-[gamma] in complicated malaria: Association with IL4 polymorphism and peripheral parasitemia. *Acta Tropica* **101**, 258-265 (2007).
117 Okeyo, W. A. *et al.* Interleukin (IL)-13 promoter polymorphisms (-7402 T/G and -4729G/A) condition susceptibility to pediatric severe malarial anemia but not circulating IL-13 levels. *BMC immunology* **14**, 15, doi:10.1186/1471-2172-14-15 (2013).
118 Koch, O. *et al.* IFNGR1 gene promoter polymorphisms and susceptibility to cerebral malaria. *J Infect Dis* **185**, 1684-1687, doi:JID010716 [pii]
10.1086/340516 (2002).
119 Sabeti, P. *et al.* CD40L association with protection from severe malaria. *Genes Immun* **3**, 286-291, doi:10.1038/sj.gene.6363877 (2002).
120 Carter, R. & Mendis, K. N. Evolutionary and historical aspects of the burden of malaria. *Clin Microbiol Rev* **15**, 564-594 (2002).
121 Wertheimer, S. P. & Barnwell, J. W. Plasmodium vivax interaction with the human Duffy blood group glycoprotein: identification of a parasite receptor-like protein. *Exp Parasitol* **69**, 340-350 (1989).
122 Sim, B. K. *et al. Plasmodium falciparum*: further characterization of a functionally active region of the merozoite invasion ligand EBA-175. *Exp Parasitol* **78**, 259-268, doi:10.1006/expr.1994.1027 (1994).
123 Li, X. *et al.* Identification of a specific region of *Plasmodium falciparum* EBL-1 that binds to host receptor glycophorin B and inhibits merozoite invasion in human red blood cells. *Mol Biochem Parasitol* **183**, 23-31, doi:10.1016/j.molbiopara.2012.01.002 (2012).
124 Lobo, C. A., Rodriguez, M., Reid, M. & Lustigman, S. Glycophorin C is the receptor for the *Plasmodium falciparum* erythrocyte binding ligand PfEBP-2 (baebl). *Blood* **101**, 4628-4631, doi:10.1182/blood-2002-10-3076 (2003).
125 Niang, M. *et al.* STEVOR is a *Plasmodium falciparum* erythrocyte binding protein that mediates merozoite invasion and rosetting. *Cell host & microbe* **16**, 81-93, doi:10.1016/j.chom.2014.06.004 (2014).

126 Tham, W. H. *et al.* Complement receptor 1 is the host erythrocyte receptor for *Plasmodium falciparum* PfRh4 invasion ligand. *Proc Natl Acad Sci U S A* **107**, 17327-17332, doi:10.1073/pnas.1008151107 (2010).
127 Crosnier, C. *et al.* Basigin is a receptor essential for erythrocyte invasion by *Plasmodium falciparum*. *Nature* **480**, 534-537, doi:10.1038/nature10606 (2011).
128 Goel, V. K. *et al.* Band 3 is a host receptor binding merozoite surface protein 1 during the *Plasmodium falciparum* invasion of erythrocytes. *Proc Natl Acad Sci U S A* **100**, 5164-5169, doi:10.1073/pnas.0834959100 (2003).
129 Spadafora, C. *et al.* Complement receptor 1 is a sialic acid-independent erythrocyte receptor of *Plasmodium falciparum*. *PLoS Pathog* **6**, e1000968, doi:10.1371/journal.ppat.1000968 (2010).
130 Grimberg, B. T. *et al. Plasmodium vivax* invasion of human erythrocytes inhibited by antibodies directed against the Duffy binding protein. *PLoS Med* **4**, e337, doi:10.1371/journal.pmed.0040337 (2007).
131 Barnwell, J. W., Nichols, M. E. & Rubinstein, P. In vitro evaluation of the role of the Duffy blood group in erythrocyte invasion by *Plasmodium vivax*. *J Exp Med* **169**, 1795-1802 (1989).
132 Gaur, D., Storry, J. R., Reid, M. E., Barnwell, J. W. & Miller, L. H. *Plasmodium falciparum* is able to invade erythrocytes through a trypsin-resistant pathway independent of glycophorin B. *Infect Immun* **71**, 6742-6746 (2003).
133 Maier, A. G. *et al. Plasmodium falciparum* erythrocyte invasion through glycophorin C and selection for Gerbich negativity in human populations. *Nat Med* **9**, 87-92, doi:10.1038/nm807 (2003).
134 Chishti, A. H., Palek, J., Fisher, D., Maalouf, G. J. & Liu, S. C. Reduced invasion and growth of *Plasmodium falciparum* into elliptocytic red blood cells with a combined deficiency of protein 4.1, glycophorin C, and p55. *Blood* **87**, 3462-3469 (1996).
135 Cortes, A., Benet, A., Cooke, B. M., Barnwell, J. W. & Reeder, J. C. Ability of *Plasmodium falciparum* to invade Southeast Asian ovalocytes varies between parasite lines. *Blood* **104**, 2961-2966, doi:10.1182/blood-2004-06-2136 (2004).
136 Gunalan, K., Gao, X., Yap, S. S., Huang, X. & Preiser, P. R. The role of the reticulocyte-binding-like protein homologues of *Plasmodium* in erythrocyte sensing and invasion. *Cell Microbiol* **15**, 35-44, doi:10.1111/cmi.12038 (2013).
137 Eaton, J. W. & Brewer, G. J. Red cell ATP and malaria infection. *Nature* **222**, 389-390 (1969).
138 Oppenheim, R. D. *et al.* BCKDH: the missing link in apicomplexan mitochondrial metabolism is required for full virulence of Toxoplasma gondii and *Plasmodium berghei*. *PLoS Pathog* **10**, e1004263, doi:10.1371/journal.ppat.1004263 (2014).
139 Levano-Garcia, J., Dluzewski, A. R., Markus, R. P. & Garcia, C. R. Purinergic signalling is involved in the malaria parasite *Plasmodium falciparum* invasion to red blood cells. *Purinergic signalling* **6**, 365-372, doi:10.1007/s11302-010-9202-y (2010).
140 Ramalingam, J. K., Hunke, C., Gao, X., Gruber, G. & Preiser, P. R. ATP/ADP binding to a novel nucleotide binding domain of the reticulocyte-binding protein Py235 of *Plasmodium yoelii*. *J Biol Chem* **283**, 36386-36396, doi:10.1074/jbc.M803102200 (2008).
141 Gilson, P. R. & Crabb, B. S. Morphology and kinetics of the three distinct phases of red blood cell invasion by *Plasmodium falciparum* merozoites. *International Journal for Parasitology* **39**, 91-96 (2009).
142 Ayi, K. *et al.* Pyruvate Kinase Deficiency and Malaria. *N Engl J Med*, NEJMoa072464, doi:10.1056/NEJMoa072464 (2008).
143 Kirk, K., Horner, H. A., Elford, B. C., Ellory, J. C. & Newbold, C. I. Transport of diverse substrates into malaria-infected erythrocytes via a pathway showing

functional characteristics of a chloride channel. *J Biol Chem* **269**, 3339-3347 (1994).
144 Saliba, K. J., Horner, H. A. & Kirk, K. Transport and metabolism of the essential vitamin pantothenic acid in human erythrocytes infected with the malaria parasite *Plasmodium falciparum*. *J Biol Chem* **273**, 10190-10195 (1998).
145 Martin, R. E. & Kirk, K. Transport of the essential nutrient isoleucine in human erythrocytes infected with the malaria parasite *Plasmodium falciparum*. *Blood* **109**, 2217-2224, doi:10.1182/blood-2005-11-026963 (2007).
146 Poole, R. C. & Halestrap, A. P. Transport of lactate and other monocarboxylates across mammalian plasma membranes. *The American journal of physiology* **264**, C761-782 (1993).
147 Quashie, N. B., Ranford-Cartwright, L. C. & de Koning, H. P. Uptake of purines in *Plasmodium falciparum*-infected human erythrocytes is mostly mediated by the human equilibrative nucleoside transporter and the human facilitative nucleobase transporter. *Malar J* **9**, 36, doi:10.1186/1475-2875-9-36 (2010).
148 Nepveu, F. & Turrini, F. Targeting the redox metabolism of *Plasmodium falciparum*. *Future medicinal chemistry* **5**, 1993-2006, doi:10.4155/fmc.13.159 (2013).
149 Jortzik, E. & Becker, K. Thioredoxin and glutathione systems in *Plasmodium falciparum*. *International journal of medical microbiology : IJMM* **302**, 187-194, doi:10.1016/j.ijmm.2012.07.007 (2012).
150 Sztajer, H. *et al.* The putative glutathione peroxidase gene of *Plasmodium falciparum* codes for a thioredoxin peroxidase. *J Biol Chem* **276**, 7397-7403, doi:10.1074/jbc.M008631200 (2001).
151 Stocker, R. *et al.* Oxidative stress and protective mechanisms in erythrocytes in relation to *Plasmodium vinckei* load. *Proc Natl Acad Sci U S A* **82**, 548-551 (1985).
152 Brizuela, M. *et al.* Treatment of erythrocytes with the 2-cys peroxiredoxin inhibitor, Conoidin A, prevents the growth of *Plasmodium falciparum* and enhances parasite sensitivity to chloroquine. *PLoS One* **9**, e92411, doi:10.1371/journal.pone.0092411 (2014).
153 Krnajski, Z., Gilberger, T. W., Walter, R. D., Cowman, A. F. & Muller, S. Thioredoxin reductase is essential for the survival of *Plasmodium falciparum* erythrocytic stages. *J Biol Chem* **277**, 25970-25975, doi:10.1074/jbc.M203539200 (2002).
154 Mendez, D., Linares, M., Diez, A., Puyet, A. & Bautista, J. M. Stress response and cytoskeletal proteins involved in erythrocyte membrane remodeling upon *Plasmodium falciparum* invasion are differentially carbonylated in G6PD A-deficiency. *Free Radic Biol Med* **50**, 1305-1313, doi:10.1016/j.freeradbiomed.2011.02.024 (2011).
155 Cyrklaff, M. *et al.* Hemoglobins S and C interfere with actin remodeling in *Plasmodium falciparum*-infected erythrocytes. *Science* **334**, 1283-1286, doi:10.1126/science.1213775 (2011).
156 Giribaldi, G., Ulliers, D., Mannu, F., Arese, P. & Turrini, F. Growth of *Plasmodium falciparum* induces stage-dependent haemichrome formation, oxidative aggregation of band 3, membrane deposition of complement and antibodies, and phagocytosis of parasitized erythrocytes. *Br J Haematol* **113**, 492-499 (2001).
157 Ayi, K., Turrini, F., Piga, A. & Arese, P. Enhanced phagocytosis of ring-parasitized mutant erythrocytes: a common mechanism that may explain protection against *falciparum* malaria in sickle trait and beta-thalassemia trait. *Blood* **104**, 3364-3371, doi:10.1182/blood-2003-11-3820 (2004).
158 Beaudry, J. T. *et al.* Ex-vivo cytoadherence phenotypes of *Plasmodium falciparum* strains from Malian children with hemoglobins A, S, and C. *PLoS One* **9**, e92185, doi:10.1371/journal.pone.0092185 (2014).

159 Cholera, R. *et al.* Impaired cytoadherence of *Plasmodium falciparum*-infected erythrocytes containing sickle hemoglobin. *Proc Natl Acad Sci U S A* **105**, 991-996, doi:10.1073/pnas.0711401105 (2008).
160 Ferreira, A. *et al.* Sickle hemoglobin confers tolerance to *Plasmodium* infection. *Cell* **145**, 398-409, doi:10.1016/j.cell.2011.03.049 (2011).
161 Cabrera, G. *et al.* The sickle cell trait is associated with enhanced immunoglobulin G antibody responses to *Plasmodium falciparum* variant surface antigens. *J Infect Dis* **191**, 1631-1638, doi:10.1086/429832 (2005).
162 Verra, F. *et al.* Haemoglobin C and S role in acquired immunity against *Plasmodium falciparum* malaria. *PLoS One* **2**, e978, doi:10.1371/journal.pone.0000978 (2007).
163 Nagababu, E., Fabry, M. E., Nagel, R. L. & Rifkind, J. M. Heme degradation and oxidative stress in murine models for hemoglobinopathies: thalassemia, sickle cell disease and hemoglobin C disease. *Blood cells, molecules & diseases* **41**, 60-66, doi:10.1016/j.bcmd.2007.12.003 (2008).
164 Orjih, A. U. Comparison of *Plasmodium falciparum* growth in sickle cells in low oxygen environment and candle-jar. *Acta Trop* **94**, 25-34, doi:10.1016/j.actatropica.2005.02.001 (2005).
165 Carlson, J., Nash, G. B., Gabutti, V., al-Yaman, F. & Wahlgren, M. Natural protection against severe *Plasmodium falciparum* malaria due to impaired rosette formation. *Blood* **84**, 3909-3914 (1994).
166 Olson, J. A. & Nagel, R. L. Synchronized cultures of *P. falciparum* in abnormal red cells: the mechanism of the inhibition of growth in HbCC cells. *Blood* **67**, 997-1001 (1986).
167 Fairhurst, R. M. *et al.* Abnormal display of PfEMP-1 on erythrocytes carrying haemoglobin C may protect against malaria. *Nature* **435**, 1117-1121, doi:10.1038/nature03631 (2005).
168 Dei-Cas, E. *et al.* In vitro growth and chloroquine sensitivity of P*lasmodium falciparum* (FCR-3 strain) in red blood cells containing HbC. *Parasitology research* **73**, 306-312 (1987).
169 Fairhurst, R. M., Fujioka, H., Hayton, K., Collins, K. F. & Wellems, T. E. Aberrant development of *Plasmodium falciparum* in hemoglobin CC red cells: implications for the malaria protective effect of the homozygous state. *Blood* **101**, 3309-3315, doi:10.1182/blood-2002-10-3105 (2003).
170 Vernes, A. J., Haynes, J. D., Tang, D. B., Dutoit, E. & Diggs, C. L. Decreased growth of *Plasmodium falciparum* in red cells containing haemoglobin E, a role for oxidative stress, and a sero-epidemiological correlation. *Trans R Soc Trop Med Hyg* **80**, 642-648 (1986).
171 Bunyaratvej, A. *et al.* Increased phagocytosis of *Plasmodium falciparum*-infected erythrocytes with haemoglobin E by peripheral blood monocytes. *Acta haematologica* **76**, 155-158 (1986).
172 Luzzi, G. A., Merry, A. H., Newbold, C. I., Marsh, K. & Pasvol, G. Protection by alpha-thalassaemia against Plasmodium falciparum malaria: modified surface antigen expression rather than impaired growth or cytoadherence. *Immunology letters* **30**, 233-240 (1991).
173 Krause, M. A. *et al.* alpha-Thalassemia impairs the cytoadherence of Plasmodium falciparum-infected erythrocytes. *PLoS One* **7**, e37214, doi:10.1371/journal.pone.0037214 (2012).
174 Senok, A. C., Nelson, E. A., Li, K. & Oppenheimer, S. J. Thalassaemia trait, red blood cell age and oxidant stress: effects on Plasmodium falciparum growth and sensitivity to artemisinin. *Trans R Soc Trop Med Hyg* **91**, 585-589 (1997).

175 Pantaleo, A. *et al.* Effect of heterozygous beta thalassemia on the phosphorylative response to *Plasmodium falciparum* infection. *Journal of proteomics* **76 Spec No.**, 251-258, doi:10.1016/j.jprot.2012.08.018 (2012).
176 Udomsangpetch, R. *et al.* Alteration in cytoadherence and rosetting of *Plasmodium falciparum*-infected thalassemic red blood cells. *Blood* **82**, 3752-3759 (1993).
177 Cappadoro, M. *et al.* Early phagocytosis of glucose-6-phosphate dehydrogenase (G6PD)-deficient erythrocytes parasitized by *Plasmodium falciparum* may explain malaria protection in G6PD deficiency. *Blood* **92**, 2527-2534 (1998).
178 Rowe, J. A. *et al.* Blood group O protects against severe *Plasmodium falciparum* malaria through the mechanism of reduced rosetting. *Proc Natl Acad Sci U S A* **104**, 17471-17476, doi:10.1073/pnas.0705390104 (2007).
179 Vigan-Womas, I. *et al.* Structural basis for the ABO blood-group dependence of *Plasmodium falciparum* rosetting. *PLoS Pathog* **8**, e1002781, doi:10.1371/journal.ppat.1002781 (2012).
180 Rowe, J. A., Moulds, J. M., Newbold, C. I. & Miller, L. H. *P. falciparum* rosetting mediated by a parasite-variant erythrocyte membrane protein and complement-receptor 1. *Nature* **388**, 292-295, doi:10.1038/40888 (1997).
181 Baum, J., Pinder, M. & Conway, D. J. Erythrocyte invasion phenotypes of *Plasmodium falciparum* in The Gambia. *Infect Immun* **71**, 1856-1863 (2003).
182 Schulman, S. *et al.* Growth of *Plasmodium falciparum* in human erythrocytes containing abnormal membrane proteins. *Proc Natl Acad Sci U S A* **87**, 7339-7343 (1990).
183 Crandall, I., Collins, W. E., Gysin, J. & Sherman, I. W. Synthetic peptides based on motifs present in human band 3 protein inhibit cytoadherence/sequestration of the malaria parasite *Plasmodium falciparum*. *Proc Natl Acad Sci U S A* **90**, 4703-4707 (1993).
184 Herrera, S. *et al.* A conserved region of the MSP-1 surface protein of *Plasmodium falciparum* contains a recognition sequence for erythrocyte spectrin. *The EMBO journal* **12**, 1607-1614 (1993).
185 Magowan, C. *et al.* Role of the *Plasmodium falciparum* mature-parasite-infected erythrocyte surface antigen (MESA/PfEMP-2) in malarial infection of erythrocytes. *Blood* **86**, 3196-3204 (1995).
186 Greth, A. *et al.* A novel ENU-mutation in ankyrin-1 disrupts malaria parasite maturation in red blood cells of mice. *PLoS One* **7**, e38999, doi:10.1371/journal.pone.0038999 (2012).
187 Buffet, P. A. *et al.* The pathogenesis of *Plasmodium falciparum* malaria in humans: insights from splenic physiology. *Blood* **117**, 381-392, doi:10.1182/blood-2010-04-202911 (2011).
188 Groom, A. C., Schmidt, E. E. & MacDonald, I. C. Microcirculatory pathways and blood flow in spleen: new insights from washout kinetics, corrosion casts, and quantitative intravital videomicroscopy. *Scanning Microsc* **5**, 159-173; discussion 173-154 (1991).
189 Buffet, P. A. *et al.* Ex vivo perfusion of human spleens maintains clearing and processing functions. *Blood* **107**, 3745-3752, doi:10.1182/blood-2005-10-4094 (2006).
190 Safeukui, I. *et al.* Retention of *Plasmodium falciparum* ring-infected erythrocytes in the slow, open microcirculation of the human spleen. *Blood* **112**, 2520-2528, doi:blood-2008-03-146779 [pii] 10.1182/blood-2008-03-146779 (2008).
191 Mohandas, N. & Gallagher, P. G. Red cell membrane: past, present, and future. *Blood* **112**, 3939-3948, doi:10.1182/blood-2008-07-161166 (2008).

192 Looareesuwan, S. *et al.* Dynamic alteration in splenic function during acute *falciparum* malaria. *N Engl J Med* **317**, 675-679, doi:10.1056/NEJM198709103171105 (1987).
193 Turrini, F. *et al.* Phagocytosis of *Plasmodium falciparum*-infected human red blood cells by human monocytes: involvement of immune and nonimmune determinants and dependence on parasite developmental stage. *Blood* **80**, 801-808 (1992).
194 Lutz, H. U. Innate immune and non-immune mediators of erythrocyte clearance. *Cellular and molecular biology* **50**, 107-116 (2004).
195 Suwanarusk, R. *et al.* The deformability of red blood cells parasitized by *Plasmodium falciparum* and P. vivax. *J Infect Dis* **189**, 190-194, doi:10.1086/380468 (2004).
196 Handayani, S. *et al.* High deformability of *Plasmodium vivax*-infected red blood cells under microfluidic conditions. *J Infect Dis* **199**, 445-450, doi:10.1086/596048 (2009).
197 Maier, A. G., Cooke, B. M., Cowman, A. F. & Tilley, L. Malaria parasite proteins that remodel the host erythrocyte. *Nature reviews. Microbiology* **7**, 341-354, doi:10.1038/nrmicro2110 (2009).
198 Cranston, H. A. *et al. Plasmodium falciparum* maturation abolishes physiologic red cell deformability. *Science* **223**, 400-403 (1984).
199 Nash, G. B., O'Brien, E., Gordon-Smith, E. C. & Dormandy, J. A. Abnormalities in the mechanical properties of red blood cells caused by *Plasmodium falciparum*. *Blood* **74**, 855-861 (1989).
200 Mills, J. P. *et al.* Effect of plasmodial RESA protein on deformability of human red blood cells harboring *Plasmodium falciparum*. *Proc Natl Acad Sci U S A* **104**, 9213-9217, doi:10.1073/pnas.0703433104 (2007).
201 Rowe, J. A., Claessens, A., Corrigan, R. A. & Arman, M. Adhesion of *Plasmodium falciparum*-infected erythrocytes to human cells: molecular mechanisms and therapeutic implications. *Expert reviews in molecular medicine* **11**, e16, doi:10.1017/S1462399409001082 (2009).
202 Chen, Q. *et al.* Identification of *Plasmodium falciparum* erythrocyte membrane protein 1 (PfEMP1) as the rosetting ligand of the malaria parasite P. falciparum. *J Exp Med* **187**, 15-23 (1998).
203 Lavstsen, T., Salanti, A., Jensen, A. T., Arnot, D. E. & Theander, T. G. Sub-grouping of *Plasmodium falciparum* 3D7 var genes based on sequence analysis of coding and non-coding regions. *Malar J* **2**, 27, doi:10.1186/1475-2875-2-27 (2003).
204 Blisnick, T. *et al.* Pfsbp1, a Maurer's cleft *Plasmodium falciparum* protein, is associated with the erythrocyte skeleton. *Mol Biochem Parasitol* **111**, 107-121 (2000).
205 Kilian, N. *et al.* Haemoglobin S and C affect the motion of Maurer's clefts in *Plasmodium falciparum*-infected erythrocytes. *Cell Microbiol* **15**, 1111-1126, doi:10.1111/cmi.12102 (2013).
206 Trelka, D. P., Schneider, T. G., Reeder, J. C. & Taraschi, T. F. Evidence for vesicle-mediated trafficking of parasite proteins to the host cell cytosol and erythrocyte surface membrane in *Plasmodium falciparum* infected erythrocytes. *Mol Biochem Parasitol* **106**, 131-145 (2000).
207 Chen, Q. *et al.* The semiconserved head structure of *Plasmodium falciparum* erythrocyte membrane protein 1 mediates binding to multiple independent host receptors. *J Exp Med* **192**, 1-10 (2000).
208 Barragan, A., Kremsner, P. G., Wahlgren, M. & Carlson, J. Blood group A antigen is a coreceptor in *Plasmodium falciparum* rosetting. *Infect Immun* **68**, 2971-2975 (2000).

209 Wellems, T. E., Hayton, K. & Fairhurst, R. M. The impact of malaria parasitism: from corpuscles to communities. *J Clin Invest* **119**, 2496-2505, doi:10.1172/JCI38307 (2009).
210 Grau, G. E. & Craig, A. G. Cerebral malaria pathogenesis: revisiting parasite and host contributions. *Future microbiology* **7**, 291-302, doi:10.2217/fmb.11.155 (2012).
211 MacPherson, G. G., Warrell, M. J., White, N. J., Looareesuwan, S. & Warrell, D. A. Human cerebral malaria. A quantitative ultrastructural analysis of parasitized erythrocyte sequestration. *The American journal of pathology* **119**, 385-401 (1985).
212 Dorovini-Zis, K. *et al.* The neuropathology of fatal cerebral malaria in malawian children. *The American journal of pathology* **178**, 2146-2158, doi:10.1016/j.ajpath.2011.01.016 (2011).
213 Turner, L. *et al.* Severe malaria is associated with parasite binding to endothelial protein C receptor. *Nature* **498**, 502-505, doi:10.1038/nature12216 (2013).
214 Lavstsen, T. *et al. Plasmodium falciparum* erythrocyte membrane protein 1 domain cassettes 8 and 13 are associated with severe malaria in children. *Proc Natl Acad Sci U S A* **109**, E1791-1800, doi:10.1073/pnas.1120455109 (2012).
215 Rogerson, S. J. & Brown, G. V. Chondroitin sulphate A as an adherence receptor for *Plasmodium falciparum*-infected erythrocytes. *Parasitology today* **13**, 70-75 (1997).
216 Beeson, J. G. *et al.* Adhesion of *Plasmodium falciparum*-infected erythrocytes to hyaluronic acid in placental malaria. *Nat Med* **6**, 86-90, doi:10.1038/71582 (2000).
217 Higgins, M. K. The structure of a chondroitin sulfate-binding domain important in placental malaria. *J Biol Chem* **283**, 21842-21846, doi:10.1074/jbc.C800086200 (2008).
218 Rogerson, S. J., Hviid, L., Duffy, P. E., Leke, R. F. & Taylor, D. W. Malaria in pregnancy: pathogenesis and immunity. *Lancet Infect Dis* **7**, 105-117, doi:10.1016/S1473-3099(07)70022-1 (2007).
219 Grau, G. E. *et al.* Platelet accumulation in brain microvessels in fatal pediatric cerebral malaria. *J Infect Dis* **187**, 461-466, doi:10.1086/367960 (2003).
220 Pain, A. *et al.* Platelet-mediated clumping of *Plasmodium falciparum*-infected erythrocytes is a common adhesive phenotype and is associated with severe malaria. *Proc Natl Acad Sci U S A* **98**, 1805-1810, doi:10.1073/pnas.98.4.1805 (2001).
221 Sun, G. *et al.* Inhibition of platelet adherence to brain microvasculature protects against severe *Plasmodium berghei* malaria. *Infect Immun* **71**, 6553-6561 (2003).
222 Srivastava, K. *et al.* Platelet factor 4 mediates inflammation in experimental cerebral malaria. *Cell host & microbe* **4**, 179-187, doi:10.1016/j.chom.2008.07.003 (2008).
223 McMorran, B. J. *et al.* Platelets kill intraerythrocytic malarial parasites and mediate survival to infection. *Science* **323**, 797-800, doi:323/5915/797 [pii] 10.1126/science.1166296 [doi] (2009).
224 Aggrey, A. A., Srivastava, K., Ture, S., Field, D. J. & Morrell, C. N. Platelet induction of the acute-phase response is protective in murine experimental cerebral malaria. *J Immunol* **190**, 4685-4691, doi:10.4049/jimmunol.1202672 (2013).
225 Craig, A. G. *et al.* The role of animal models for research on severe malaria. *PLoS Pathog* **8**, e1002401, doi:10.1371/journal.ppat.1002401 (2012).
226 Yanez, D. M., Manning, D. D., Cooley, A. J., Weidanz, W. P. & van der Heyde, H. C. Participation of lymphocyte subpopulations in the pathogenesis of experimental murine cerebral malaria. *J Immunol* **157**, 1620-1624 (1996).

227 Amani, V. *et al.* Involvement of IFN-gamma receptor-medicated signaling in pathology and anti-malarial immunity induced by *Plasmodium berghei* infection. *Eur J Immunol* **30**, 1646-1655, doi:10.1002/1521-4141(200006)30:6<1646::AID-IMMU1646>3.0.CO;2-0 (2000).
228 Grau, G. E. *et al.* Tumor necrosis factor (cachectin) as an essential mediator in murine cerebral malaria. *Science* **237**, 1210-1212 (1987).
229 Engwerda, C. R. *et al.* Locally up-regulated lymphotoxin alpha, not systemic tumor necrosis factor alpha, is the principle mediator of murine cerebral malaria. *J Exp Med* **195**, 1371-1377 (2002).
230 Hermsen, C., van de Wiel, T., Mommers, E., Sauerwein, R. & Eling, W. Depletion of CD4+ or CD8+ T-cells prevents *Plasmodium berghei* induced cerebral malaria in end-stage disease. *Parasitology* **114 (Pt 1)**, 7-12 (1997).
231 Bongfen, S. E. *et al.* An N-Ethyl-N-Nitrosourea (ENU)-Induced Dominant Negative Mutation in the JAK3 Kinase Protects against Cerebral Malaria. *PloS one* **7**, e31012, doi:10.1371/journal.pone.0031012 (2012).
232 Claser, C. *et al.* CD8+ T cells and IFN-gamma mediate the time-dependent accumulation of infected red blood cells in deep organs during experimental cerebral malaria. *PLoS One* **6**, e18720, doi:10.1371/journal.pone.0018720 (2011).
233 Renia, L. *et al.* Cerebral malaria: mysteries at the blood-brain barrier. *Virulence* **3**, 193-201, doi:10.4161/viru.19013 (2012).
234 Wassmer, S. C. *et al.* TGF-beta1 released from activated platelets can induce TNF-stimulated human brain endothelium apoptosis: a new mechanism for microvascular lesion during cerebral malaria. *J Immunol* **176**, 1180-1184 (2006).
235 Renia, L. *et al.* Pathogenic T cells in cerebral malaria. *Int J Parasitol* **36**, 547-554, doi:10.1016/j.ijpara.2006.02.007 (2006).
236 Poh, C. M., Howland, S. W., Grotenbreg, G. M. & Renia, L. Damage to the blood-brain barrier during experimental cerebral malaria results from synergistic effects of CD8+ T cells with different specificities. *Infect Immun* **82**, 4854-4864, doi:10.1128/IAI.02180-14 (2014).
237 Hood, A. T., Fabry, M. E., Costantini, F., Nagel, R. L. & Shear, H. L. Protection from lethal malaria in transgenic mice expressing sickle hemoglobin. *Blood* **87**, 1600-1603 (1996).
238 Carter, R. & Miller, L. H. Evidence for environmental modulation of gametocytogenesis in *Plasmodium falciparum* in continuous culture. *Bull World Health Organ* **57 Suppl 1**, 37-52 (1979).
239 Trager, W., Gill, G. S., Lawrence, C. & Nagel, R. L. *Plasmodium falciparum*: enhanced gametocyte formation in vitro in reticulocyte-rich blood. *Exp Parasitol* **91**, 115-118, doi:10.1006/expr.1998.4347 (1999).
240 Smalley, M. E. & Brown, J. *Plasmodium falciparum* gametocytogenesis stimulated by lymphocytes and serum from infected Gambian children. *Trans R Soc Trop Med Hyg* **75**, 316-317 (1981).
241 Bruce, M. C., Alano, P., Duthie, S. & Carter, R. Commitment of the malaria parasite *Plasmodium falciparum* to sexual and asexual development. *Parasitology* **100 Pt 2**, 191-200 (1990).
242 Lingnau, A., Margos, G., Maier, W. A. & Seitz, H. M. The effects of hormones on the gametocytogenesis of *Plasmodium falciparum* in vitro. *Applied parasitology* **34**, 153-160 (1993).
243 Trager, W. What triggers the gametocyte pathway in *Plasmodium falciparum*? *Trends Parasitol* **21**, 262-264, doi:10.1016/j.pt.2005.04.005 (2005).
244 Eksi, S. *et al. Plasmodium falciparum* gametocyte development 1 (Pfgdv1) and gametocytogenesis early gene identification and commitment to sexual development. *PLoS Pathog* **8**, e1002964, doi:10.1371/journal.ppat.1002964 (2012).

245 Schneider, P. *et al.* Quantification of *Plasmodium falciparum* gametocytes in differential stages of development by quantitative nucleic acid sequence-based amplification. *Mol Biochem Parasitol* **137**, 35-41, doi:10.1016/j.molbiopara.2004.03.018 (2004).
246 Dyer, M. & Day, K. P. Regulation of the rate of asexual growth and commitment to sexual development by diffusible factors from in vitro cultures of *Plasmodium falciparum*. *Am J Trop Med Hyg* **68**, 403-409 (2003).
247 Gouagna, L. C. *et al.* Genetic variation in human HBB is associated with *Plasmodium falciparum* transmission. *Nat Genet* **42**, 328-331, doi:10.1038/ng.554 (2010).
248 Lawaly, Y. R. *et al.* Heritability of the human infectious reservoir of malaria parasites. *PLoS One* **5**, e11358, doi:10.1371/journal.pone.0011358 (2010).
249 Schwegmann, A. & Brombacher, F. Host-Directed Drug Targeting of Factors Hijacked by Pathogens. *Sci. Signal.* **1**, re8-, doi:10.1126/scisignal.129re8 (2008).
250 Kuijl, C. *et al.* Intracellular bacterial growth is controlled by a kinase network around PKB/AKT1. *Nature* **450**, 725-730 (2007).
251 Elkington, P. T. & Friedland, J. S. Matrix metalloproteinases in destructive pulmonary pathology. *Thorax* **61**, 259-266, doi:10.1136/thx.2005.051979 (2006).
252 Maiga, M. *et al.* Successful Shortening of Tuberculosis Treatment Using Adjuvant Host-Directed Therapy with FDA-Approved Phosphodiesterase Inhibitors in the Mouse Model. *PloS one* **7**, e30749, doi:10.1371/journal.pone.0030749 (2012).
253 Stanley, S. A. *et al.* Identification of host-targeted small molecules that restrict intracellular *Mycobacterium tuberculosis* growth. *PLoS Pathog* **10**, e1003946, doi:10.1371/journal.ppat.1003946 (2014).
254 Mayer-Barber, K. D. *et al.* Host-directed therapy of tuberculosis based on interleukin-1 and type I interferon crosstalk. *Nature* **511**, 99-103, doi:10.1038/nature13489 (2014).
255 Ray, N. Maraviroc in the treatment of HIV infection. *Drug Des Devel Ther* **2**, 151-161 (2009).
256 Yuan, Y. *et al.* A combination of polymorphic mutations in V3 loop of HIV-1 gp120 can confer noncompetitive resistance to maraviroc. *Virology* **413**, 293-299, doi:10.1016/j.virol.2011.02.019 (2011).
257 Delobel, P. *et al.* Shift in phenotypic susceptibility suggests a competition mechanism in a case of acquired resistance to maraviroc. *Aids* **24**, 1382-1384, doi:10.1097/QAD.0b013e328338b7a6 (2010).
258 Westby, M. *et al.* Reduced maximal inhibition in phenotypic susceptibility assays indicates that viral strains resistant to the CCR5 antagonist maraviroc utilize inhibitor-bound receptor for entry. *Journal of virology* **81**, 2359-2371, doi:10.1128/JVI.02006-06 (2007).
259 Krumm, S. A. *et al.* Potent host-directed small-molecule inhibitors of myxovirus RNA-dependent RNA-polymerases. *PloS one* **6**, e20069, doi:10.1371/journal.pone.0020069 (2011).
260 Konig, R. *et al.* Human host factors required for influenza virus replication. *Nature* **463**, 813-817, doi:10.1038/nature08699 (2010).
261 Karlas, A. *et al.* Genome-wide RNAi screen identifies human host factors crucial for influenza virus replication. *Nature* **463**, 818-822, doi:10.1038/nature08760 (2010).
262 Sicard, A. *et al.* Activation of a PAK-MEK signalling pathway in malaria parasite-infected erythrocytes. *Cell Microbiol* **13**, 836-845, doi:10.1111/j.1462-5822.2011.01582.x (2011).
263 Smith, C. M. *et al.* Red cells from ferrochelatase-deficient erythropoietic protoporphyria patients are resistant to growth of malarial parasites. *Blood*, doi:10.1182/blood-2014-04-567149 (2014).

264 Jallow, M. *et al.* Genome-wide and fine-resolution association analysis of malaria in West Africa. *Nat Genet*, doi:ng.388 [pii] 10.1038/ng.388 [doi] (2009).
265 Timmann, C. *et al.* Genome-Wide Linkage Analysis of Malaria Infection Intensity and Mild Disease. *PLoS Genet* **3**, e48 (2007).
266 Lee, J. C. *et al.* Human SNP links differential outcomes in inflammatory and infectious disease to a FOXO3-regulated pathway. *Cell* **155**, 57-69, doi:10.1016/j.cell.2013.08.034 (2013).
267 Fortin, A. *et al.* Identification of a new malaria susceptibility locus (Char4) in recombinant congenic strains of mice. *Proc Natl Acad Sci U S A* **98**, 10793-10798, doi:10.1073/pnas.191288998 191288998 [pii] (2001).
268 Hernandez-Valladares, M. *et al.* Confirmation and dissection of QTL controlling resistance to malaria in mice. *Mamm Genome* **15**, 390-398, doi:10.1007/s00335-004-3042-4 [doi] (2004).
269 Min-Oo, G. *et al.* Complex genetic control of susceptibility to malaria: positional cloning of the Char9 locus. *J Exp Med* **204**, 511-524, doi:jem.20061252 [pii] 10.1084/jem.20061252 [doi] (2007).
270 Min-Oo, G. *et al.* Mapping of Char10, a novel malaria susceptibility locus on mouse chromosome 9. *Genes Immun* **11**, 113-123 (2009).
271 Laroque, A. *et al.* Genetic control of susceptibility to infection with *Plasmodium chabaudi chabaudi AS* in inbred mouse strains. *Genes Immun* **13**, 155-163, doi:10.1038/gene.2011.67 (2012).
272 Bagot, S. *et al.* Identification of two cerebral malaria resistance loci using an inbred wild-derived mouse strain. *Proc Natl Acad Sci U S A* **99**, 9919-9923, doi:10.1073/pnas.152215199 (2002).
273 Ohno, T. & Nishimura, M. Detection of a new cerebral malaria susceptibility locus, using CBA mice. *Immunogenetics* **56**, 675-678, doi:10.1007/s00251-004-0739-1 (2004).
274 Campino, S. *et al.* Genetic control of parasite clearance leads to resistance to *Plasmodium berghei* ANKA infection and confers immunity. *Genes Immun* **6**, 416-421, doi:10.1038/sj.gene.6364219 (2005).
275 Berghout, J. *et al.* Identification of a novel cerebral malaria susceptibility locus (Berr5) on mouse chromosome 19. *Genes Immun* **11**, 310-318, doi:10.1038/gene.2009.79 (2010).
276 Richer, E., Qureshi, S. T., Vidal, S. M. & Malo, D. Chemical mutagenesis: a new strategy against the global threat of infectious diseases. *Mamm Genome* **19**, 309-317, doi:10.1007/s00335-008-9114-0 [doi] (2008).
277 Justice, M. J., Noveroske, J. K., Weber, J. S., Zheng, B. & Bradley, A. Mouse ENU mutagenesis. *Hum Mol Genet* **8**, 1955-1963, doi:ddc219 [pii] (1999).
278 Noveroske, J. K., Weber, J. S. & Justice, M. J. The mutagenic action of N-ethyl-N-nitrosourea in the mouse. *Mamm Genome* **11**, 478-483 (2000).
279 Russell, W. L. *et al.* Specific-locus test shows ethylnitrosourea to be the most potent mutagen in the mouse. *Proc Natl Acad Sci U S A* **76**, 5818-5819 (1979).
280 Cordes, S. P. N-ethyl-N-nitrosourea mutagenesis: boarding the mouse mutant express. *Microbiol Mol Biol Rev* **69**, 426-439, doi:10.1128/MMBR.69.3.426-439.2005 (2005).
281 Weiss, J. *et al.* ENU mutagenesis in mice identifies candidate genes for hypogonadism. *Mamm Genome*, doi:10.1007/s00335-011-9388-5 (2012).
282 Sandell, L. L. *et al.* A phenotype-driven ENU mutagenesis screen identifies novel alleles with functional roles in early mouse craniofacial development. *Genesis* **49**, 342-359, doi:10.1002/dvg.20727 (2011).

283 Dauphinee, S. M. *et al.* Characterization of two ENU-induced mutations affecting mouse skeletal morphology. *G3* **3**, 1753-1758, doi:10.1534/g3.113.007310 (2013).
284 Yates, L. *et al.* ENU mutagenesis as a tool for understanding lung development and disease. *Biochem Soc Trans* **37**, 838-842, doi:10.1042/BST0370838 (2009).
285 Casrouge, A. *et al.* Herpes simplex virus encephalitis in human UNC-93B deficiency. *Science* **314**, 308-312, doi:1128346 [pii] 10.1126/science.1128346 [doi] (2006).
286 Zhang, S. Y. *et al.* TLR3 deficiency in patients with herpes simplex encephalitis. *Science* **317**, 1522-1527, doi:317/5844/1522 [pii] 10.1126/science.1139522 [doi] (2007).
287 Eva, M. M. *et al.* Altered IFN-gamma-mediated immunity and transcriptional expression patterns in N-Ethyl-N-nitrosourea-induced STAT4 mutants confer susceptibility to acute typhoid-like disease. *J Immunol* **192**, 259-270, doi:10.4049/jimmunol.1301370 (2014).
288 Yuki, K. E. *et al.* Suppression of hepcidin expression and iron overload mediate Salmonella susceptibility in ankyrin 1 ENU-induced mutant. *PLoS One* **8**, e55331, doi:10.1371/journal.pone.0055331 (2013).
289 Kennedy, J. M. *et al.* CCDC88B is a novel regulator of maturation and effector functions of T cells during pathological inflammation. *J Exp Med* **211**, 2519-2535, doi:10.1084/jem.20140455 (2014).
290 Buske, F., French, H., Smith, M. & Bauer, D. NGSANE: Lightweight Production Informatics Framework for High Throughput Data Analysis. *Bioinformatics* (under review).
291 Li, H. & Durbin, R. Fast and accurate long-read alignment with Burrows-Wheeler transform. *Bioinformatics* **26**, 589-595, doi:10.1093/bioinformatics/btp698 (2010).
292 Langmead, B. & Salzberg, S. L. Fast gapped-read alignment with Bowtie 2. *Nature methods* **9**, 357-359, doi:10.1038/nmeth.1923 (2012).
293 Li, H. *et al.* The Sequence Alignment/Map format and SAMtools. *Bioinformatics* **25**, 2078-2079, doi:10.1093/bioinformatics/btp352 (2009).
294 McKenna, A. *et al.* The Genome Analysis Toolkit: a MapReduce framework for analyzing next-generation DNA sequencing data. *Genome research* **20**, 1297-1303, doi:10.1101/gr.107524.110 (2010).
295 Wang, K., Li, M. & Hakonarson, H. ANNOVAR: functional annotation of genetic variants from high-throughput sequencing data. *Nucleic acids research* **38**, e164, doi:10.1093/nar/gkq603 (2010).
296 Cong, L. *et al.* Multiplex genome engineering using CRISPR/Cas systems. *Science* **339**, 819-823, doi:10.1126/science.1231143 (2013).
297 Ran, F. A. *et al.* Double nicking by RNA-guided CRISPR Cas9 for enhanced genome editing specificity. *Cell* **154**, 1380-1389, doi:10.1016/j.cell.2013.08.021 (2013).
298 Laemmli, U. Cleavage of structural proteins during the assembly of the head of bacteriophage T4. *Nature* **227**, 680-685 (1970).
299 Chen, K. *et al.* Resolving the distinct stages in erythroid differentiation based on dynamic changes in membrane protein expression during erythropoiesis. *Proc Natl Acad Sci U S A* **106**, 17413-17418, doi:10.1073/pnas.0909296106 (2009).
300 Trager, W. & Jensen, J. B. Human malaria parasites in continuous culture. *Science* **193**, 673-675 (1976).
301 Rivadeneira, E. M., Wasserman, M. & Espinal, C. T. Separation and concentration of schizonts of *Plasmodium falciparum* by Percoll gradients. *The Journal of protozoology* **30**, 367-370 (1983).

302 An, X. *et al.* Global transcriptome analyses of human and murine terminal erythroid differentiation. *Blood* **123**, 3466-3477, doi:10.1182/blood-2014-01-548305 (2014).
303 Lowy, B. & Dorfman, B. Z. Adenylosuccinase activity in human and rabbit erythrocyte lysates. *J Biol Chem* **245**, 3043-3046 (1970).
304 Lowy, B. A., Williams, M. K. & London, I. M. Enzymatic deficiencies of purine nucleotide synthesis in the human erythrocyte. *J Biol Chem* **237**, 1622-1625 (1962).
305 Hitomi, Y. *et al.* Inosine triphosphate protects against ribavirin-induced adenosine triphosphate loss by adenylosuccinate synthase function. *Gastroenterology* **140**, 1314-1321, doi:10.1053/j.gastro.2010.12.038 (2011).
306 Ashby, B. & Frieden, C. Adenylate deaminase. Kinetic and binding studies on the rabbit muscle enzyme. *J Biol Chem* **253**, 8728-8735 (1978).
307 Rundell, K. W., Tullson, P. C. & Terjung, R. L. Altered kinetics of AMP deaminase by myosin binding. *The American journal of physiology* **263**, C294-299 (1992).
308 Tovmasian, E. K., Hairapetian, R. L., Bykova, E. V., Severin, S. E., Jr. & Haroutunian, A. V. Phosphorylation of the skeletal muscle AMP-deaminase by protein kinase C. *FEBS Lett* **259**, 321-323 (1990).
309 Askari, A. Erythrocytes: 5' -adenylic acid deaminase requirement for ammonia or monovalent metal ion. *Science* **141**, 44-45 (1963).
310 Tavazzi, B. *et al.* Energy metabolism and lipid peroxidation of human erythrocytes as a function of increased oxidative stress. *European journal of biochemistry / FEBS* **267**, 684-689 (2000).
311 Yoshino, M., Kawamura, Y. & Ogasawara, N. Regulation of AMP deaminase from chicken erythrocytes. A kinetic study of the allosteric interactions. *Journal of biochemistry* **80**, 299-308 (1976).
312 Mahnke, D. K. & Sabina, R. L. Calcium activates erythrocyte AMP deaminase [isoform E (AMPD3)] through a protein-protein interaction between calmodulin and the N-terminal domain of the AMPD3 polypeptide. *Biochemistry* **44**, 5551-5559, doi:10.1021/bi048121p (2005).
313 Mahnke-Zizelman, D. K. & Sabina, R. L. N-terminal sequence and distal histidine residues are responsible for pH-regulated cytoplasmic membrane binding of human AMP deaminase isoform E. *J Biol Chem* **277**, 42654-42662, doi:10.1074/jbc.M203473200 (2002).
314 Sims, B. *et al.* Regulation of AMP deaminase by phosphoinositides. *J Biol Chem* **274**, 25701-25707 (1999).
315 Thakkar, J. K., Janero, D. R., Yarwood, C. & Sharif, H. M. Modulation of mammalian cardiac AMP deaminase by protein kinase C-mediated phosphorylation. *Biochem J* **291 (Pt 2)**, 523-527 (1993).
316 Bader-Meunier, B. *et al.* Long-term evaluation of the beneficial effect of subtotal splenectomy for management of hereditary spherocytosis. *Blood* **97**, 399-403 (2001).
317 Kurata, M., Suzuki, M. & Agar, N. S. Antioxidant systems and erythrocyte life-span in mammals. *Comparative biochemistry and physiology. B, Comparative biochemistry* **106**, 477-487 (1993).
318 Lang, F. & Qadri, S. M. Mechanisms and significance of eryptosis, the suicidal death of erythrocytes. *Blood purification* **33**, 125-130, doi:10.1159/000334163 (2012).
319 Lui, J. C. *et al.* Cordycepin induced eryptosis in mouse erythrocytes through a Ca2+-dependent pathway without caspase-3 activation. *Archives of toxicology* **81**, 859-865, doi:10.1007/s00204-007-0214-5 (2007).

320 Lau, I. P. *et al.* In vitro effect of CTAB- and PEG-coated gold nanorods on the induction of eryptosis/erythroptosis in human erythrocytes. *Nanotoxicology* **6**, 847-856, doi:10.3109/17435390.2011.625132 (2012).
321 Vota, D. M., Crisp, R. L., Nesse, A. B. & Vittori, D. C. Oxidative stress due to aluminum exposure induces eryptosis which is prevented by erythropoietin. *Journal of cellular biochemistry* **113**, 1581-1589, doi:10.1002/jcb.24026 (2012).
322 Wang, S. B., Dale, G. L., Song, P., Viollet, B. & Zou, M. H. AMPK alpha 1 Deletion Shortens Erythrocyte Life Span in Mice ROLE OF OXIDATIVE STRESS. *Journal of Biological Chemistry* **285**, 19976-19985, doi:Doi 10.1074/Jbc.M110.102467 (2010).
323 Bhavsar, S. K., Gu, S., Bobbala, D. & Lang, F. Janus kinase 3 is expressed in erythrocytes, phosphorylated upon energy depletion and involved in the regulation of suicidal erythrocyte death. *Cellular physiology and biochemistry : international journal of experimental cellular physiology, biochemistry, and pharmacology* **27**, 547-556, doi:10.1159/000329956 (2011).
324 Attanasio, P. *et al.* Stimulation of eryptosis by anti-A IgG antibodies. *Cellular physiology and biochemistry : international journal of experimental cellular physiology, biochemistry, and pharmacology* **20**, 591-600, doi:10.1159/000107542 (2007).
325 Lang, E. *et al.* Conjugated bilirubin triggers anemia by inducing erythrocyte death. *Hepatology* **61**, 275-284, doi:10.1002/hep.27338 (2015).
326 Lang, E. & Lang, F. Mechanisms and pathophysiological significance of eryptosis, the suicidal erythrocyte death. *Seminars in cell & developmental biology*, doi:10.1016/j.semcdb.2015.01.009 (2015).
327 Yamada, Y., Goto, H., Wakamatsu, N. & Ogasawara, N. A rare case of complete human erythrocyte AMP deaminase deficiency due to two novel missense mutations in AMPD3. *Hum Mutat* **17**, 78, doi:10.1002/1098-1004(2001)17:1<78::AID-HUMU21>3.0.CO;2-B (2001).
328 Cheng, J. *et al.* AMPD3-deficient mice exhibit increased erythrocyte ATP levels but anemia not improved due to PK deficiency. *Genes to cells : devoted to molecular & cellular mechanisms* **17**, 913-922, doi:10.1111/gtc.12006 (2012).
329 Obrador, R., Musulin, S. & Hansen, B. Red blood cell storage lesion. *Journal of veterinary emergency and critical care*, doi:10.1111/vec.12252 (2014).
330 Lei, J. & Mackey, M. C. Understanding and treating cytopenia through mathematical modeling. *Advances in experimental medicine and biology* **844**, 279-302, doi:10.1007/978-1-4939-2095-2_14 (2014).
331 Horwitz, M., Benson, K. F., Person, R. E., Aprikyan, A. G. & Dale, D. C. Mutations in ELA2, encoding neutrophil elastase, define a 21-day biological clock in cyclic haematopoiesis. *Nat Genet* **23**, 433-436, doi:10.1038/70544 (1999).
332 Weiden, P. L., Robinett, B., Graham, T. C., Adamson, J. & Storb, R. Canine cyclic neutropenia. A stem cell defect. *J Clin Invest* **53**, 950-953, doi:10.1172/JCI107636 (1974).
333 Dale, D. C. *et al.* Mutations in the gene encoding neutrophil elastase in congenital and cyclic neutropenia. *Blood* **96**, 2317-2322 (2000).
334 Grenda, D. S. *et al.* Mutations of the ELA2 gene found in patients with severe congenital neutropenia induce the unfolded protein response and cellular apoptosis. *Blood* **110**, 4179-4187, doi:10.1182/blood-2006-11-057299 (2007).
335 Cortes, J. E., Talpaz, M. & Kantarjian, H. Chronic myelogenous leukemia: a review. *The American journal of medicine* **100**, 555-570 (1996).
336 Mackey, M. C. Periodic auto-immune hemolytic anemia: an induced dynamical disease. *Bulletin of mathematical biology* **41**, 829-834 (1979).
337 Belair, J., Mackey, M. C. & Mahaffy, J. M. Age-structured and two-delay models for erythropoiesis. *Mathematical biosciences* **128**, 317-346 (1995).

338 Gardner, M. J. *et al.* Genome sequence of the human malaria parasite *Plasmodium falciparum*. *Nature* **419**, 498-511, doi:10.1038/nature01097 (2002).
339 Cassera, M. B., Zhang, Y., Hazleton, K. Z. & Schramm, V. L. Purine and pyrimidine pathways as targets in *Plasmodium falciparum*. *Current topics in medicinal chemistry* **11**, 2103-2115 (2011).
340 Carter, N. S. *et al.* Isolation and functional characterization of the PfNT1 nucleoside transporter gene from *Plasmodium falciparum*. *J Biol Chem* **275**, 10683-10691 (2000).
341 Reyes, P. *et al.* Enzymes of purine and pyrimidine metabolism from the human malaria parasite, *Plasmodium falciparum*. *Mol Biochem Parasitol* **5**, 275-290 (1982).
342 Ma, J. *et al.* Subcellular localization of adenylate kinases in *Plasmodium falciparum*. *FEBS Lett* **586**, 3037-3043, doi:10.1016/j.febslet.2012.07.013 (2012).
343 Sana, T. R. *et al.* Global mass spectrometry based metabolomics profiling of erythrocytes infected with *Plasmodium falciparum*. *PLoS One* **8**, e60840, doi:10.1371/journal.pone.0060840 (2013).
344 Laourdakis, C. D., Merino, E. F., Neilson, A. P. & Cassera, M. B. Comprehensive quantitative analysis of purines and pyrimidines in the human malaria parasite using ion-pairing ultra-performance liquid chromatography-mass spectrometry. *Journal of chromatography. B, Analytical technologies in the biomedical and life sciences* **967**, 127-133, doi:10.1016/j.jchromb.2014.07.012 (2014).
345 Yap, G. S. & Stevenson, M. M. *Plasmodium chabaudi* AS: erythropoietic responses during infection in resistant and susceptible mice. *Exp Parasitol* **75**, 340-352, doi:0014-4894(92)90219-Z [pii] (1992).
346 Min-Oo, G. *et al.* Pyruvate kinase deficiency in mice protects against malaria. *Nat Genet* **35**, 357-362, doi:10.1038/ng1260 [doi]
ng1260 [pii] (2003).
347 Kotlyar, S. *et al.* Spleen volume and clinical disease manifestations of severe *Plasmodium falciparum* malaria in African children. *Trans R Soc Trop Med Hyg* **108**, 283-289, doi:10.1093/trstmh/tru040 (2014).
348 Chang, K. H., Tam, M. & Stevenson, M. M. Modulation of the course and outcome of blood-stage malaria by erythropoietin-induced reticulocytosis. *J Infect Dis* **189**, 735-743, doi:JID31267 [pii]
10.1086/381458 [doi] (2004).
349 Omodeo-Sale, F. *et al.* Accelerated senescence of human erythrocytes cultured with *Plasmodium falciparum*. *Blood* **102**, 705-711, doi:10.1182/blood-2002-08-2437 (2003).
350 Lelliott, P. M., Lampkin, S., McMorran, B. J., Foote, S. J. & Burgio, G. A flow cytometric assay to quantify invasion of red blood cells by rodent *Plasmodium parasites in vivo*. *Malar J* **13**, 100, doi:10.1186/1475-2875-13-100 (2014).
351 Engwerda, C. R., Beattie, L. & Amante, F. H. The importance of the spleen in malaria. *Trends Parasitol* **21**, 75-80, doi:10.1016/j.pt.2004.11.008 (2005).
352 Abdalla, S. H. Hematopoiesis in human malaria. *Blood Cells* **16**, 401-416; discussion 417-409 (1990).
353 Chang, K. H. & Stevenson, M. M. Malarial anaemia: mechanisms and implications of insufficient erythropoiesis during blood-stage malaria. *Int J Parasitol* **34**, 1501-1516, doi:S0020-7519(04)00213-9 [pii]
10.1016/j.ijpara.2004.10.008 [doi] (2004).
354 Leowattana, W., Krudsood, S., Tangpukdee, N., Brittenham, G. & Looareesuwan, S. Defective erythropoietin production and reticulocyte response in acute *Plasmodium falciparum* malaria-associated anemia. *Southeast Asian J Trop Med Public Health* **39**, 581-588 (2008).

355 Kurtzhals, J. A. *et al.* Reversible suppression of bone marrow response to erythropoietin in *Plasmodium falciparum* malaria. *Br J Haematol* **97**, 169-174 (1997).
356 Casals-Pascual, C. *et al.* Suppression of erythropoiesis in malarial anemia is associated with hemozoin *in vitro* and *in vivo*. *Blood* **108**, 2569-2577, doi:10.1182/blood-2006-05-018697 (2006).
357 Keller, C. C. *et al.* Suppression of a novel hematopoietic mediator in children with severe malarial anemia. *Infect Immun* **77**, 3864-3871, doi:10.1128/IAI.00342-09 (2009).
358 Weiss, G. & Goodnough, L. T. Anemia of Chronic Disease. *N Engl J Med* **352**, 1011-1023, doi:10.1056/NEJMra041809 (2005).
359 Thawani, N., Tam, M. & Stevenson, M. M. STAT6-mediated suppression of erythropoiesis in an experimental model of malarial anemia. *Haematologica* **94**, 195-204, doi:haematol.13422 [pii] 10.3324/haematol.13422 [doi] (2009).
360 Peatey, C. L. *et al.* Enhanced gametocyte formation in erythrocyte progenitor cells: a site-specific adaptation by *Plasmodium falciparum*. *J Infect Dis* **208**, 1170-1174, doi:10.1093/infdis/jit309 (2013).
361 Paul, R. E., Coulson, T. N., Raibaud, A. & Brey, P. T. Sex determination in malaria parasites. *Science* **287**, 128-131 (2000).
362 Carter, R. Studies on enzyme variation in the murine malaria parasites *Plasmodium berghei, P. yoelii, P. vinckei* and *P. chabaudi* by starch gel electrophoresis. *Parasitology* **76**, 241-267 (1978).
363 Rest, J. R. Cerebral malaria in inbred mice. I. A new model and its pathology. *Trans R Soc Trop Med Hyg* **76**, 410-415 (1982).
364 Dluzewski, A. R., Nash, G. B., Wilson, R. J., Reardon, D. M. & Gratzer, W. B. Invasion of hereditary ovalocytes by *Plasmodium falciparum* in vitro and its relation to intracellular ATP concentration. *Mol Biochem Parasitol* **55**, 1-7 (1992).
365 Jewell, J. L. & Guan, K. L. Nutrient signaling to mTOR and cell growth. *Trends in biochemical sciences* **38**, 233-242, doi:10.1016/j.tibs.2013.01.004 (2013).
366 Carazo-Salas, R. E. *et al.* Generation of GTP-bound Ran by RCC1 is required for chromatin-induced mitotic spindle formation. *Nature* **400**, 178-181, doi:10.1038/22133 (1999).
367 Dontfraid, F. F. & Chakrabarti, D. Cloning and expression of a cDNA encoding the homologue of Ran/TC4 GTP-binding protein from *Plasmodium falciparum*. *Biochem Biophys Res Commun* **201**, 423-429, doi:10.1006/bbrc.1994.1718 (1994).
368 Sultan, A. A., Richardson, W. A., Alano, P., Arnot, D. E. & Doerig, C. Cloning and characterisation of a *Plasmodium falciparum* homologue of the Ran/TC4 signal transducing GTPase involved in cell cycle control. *Mol Biochem Parasitol* **67**, 339 (1994).
369 Brouhard, G. & Sept, D. Microtubules: sizing up the GTP cap. *Curr Biol* **22**, R802-803, doi:10.1016/j.cub.2012.07.050 (2012).
370 Asante, K. P. *et al.* Safety and efficacy of the RTS,S/AS01E candidate malaria vaccine given with expanded-programme-on-immunisation vaccines: 19 month follow-up of a randomised, open-label, phase 2 trial. *Lancet Infect Dis* **11**, 741-749, doi:10.1016/S1473-3099(11)70100-1 (2011).
371 Bittner, A. N., Kriel, A. & Wang, J. D. Lowering GTP level increases survival of amino acid starvation but slows growth rate for Bacillus subtilis cells lacking (p)ppGpp. *Journal of bacteriology* **196**, 2067-2076, doi:10.1128/JB.01471-14 (2014).

372 Staines, H. M., Ellory, J. C. & Kirk, K. Perturbation of the pump-leak balance for Na(+) and K(+) in malaria-infected erythrocytes. *Am J Physiol Cell Physiol* **280**, C1576-1587 (2001).
373 Brand, V. B. *et al.* Dependence of *Plasmodium falciparum* in vitro growth on the cation permeability of the human host erythrocyte. *Cellular physiology and biochemistry : international journal of experimental cellular physiology, biochemistry, and pharmacology* **13**, 347-356, doi:75122 (2003).
374 Allen, R. J. & Kirk, K. The membrane potential of the intraerythrocytic malaria parasite *Plasmodium falciparum*. *J Biol Chem* **279**, 11264-11272, doi:10.1074/jbc.M311110200 (2004).
375 Pan, D. *et al.* K-Cl cotransporter gene expression during human and murine erythroid differentiation. *J Biol Chem* **286**, 30492-30503, doi:10.1074/jbc.M110.206516 (2011).
376 Bize, I., Taher, S. & Brugnara, C. Regulation of K-Cl cotransport during reticulocyte maturation and erythrocyte aging in normal and sickle erythrocytes. *Am J Physiol Cell Physiol* **285**, C31-38, doi:10.1152/ajpcell.00447.2002 (2003).
377 Su, W. *et al.* Mouse K-Cl cotransporter KCC1: cloning, mapping, pathological expression, and functional regulation. *The American journal of physiology* **277**, C899-912 (1999).
378 Friedman, M. J., Roth, E. F., Nagel, R. L. & Trager, W. *Plasmodium falciparum*: physiological interactions with the human sickle cell. *Exp Parasitol* **47**, 73-80 (1979).
379 Kossodo, S. *et al.* Interleukin-10 modulates susceptibility in experimental cerebral malaria. *Immunology* **91**, 536-540 (1997).
380 de Los Heros, P. *et al.* WNK3 bypasses the tonicity requirement for K-Cl cotransporter activation via a phosphatase-dependent pathway. *Proc Natl Acad Sci U S A* **103**, 1976-1981, doi:10.1073/pnas.0510947103 (2006).
381 de Los Heros, P. *et al.* The WNK-regulated SPAK/OSR1 kinases directly phosphorylate and inhibit the K+-Cl- co-transporters. *Biochem J* **458**, 559-573, doi:10.1042/BJ20131478 (2014).
382 Mori, T. *et al.* Chemical library screening for WNK signalling inhibitors using fluorescence correlation spectroscopy. *Biochem J* **455**, 339-345, doi:10.1042/BJ20130597 (2013).
383 Kikuchi, E. *et al.* Discovery of Novel SPAK Inhibitors That Block WNK Kinase Signaling to Cation Chloride Transporters. *Journal of the American Society of Nephrology : JASN*, doi:10.1681/ASN.2014060560 (2014).
384 Singh, S., Alam, M. M., Pal-Bhowmick, I., Brzostowski, J. A. & Chitnis, C. E. Distinct external signals trigger sequential release of apical organelles during erythrocyte invasion by malaria parasites. *PLoS Pathog* **6**, e1000746, doi:10.1371/journal.ppat.1000746 (2010).
385 Singh, S., More, K. R. & Chitnis, C. E. Role of calcineurin and actin dynamics in regulated secretion of microneme proteins in *Plasmodium falciparum* merozoites during erythrocyte invasion. *Cell Microbiol* **16**, 50-63, doi:10.1111/cmi.12177 (2014).
386 Tiffert, T. *et al.* The hydration state of human red blood cells and their susceptibility to invasion by *Plasmodium falciparum*. *Blood* **105**, 4853-4860, doi:2004-12-4948 [pii]
10.1182/blood-2004-12-4948 (2005).
387 Simpson, J. A., Aarons, L., Collins, W. E., Jeffery, G. M. & White, N. J. Population dynamics of untreated *Plasmodium falciparum* malaria within the adult human host during the expansion phase of the infection. *Parasitology* **124**, 247-263 (2002).

388 Langhorne, J. *et al.* Dendritic cells, pro-inflammatory responses, and antigen presentation in a rodent malaria infection. *Immunological reviews* **201**, 35-47, doi:10.1111/j.0105-2896.2004.00182.x (2004).
389 Amante, F. H. *et al.* Immune-mediated mechanisms of parasite tissue sequestration during experimental cerebral malaria. *J Immunol* **185**, 3632-3642, doi:10.4049/jimmunol.1000944 (2010).
390 Matz, J. M. *et al.* In Vivo Function of PTEX88 in Malaria Parasite Sequestration and Virulence. *Eukaryotic cell* **14**, 528-534, doi:10.1128/EC.00276-14 (2015).
391 D'Ombrain, M. C. *et al. Plasmodium falciparum* erythrocyte membrane protein-1 specifically suppresses early production of host interferon-gamma. *Cell host & microbe* **2**, 130-138, doi:10.1016/j.chom.2007.06.012 (2007).
392 Urban, B. C. *et al. Plasmodium falciparum*-infected erythrocytes modulate the maturation of dendritic cells. *Nature* **400**, 73-77, doi:10.1038/21900 (1999).
393 Millington, O. R., Di Lorenzo, C., Phillips, R. S., Garside, P. & Brewer, J. M. Suppression of adaptive immunity to heterologous antigens during *Plasmodium* infection through hemozoin-induced failure of dendritic cell function. *Journal of biology* **5**, 5, doi:10.1186/jbiol34 (2006).
394 Mockenhaupt, F. P. *et al. Plasmodium falciparum* infection: influence on hemoglobin levels in alpha-thalassemia and microcytosis. *J Infect Dis* **180**, 925-928, doi:10.1086/314959 (1999).
395 Wellems, T. E. & Fairhurst, R. M. An evolving picture of the interactions between malaria parasites and their host erythrocytes. *Cell research* **22**, 453-456, doi:10.1038/cr.2012.14 (2012).

Appendix

Appendix A: Steady–state purine analysis of Ampd3^{T689A}

Relative ratios (RR) of metabolites measured by HPLC/MS in mature RBCs of WT, Ampd3$^{T689A/+}$ and Ampd3$^{T689A/T689A}$ (n=4). Bold indicates metabolites for which P<0.05. (-) Indicates where RR could not be calculated because level of metabolite was too low to measure, or where level of metabolite was only high enough to measure in 1 sample so P or SEM could not be calculated. P values were calculated using the studen't T test.

	Average RR ± SEM			P values	
	WT	T689A/+	T689A/T689A	WT vs T689A/+	WT vs T689A/T689A
1* ADP	**0.102 ± 0.009**	**0.029 ± 0.003**	**0.067 ± 0.007**	**0.002**	**0.022**
1* Arginine	1.620 ± 0.132	1.289 ± 0.240	2.879 ± 0.463	0.300	0.068
1* cis-Aconitic acid	- ± -	- ± -	- ± -	-	-
1* Citrulline	0.015 ± 0.001	0.018 ± 0.001	0.018 ± 0.002	0.130	0.254
1* Cytidine	- ± -	0.004 ± 0.001	0.216 ± 0.031	-	-
1* D-Glucosamine (NPS)	**0.015 ± 0.005**	**0.034 ± 0.003**	**0.053 ± 0.006**	**0.021**	**0.003**
1* D-Glucuronolactone	**0.165 ± 0.029**	**0.178 ± 0.040**	**0.066 ± 0.004**	**0.823**	**0.041**
1* D-ribose-5-phosphate	**0.007 ± 0.000**	**0.007 ± 0.001**	**0.017 ± 0.001**	**0.988**	**0.002**
1* Fumarate	**1.263 ± 0.154**	**1.255 ± 0.049**	**4.119 ± 0.579**	**0.962**	**0.013**
1* GDP-mannose	**0.105 ± 0.011**	**0.076 ± 0.009**	**2.236 ± 0.388**	**0.264**	**0.012**
1* Gluconate	- ± -	- ± -	4.862 ± 0.410	-	-
1* Glutamate	**6.116 ± 0.813**	**8.148 ± 0.647**	**11.582 ± 1.380**	**0.101**	**0.020**
1* Glutamine	**0.090 ± 0.006**	**0.094 ± 0.006**	**0.153 ± 0.011**	**0.644**	**0.005**
1* GTP	**0.068 ± 0.009**	**0.139 ± 0.020**	**5.047 ± 0.862**	**0.030**	**0.010**
1* Guanine	0.007 ± 0.003	0.005 ± 0.001	0.007 ± 0.002	0.525	0.970
1* Histidine	**1.305 ± 0.160**	**1.002 ± 0.085**	**0.279 ± 0.028**	**0.161**	**0.007**
1* Leucine	0.102 ± 0.017	0.094 ± 0.007	0.318 ± 0.038	0.729	0.006
1* L-Threonine	0.667 ± 0.074	0.626 ± 0.035	0.757 ± 0.132	0.644	0.577
1* L-Valine	**0.009 ± 0.004**	**- ± -**	**0.052 ± 0.005**	**-**	**0.000**
1* Lysine	**2.091 ± 0.249**	**1.791 ± 0.286**	**5.635 ± 1.029**	**0.458**	**0.037**
1* Methionine	0.035 ± -	0.046 ± -	0.141 ± 0.024	-	-
1* Orotate	0.352 ± 0.091	0.349 ± 0.084	0.148 ± 0.020	0.978	0.107
1* Proline	**0.241 ± 0.017**	**0.263 ± 0.020**	**0.633 ± 0.058**	**0.435**	**0.004**
1* S-Adenosyl-L-methionine	0.067 ± 0.019	0.093 ± 0.014	0.174 ± 0.021	0.527	0.077
1* Serotonin	0.001 ± 0.000	0.001 ± 0.000	0.001 ± 0.000	0.197	0.146
1* UDP	**- ± -**	**- ± -**	**- ± -**	**-**	**-**
1* UMP	**0.002 ± 0.000**	**0.002 ± 0.000**	**0.028 ± 0.002**	**0.184**	**0.000**
1* Uric Acid	0.888 ± 0.143	0.918 ± 0.045	0.858 ± 0.079	0.874	0.879
1* Uridine	0.067 ± 0.001	0.195 ± 0.048	1.281 ± 0.411	0.076	0.060
2* 3',5'-Cyclic AMP	- ± -	- ± -	- ± -	-	-
2* Acetyl-CoA	0.017 ± -	- ± -	- ± -	-	-
2* Allantoin	0.160 ± 0.038	0.229 ± 0.000	0.252 ± 0.036	0.425	0.343
2* Asparagine	**0.006 ± 0.001**	**0.008 ± 0.000**	**0.022 ± 0.003**	**0.045**	**0.007**
2* Aspartic Acid	**1.045 ± 0.186**	**1.987 ± 0.281**	**11.471 ± 1.744**	**0.036**	**0.009**
2* ATP	**9.368 ± 0.927**	**1.830 ± 0.263**	**3.253 ± 0.445**	**0.003**	**0.003**
2* Citrate	- ± -	1.204 ± -	9.653 ± 1.506	-	-

	Average RR ± SEM			P values	
	WT	T689A/+	T689A/T689A	WT vs T689A/+	WT vs T689A/T689A
2* D-Fructose 1,6-bisphosphate	**0.728 ± 0.074**	**0.127 ± 0.002**	**0.765 ± 0.266**	**0.004**	**0.937**
2* D-Glucuronate	0.083 ± 0.019	0.062 ± 0.003	0.041 ± 0.009	0.334	0.107
2* FAD	**0.070 ± 0.002**	**- ± -**	**0.131 ± -**	**-**	**-**
2* GDP	**0.026 ± 0.004**	**0.062 ± 0.001**	**4.045 ± 0.795**	**0.002**	**0.015**
2* IDP	- ± -	- ± -	- ± -	-	-
2* NAD+	**6.655 ± 1.569**	**2.189 ± 0.426**	**1.545 ± 0.272**	**0.061**	**0.045**
2* NADP+	**0.231 ± 0.023**	**0.064 ± 0.004**	**0.351 ± 0.057**	**0.005**	**0.124**
2* Orotidine	**2.191 ± 0.111**	**3.357 ± 0.188**	**3.301 ± 0.459**	**0.004**	**0.091**
2* UDP-glucose	**6.309 ± 0.826**	**2.081 ± 0.223**	**11.596 ± 1.464**	**0.011**	**0.027**
2* Uracil	0.183 ± -	0.165 ± 0.016	0.281 ± 0.054	-	-
3* Alanine	**0.158 ± 0.019**	**0.171 ± 0.011**	**0.366 ± 0.048**	**0.560**	**0.016**
3* AMP	**4.378 ± 0.458**	**1.518 ± 0.216**	**5.807 ± 0.735**	**0.004**	**0.159**
3* CMP	- ± -	0.000 ± 0.000	0.007 ± 0.000	-	-
3* dAMP	0.005 ± 0.002	0.008 ± 0.003	0.005 ± 0.002	0.517	0.928
3* dCMP	- ± -	- ± -	- ± -	-	-
3* D-Fructose	1.059 ± 0.386	0.176 ± 0.109	0.331 ± 0.076	0.103	0.155
3* D-Fructose-6-phosphate	**1.329 ± 0.190**	**0.489 ± 0.097**	**1.543 ± 0.165**	**0.014**	**0.428**
3* dIMP	0.002 ± -	- ± -	- ± -	-	-
3* FMN	- ± -	- ± -	0.024 ± -	-	-
3* GMP	**0.012 ± 0.003**	**0.050 ± 0.001**	**1.408 ± 0.250**	**0.000**	**0.011**
3* IMP	**0.076 ± 0.015**	**0.206 ± 0.011**	**0.351 ± 0.051**	**0.001**	**0.010**
4* CTP	- ± -	- ± -	0.216 ± 0.031	-	-
4* D-Glucose	1.097 ± 0.616	0.070 ± 0.006	0.328 ± 0.068	0.194	0.301
4* dGMP	0.000 ± 0.000	0.000 ± -	0.001 ± -	-	-
4* Hexanoic acid	0.055 ± 0.021	0.091 ± 0.030	0.037 ± 0.000	0.394	0.542
4* L-Tryptophan	0.003 ± -	0.013 ± -	0.057 ± 0.008	-	-
4* UDP-D-galactose	**6.309 ± 0.826**	**2.081 ± 0.223**	**11.596 ± 1.464**	**0.011**	**0.027**
4* UDP-N-acetyl-D-glucosamine	**0.042 ± 0.002**	**0.021 ± 0.001**	**0.214 ± 0.016**	**0.001**	**0.001**
4* Xanthine	**0.267 ± 0.037**	**0.228 ± 0.031**	**0.745 ± 0.106**	**0.454**	**0.015**
5* NADH	0.561 ± 0.277	0.094 ± 0.048	0.211 ± 0.052	0.190	0.298
5-Hyroxytryptophan	- ± -	- ± -	0.002 ± 0.000	-	-
Adenosine	- ± -	- ± -	0.007 ± 0.003	-	-
Hypoxanthine	**1.110 ± 0.127**	**1.645 ± 0.328**	**0.498 ± 0.035**	**0.205**	**0.014**
Malonic Acid	0.002 ± 0.000	0.005 ± 0.001	0.012 ± 0.004	0.114	0.135
Sedoheptulose 7-phosphate	**0.990 ± 0.038**	**0.364 ± 0.023**	**2.225 ± 0.099**	**0.000**	**0.000**
sn-glycero-3-Phospho-1-inositol	**0.001 ± 0.000**	**0.003 ± 0.000**	**0.002 ± 0.000**	**0.007**	**0.004**

Appendix B: Ethics Approvals

UTAS

University of Tasmania
Animal Ethics Committee
ETHICS APPROVAL PERMIT

University of Tasmania
Research Services
Phone: (03) 62267283
Facsimile: (03) 62267148
Email:Animal.Ethics@utas.edu.au

To: Professor SJ Foote, Menzies Research Institute, Box 23

From: Nicola Hodgman, Executive Officer, Animal Ethics Committee

Date: Monday, 23 March 2009

Project: A0010470 Discovery of malarial resistance genes using ENU mutagenesis in mice and the study of these and other genes as antimalarial therapeutic targets

Approved on: 20/03/2009

Approval expires: 20/03/2012

Annual Report 1 due: 20/03/2010

PLEASE READ THIS PERMIT CAREFULLY AS APPROVAL MAY BE WITHDRAWN FOR PROJECTS THAT DO NOT COMPLY WITH THE CONDITIONS OUTLINED BELOW.

The Animal Ethics Committee on 20/03/2009 approved this project 20/03/2012 subject to the review and approval of an annual report due on the anniversary date of approval each year. You will receive an email reminder of this 4 weeks before the report is due.

If the project is to continue past 20/03/2012 a new initial application will need to be submitted as a project can only be approved for a maximum of 3 years.

As Chief Investigator on the project, you are responsible for ensuring:

(a) that all aspects of the work conform to the requirements of the current edition of the *Australian code of practice for the care and use of animals for scientific purposes*

(b) that a full record is maintained of all animals used in this project; and

(c) that any animals under an experimental regime are clearly identified. On this point, the Committee requests that you use an identification card on the cage or enclosure as illustrated on the following page. This identification is not required for animals being held as stock but only for those under the experimental regime.

(d) that you contact the Animal Welfare Officer (Dr Barrie Wells) to advise him of when and where your experiments will be conducted. Sufficient notice needs to be given so that if the AWO wishes to make an inspection, this can be easily arranged. Dr Wells can be contacted on 0427680782 or email barrie.wells@utas.edu.au

The Animal Ethics Committee is to be promptly notified of any unexpected, adverse events which occur during the period of the approved project and which may impact on the welfare of the animals. (2.2.28 *Australian Code of Practice*).

Autopsy by a qualified veterinarian should be performed when animals die unexpectedly. Any foreseeable departure from this requirement must have been outlined and approved in the initial application.

Approval permit for project A0010470 approved 20/03/2009

Detailed experimental records must be kept and must be available to the Committee on request.

Conditions which apply to some projects only:
(i) If the investigation necessitates a Parks & Wildlife permit you are required to send a copy of this permit to the AEC Secretary before commencing work.
(ii) If you intend to obtain laboratory animals directly from a source other than the University Central Animal House, the Animal Welfare Officer must be notified when the order is placed and when the animals are received.

Special Conditions of approval (if applicable):
There are no special conditions of approval applicable to this project.

Nicola Hodgman

Approval permit for project A0010470 approved 20/03/2009

UNIVERSITY OF TASMANIA ANIMAL ETHICS COMMITTEE		
Ethics Number	A0010470	
Project Name	Discovery of malarial resistance genes using ENU mutagenesis in mice and the study of these and other genes as antimalarial therapeutic targets	
Chief Investigator	Professor SJ Foote	Phone
School	Menzies Research Institute	
Person responsible for day-to-day care		Phone
Starting date	20/03/2009	
Approved to	20/03/2012 (subject to annual review)	
Emergency Contact		Phone

Approval permit for project A0010470 approved 20/03/2009

University of Tasmania
Animal Ethics Committee

Research Services
University of Tasmania
Private Bag 01
Hobart, Tasmania 7001
Tel: (03) 6226 7283
Fax: (03) 6226 7148
Email: animal.ethics@utas.edu.au

ASSOCIATE INVESTIGATOR

Please note the intention of this form is to provide the AEC with sufficient information to assess the competency and level of supervision of the applicant.

APPLICATION TO ADD A NEW ASSOCIATE INVESTIGATOR TO AN APPROVED PROJECT	
Project No:	A010470
Title of approved investigation:	Discovery of malarial resistance genes using ENU mutagenesis in mice and the study of these and other genes as antimalarial therapeutic targets
Responsible investigator:	Professor Simon Foote

1. **Details of new investigator**

Name (include title, name and position/research level):	**Andreas GRETH, PhD student**
School or Discipline:	**Menzies Research Institute**
Internal box number:	**23**
Postal Address:	**Private Bag 23, Hobart, TAS 7001**
Phone (business and mobile):	**6226 4637**
Fax:	**6226 7704**
Email:	

Name (include title, name and position/research level):	**Preethi MAYURA GURU, RA**
School or Discipline:	**Menzies Research Institute**
Internal box number:	**23**
Postal Address:	**Private Bag 23, Hobart, TAS 7001**
Phone (business and mobile):	**6226 7734**
Fax:	**6226 7704**
Email:	**Preethi.mayuraGuru@utas.edu.au**

Name (include title, name and position/research level):	**Elinor Hortle, Hons student**
School or Discipline:	**Menzies Research Institute**
Internal box number:	**23**
Postal Address:	**Private Bag 23, Hobart, TAS 7001**
Phone (business and mobile):	**6226 4637**
Fax:	**6226 7704**
Email:	**ejhortle@postoffice.utas.edu.au**

2. Date of commencement in the approved investigation

Please type in the box which will expand

Greth – as soon as approval is given

Mayura guru - as soon as approval is given

Hortle – as soon as approval is given

3. Role within the approved investigation (include procedures, techniques and SOP's to be undertaken by the applicant)

Please type in the box which will expand

Greth – PhD student working on several lines of mice segregating resistant mutations for malarial infection.

Mayura guru – RA working on technical support for this project.

Hortle - Hons student working on several lines of mice segregating resistant mutations for malarial infection.

Fleur Rodda will start training Preethi Mayura guru , Andreas Greth and Elinor Hortle on many techniques associated with this work. These will include tail bleeding, venesection, injecting parasites, killing mice by either cervical dislocation, or gas.

4. Experience with nominated procedures

Please type in the box which will expand

Greth – None

Mayura guru –has previous experience on many techniques associated with this work. This includes tail bleeding, venesection, tail-vein, sub-cutaneous and intra peritoneal injections, killing mice by either cervical dislocation, or gas. All techniques will initially be supervised by Fleur Rodda

Hortle - none

5. Experience with nominated species

Please type in the box which will expand

Greth – None

Mayura guru – has previous experience on many techniques associated with this work. This includes tail bleeding, venesection, tail-vein, sub-cutaneous and intra peritoneal injections, killing mice by either cervical dislocation, or gas. All techniques will initially be supervised by Fleur Rodda

Hortle - none

6. If inexperienced with either species or procedures(s), how will experience be gained? (detailed information on training and supervision should be included)

Please type in the box which will expand

Greth, Mayura guru and Hortle will be assessed and trained by Fleur Rodda.

DECLARATIONS

I am familiar with the *Australian code of practice for the care and use of animals for scientific purposes* 2004. I accept that I have a responsibility to ensure that the investigations and procedures proposed in this form are conducted fully within the conditions laid down by the Code and I undertake not to use any animals or carry out any procedures which have not been approved by the Committee. I accept that the responsible investigator has ultimate responsibility for the project.

Name of New Associate Investigator: Andreas Greth

Signature: 1/3/2010

Date:

I am familiar with the *Australian code of practice for the care and use of animals for scientific purposes* 2004. I accept that I have a responsibility to ensure that the investigations and procedures proposed in this form are conducted fully within the conditions laid down by the Code and I undertake not to use any animals or carry out any procedures which have not been approved by the Committee. I accept that the responsible investigator has ultimate responsibility for the project.

Name of New Associate Investigator: Preethi Mayura guru

Signature:

Date: 1/3/10

I am familiar with the *Australian code of practice for the care and use of animals for scientific purposes* 2004. I accept that I have a responsibility to ensure that the investigations and procedures proposed in this form are conducted fully within the conditions laid down by the Code and I undertake not to use any animals or carry out any procedures which have not been approved by the Committee. I accept that the responsible investigator has ultimate responsibility for the project.

Name of New Associate Investigator: Elinor Hortle

Signature:

Date: 1-3-10

Name of Responsible Investigator: Professor Simon Foote

Signature:

Date: 08/03/10

ANIMAL RESEARCH AUTHORITY (ARA)

MACQUARIE UNIVERSITY

AEC Reference No.: 2012/019-3 **Date of Expiry:** 19 April 2014

Full Approval Duration: *20 April 2012 to 19 April 2015 (36 Months)*

This ARA remains in force until the Date of Expiry (unless suspended, cancelled or surrendered) **and will only be renewed upon receipt of a satisfactory Progress Report before expiry (see Approval email for submission details).**

Principal Investigator:
Prof Simon Foote
ASAM
simon.foote@mq.edu.au
0407 855 438

Other people participating

Shelley Lampkin	0439 617 344
Andreas Greth	0405 415 984
Patrick Lelliott	0450 314 761
Elinor Hortle	0400 067 447
Hong Ming Huang	0411 299 659

Associate Investigators:

Gaetan Burgio	0400 249 745
Brendan McMorran	0400 391 529
Bernardette Schnider	0451 875 457
Ju Wen Loke	0402 623 226

In case of emergency, please contact:
the Principal Investigator /
Associate Investigator named above
or Manager, CAF: 9850 7780 / 0428 861 163, and
Animal Welfare Officer: 9850 7758 / 0439 497 383

The above-named are authorised by MACQUARIE UNIVERSITY ANIMAL ETHICS COMMITTEE to conduct the following research:

Title of the project: **Discovery of malarial resistance genes using ENU mutagenesis in mice and the study of these and other genes as antimalarial therapeutic targets**

Purpose: **4 - Research : Human or animal health and welfare**

Aims:
1. **To cause mutations in the sperm of mice using Ethyl Nitrosourea (ENU)**
2. **To screen the progeny of ENU-treated mice for resistance to malarial infection**
3. **To examine the biological characteristics (including genotyping) of the malarial-resistant mice**

Surgical Procedures category: 7 (Major Physiological Challenge), 8 (Death as an endpoint)

All procedures must be performed as per the AEC-approved protocol, unless stated otherwise by the AEC and/or AWO.

Maximum numbers approved (for the Full Approval Duration):

Species	Strain	Age/Sex/Weight	Total	Supplier/Source
01: Mice	SJL, C57BL/6, C3H/He, BALB/c, 129/Sv, CAST/Ei	m/f/18-30g	16000	ARC/Jax/CAF or other
		Total	**16000**	

Location of research:

Location	*Full street address*
Australian School of Advanced Medicine (ASAM)	Level 1, Clinic Building, 2 Technology Place, Macquarie University NSW 2109
Central Animal Facility (CAF)	Building F9A, Research Park Drive, Macquarie University NSW 2109

Amendments approved by the AEC since initial approval:
1. *Addition of Bernardette Schnider as Associate Investigator* ***on the condition that there is proper supervision at all times*** *(Approved November 2012, ratified at AEC 6 December 2012 meeting).*
2. *Addition of Ju Wen Ian Loke as Associate Investigator (Approved Feb 2013, ratified March 2013)*

Conditions of Approval: N/A

Being animal research carried out in accordance with the Code of Practice for a recognised research purpose and in connection with animals (other than exempt animals) that have been obtained from the holder of an animal suppliers licence.

Professor Mark Connor (Chair, Animal Ethics Committee) **Approval Date:** 14 March 2013

Adapted from Form C (issued under part IV of the Animal Research Act, 1985)